UNIVERSITY OF CALIFORNIA, SAN DIEGO

Sphingosine-1-Phosphate Effects

on Cardiac Fibroblasts and Myocytes

A Dissertation submitted in partial satisfaction of the requirements for the degree

Doctor of Philosophy

in

Bioengineering

by

Lee K. Landeen

Committee in charge:

Professor Wayne R. Giles, Chair
Professor Gabriel A. Silva, Co-Chair
Professor Shu Chien
Professor Christopher Glass
Professor Paul Insel
Professor Hugh Rosen

2007

The Dissertation of Lee K. Landeen is approved, and it is acceptable in quality and form for publication on microfilm:

Co-Chair

Chair

University of California, San Diego

2007

DEDICATION

This is dedicated in part to
my partner,
my family,
and my friends
who supported me along the way.

TABLE OF CONTENTS

LIST OF TABLES

LIST OF FIGURES

ACKNOWLEDGEMENTS

I would first like to thank my advisor, Dr. Wayne Giles, for his guidance, mentoring, and support during my dissertation. He was very encouraging and willing to let me pursue areas of research which I found interesting. I would also like to thank my other committee members for their willingness to participate and for their scientific contributions and suggestions.

I am indebted to several people for their assistance during my research. The greatest thanks go to Nakon Aroonsakool for his technical assistance in the lab. Likewise, I thank other lab members, both past and present including Betty Hu, Dr. Martin Fink, Sahar Soleymani, Dr. Rikuo Ochi, Dorothy Dederko, Dr. Richard Kondo, Colleen Kondo, Dr. Lisa Chilton, Ricardo Goméz García, Dr. Robert Clark, Sheila Crombie, and Caroline Collins. I would like to thank others at UCSD who assisted in various ways: Ian Lian, Dr. Jason Haga, Gerry Norwich, Marie Davidson, and Iveta Kalcheva.

Dr. Ken Spitzer of the Nora Eccles Harrison Cardiovascular Research and Training Center (University of Utah) was instrumental in providing guidance and technical support for the myocyte studies. Dr. Richard Proia of the National Institute of Diabetes, Digestive and Kidney Diseases was most generous in sharing his S1P receptor deficient mice, and Kim Weldy was valued for maintaining the breeding colonies, under the cooperation of Dr. Masahijo Hoshijima. I am appreciative of the technical assistance provided by Drs. Victor Panchenco and Dr. Antonio Guia of AVIVA Biosciences (San

Diego, CA). Likewise, I thank Rick Logemann and Abe Mara of Bio-Imaging Solutions for their technical assistance with the confocal microscope.

I would like to thank several investigators for allowing me use of their instruments and/or shared facilities including Dr. Shu Chien (initial lab space, quantitative PCR machine, and flow cytometer), Dr. Gabe Silva (confocal microscope), Dr. Masahijo Hoshijima (TaqMan PCR instrument), and Dr. Amy Sung (Bioengineering Core lab space).

Several chapters of this thesis have been submitted in part for publication in which the dissertation author was the primary investigator and author. Chapters 2 and 3 are being published in the following manuscript: Landeen L.K., Aroonsakool N., Haga J.H., Hu B.S., Giles W.R., Sphingosine-1-Phosphate Receptor Expression in Cardiac Fibroblast Cells is Modulated by in vitro Culture Conditions, *American Journal of Physiology: Heart and Circulatory Physiology,* 2007 (in press). Chapter 5 has been submitted for publication and is currently in revision: Landeen L.K., Hu B.S., Haga J.H., Aroonsakool N., Giles W.R., Mechanisms of the Negative Inotropic Effects of Sphinogine-1-Phosphate in Adult Mouse Ventricular Myocytes, *American Journal of Physiology: Heart and Circulatory Physiology..*

This research was supported in part by a grant from the American Heart Association Western States Affiliate (0555040Y). Lastly, I would like to acknowledge the financial support of my graduate research fellowship from the National Science Foundation.

VITA

Education

1987	B.S., Microbiology, University of Arizona
1989	M.S., Microbiology, University of Arizona
2007	Ph.D., Bioengineering, University of California, San Diego

Professional Experience

1989-2002	Manufacturing Associate (I, II), Research Associate (I-IV), Research Scientist, Project Manager, Advanced Tissue Sciences, Inc., La Jolla, CA
2002	Consultant, Advanced Tissue Sciences, Inc., La Jolla, CA
2004	Consultant, Smith & Nephew Wound Management, La Jolla, CA
2006	Consultant, Accurate Consulting, Inc., San Diego, CA

Fellowships

2003-2004	Jacobs School Fellowship
2004-2006	National Science Foundation Graduate Research Fellowship

Publications

Landeen LK, Dederko DA, Hu BS, Aroonsakool N, Haga JH, Giles WR. Mechanisms of the Negative Inotropic Effects of Sphinogine-1-Phosphate in Adult Mouse Ventricular Myocytes. *American Journal of Physiology: Heart and Circulatory Physiology*. 2007 (in submission).

Hu BS, Landeen LK, Aroonaskool N, Giles WR. An Analysis of the Effects of Stretch on IGF-1 Secretion from Rat Ventricular Fibroblasts. *American Journal of Physiology: Heart and Circulatory Physiology*. 2007 (in press).

Landeen LK, Aroonsakool N, Haga JH, Hu BS, Giles WR. Sphingosine-1-Phosphate Receptor Expression in Cardiac Fibroblast Cells is Modulated by in vitro Culture Conditions. *American Journal of Physiology: Heart and Circulatory Physiology*. 2007 (in press).

Sherwood JK, Riley SL, Palazzolo R, Brown SC, Monkhouse DC, Coates M, Griffith LG, Landeen LK, Ratcliffe A. A Three-Dimensional Osteochondral Composite Scaffold for Articular Cartilage Repair. *Biomaterials*. 2002. 23/24:4739-4751.

Kellar RS, Landeen LK, Shepherd BR, Ratcliffe A, Naughton GK, Williams SK. Scaffold-Based, Three-Dimensional Human Fibroblast Cultures Provide a Structural Matrix That Supports Angiogenesis in Ischemic Heart Tissue. *Circulation*. 2001. 104:2063-2068.

Zeltinger J, Landeen LK , Alexander HG, Kidd ID, Sibanda B. Development and Characterization of Tissue Engineered Aortic Valves. *Tissue Engineering*. 2001. 7(1):9-22.

Landeen, LK, Zeltinger J, Lee AL, Alexander HG, Graham, DA, Ratcliffe T, and Naughton GK. Tissue Engineered Vascular Grafts. *Stent Graft Update*. Ed. Vossoughi J, Kipshidze N, Karanian JW. Medical and Engineering Publishers, Inc., Washington, DC. 2000. 89-111.

Halberstadt CR, Hardin R, Bezverkov K, Snyder D, Allen L, Landeen L. The In Vitro Growth of a 3-D Human Dermal Replacement Using a Single-Pass Perfusion System. *Biotechnology and Bioengineering*. 1994. 43(8):740-746.

Slivka SR, Landeen LK, Ziegler F, Zimber MP, Bartel RL. Characterization, Barrier Function, and Drug Metabolism of an In Vitro Skin Model. *Journal of Investigative Dermatology*. 1993. 100(1):40-46.

Zeigler FC, Landeen L, Naughton GK, Slivka SR. Tissue-Engineered, Three-Dimensional Human Dermis to Study Extracellular Matrix Formation in Wound Healing. Journal of Toxicology: *Cutaneous and Ocular Toxicology*. 1993. 12(4):303-312.

Landeen LK, Zeigler FC, Halberstadt C, Cohen R, Slivka SR. Characterization of a Human Dermal Replacement. *Wounds*. 1992. 4(5):167-175.

Slivka SR, Landeen L, Naughton GK, Bartel RL. Regulation of Collagen Deposition by Human Fibroblasts Grown in a Three Dimensional Skin Culture System. *In Vitro Toxicology: Mechanisms and New Technology*. Ed. Alan M. Goldberg. Mary Ann Liebert, Inc., New York. 1991. 8:335-342.

Slivka SR, Landeen L, Zimber MP, Bartel RL. Characterization of a Three-Dimensional Human Skin Culture Model for In Vitro Percutaneous Absorption Studies. *Pharmaceutical Research.* 1991. 17-21.

Yahya MT, Landeen LK, Messina MC, Kutz SM, Shulze R, Gerba CP. Disinfection of Bacteria in Water Systems by Using Electrolytically Generated Copper:Silver and Reduced Levels of Free Chlorine. *Canadian Journal of Microbiology*. 1990. 36(2):109-116.

Landeen LK, Yahya MT, Gerba CP. Efficacy of Copper and Silver Ions and Reduced Levels of Free Chlorine in Inactivation of *Legionella pneumophila*. *Applied and Environmental Microbiology*. 1989. 55(12):3045-3050.

Landeen, LK, Yahya MT, Kutz SM, and Gerba CP. Microbiological Evaluation of Copper:Silver Disinfection Units for Use in Swimming Pools. *Water Science and Technology*. 1989. 21(3):267-270.

Rose JB, Landeen LK, Riley KR, and Gerba CP. Evaluation of Immunofluorescence Techniques for Detection of *Cryptosporidium* oocytes and *Giardia* cysts from

Environmental Samples. *Applied and Environmental Microbiology*. 1989. 55(12):3189-3196.

Yahya MT, Landeen LK, Kutz SM, Gerba CP. Inactivation of Legionella pneumophila by Exposure to Copper:Silver Ions and Reduced Levels of Free Chlorine. *Water Pollution Control Federation Specialty Conference Series*, "Microbial Aspects of Surface Water Quality". 1989. Chicago, IL. 82-95.

Yahya MT, Landeen LK, Kutz SM, Gerba CP. Swimming Pool Disinfection: an Evaluation of the Efficacy of Copper:Silver Ions. *Journal of Environmental Health*. 1989. 51(5):282-285.

Patents

Ratcliffe A, Mansbridge JN, Landeen LK, Pinney E, Edison LJ. Cultures of Three Dimensional Tissues and Uses Thereof. U.S. Application Serial No. 11/216,574.

Naughton GK, Horwitz DL, Applegate M, Zeltinger J, Mansbridge JN, Kern A, Landeen LK, Ratcliffe A. Conditioned Cell Culture Medium Compositions and Methods of Use. U.S. Patent #7,118,746.

Naughton GK, Naughton BA, Purchio AF, Landeen LK, Zeltinger J, Campbell TD. Three-Dimensional Human Cell Cultures on Cardiac Valve Frameworks and Their Uses. U.S. Application Serial No. 08/488,165.

Peterson A, Landeen L, Bennett J, Gee J, Chesla S, Zeltinger J, Flatt JH, Applegate M, Dunkelman N, Kemmerrer S. Apparatus and Method for Simulating in vivo Conditions While Seeding and Culturing Three-Dimensional Tissue Constructs. Issued 9-19-00. U.S. Patent #6,121,042.

Peterson A, Landeen LK, Bennett JW, Gee Chesla S, JM, Zeltinger J. Apparatus for Sterilizing, Seeding , Culturing, Storing, Shipping and Testing Tissue, Synthetic or Mechanical Heart Valves or Valve Segments. U.S. Patent #5,846,828.

Peterson A, Landeen L, Zeltinger J. Apparatus for Sterilizing, Seeding, Culturing, Storing, Shipping and Testing Tissue, Synthetic or Native Vascular Grafts. Issued 8-11-98. U.S. Patent #5,792,603.

Slivka SR, Landeen LK. Three-Dimensional Stromal Cell and Tissue Culture System. Issued 12-26-95. U.S. Patent #5,478,739.

Awards and Honors

Phi Kappa Phi Honor Society
Phi Beta Kappa Honor Society
Phi Eta Sigma Honor Society

Outstanding Senior, Microbiology Department, University of Arizona
Outstanding Senior, Faculty of Sciences, College of Arts and Sciences, University of Arizona
National Dean's List
United States National Collegiate Award Winner
University of Arizona General Academic Scholarship

Activities

1990	Volunteer, AIDS Foundation
1991-1996	Volunteer, The Center for Social Services
1993-1996	Recording Secretary, The Center for Social Services
1997-2001	Volunteer and Participant, AIDS Walk
2000-2003	Founder, President, Chair of Board of Directors, Lambda Biotechnology Association
2003-2005	Secretary, Board of Directors, Lambda Biotechnology Association
2005-2007	Treasurer, Board of Directors, Lambda Biotechnology Association

Fields of Study

Major Field: Bioengineeing

Studies in Electrophysiology
Professor Wayne Giles

Studies in Physiology
Professor Wayne Giles

ABSTRACT OF THE DISSERATION

Sphingosine-1-Phosphate Effects on Cardiac Fibroblasts and Myocytes

by

Lee K. Landeen

Doctor of Philosophy in Bioengineering

University of California, San Diego, 2007

Professor Wayne R. Giles, Chair

Professor Gabriel A. Silva, Co-Chair

The bioactive molecule sphingosine-1-phosphate (S1P) activates five recognized G-protein coupled receptors ($S1P_{1-5}$) to affect various tissues, including myocardium. Activation of these receptors and the ability to affect functional responses including

differentiation, migration, contraction, and ionic currents in isolated cardiac fibroblasts (CFb) and myocytes was investigated.

CFb are essential components of myocardium, and study of their cell signaling and physiology is required for a number of emerging disciplines. However, in order to conduct meaningful studies on CFb, methods for selective, reproducible cell isolations are necessary. A protocol was therefore developed that significantly reduced resident macrophage levels in CFb isolates and utilized more CFb-specific markers, instead of, or in addition to, more commonly used cytoskeletal markers.

Primary isolated, purified mouse CFb express predominantly $S1P_{1-3}$; however, the relative levels of these receptor subtypes are modulated with time and by culture conditions. Co-culture with macrophages altered CFb S1P receptor levels relative to controls. Further investigations using known macrophage-secreted factors (e.g. TFGβ1, TNFα, and PDGF-BB) all altered S1P receptor subtypes. Low serum concentrations increased $S1P_2$, which was diminished using a Rho-associated protein kinase inhibitor. Similarly, elevated $S1P_3$ levels by PDGF-BB were diminished using a Rac1 inhibitor. $S1P_2$ and $S1P_3$ (which activate Rho and Rac pathways, respectively) regulate cell migration, and CFb isolated from $S1P_3$-null mice had reduced migration. These results highlight the importance of demonstrating CFb culture purity in functional studies of S1P and present conditions that modulate S1P receptor expression in CFb.

CFb were characterized using novel patch-clamping technology platforms to assess potassium channel currents and the effect of S1P on CFb electrophysiology. Both K_v and K_{ir} currents were identified by conventional and patch-on-a-chip platforms;

however, chip platforms were more likely to activate mechanosensitive ion channels. S1P strongly activated both inward and outward currents in adult rat CFb.

Lastly, mouse ventricular myoycte contractility was investigated experimentally and through mathematical modeling to characterize signaling pathways involved in S1P-regulated negative inotropy. S1P reduced cell shortening via $S1P_1$ and $S1P_3$. In particular, $S1P_1$ reduced L-type calcium channel activity and activated an acetylcholine-like potassium current to alter action potential duration and intracellular calcium concentrations.

CHAPTER 1

INTRODUCTION

1.1 Abstract

This chapter reviews and provides background information on several topics discussed within the dissertation. Rather than serving as an exhaustive literature review, it is meant instead to familiarize the reader first with the molecule sphingosine-1-phosphate (S1P), which was a focal point of study. Towards that, this chapter will describe the basic structure and metabolism of the molecule, the receptors for which it serves as ligand, and some of the reported physiological effects in cells and the cardiovascular system upon exposure. Lastly, this chapter discusses the cardiac fibroblast, its phenotypic characterization, and its importance to myocardial electrophysiology. The interrelationships between the cardiac fibroblast and the myocyte in normal and pathphysiological conditions are increasingly being recognized and it is important to discuss these. Additional, relevant and more specific background material will be presented within the introduction and discussion sections of the remaining chapters, in context with the derived experimental results.

1.2 Sphingolipids

Sphingolipids are amphipathetic molecules with a large degree of structural variety and function that were first named by J.L.W. Thudichum in the late nineteenth century (1884).[32,82] Sphingolipids structurally contain a hydrophobic domain (one of five sphingoid bases with one of twenty fatty acid acyl chains) and a hydrophilic domain

(either phosphate, phosphorylcholine, or one of five hundred carbohydrate residues). The structural definition of sphinoglipids is shown in Figure 1.1. They are one of three main classes of cell membrane lipids (the others being glycerolipids and sterols) and are found in all higher life forms and some prokaryotes and viruses.[82] Sphingolipids are concentrated in lipid rafts on the outer plasma membrane, but are also found in mitochondria, the endoplasmic reticulum, and the Golgi apparatus (from where they are synthesized and transported).[32]

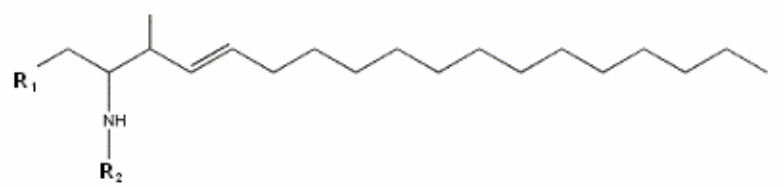

R1	*R2*	*Name*
H	OH	sphingosine
H	PO_4	sphingosine-1-phosphate
fatty acid	OH	ceramide
fatty acid	phosphocholine	sphingomyeline
fatty acid	galactose	cerebroside

Figure 1.1 Sphingolipid Structure and Representative Modifying Groups.[107]

In common with other glycolipds, sphingolipids are involved in cell-cell communication and intracellular signaling pathways. Sphingolipids may function as primary messengers via ligand binding to extracellular transmembrane receptors or as secondary messengers which act intracellularly.[82]

The concept of a sphingolipid rheostat has been proposed by several investigators to help describe the balance between cell survival and apoptotic events. Three important sphingolipids involved in this delicate balance are ceramide, sphingosine-1-phosphate

(S1P), and their intermediate molecular product, sphingosine (see Figure 1.2). Whereas ceramide or sphingosine have been associated with cell growth arrest, apoptosis, and inhibition of calcium release-activated calcium current, S1P has been associated with cell growth, motility, cell survival, and calcium regulation.[108]

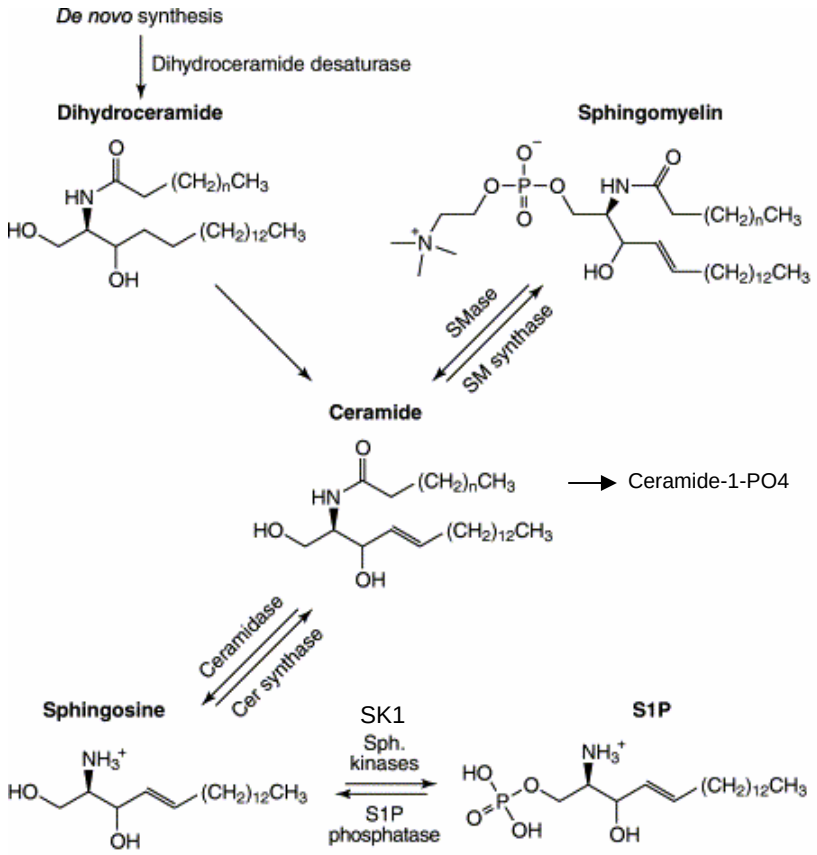

Figure 1.2 Metabolic Pathway of S1P and Its Intermediates. Modified from Rosen and Liao (2003).[103]

1.3 Sphingosine-1-Phosphate

S1P is derived from the ATP-mediated phosphorylation of sphingosine (at the 1-OH position) by one of two sphingosine kinase (SK) isoforms.[17] S1P is present in greater quantities than its precursors sphingosine or ceramide. The conversion of

sphingosine to S1P is rapid and can be formed either within the cytosol (where S1P predominates) or in the extracellular space, since SK is constitutively secreted (in small amounts) into the extracellular space. When exposed to sphingosine, S1P is significantly detected within 5 minutes, peaks at 60 minutes, but is still detected above baseline levels for up to 8 hours.[132] S1P may be degraded by S1P lyase into the byproducts trans-hexadecenol and ethanolamine-phosphate.

S1P is a normal component of serum and plasma,[20,42,99] where it binds to albumin and high density lipoprotein (HDL). S1P plasma levels in C57Bl/6 mice have been recorded as high as 1.3 μM.[47] Whether these are representative of true in vivo levels or are slightly elevated is unknown, due to the potential for bias by platelet activation and S1P release during blood collection. Although it is commonly believed that activated platelets[130] are the primary source for circulating levels of S1P, recent data (T. Hla, unpublished results) suggests that endothelial cells within the liver are primary contributors. This discovery was made by measuring plasma levels in mice depleted of platelets, red blood cells, or hematopoeitic cells. Serum concentrations in those mice were relatively constant. However, mice having undergone hepatectomies exhibited significantly reduced levels of circulating S1P.

While specific effects of S1P depend on cell type, the complement of S1P receptor expression, and associated G proteins (reviewed in [31,32,99,109]), S1P is known to affect physiological responses including heart rate,[105] arterial vasoconstriction,[16] endothelial cell integrity,[34] immune cell functions,[78,105] proliferation,[59,93,132] motility,[1,104] intracellular calcium ($[Ca^{++}]_i$) regulation,[36,56,83,84,117,132] cell survival, and ion channel current activation.[77,117]

1.4 S1P Receptors

S1P binds with high affinity (K_d values vary between 1-60 nM) to five distinct G protein coupled receptors (GPCR).[15] Recently, three other receptors (gpr3, gpr6, and gpr12) have been identified that also interact with S1P.[116] GPCR are a class of seven-pass transmembrane proteins that utilize guanine nucleotide binding proteins as intermediaries between the agonist-stimulated receptors and the downstream effector/signal generators. G proteins are heterotrimeric complexes consisting of an α, β, and γ subunit, each of which localizes primarily at the plasma membrane. Upon receptor activation, guanosine diphosphate (GDP) bound to the α subunit is exchanged for guanosine triphosphate (GTP). This releases the α subunit from the βγ subunit dimer and both are free to interact with their respective effector molecule(s), thus allowing for a highly complex array of signaling pathways. Hydrolysis of GTP to GDP by the α unit allows it to reassociate with the βγ dimmer.[29]

The GPCR to which S1P (and the related lysophospholipid lysophosphatidic acid, [LPA]) bind were originally termed endothelial differentiation gene (EDG) receptors, based on their first reported discovery in endothelial cells. Because the original nomenclature of these receptors was not entirely representative of their later determined functions, they have since been renamed according to the International Union of Pharmacology (IUPHAR) guidelines in the late 1990s. These guidelines specify receptor names based on the particular ligand and the order of publication.[15] Furthermore, the usage of the abbreviation S1P (for sphingosine-1-phosphate) was adopted over other

alternatives (e.g. SPP or Sph-P). A listing of the eight recognized lysophospholipid receptors is presented in Table 1.1.

Table 1.1 S1P and LPA Receptor Nomenclature[15]

Agonist Ligand	*IUPHAR Nomenclature*	*Receptor Code*	*EDG Name*	*Alternative Names*
LPA	LPA_1	2.1:LPL:2:LPA1	EDG-2	LP_{A1}, vzg-1, rec1.3
LPA	LPA_2	2.1:LPL:4:LPA2	EDG-4	LP_{A2}
LPA	LPA_3	2.1:LPL:7:LPA3	EDG-7	LP_{A3}
S1P	$S1P_1$	2.1:LPL:1:S1P1	EDG-1	LP_{B1}
S1P	$S1P_2$	2.1:LPL:3:S1P2	EDG-5	LP_{B2}, AGR16, H218
S1P	$S1P_3$	2.1:LPL:5:S1P3	EDG-3	LP_{B3}
S1P	$S1P_4$	2.1:LPL:6:S1P4	EDG-6	LP_{B4}
S1P	$S1P_5$	2.1:LPL:8:S1P5	EDG-8	LP_{B5}, nrg-1

Thus, S1P can induce significant and varied changes in target cell function at nanomolar concentrations[84] through its complex G-protein signaling pathways. $S1P_1$ couples exclusively to pertussis toxin (PTX)-sensitive G_i and can inhibit cAMP production and mediates phospholipase C (PLC) activation. $S1P_2$ and $S1P_3$ in contrast can couple to several G-proteins including G_q, $G_{i/o}$, and $G_{12/13}$. However, though $S1P_2$ and $S1P_3$ share overlapping G-proteins, the effector proteins of each pathway differs. $S1P_3$ is involved in proliferation, migration, survival and morphogenesis. $S1P_3$ can mediate G_i inhibition of cAMP and induce PLC activation through a PTX-insensitive pathway. $S1P_3$ can activate Rac via $G_{12/13}$ and, to a much lesser extent, Rho. $S1P_2$ (acting via $G_{12/13}$) is the primary Rho activation receptor by S1P.[31,43,44,99] A listing of classical S1P receptor subtypes and their associated G-proteins is presented in Table 1.2.

Figure 1.3 illustrates signaling pathways and downstream effecter molecules of the S1P receptor subtypes.

The orphan GPCR gpr3, gpr6, and gpr12 appear to have somewhat contradictory and opposing signaling pathways in that they are reported to have constitutive activity with dual coupling to both G_s and G_i. However, due to the absence of reports on whether these newer S1P-activated GPCR are expressed in cardiac tissue, they will not be discussed further.

Table 1.2 S1P Receptor and G-protein Associations[108]

Receptor	G_i	G_q	G_{13}	G_{12}	G_s
$S1P_1$ (EDG1)	✓				
$S1P_2$ (EDG5)	✓	✓	✓	✓	?
$S1P_3$ (EDG3)	✓	✓	✓	✓	
$S1P_4$ (EDG6)	✓			✓	
$S1P_5$ (EDG8)	✓				

Several S1P receptor null mice have been developed in which the progeny have varying degrees of functional deficiencies.[129] $S1P_1$-null mice are embryonic lethal. This lethality is due to hemorrhaging resulting from compromised vascular smooth muscle cell (VSMC) migration.[73] VSMC from $S1P_1$-null mice have compromised Rac signaling and cell migration.[73] This loss in function prevents pericytes from migrating towards capillary endothelial cells to stabilize newly forming vessel structures. Whereas neither $S1P_2$-[44] nor $S1P_3$-null[43] mice are embryonic lethal, double-null $S1P_{1,2}$ and $S1P_{1,3}$ and triple-null $S1P_{1,2,3}$ mice do result in embryonic lethality. These findings emphasize the importance of $S1P_1$ in early vascular development.[63]

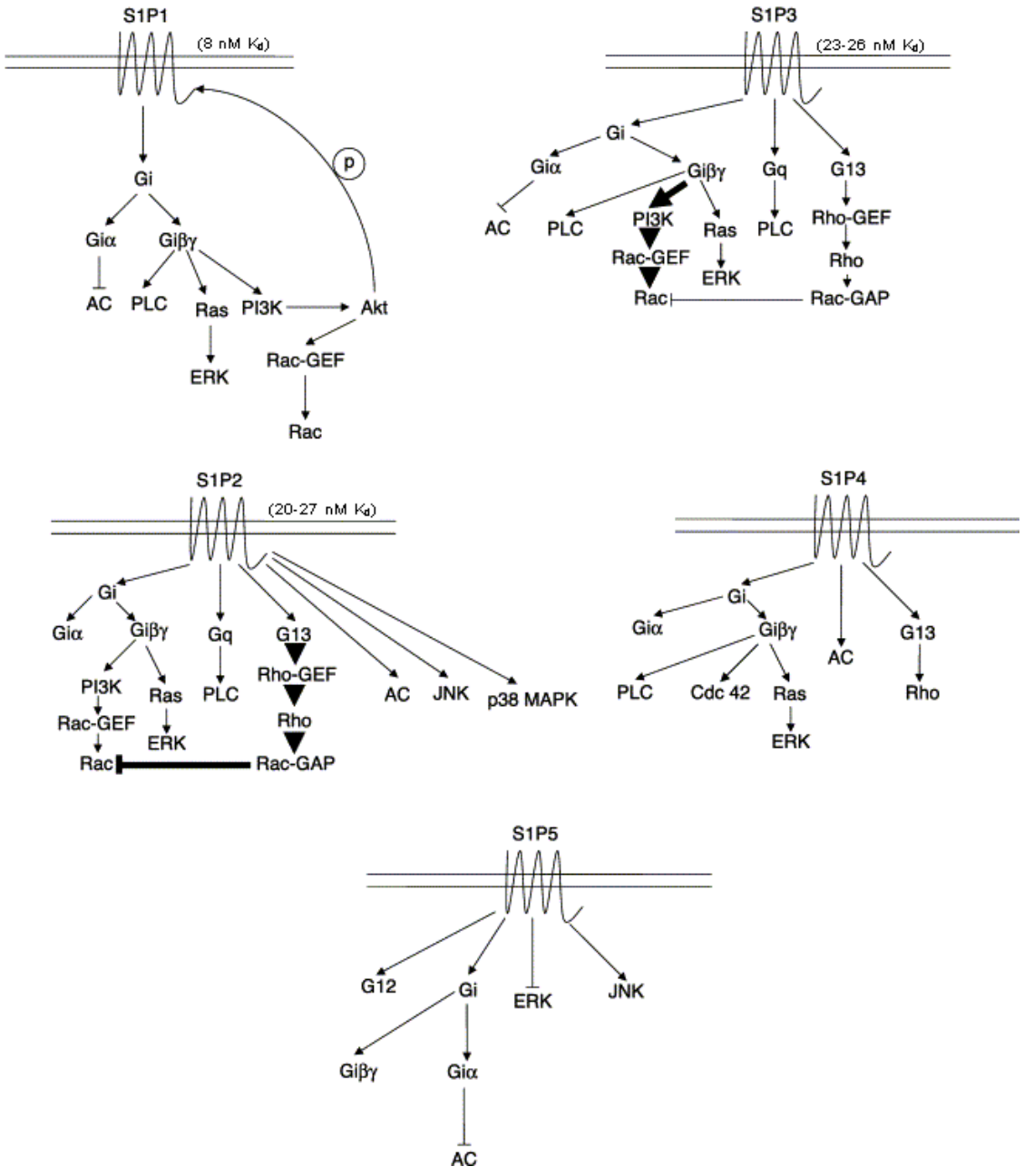

Figure 1.3 S1P Receptor Subtype Signaling Pathways. Modified from Taha et al., 2004.[112]

Cells from $S1P_2$ null mice have decreased Rho activation but normal PLC activation and intracellular calcium ($[Ca^{++}]_i$) mobilization. $S1P_3$-null mice appear to have a relatively normal phenotype, except for impaired PLC signaling.[43] Therefore, $S1P_3$ may not be as important during normal development. As mentioned earlier, $S1P_2$ and $S1P_3$ can signal through common G-proteins. For example, although both receptor subtypes can signal through Rho, $S1P_3$ does not utilize this pathway to any extent since Rho activation is unaffected in cells from $S1P_3$ null mice. In contrast, cells from $S1P_{2,3}$ double-null mice exhibit a complete loss of Rho activation. Additionally, these cells are noted to have significant defects in PLC activation and $[Ca^{++}]_i$ mobilization.[44] Lastly, cells from $S1P_{2,3}$ double-null mice had little effect on adenylyl cyclase (AC) inhibition, suggesting that G_i signaling is less important for these S1P receptor subtypes.[44]

A summary the phenotype for several of these genetically altered mice is presented in Table 1.3.

Table 1.3 S1P Receptor Knock-Out Mice and Phenotype

Receptor	*Observations*	*Normal Expression*
$S1P_1$ null	• Death between E12.5-E14.5 • Incomplete vascular maturation • Inability to activate Rac in SMC	• ubiquitous • cardiomyocyte sarcolemma • endothelial cells (EC) of human cardiac vessels
$S1P_2$ null	• Epileptic seizure at 3-6 weeks • decreased Rho activation	• smooth muscle cells (SMC) of human aorta
$S1P_3$ null	• Relatively unaffected phenotype • Impaired PLC activation • Minimal affect on adenylyl cyclase inhibition • Rho activation unaffected	• Ubiquitous • SMC of human aorta • EC

1.5 Expression and Distribution of S1P Receptors

S1P receptors can be found on virtually every cell type. However, the relative amounts and distribution can vary depending on species, tissue and cell type. In the human cardiovascular system, $S1P_1$, $S1P_2$, and $S1P_3$ are expressed in both the adult and fetal heart. $S1P_1$ is expressed strongly in EC of the aorta and endocardium and within the myocardium. $S1P_2$ is expressed weakly within the myocardium. Surprisingly, although $S1P_2$ is present in aortic artery SMC, it is reportedly absent in coronary artery SMC. $S1P_3$, on the other hand, is moderately expressed in myocardial tissue, but is strongly expressed in SMC of both the aorta and coronary artery.[80] In rats, $S1P_1$, $S1P_2$, and $S1P_3$ are all expressed in atrial and ventricular myocytes.[72] Table 1.4 summarizes these findings.

$S1P_4$ (EDG6) and $S1P_5$ (EDG8) are reportedly not as highly expressed in cardiac tissue[72] or macrophages.[41] For these reasons, the studies presented herein focus on expression of $S1P_1$, $S1P_2$, and $S1P_3$ subtypes.

Table 1.4 S1P Receptor Distribution in Cardiac Tissues

Species	*Tissue*	*Cell*	*$S1P_1$*	*$S1P_2$*	*$S1P_3$*
Human	Cardiac vessel	EC	✓		
Human	Myocardium	Myocyte	✓	✓	✓
Human	Aorta	SMC		✓	✓
Human	Cardiac vessel	SMC			✓
Rodent	Atria	Myocyte	✓	✓	✓
Rodent	Ventricle	Myocyte	✓	✓	✓

1.6 Electrophysiological and Functional Responses to S1P

Tissue-specific expression of ion channels is known to affect atrial and ventricular myocyte action potential (AP) waveforms.[7,37,74] S1P also has varying effects in different heart regions which may be related to differential expression of S1P receptor subtypes. In canine sino-atrial node (SAN) myocytes, S1P at high levels can increase heart rate.[111] However, in rabbit SAN myocytes,[39,77] S1P increases cycle length, decreases resting mean potential, and decreases isoproteranol-stimulated pacing, but appears to have no effect on L-type calcium channel currents (I_{CaL}).[39] This effect in rabbit SAN myocytes is due to an activation of an inwardly rectifying potassium (K^+) current very similar to acetylcholine-activated K^+ currents (I_{KAch}). The activation of I_{KAch} by S1P has been demonstrated conclusively in guinea pig[9] and human[40] atrial myocytes. In rats, intravenously administered S1P slows heart rate.[110] In rat ventricle, S1P can depress ventricular myocyte excitability by reducing sodium current (I_{Na})[77] and inducing Ca^{++} overload. In voltage-clamped mouse atrial myocytes, S1P causes a hyperpolarization that results in increased cycle length and activates a weakly inwardly rectifying current, similar to $I_{KAch.}$[88]

One of the few studies on the effects of S1P on fibroblasts has shown S1P to hyperpolarize the embryonic mouse fibroblast cell line NIH3T3 by increasing K^+ efflux.[100] After exposure to 10 nM (10^{-8} M) S1P, the resting mean potential changed from approximately -30 mV to approximately -45 mV. This hyperpolarization was dose-dependent between 10^{-8} and 10^{-5} M S1P and was sensitive to blockade by charybdotoxin (300 nM), suggesting involvement of Ca^{++}-activated K^+ channels (K_{Ca}).

S1P can affect other cellular functions. S1P was first shown to stimulate cell proliferation and increase in intracellular calcium by Zhang, et al.[132] In those studies using Swiss 3T3 fibroblasts, calcium levels were rapidly increased (within 15 seconds) from intracellular stores and it was suggested that this mobilization of calcium involved intracellular second message signaling. Ghosh, et al.[36] later proposed that sphingosine must be phosphorylated into S1P intracellularly to have an effect on intracellular calcium rises.

S1P (and LPA) are known to activate chloride channels in a number of cell types.[131] For example, this has been shown for human lung fibroblasts at S1P concentrations of 1 μM. These chloride currents were increased in density in cells differentiated to a myofibroblast phenotype using TGFβ. When chloride channels were blocked with inhibitors, this myofibroblast differentiation was diminished.[131] Chloride channels (e.g. CLIC-4) have been shown to be involved in the differentiation of breast fibroblasts to myofibroblasts,[102] indicating that this response may be widespread among fibroblasts. In the study by Yin, et al.,[131] specific S1P receptor isotype(s) involvement was not determined, although these cells expressed $S1P_{1-3}$ in relative abundance.

S1P is known to activate a number of ionic currents in various cells.[88,100,122,131] These include: (i) a weakly inwardly rectifying potassium channel similar to KAch in mouse atrial myocytes; (ii) a calcium-activated potassium channel in NIH3T3 fibroblasts; and (iii) a chloride channel in corneal keratocytes and human lung fibroblasts.

Table 1.5 Activation of Ionic Currents by S1P

Species	*Cell Type*	*Current*
Rabbit	SAN Myocyte	KAch
Guinea Pig	Atrial Myocyte	KAch
Human	Atrial Myocyte	KAch
Mouse	Atrial Myoycte	KAch
Rat	Ventricular Myocyte	Na^+
Mouse	Embryonic Fibroblast (NIH3T3)	K_{Ca}
Human	Lung Fibroblast	Cl^-
Rabbit	Corneal Keratocytes	Cl^-

In studies using Swiss 3T3 fibroblasts, S1P was mitogenic at 0.5 μM with maximal stimulation at 2-5 μM. At its optimal concentration, S1P was found to be more mitogenic than insulin and as mitogenic as epidermal growth factor (EGF). Additionally, the effects of S1P were synergistic when used in combination with either EGF or insulin, but not when used with sphingosine.

S1P and activation of S1P receptors can affect migration in a variety of cell types.[55,60,69,75,91,95,104,113,114] It is generally recognized that activation of $S1P_1$ and $S1P_3$ are pro-migratory, whereas activation of $S1P_2$ is anti-migratory. This differential response has been attributed to distinct signaling pathways that activate predominantly Rac or Rho.

1.7 Myocyte Electrophysiology

The waveform of the myocyte action potential (AP) is determined by the underlying ionic currents. Thus, myocytes from different anatomical locations (e.g. SAN, atrium, or ventricle, or within sub-regions of the ventricle) each has a characteristic shape to the action potential.[6,37,62,74] The studies presented in Chapter 5 involved ventricular

myocytes of the adult mouse. Therefore, this section will be limited to discussions regarding this cell type.

The AP is initiated when the membrane potential (which is approximately -80 mV in the resting state) becomes sufficiently depolarized to activate voltage-gated sodium channels. This results in a very strong and rapid inward I_{Na} (maximal at approximately -40 mV) which further depolarizes the myocyte. When the membrane potential reaches approximately -20 mV, voltage-gated calcium channels become activated.[5] Inward calcium entry through L-type calcium channels (also called dihydropyridine receptors) located along the T-tubules of the cell membrane (or sarcolemma) initiates a calcium amplification process termed calcium-induced calcium release (CICR). This process occurs when L-type calcium current (I_{CaL}) activates ryanodine receptors, located on the sarcoplasmic reticulum (SR) and in close proximity to the L-type calcium channels, to release large amounts of calcium from the SR. The increased intracellular calcium concentrations serve two purposes: (i) to initiate myofilament contraction, and (ii) to extend the plateau phase of the AP waveform.[3,4] This helps explain why the AP in ventricular myocytes is broader than that of atrial myocytes.

K^+ currents are also very important in the AP and are involved with nearly every phase of the AP waveform. The first K^+ current activated is the transient outward current (I_{to}) which helps control depolarization and overshoot. Repolarization is initiated by other outward K^+ currents, and K^+ current further help stabilize the resting membrane potential.[7]

A representation of a mouse ventricular AP is presented in Figure 1.4. This AP waveform was generated using a mathematical model of the adult mouse ventricular myocyte. As depicted, the action potential duration is approximately 40 ms.

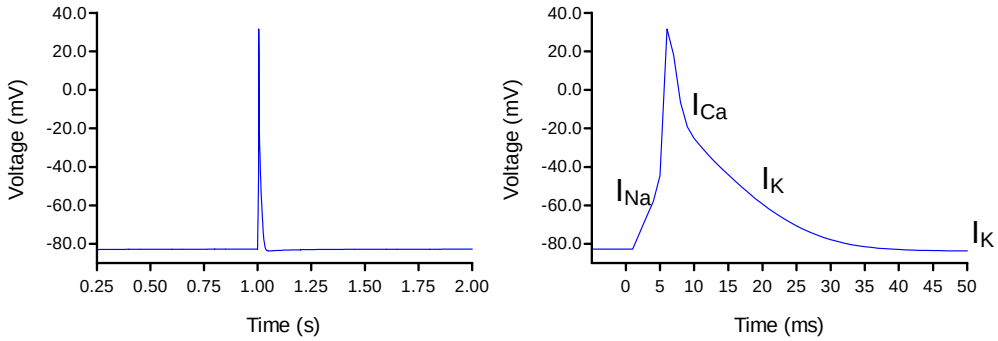

Figure 1.4 Simulated AP of the adult mouse ventricular myocyte using two time scales. Important ionic currents at the various phases are noted. This AP waveform was generated using the Bondarenko model.[5]

1.8 Cardiac Fibroblast Anatomical Location

Fibroblasts are found in virtually every organ and tissue. Within the heart, cardiac fibroblasts are found associated with myocytes and associated with the endoysial collagen weave network within the myocardium.[38] Although myocytes comprise the majority cell type based on cell mass, cardiac fibroblasts comprise the majority of non-myocyte cell type numbers. While their physiological role has been traditionally associated with extracellular matrix (ECM) deposition and wound repair, CFb are being increasingly recognized for their roles in electrophysiology and hormonal regulation.

Cardiac fibroblasts lie adjacent to myocytes and are found surrounding clusters of 2-5 myocytes, but are not found in-between myocyte clusters. Cardiac fibroblasts form junctions with other fibroblasts and myocytes via connexins (Cx). Connexins are the

structural subunits of gap junctions which allow intracellular communication between joined cells for the passage of ions and small molecules (e.g. cAMP). In ultrastructural immunohistological surveys of myocardium, Cx43 was found between adjacent fibroblasts and on the lateral margins of intercalated disks where fibroblast-myocyte contact was noted. Intracellular junctions between fibroblasts themselves occurs primarily via Cx45.[38] This provides physical evidence for potential of fibroblast-myocyte electrical coupling.

1.9 Cardiac Fibroblast Electrophysiology

Kamkin and Kiseleva[48-52,57,58,61] published some of the first electrophysiological data on cardiac fibroblasts. They showed that these cells express Ca^{++}- and stretch-activated ion channels. Other types of fibroblasts have been demonstrated to express a variety of ion channels. Dermal fibroblasts have been shown to have Kv, K_{Ca}, inwardly-rectifying K^+ (Kir), Na^+, and osmotically activated Cl^- currents.[21] Furthermore, studies of patch- clamped, rat ventricular cardiac fibroblasts (and myofibroblasts)[13] demonstrated that nearly all of these cells express I_{Kv} (with Kv1.6 showing the strongest expression by PCR), and most also express a Ba^{++}-sensitive strongly inwardly rectifying background K^+ current (I_{Kir}, with Kir2.1 and Kir6.1 showing the strongest expressions by PCR).

1.10 Cardiac Fibroblast and Myocyte Coupling

Though non-excitable themselves, cardiac fibroblasts play important roles in cardiomyocyte electrophysiology. Cardiac fibroblasts are known to have very high

membrane resistances (in the GΩ range[49]) and may thus act as insulators to decrease conduction and propagation velocities.[127] Thus, they are speculated at contributing to larger delays and arrhythmias in fibrotic myocardium. This has been confirmed in vitro, whereby cardiac fibroblasts can delay propagation between 11-68 msec if inserted experimentally between cardiomyocytes.[35] If experimentally transfected with the voltage-sensitive K^+ channel, Kv1.3, cardiac fibroblasts can electrically couple with cardiomyocytes; however, these transfected cells still caused alterations in electrical conduction.[24]

The electrotonic interactions between myocytes and fibroblasts have also been investigated through mathematical modeling.[76] When *in silico* cardiac fibroblasts were electrically coupled to a single *in silico* myocyte, action potential duration was significantly shortened. This effect was enhanced as the number of fibroblasts increased.

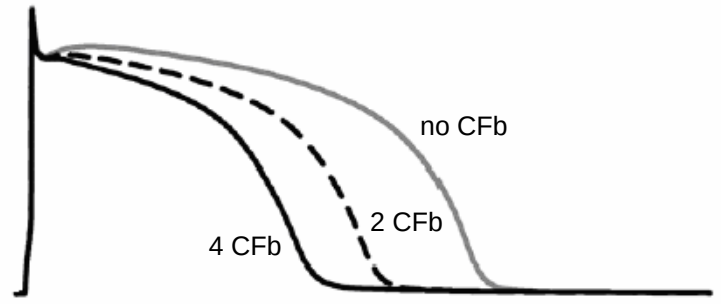

Figure 1.5 Mathematical modeling of cardiac fibroblast coupling on myocyte action potential duration. Modified from MacCannell and Giles (2007).[76]

1.11 Cardiac Fibroblast Identification and Characterization

Part of the difficulty of identifying fibroblasts is the lack of consensus on what exactly a fibroblast is and from where they originate. Cardiac fibroblasts are believed to

be derived from bone marrow-derived mesoangioblasts, a progenitor common to endothelial cells and fibroblasts. It has also been demonstrated in avian development that cardiac fibroblasts derive from the epicardium during coronary morphogenesis via mesenchymal transformation.[19] Lastly, circulating fibroblast precursors (fibrocytes) that originate within bone marrow have been described as well, although these may be involved more during wound repair and regeneration rather than during development.[8]

Identification of fibroblasts is often by phenotype, production of ECM proteins, or by positive immunolabeling to various cytoskeletal proteins. Adding to this difficulty are that fibroblasts may differ regionally or anatomically, may be under various stages of differentiation, and can vary in phenotype from species to species. For example, human fibroblasts are more spindle-shaped at confluence, whereas mouse fibroblasts have a pavement-like appearance.[30]

One marker that has been proposed to be expressed in all fibroblasts[45] is fibroblast specific protein 1 (FSP1), a class S100 calcium-binding protein, that also appears to have involvement with migration.[90] In tissues, strong expression of FSP1 was found in lung and spleen, weak expression in kidney, muscle, and heart and undetectable expression in brain and liver. However, this marker can be upregulated in epithelial cells subjected to persistent chemical exposure to TGFβ, EGF, or bFGF, making it seem less fibroblast specific.

Using a green fluorescent protein (GFP)-tagged FSP1 promoter, Iwano, et al.[45] described the epithelial-mesenchymal transition (EMT) of kidney epithelial cells to fibroblasts based on the expression of FSP1, the ability of these cells to produce matrix

metalloprotease (MMP)-2, vimentin, collagen type I and αSMactin, and a change in cell morphology resembling stromal cells. However, presence of FSP1 and collagen type I or αSMactin are not co-indicated for all fibroblast populations.[89] Additional studies using alveolar epithelial cells have shown the ability of these cells to acquire fibroblast-like characteristics under selective culture conditions.[125] Finally, transdifferentiation has been reported for SMC in which these cells were noted to demonstrate a macrophage-like phenotype following cholesterol loading.[101]

Immunolabeling against vimentin, collagen type I or smooth muscle actin alpha (αSMactin) are not necessarily suitable fibroblast markers[89] as these proteins can also be expressed in a number of other cell types including SMC and macrophages.[46,85]

Recently, a cell surface receptor has been described that reportedly can identify cardiac fibroblasts within developing and adult myocardial tissue.[38,86] Discoidin domain receptor 2 (DDR2) is a non-integrin tyrosine kinase receptor that is activated (autophosphorylated) by fibrillar (triple-helical structure) collagen, primarily types I and III,[92,106,120] and is distinct from collagen-binding integrins.[119] DDR2 is present in 11.5-20 day-old embryos, neonatal rat hearts, and also in adult rat hearts. DDR2 has been used as a cardiac fibroblast marker due to its association with the collagen matrix[38] and reported absence (by Western blotting) in SMC, EC, or myocytes. Goldsmith et al.[38] further propose that DDR2 might be involved in collagen remodeling of the heart.

The activation kinetics of DDR2 are very slow[25,92,120] compared to other tyrosine kinase receptors, but it has been shown to be involved in fibroblast proliferation,

migration and differentiation. DDR2 activation by fibrillar collagen upregulates MMP-1,[120] and MMP-2 promoter activity in dermal fibroblasts requires DDR2 activation.[92]

DDR2 has been shown to be associated with pathologies of fibroblasts and SMC. DDR2-deficient mice exhibit dwarfism by long-bone shortening, and skin fibroblasts isolated from these mice have impaired proliferation abilities.[67] In hepatic stellate cells (liver fibroblasts), it has been suggested that DDR2 perpetuates a fibrotic response by its slow activation/inactivation kinetics, MMP-1 upregulation and autocrine regulation.[92] DDR2 has been found in atherosclerotic lesions and lymphangioleiomyomatosis (LAM). Whereas DDR2 message levels were not different in normal vs. atherosclerotic lesioned arteries, DDR2 was upregulated in LAM nodules.[25] SMC transfected to overexpress DDR2 were capable of higher MMP-1 levels, more pronounced collagen and elastin degradation, and less collagen production.[25]

DDR2 is related to another discoidin domain receptor, DDR1. Like DDR2, DDR1 is involved in cell attachment, migration and proliferation also; however, its ligands are collagens[120] such as those found in basement membrane (e.g. collagen type IV). And, while there are five alternative splicing isoforms (a-e) of DDR1, no isoforms have been reported for DDR2. DDR1 is constituitively expressed in epithelial cells and is upregulated in leukocytes (neutrophils, monocytes, Mϕ, and lymphocytes) upon activation.[53] DDR1 can also be found in fibroblasts.[14]

1.12 Cardiac Myofibroblast Phenotype

When fibroblasts shift to an ECM-synthesizing phenotype, they are termed myofibroblasts. This transdifferentiation is regulated by a complex mix of environmental and regulatory factors. The term myofibroblast can mean many things to many people, depending on their area of training and organ system of interest. However, one useful definition is that of a cell which: expresses vimentin and smooth muscle alpha actin (SM α-actin); contains abundant rough endoplasmic reticulum, a Golgi apparatus, and collagen secretion granules; exhibits peripheral myofilaments with focal densities (stress fibers) and fibronexus junctions; and expresses gap junctions and other actin-associated nondesmosomal junctions.[23]

Myofibroblasts are generally characterized by expression of SM α-actin, stress fibers, and the embryonal isoform of myosin heavy chain,[23,23,28,98] although there is conflicting data on the presence of other SMC markers such as desmin and smooth muscle myosin heavy chains.[28] Regardless, it is through the expressed contractile proteins that the cells manifest wound contraction and scarification. During wound healing, resident CFb undergo differentiation to the myofibroblast phenotype which is largely responsible for the synthesis, secretion and remodeling of the ECM. Myofibroblasts are collagen-producing cells and appearance of SM α-actin has been positively correlated with collagen content.[98]

Inducers of myofibroblasts include mechanical stress[123] and transforming growth factor beta-1 (TGFβ-1), a pluripotent mitogen that can regulate collagenesis, increase stress fiber formation, increase atrial natriuretic peptide (ANP) levels, and induce

connective tissue growth factor (CTGF) in fibroblasts and myofibroblasts.[10,66,68,70,71,115,118] Myofibroblasts, in turn, secrete TGFβ-1 at basal levels greater than fibroblasts.[11] TGFβ-1 can further act in autocrine and paracine signaling pathways to regulate angiotensin II (Ang II) receptor (AT1) expression and membrane-bound angiotensin-converting enzyme (ACE). ACE regulates local concentrations of Ang II, which, in turn, modulates the expression of TGFβ-1.[54,97,124,124]

Several growth factor signaling pathways and their effects on cardiac fibroblasts are depicted in Figure 1.6.

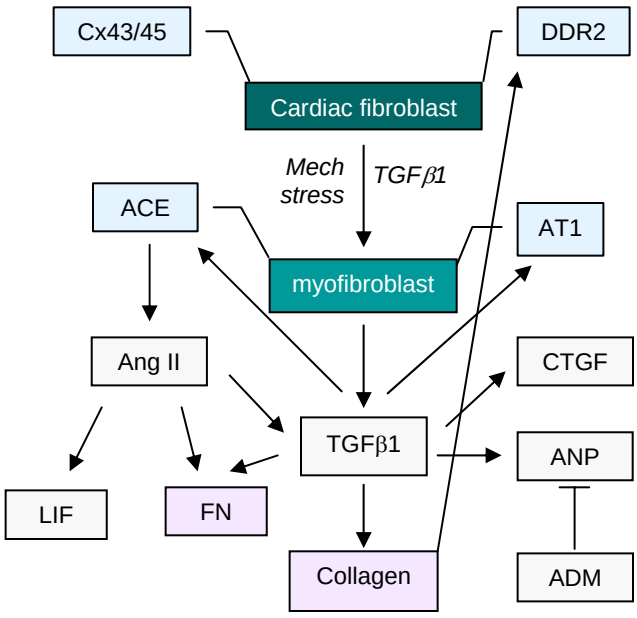

Figure 1.6 Molecules that can affect cardiac fibroblast and myofibroblast phenotype. Cell surface structures are shown in light blue. Extracellular matrix molecules are shown in pink.

1.13 Macrophages

Macrophages are resident cells within normal tissues and are primarily recognized for their role in phagocytosis of microbial and cellular debris. However, they secrete a number of factors that influence the wound healing and remodeling process. Macrophage activation (e.g. by bacterial lipopolysaccharide stimulation of toll-like receptors [TLR] on monocytes) induces tumor necrosis factor α (TNFα), granulocyte macrophage colony stimulating factor (GM-CSF), and adrenomedullin (AM) secretion. TNFα stimulates ceramide levels and can lead to cell apoptosis,[18,94,128] GM-CSF can serve as a recruiting and differentiation factor for additional macrophage,[26,64,96,121] and AM, in turn, can increase TNFα production.[65,96] Macrophages also contain ACE and can participate in TGFβ-1 pathways.

Macrophages increase uptake of oxidized low density lipoprotein (LDL) and acetylated-LDL when exposed to fibronectin (or RGD-containing peptides)[2] and collagen type I,[12] respectively, and this has been shown to play a potential role in arthleroma formation. Collagen can interact with macrophages through DDR1. DDR1 is expressed as monocytes differentiate to macrophages, and interaction of DDR1b with collagen can upregulate several factors including IL-8, macrophage inflammatory protein-1α, and MCP-1.[79]

Macrophages have been characterized by patch clamping techniques and been shown to have RMP of approximately -70 mV. They can be induced to have action potentials (AP) that are calcium-mediated and sodium-insensitive and display voltage-dependent inward and outward currents such as K_{Ca} and Kir.[33,81,126]

Macrophage-like cells have been reported to be strongly attached to myocytes of normal myocardium by scanning electron microscopic evaluation[87]. This association may be mediated by gap junction formation since macrophages have been shown to express Cx43 and can couple to each other[22,27]. Thus, direct cell contact, as well as cytokine and growth factor interactions, may contribute to macrophage interactions with the two major cell types (myocytes and cardiac fibroblasts) in the heart to alter physiological behavior.

1.14 Objectives

The objectives of the dissertation were to investigate the responses of S1P on cardiac fibroblast and myocyte phenotype and functional performance. Specifically, they were: (i) to determine whether S1P or other soluble factors can modulate the relative levels of S1P receptors expressed on cardiac fibroblasts, (ii) to determine how S1P can alter the electrophysiology of resting cardiac fibroblasts, and (iii) to determine the signaling pathway(s) responsible for the negative inotropic effects observed in myocytes after exposure to S1P. The findings from these studies should enhance the overall understanding of fibroblast and myocyte responses in physiological or pathophysiological situations where S1P levels may be elevated.

1.15 References

1. Baudhuin,L.M. *et al.* $S1P_3$-mediated Akt activation and cross-talk with platelet-derived growth factor receptor (PDGFR). *FASEB J.* 18, 341-343 (2004).

2. Beppu,M., Hora,M., Watanabe,M. & Kikugawa,K. Binding and uptake of oxidized low density lipoprotein (LDL) by macrophage scavenger receptors are enhanced by substrate-bound fibronectin. *Biol. Pharm. Bull.* 18, 802-809 (1995).

3. Bers,D.M. Cardiac excitation-contraction coupling. *Nature.* 415, 198-205 (2002).

4. Bers,D.M. & Guo,T. Calcium signaling in cardiac ventricular myocytes. *Ann. N. Y. Acad. Sci.* 1047:86-98., 86-98 (2005).

5. Bondarenko,V.E., Szigeti,G.P., Bett,G.C., Kim,S.J. & Rasmusson,R.L. Computer model of action potential of mouse ventricular myocytes. *Am. J. Physiol Heart Circ. Physiol* 287, H1378-H1403 (2004).

6. Boyett,M.R., Honjo,H. & Kodama,I. The sinoatrial node, a heterogeneous pacemaker structure. *Cardiovasc. Res.* 47, 658-687 (2000).

7. Brouillette,J., Clark,R.B., Giles,W.R. & Fiset,C. Functional properties of K^+ currents in adult mouse ventricular myocytes. *J. Physiol* 559, 777-798 (2004).

8. Bucala,R., Spiegel,L.A., Chesney,J., Hogan,M. & Cerami,A. Circulating fibrocytes define a new leukocyte subpopulation that mediates tissue repair. *Mol. Med.* 1, 71-81 (1994).

9. Bunemann,M. *et al.* Activation of muscarinic K^+ current in guinea-pig atrial myocytes by sphingosine-1-phosphate. *Journal of Physiology* 489, 701-707 (1995).

10. Cameron,V.A. *et al.* Atrial (ANP) and brain natriuretic peptide (BNP) expression after myocardial infarction in sheep: ANP is synthesized by fibroblasts infiltrating the infarct. *Endocrinology* 141, 4690-4697 (2000).

11. Campbell,S.E. & Katwa,L.C. Angiotensin II stimulated expression of transforming growth factor-beta1 in cardiac fibroblasts and myofibroblasts. *J. Mol. Cell Cardiol.* 29, 1947-1958 (1997).

12. Chen,Q., Wei,E., Chen,X., Wang,N. & Jurgens,G. Interactions between macrophages and oxidized low density lipoprotein in the presence of type I collagen. *Biofactors* 6, 131-138 (1997).

13. Chilton,L. *et al.* K^+ currents regulate the resting membrane potential, proliferation, and contractile responses in ventricular fibroblasts and myofibroblasts. *Am. J. Physiol Heart Circ. Physiol* 288, H2931-H2939 (2005).

14. Chin,G.S. *et al.* Cellular signaling by tyrosine phosphorylation in keloid and normal human dermal fibroblasts. *Plast. Reconstr. Surg.* 106, 1532-1540 (2000).

15. Chun,J. *et al.* International Union of Pharmacology. XXXIV. Lysophospholipid receptor nomenclature. *Pharmacol. Rev.* 54, 265-269 (2002).

16. Coussin,F., Scott,R.H., Wise,A. & Nixon,G.F. Comparison of sphingosine 1-phosphate-induced intracellular signaling pathways in vascular smooth muscles: differential role in vasoconstriction. *Circ Res.* 91, 151-157 (2002).

17. Curfman,C. & Liotta,D. Synthesis of sphingosine and sphingoid bases. *Methods Enzymol.* 311:391-440., 391-440 (2000).

18. Cuvillier,O. *et al.* Suppression of ceramide-mediated programmed cell death by sphingosine-1-phosphate. *Nature* 381, 800-803 (1996).

19. Dettman,R.W., Denetclaw,W., Jr., Ordahl,C.P. & Bristow,J. Common epicardial origin of coronary vascular smooth muscle, perivascular fibroblasts, and intermyocardial fibroblasts in the avian heart. *Dev. Biol.* 193, 169-181 (1998).

20. Edsall,L.C. & Spiegel,S. Enzymatic measurement of sphingosine 1-phosphate. *Anal. Biochem.* 272, 80-86 (1999).

21. Estacion,M. Characterization of ion channels seen in subconfluent human dermal fibroblasts. *J. Physiol* 436:579-601., 579-601 (1991).

22. Eugenin,E.A., Branes,M.C., Berman,J.W. & Saez,J.C. TNF-alpha plus IFN-gamma induce connexin43 expression and formation of gap junctions between human monocytes/macrophages that enhance physiological responses. *J. Immunol.* 170, 1320-1328 (2003).

23. Eyden,B. The myofibroblast: an assessment of controversial issues and a definition useful in diagnosis and research. *Ultrastruct. Pathol.* 25, 39-50 (2001).

24. Feld,Y. *et al.* Electrophysiological modulation of cardiomyocytic tissue by transfected fibroblasts expressing potassium channels: a novel strategy to manipulate excitability. *Circulation* 105, 522-529 (2002).

25. Ferri,N., Carragher,N.O. & Raines,E.W. Role of discoidin domain receptors 1 and 2 in human smooth muscle cell-mediated collagen remodeling: potential implications in atherosclerosis and lymphangioleiomyomatosis. *Am. J. Pathol.* 164, 1575-1585 (2004).

26. Fitzgerald,S.M. *et al.* GM-CSF induction in human lung fibroblasts by IL-1beta, TNF-alpha, and macrophage contact. *J. Interferon Cytokine Res.* 23, 57-65 (2003).

27. Fortes,F.S. *et al.* Modulation of intercellular communication in macrophages: possible interactions between GAP junctions and P2 receptors. *J. Cell Sci.* 117, 4717-4726 (2004).

28. Frangogiannis,N.G., Michael,L.H. & Entman,M.L. Myofibroblasts in reperfused myocardial infarcts express the embryonic form of smooth muscle myosin heavy chain (SMemb). *Cardiovasc. Res.* 48, 89-100 (2000).

29. Freissmuth,M., Waldhoer,M., Bofill-Cardona,E. & Nanoff,C. G protein antagonists. *Trends Pharmacol. Sci.* 20, 237-245 (1999).

30. Freshney,R.I. Culture of animal cells. Wiley-Liss, New York (2005).

31. Fukushima,N., Ishii,I., Contos,J.J., Weiner,J.A. & Chun,J. Lysophospholipid receptors. *Annu. Rev. Pharmacol. Toxicol.* 41:507-34., 507-534 (2001).

32. Futerman,A.H. & Hannun,Y.A. The complex life of simple sphingolipids. *Eur. Mol. Biol. Organization* 5, 777-782 (2004).

33. Gallin,E.K. Electrophysiological properties of macrophages. *Fed. Proc.* 43, 2385-2389 (1984).

34. Garcia,J.G.N. *et al.* Sphingosine 1-phosphate promotes endothelial cell barrier integrity by Edg-dependent cytoskeletal rearrangement. *Journal of Clinical Investigation* 108, 689 (2001).

35. Gaudesius,G., Miragoli,M., Thomas,S.P. & Rohr,S. Coupling of cardiac electrical activity over extended distances by fibroblasts of cardiac origin. *Circ. Res.* 93, 421-428 (2003).

36. Ghosh,T.K., Bian,J. & Gill,D.L. Intracellular calcium release mediated by sphingosine derivatives generated in cells. *Science* 248, 1653-1656 (1990).

37. Giles,W.R. & Imaizumi,Y. Comparison of potassium currents in rabbit atrial and ventricular cells. *J. Physiol* 405:123-45., 123-145 (1988).

38. Goldsmith,E.C. *et al.* Organization of fibroblasts in the heart. *Dev. Dyn.* 230, 787-794 (2004).

39. Guo,J., MacDonell,K.L. & Giles,W.R. Effects of sphingosine 1-phosphate on pacemaker activity in rabbit sino-atrial node cells. *Pflugers Arch.* 438, 642-648 (1999).

40. Himmel,H.M., Pietsch,M., Streller,U., Graf,E.M. & Ravens,U. Changes in morphology and inward rectifier currents in human atrial myocytes depend on culture conditions. *Basic Res. Cardiol.* 97, 434-444 (2002).

41. Hornuss,C., Hammermann,R., Fuhrmann,M., Juergens,U.R. & Racke,K. Human and rat alveolar macrophages express multiple EDG receptors. *Eur. J. Pharmacol.* 19;429, 303-308 (2001).

42. Igarashi,Y. & Yatomi,Y. Sphingosine 1-phosphate is a blood constituent released from activated platelets, possibly playing a variety of physiological and pathophysiological roles. *Acta Biochim. Pol.* 45, 299-309 (1998).

43. Ishii,I. *et al.* Selective loss of sphingosine 1-phosphate signaling with no obvious phenotypic abnormality in mice lacking its G protein-coupled receptor, LP(B3)/EDG-3. *J. Biol. Chem.* 276, 33697-33704 (2001).

44. Ishii,I. *et al.* Marked perinatal lethality and cellular signaling deficits in mice null for the two sphingosine 1-phosphate (S1P) receptors, S1P(2)/LP(B2)/EDG-5 and S1P(3)/LP(B3)/EDG-3. *J. Biol. Chem.* 277, 25152-25159 (2002).

45. Iwano,M. *et al.* Evidence that fibroblasts derive from epithelium during tissue fibrosis. *J. Clin. Invest* 110, 341-350 (2002).

46. Jabs,A., Moncada,G.A., Nichols,C.E., Waller,E.K. & Wilcox,J.N. Peripheral blood mononuclear cells acquire myofibroblast characteristics in granulation tissue. *J. Vasc. Res.* 42, 174-180 (2005).

47. Jiang,X. & Han,X. Characterization and direct quantitation of sphingoid base-1-phosphates from lipid extracts: a shotgun lipidomics approach. *J. Lipid Res.* 47, 1865-1873 (2006).

48. Kamkin,A. *et al.* Cardiac fibroblasts and the mechano-electric feedback mechanism in healthy and diseased hearts. *Prog. Biophys. Mol. Biol.* 82, 111-120 (2003).

49. Kamkin,A. *et al.* Mechanically induced potentials in fibroblasts from human right atrium. *Exp. Physiol* 84, 347-356 (1999).

50. Kamkin,A. *et al.* Mechanically induced potentials in atrial fibroblasts from rat hearts are sensitive to hypoxia/reoxygenation. *Pflugers Arch.* 446, 169-174 (2003).

51. Kamkin,A. *et al.* A possible role for atrial fibroblasts in postinfarction bradycardia. *Am. J. Physiol Heart Circ. Physiol* 282, H842-H849 (2002).

52. Kamkin,A.G. & Kiseleva,I.S. Heart fibroblasts, the mechanism of the appearance of their potentials and their possible role in regulating cardiac work. *Usp. Fiziol. Nauk* 29, 72-102 (1998).

53. Kamohara,H., Yamashiro,S., Galligan,C. & Yoshimura,T. Discoidin domain receptor 1 isoform-a (DDR1alpha) promotes migration of leukocytes in three-dimensional collagen lattices. *FASEB J.* 15, 2724-2726 (2001).

54. Katoh,M. *et al.* Cardiac angiotensin II receptors are upregulated by long-term inhibition of nitric oxide synthesis in rats. *Circ. Res.* 83, 743-751 (1998).

55. Kimura,T. *et al.* Sphingosine 1-phosphate stimulates proliferation and migration of human endothelial cells possibly through the lipid receptors, Edg-1 and Edg-3. *Biochemical Journal* 348, 71-76 (2000).

56. Kindman,L.A., Kim,S., McDonald,T.V. & Gardner,P. Characterization of a novel intracellular sphingolipid-gated Ca^{2+}- permeable channel from rat basophilic leukemia cells. *J Biol. Chem.* 269, 13088-13091 (1994).

57. Kiseleva,I., Kamkin,A., Kohl,P. & Lab,M.J. Calcium and mechanically induced potentials in fibroblasts of rat atrium. *Cardiovasc. Res.* 32, 98-111 (1996).

58. Kiseleva,I. *et al.* Electrophysiological properties of mechanosensitive atrial fibroblasts from chronic infarcted rat heart. *J. Mol. Cell Cardiol.* 30, 1083-1093 (1998).

59. Kiss,Z., Crilly,K.S. & Anderson,W.H. Extracellular sphingosine 1-phosphate stimulates formation of ethanolamine from phosphatidylethanolamine: modulation of sphingosine 1-phosphate-induced mitogenesis by ethanolamine. *Biochem. J.* 328, 383-391 (1997).

60. Kluk,M.J. & Hla,T. Role of the sphingosine 1-phosphate receptor EDG-1 in vascular smooth muscle cell proliferation and migration. *Circulation Research* 89, 496-502 (2001).

61. Kohl,P., Kamkin,A.G., Kiseleva,I.S. & Noble,D. Mechanosensitive fibroblasts in the sino-atrial node region of rat heart: interaction with cardiomyocytes and possible role. *Exp. Physiol* 79, 943-956 (1994).

62. Kondo,R.P. *et al.* Comparison of contraction and calcium handling between right and left ventricular myocytes from adult mouse heart: a role for repolarization waveform. *J. Physiol.* 571, 131-146 (2006).

63. Kono,M. *et al.* The sphingosine-1-phosphate receptors $S1P_1$, $S1P_2$, and $S1P_3$ function coordinately during embryonic angiogenesis. *J. Biol. Chem.* 279, 29367-29373 (2004).

64. Krutzik,S.R. *et al.* TLR activation triggers the rapid differentiation of monocytes into macrophages and dendritic cells. *Nat. Med.* 11, 653-660 (2005).

65. Kubo,A. *et al.* Production of adrenomedullin in macrophage cell line and peritoneal macrophage. *J. Biol. Chem.* 273, 16730-16738 (1998).

66. Kunz-Schughart,L.A., Wenninger,S., Neumeier,T., Seidl,P. & Knuechel,R. Three-dimensional tissue structure affects sensitivity of fibroblasts to TGF-beta 1. *Am. J. Physiol Cell Physiol* 284, C209-C219 (2003).

67. Labrador,J.P. *et al.* The collagen receptor DDR2 regulates proliferation and its elimination leads to dwarfism. *EMBO Rep.* 2, 446-452 (2001).

68. Leask,A., Holmes,A. & Abraham,D.J. Connective tissue growth factor: a new and important player in the pathogenesis of fibrosis. *Curr. Rheumatol. Rep.* 4, 136-142 (2002).

69. Lepley,D., Paik,J.H., Hla,T. & Ferrer,F. The G protein-coupled receptor $S1P_2$ regulates Rho/Rho kinase pathway to inhibit tumor cell migration. *Cancer Res.* 65, 3788-3795 (2005).

70. Lijnen,P., Petrov,V. & Fagard,R. Transforming growth factor-beta 1-mediated collagen gel contraction by cardiac fibroblasts. *J. Renin. Angiotensin. Aldosterone. Syst.* 4, 113-118 (2003).

71. Lijnen,P., Petrov,V., Rumilla,K. & Fagard,R. Transforming growth factor-beta 1 promotes contraction of collagen gel by cardiac fibroblasts through their differentiation into Myofibroblasts. *Methods Find. Exp. Clin. Pharmacol.* 25, 79-86 (2003).

72. Liliom,K. *et al.* Sphingosylphosphocholine is a naturally occurring lipid mediator in blood plasma: a possible role in regulating cardiac function via sphingolipid receptors. *Biochem. J.* 355, 189-197 (2001).

73. Liu,Y. *et al.* Edg-1, the G protein-coupled receptor for sphingosine-1-phosphate, is essential for vascular maturation. *J. Clin. Invest* 106, 951-961 (2000).

74. Lomax,A.E., Kondo,C.S. & Giles,W.R. Comparison of time- and voltage-dependent K^+ currents in myocytes from left and right atria of adult mice. *Am. J. Physiol Heart Circ. Physiol* 285, H1837-H1848 (2003).

75. Long,J.S., Natarajan,V., Tigyi,G., Pyne,S. & Pyne,N.J. The functional PDGFbeta receptor-$S1P_1$ receptor signaling complex is involved in regulating migration of mouse embryonic fibroblasts in response to platelet derived growth factor. *Prostaglandins Other Lipid Mediat.* 80, 74-80 (2006).

76. MacCannell,K.A. *et al.* A Mathematical Model of Electrotonic Interactions between Ventricular Myocytes and Fibroblasts. *Biophys. J.* in press, (2007).

77. MacDonell,K.L., Severson,D.L. & Giles,W.R. Depression of excitability by sphingosine-1-phosphate in rat ventricular myocytes. *American Journal of Physiology* 275, H2291-H2299 (1998).

78. Martino,A. *et al.* Sphingosine 1-Phosphate Interferes on the Differentiation of Human Monocytes into Competent Dendritic Cells. *Scand. J. Immunol.* 65, 84-91 (2007).

79. Matsuyama,W., Wang,L., Farrar,W.L., Faure,M. & Yoshimura,T. Activation of discoidin domain receptor 1 isoform b with collagen up-regulates chemokine production in human macrophages: role of p38 mitogen-activated protein kinase and NF-kappa B. *J. Immunol.* 172, 2332-2340 (2004).

80. Mazurais,D. *et al.* Cell type-specific localization of human cardiac S1P receptors. *J. Histochem. Cytochem.* 50, 661-670 (2002).

81. McCann,F.V., Cole,J.J., Guyre,P.M. & Russell,J.A. Action potentials in macrophages derived from human monocytes. *Science* 219, 991-993 (1983).

82. Merrill,A.H.J. & Sweeley,C.C. Biochemistry of Lipids, Lipoproteins and Membranes. Vance,D.E. & Vance,J.E. (eds.), pp. 309-339 (Elsevier Science B.V., Amsterdam,1996).

83. Meyer zu,H.D. Lysophospholipid receptor-dependent and -independent calcium signaling. *J. Cell Biochem.* 92, 937-948 (2004).

84. Meyer zu,H.D., Himmel,H.M. & Jakobs,K.H. Sphingosylphosphorylcholine-biological functions and mechanisms of action. *Biochim. Biophys. Acta* 1582, 178-189 (2002).

85. Mor-Vaknin,N., Punturieri,A., Sitwala,K. & Markovitz,D.M. Vimentin is secreted by activated macrophages. *Nat. Cell Biol.* 5, 59-63 (2003).

86. Morales,M.O., Price,R.L. & Goldsmith,E.C. Expression of discoidin domain receptor 2 (DDR2) in the developing heart. *Microsc. Microanal.* 11, 260-267 (2005).

87. Nag,A.C. Study of non-muscle cells of the adult mammalian heart: a fine structural analysis and distribution. *Cytobios* 28, 41-61 (1980).

88. Ochi,R., Momose,Y., Oyama,K. & Giles,W.R. Sphingosine-1-phosphate effects on guinea pig atrial myocytes: Alterations in action potentials and K^+ currents. *Cardiovasc. Res.* 70, 88-96 (2006).

89. Okada,H. *et al.* Progressive renal fibrosis in murine polycystic kidney disease: an immunohistochemical observation. *Kidney Int.* 58, 587-597 (2000).

90. Okada,H., Danoff,T.M., Kalluri,R. & Neilson,E.G. Early role of Fsp1 in epithelial-mesenchymal transformation. *Am. J. Physiol* 273, F563-F574 (1997).

91. Okamoto,H. *et al.* Inhibitory regulation of Rac activation, membrane ruffling, and cell migration by the G protein-coupled sphingosine-1-phosphate receptor EDG5 but not EDG1 or EDG3. *Mol. Cell Biol.* 20, 9247-9261 (2000).

92. Olaso,E. *et al.* DDR2 receptor promotes MMP-2-mediated proliferation and invasion by hepatic stellate cells. *J. Clin. Invest* 108, 1369-1378 (2001).

93. Olivera,A. & Spiegel,S. Sphingosine-1-phosphate as second messenger in cell proliferation induced by PDGF and FCS mitogens. *Nature* 365, 557-560 (1993).

94. Osawa,Y. *et al.* Roles for C16-ceramide and sphingosine 1-phosphate in regulating hepatocyte apoptosis in response to tumor necrosis factor-alpha. *J. Biol. Chem.* 280, 27879-27887 (2005).

95. Paik,J.H., Chae,S.-S., Lee,M.-J., Thangada,S. & Hla,T. Sphingosine 1-phosphate-induced endothelial cell migration requires the expression of EDG-1 and EDG-3 receptors and Rho-dependent activation of αvβb and β1 containing integrins. *Journal of Biological Chemistry* 276, 11830-11837 (2001).

96. Paine,R., III *et al.* Impaired functional activity of alveolar macrophages from GM-CSF-deficient mice. *Am. J. Physiol Lung Cell Mol. Physiol* 281, L1210-L1218 (2001).

97. Petrov,V.V., Fagard,R.H. & Lijnen,P.J. Transforming growth factor-beta(1) induces angiotensin-converting enzyme synthesis in rat cardiac fibroblasts during their differentiation to myofibroblasts. *J. Renin. Angiotensin. Aldosterone. Syst.* 1, 342-352 (2000).

98. Petrova,R. *et al.* Advanced glycation endproduct-induced calcium handling impairment in mouse cardiac myocytes. *J. Mol. Cell Cardiol.* 34, 1425-1431 (2002).

99. Pyne,S. & Pyne,N.J. Sphingosine 1-phosphate signalling in mammalian cells. *Biochem. J.* 349, 385-402 (2000).

100. Repp,H., Birringer,J., Koschinski,A. & Dreyer,F. Activation of a Ca^{2+}-dependent K^+ current in mouse fibroblasts by sphingosine-1-phosphate involves the protein tyrosine kinase c-Src. *Naunyn Schmiedebergs Arch. Pharmacol.* 363, 295-301 (2001).

101. Rong,J.X., Shapiro,M., Trogan,E. & Fisher,E.A. Transdifferentiation of mouse aortic smooth muscle cells to a macrophage-like state after cholesterol loading. *Proc. Natl. Acad. Sci. U. S. A* 100, 13531-13536 (2003).

102. Ronnov-Jessen,L., Villadsen,R., Edwards,J.C. & Petersen,O.W. Differential expression of a chloride intracellular channel gene, CLIC4, in transforming growth factor-beta1-mediated conversion of fibroblasts to myofibroblasts. *Am. J. Pathol.* 161, 471-480 (2002).

103. Rosen,H. & Liao,J. Sphingosine 1-phosphate pathway therapeutics: a lipid ligand-receptor paradigm. *Curr. Opin. Chem. Biol.* 7, 461-468 (2003).

104. Rosenfeldt,H.M. *et al.* EDG-1 links the PDGF receptor to Src and focal adhesion kinase activation leading to lamellipodia formation and cell migration. *FASEB J.* 15, 2649-2659 (2001).

105. Sanna,M.G. *et al.* Sphingosine 1-phosphate (S1P) receptor subtypes $S1P_1$ and $S1P_3$, respectively, regulate lymphocyte recirculation and heart rate. *J. Biol. Chem.* 279, 13839-13848 (2004).

106. Shrivastava,A. *et al.* An orphan receptor tyrosine kinase family whose members serve as nonintegrin collagen receptors. *Mol. Cell* 1, 25-34 (1997).

107. Snook,C.F., Jones,J.A. & Hannun,Y.A. Sphingolipid-binding proteins. *Biochim. Biophys. Acta.* 1761, 927-946 (2006).

108. Spiegel,S. & Milstien,S. Sphingosine 1-phosphate, a key cell signaling molecule. *J. Biol. Chem.* 19;277, 25851-25854 (2002).

109. Spiegel,S. & Milstien,S. Sphingosine-1-phosphate: an enigmatic signalling lipid. *Nat. Rev. Mol. Cell Biol.* 4, 397-407 (2003).

110. Sugiyama,A., Aye,N.N., Yatomi,Y., Ozaki,Y. & Hashimoto,K. Effects of sphingosine 1-phosphate, a naturally occurring biologically active lysophospholipid, on the rat cardiovascular system. *Jpn. J. Pharmacol.* 82, 338-342 (2000).

111. Sugiyama,A., Yatomi,Y., Ozaki,Y. & Hashimoto,K. Sphingosine 1-phosphate induces sinus tachycardia and coronary vasoconstriction in the canine heart. *Cardiovasc. Res.* 46, 119-125 (2000).

112. Taha,T.A., Argraves,K.M. & Obeid,L.M. Sphingosine-1-phosphate receptors: receptor specificity versus functional redundancy. *Biochim. Biophys. Acta* 1682, 48-55 (2004).

113. Takuwa,Y. Subtype-specific differential regulation of Rho family G proteins and cell migration by the Edg family sphingosine-1-phosphate receptors. *Biochim. Biophys. Acta.* 1582, 112-120 (2002).

114. Tamama,K. *et al.* Extracellular mechanism through the Edg family of receptors might be responsible for sphingosine-1-phosphate-induced regulation of DNA synthesis and migration of rat aortic smooth-muscle cells. *Biochem. J.* 353, 139-146 (2001).

115. Thibault,G. *et al.* Upregulation of alpha(8)beta(1)-integrin in cardiac fibroblast by angiotensin II and transforming growth factor-beta1. *Am. J. Physiol Cell Physiol* 281, C1457-C1467 (2001).

116. Uhlenbrock,K., Gassenhuber,H. & Kostenis,E. Sphingosine 1-phosphate is a ligand of the human gpr3, gpr6 and gpr12 family of constitutively active G protein-coupled receptors. *Cell Signal.* 14, 941-953 (2002).

117. van Koppen,C. *et al.* Activation of a high affinity Gi protein-coupled plasma membrane receptor by sphingosine-1-phosphate. *J. Biol. Chem.* 271, 2082-2087 (1996).

118. Vaughan,M.B., Howard,E.W. & Tomasek,J.J. Transforming growth factor-beta1 promotes the morphological and functional differentiation of the myofibroblast. *Exp. Cell Res.* 257, 180-189 (2000).

119. Vogel,W. *et al.* Discoidin domain receptor 1 is activated independently of beta(1) integrin. *J. Biol. Chem.* 275, 5779-5784 (2000).

120. Vogel,W., Gish,G.D., Alves,F. & Pawson,T. The discoidin domain receptor tyrosine kinases are activated by collagen. *Mol. Cell* 1, 13-23 (1997).

121. Vyalov,S., Desmouliere,A. & Gabbiani,G. GM-CSF-induced granulation tissue formation: relationships between macrophage and myofibroblast accumulation. *Virchows Arch. B Cell Pathol. Incl. Mol. Pathol.* 63, 231-239 (1993).

122. Wang,J., Carbone,L.D. & Watsky,M.A. Receptor-mediated activation of a Cl^- current by LPA and S1P in cultured corneal keratocytes. *Invest Ophthalmol. Vis. Sci.* 43, 3202-3208 (2002).

123. Wang,J., Chen,H., Seth,A. & McCulloch,C.A. Mechanical force regulation of myofibroblast differentiation in cardiac fibroblasts. *Am. J. Physiol Heart Circ. Physiol* 285, H1871-H1881 (2003).

124. Weber,K.T. & Sun,Y. Recruitable ACE and tissue repair in the infarcted heart. *J. Renin. Angiotensin. Aldosterone. Syst.* 1, 295-303 (2000).

125. Willis,B.C. *et al.* Induction of epithelial-mesenchymal transition in alveolar epithelial cells by transforming growth factor-beta1: potential role in idiopathic pulmonary fibrosis. *Am. J. Pathol.* 166, 1321-1332 (2005).

126. Woehlck,H.J. & McCann,F.V. Action potentials in human macrophages are calcium spikes. *Cell Biol. Int. Rep.* 10, 517-525 (1986).

127. Wolk,R., Cobbe,S.M., Hicks,M.N. & Kane,K.A. Functional, structural, and dynamic basis of electrical heterogeneity in healthy and diseased cardiac muscle: implications for arrhythmogenesis and anti-arrhythmic drug therapy. *Pharmacol. Ther.* 84, 207-231 (1999).

128. Xia,P., Wang,L., Gamble,J.R. & Vadas,M.A. Activation of sphingosine kinase by tumor necrosis factor-alpha inhibits apoptosis in human endothelial cells. *J. Biol. Chem.* 274, 34499-34505 (1999).

129. Yang,A.H., Ishii,I. & Chun,J. In vivo roles of lysophospholipid receptors revealed by gene targeting studies in mice. *Biochim. Biophys. Acta* 1582, 197-203 (2002).

130. Yatomi,Y., Ruan,F., Hakomori,S. & Igarashi,Y. Sphingosine-1-phosphate: a platelet-activating sphingolipid released from agonist-stimulated human platelets. *Blood* 86, 193-202 (1995).

131. Yin,Z. & Watsky,M.A. Chloride channel activity in human lung fibroblasts and myofibroblasts. *Am. J. Physiol Lung Cell Mol. Physiol.* 288, L1110-L1116 (2005).

132. Zhang,H. *et al.* Sphingosine-1-phosphate, a novel lipid, involved in cellular proliferation. *J. Cell Biol.* 114, 155-167 (1991).

CHAPTER 2

PURIFICATION OF CARDIAC FIBROBLAST CULTURES

2.1 Abstract

Cardiac fibroblasts (CFb) are essential components of myocardial tissue and study of their cell signaling and physiology is required for a number of emerging disciplines. Meaningful studies of CFb, however, necessitate methods for selective, reproducible cell isolations. CFb culture purity is commonly based on an absence of endothelial markers and positive immunoreactivity to cytoskeletal proteins vimentin and smooth muscle α-actin. Macrophages (MΦ) also reside within normal cardiac tissues and often co-isolate with CFb. Furthermore, MΦ can express cytoskeletal proteins used to identify CFb, as well as other common cell surface receptors. We therefore investigated whether MΦ may be present in CFb cultures.

The objectives of this study were to (i) characterize MΦ levels in CFb cultures from adult mouse and rat hearts, (ii) identify markers that can aid in differentiating cell type, and (iii) develop methods for improving CFb culture purity. Our results indicate that MΦ may comprise up to 10% of non-myocytes in primary digested myocardium and that MΦ can still be detected in cultures after several weeks. A protocol was developed that significantly reduces MΦ levels using a pre-plating step in cold cation-chelating buffer, followed by magnetic antibody cell sorting. We further show that MΦ can co-migrate with CFb, and show that co-culture with MΦ can alter expression levels of sphingosine-1-phosphate cell surface receptors. MΦ may therefore interfere with the

interpretation of CFb studies. These results highlight the importance of better characterization of CFb cultures and provide a means for improved cell purity.

2.2 Introduction

Consistently obtaining highly purified cell cultures, which do not include any significant contaminating cell types, remains a considerable challenge when working with primary isolates from organs and tissues. However, this initial step is a requirement for many current molecular and cellular physiology studies in the cardiovascular system. Examples include: (i) receptor characterization/signaling studies, where receptors may be common among various cell types; (ii) cytokine and growth factor studies, where contaminating cell types might secrete stimulatory or inhibitory factors, thus affecting the targeted cell population; or (iii) electrophyisiological studies from cell populations, where cell coupling through gap junctions could complicate the interpretation of underlying ion-channel-based mechanisms.

Mammalian cardiac tissue consists of a number of different cell types. Although myocardium is mainly composed of myocytes (approximately 50%), in terms of cell mass, non-myocytes comprise the majority (65-70%) of cells within the ventricle. These non-myocytes include endothelial cells, pericytes, smooth muscle cells, and cardiac fibroblasts (CFb).[94] In the mammalian myocardium, non-myocytes also provide essential functions. For example, CFb, which constitute the significant majority non-myocyte cell type, secrete and maintain the interstitial collagen (collagen types I and III).[33] The collagen matrix helps to anchor and align myocytes. CFb also secrete a variety of cytokines and growth factors that can have autocrine and paracrine effects. In both

ventricles, CFb are found interspersed between myofibers and are attached to the ECM, to myocytes, and to other CFb.[51,94] In addition, cells with specialized for immunological roles (e.g. macrophages [MΦ] and dendritic cells) are present in the myocardium, as well as within the circulatory system (e.g. monocytes, neutrophils, and lymphocytes).[33,51,94]

Many assessments of CFb culture purity[1,18,66,129,131] maintain that they are at least 95% pure. Rarely is quantitative data provided. Instead this determination is usually based on several commonly used cell markers, including positive immunostaining for vimentin (or α smooth muscle actin [SMactin] for myofibroblasts [myoFb]) and negative staining for endothelial cells.

The literature is limited regarding the presence of MΦ in cardiac cultures. This is surprising since MΦ are noted as normal resident cells within tissues and organs and can readily differentiate from circulating peripheral blood monocytes.[7,10,73,90] In the heart, MΦ are found within the pericardial sac and are interspersed within the myocardium, where they are closely associated with myocytes and CFb.[94] On this basis, it is expected that MΦ should be regularly obtained during isolation procedures for CFb.

Isolation of CFb from adult myocardium is commonly performed by retrograde perfusion through the aorta and enzymatic digestion of the extracellular matrix. Following physical separation of myocytes using centrifugation, the CFb are allowed to attach to tissue culture plastic over 1-2 hr. Washing the cultures after this attachment period takes advantage of fibroblasts relatively faster attachment rates than endothelial cells and removes other non-adherent cells (e.g. lymphocytes).

However, MΦ are also capable of attaching to tissue culture plastic through integrin-dependent and integrin-independent mechanisms. MΦ express several integrins that bind to extracellular matrix proteins (e.g. collagen and fibronectin)[69] often utilized to facilitate cell attachment. Additionally, MΦ are capable of adhering to surfaces in a calcium-independent, integrin-independent manner through scavenger receptors expressed on their surface membranes.[65]

MΦ are known to secrete paracrine factors that are capable of rapidly changing target cell behavior and phenotype. These include interleukins, cytokines, and growth factors.[4,64,85,88,113,114] For example, MΦ secrete TNFα, which can induce apoptosis in a variety of cells[48], transforming growth factor beta-1 (TGFβ1), which can stimulate fibroblast differentiation to a myofibroblast phenotype[80], and PDGF, which can stimulate fibroblast proliferation.[96] MΦ may also generate reactive oxygen species (ROS) (e.g. H_2O_2) that can modulate a variety of cellular responses including ion channel activation and intracellular signaling pathways in CFb.[24,25,134] Lastly, MΦ are also a source of sphingosine-1-phosphate (S1P).[91]

To identify CFb, positive immunoreactivity for vimentin and smooth muscle α-actin as markers of undifferentiated and differentiated (i.e. myofibroblasts) phenotypes, respectively, are often used.[36,58,132] To validate the absence of endothelial cells, an absence of immunoreactivity for endothelial markers such as von Willibrand factor or VE-cadherin or an absence of acetylated low density lipoprotein uptake are often used.[53,54] However, vimentin and smooth muscle α-actin are also reported to be expressed in monocytes/ MΦ.[26,92]

Since monocytes/ MΦ are present in mammalian ventricular tissue, are capable of rapidly adhering to tissue culture plastic surfaces, and share common cytoskeletal markers, it seemed likely that MΦ contamination of cardiac cultures may be more prevalent than had been reported. An essential part of our study was therefore to improve CFb culture purity since MΦ can affect CFb phenotype. To investigate this, the levels of MΦ in native rodent cardiac tissues and at various stages of CFb cell isolation have been quantified by microscopy, flow cytometry and real-time PCR. Methods for reducing or removing MΦ from cardiac cultures, and thereby enriching the population of CFb, have been developed. Cytoskeletal markers commonly used in the identification of CFb have been examined using purified CFb and MΦ. In addition, these cell types have been compared for their specificity to a recently described CFb-specific marker, discoidin domain receptor 2 (DDR2).[51,93]

2.3 Methods

2.3.1 Cell Isolation

Hearts from heparinized adult C57Bl/6 mice or adult Sprague-Dawley rats were isolated under isoflurane anesthesia and placed in calcium-free Tyrodes buffer (130 mM NaCl, 5.4 mM KCl, 0.3 mM Na_2HPO_4, 1 mM $MgCl_2$, 10 mM HEPES, 5.5 mM glucose, 30 mM taurine, 10 mM 2,3 butanedione monoxime, 2 mM creatine, and 2 mM carnitine; pH 7.2-7.4).[14,105,118,119] After cannulation of the aorta with a blunt-end 21G (for mice) or 18G (for rat) needle, the heart was retrograde perfused with Tyrodes buffer to ensure clearing of the coronary arteries. The hearts were then placed on a Langendorff

apparatus and perfused at 3-5 ml/min (for mouse) or 5-7 ml/min (for rat) for 5 min with oxygenated, 37°C Tyrodes buffer. After an additional 10-15 min of enzymatic digestion in Tyrodes buffer containing collagenase type 2 (1 mg/ml, Worthington) and 40 μM $CaCl_2$, the ventricles were removed, gently triturated and filtered through 100-μm nylon mesh into modified Krebs-Henseleit buffer (100 mM K-glutamate, 10 mM K-aspartate, 25 mM KCl, 10 mM KH_2PO_4, 2 mM $MgSO_4$, 0.5 mM EGTA, 5 mM HEPES, 1% BSA, 20 mM glucose, 20 mM taurine, and 5 mM creatine; pH 7.2-7.4). Myocyte populations were removed by mild centrifugation (1 min, 50 x g, repeated twice). The CFb-containing supernatant was pelleted (5 min, 750 x g), resuspended, and pelleted again through a density gradient (4% bovine serum albumin [BSA] in Tyrodes buffer) to remove debris. The CFb-containing pellet was resuspended in 37°C culture medium (Dulbecco's Modified Eagles Medium supplemented with 10% fetal bovine serum, L-glutamine, sodium pyruvate, and antibiotic-antimycotic), plated onto tissue culture plastic, and allowed to incubate for 30-40 min (for rat) or 50-60 min (for mouse) in a humidified, 5% CO_2 incubator at 37°C. After the attachment period, non-adherent cells were removed by aspiration, the surfaces gently washed twice with calcium- and magnesium-free phosphate buffered saline (Ca^{++}/Mg^{++}-free PBS), and the cells were incubated with fresh culture medium.

Peritoneal MΦ were isolated from anesthetized adult mice by intraperitoneal lavage with MΦ buffer (Ca^{++}/Mg^{++}-free PBS containing 2 mM EDTA and 0.5% BSA) and gentle abdominal massage for 1 min, similar to methods previously described.[65]

All animal procedures were approved by the UCSD Institutional Animal Care and Use Committee and adhered to *Guidelines for the Care and Use of Laboratory Animals* (©1996).

2.3.2 MΦ Removal

After removal of myocytes from primary-digested myocardium, the CFb-containing pellet was resuspended in ice-cold MΦ buffer (5 ml) and incubated on tissue culture plastic for 30 min at 4-8°C. The non-adherent cells (containing CFb) were collected and layered onto the 4% BSA density gradient and then processed as described above. The adherent MΦ were washed and kept for further analysis of defined cell type from the same heart.

Additional removal of MΦ was accomplished via cell sorting using magnetic particle-conjugated antibody technology (Miltenyi Biotech, Auburn, CA). Cells were pelleted and resuspended in cold MΦ buffer and reacted with anti-CD11b antibodies as per manufacturer's instructions. CD11b (integrin α_M,) reacts primarily with myeloid-derived cells, including monocytes and MΦ. Both the positive (MΦ-containing) and negative (CFb-containing) cell fractions were collected for analysis.

2.3.3 Immunostaining

Selected cell populations were seeded onto glass chamber slides and fixed in phosphate buffered paraformaldehyde (PFA) (81 mM Na_2HPO_4, 19 mM NaH_2PO_4, 4% PFA)[106] for 10-20 min at room temperature, then stored at 4°C in 1% PFA. Cells were

permeabilized in 0.3% Triton X-100 detergent, and blocked in BSA and non-immune sera. Primary or directly conjugated antibodies were as follows: DDR2 (Santa Cruz Biotechnology, Santa Cruz, CA), CD68-FITC (Serotec, Raleigh, NC), CD64 (Santa Cruz Biotechnology), F4/80-FITC (Caltag Laboratories, Carlsbad, CA), F4/80-PE (eBioscience, San Diego, CA), vimentin (Sigma, St. Louis, MO), and smooth muscle α-actin (Sigma). Cells were washed with Ca^{++}/Mg^{++}-free PBS containing 0.05% Tween-20 and 1% BSA (Rockland, Gilbertsville, PA). Pre-treatment of MΦ with an anti-CD16/32 antibody (BD Pharmingen, San Jose, CA) was used to block FcγIII/II receptors and non-specific antibody binding.[98] Visualization was achieved using fluorochrome-conjugated secondary antibodies as follows: rabbit anti-goat IgG FITC (Sigma) or sheep anti-mouse IgG FITC (Sigma). Isotype IgG control samples were incubated at comparable immunoglobulin concentrations. Lastly, nuclei were visualized by counterstaining with DAPI (Sigma).

Digital images were captured on a $1.37x10^6$ pixel CCD camera (Hamamatsu Photonic Systems, Bridgewater, NJ) using ImagePro Plus 5.0 (MediaCybernetics, Silver Spring, MD), an Olympus IX-81 inverted epifluorescent microscope, and appropriate filter sets. Identical exposure times were used for isotype controls and samples, and all images were subjected to equivalent post-image processing.

2.3.4 Flow Cytometry

Cells in suspension were fixed and processed as above or using IntraCyte FACS kit reagents (Orion Biosolutions, Carlsbad, CA). Stained cells and their isotype controls were resuspended in FACScan buffer (BD Biosciences) and analyzed using a BD

FACScan flow cytometer. Cell populations of interest were gated to count a minimum of 10,000 events based on forward scatter (FSC) and side scatter (SSC) of control samples. Histogram data sets were analyzed by CellQuest software (BD Biosciences) by gating to isotype controls.

2.3.5 PCR

Cells were lysed and total RNA from tissues or cells was isolated by silica-gel columns using RNeasy kits (QIAGEN, Valencia, CA) and eluted in water as per manufacturer's instructions. Complementary DNA (cDNA) was reverse transcribed from mRNA by oligo-dT priming and Omniscript reverse transcriptase (QIAGEN). Expression levels of gene targets in mice and rats were characterized by SYBR Green[3] quantitative real-time PCR (qPCR) of cDNA using specific primer sets as listed in Tables 2.1 and 2.2, respectively, and were amplified using a BioRad MyIQ Cycler. Expression levels were normalized to the housekeeping gene glyceraldehyde-3-phosphate dehydrogenase (GAPDH). Additionally, expression levels of S1P receptor isotypes were performed using Applied Biosystems (Foster City, CA) TaqMan® primer/probe sets on an ABI 7300 Real Time PCR System as follows: $S1P_1$ (Mm00514644_m1), $S1P_2$ (Mm01177794_m1), $S1P_3$ (Mm00515669_m1), and GAPDH (Mm99999915_g1).

Table 2.1 Mouse Primer Sets

Gene Target	*Forward Primer*	*Reverse Primer*
GAPDH	5'-AACTTTGGCATTGTGGAAGG-3'	5'-ACACATTGGGGGTAGGAACA-3'
DDR2	5'-CCGAAAGCTTCCAGAGTTTG-3'	5'-TTCTCCCAGCTTCTCCTTGA-3'
CD64	5'-GTTAATGCCACCAAGGCTGT-3'	5'-ACCTGTATTCGCCACTGTCC-3'
CD68	5'-CCAATTCAGGGTGGAAGAAA-3'	5'-CTCGGGCTCTGATGTAGGTC-3'
MSR1*	5'-CTGGACAAACTGGTCCACCT-3'	5'-TCCCCTTCTCTCCCTTTTGT-3'
$S1P_4$	5'-GGCTACTGGCAGCTATCCTG-3'	5'-AAGGCCACCAAGATCATCAG-3'
$S1P_5$	5'-GATCCCTTCCTGGGTCTAGC-3'	5'-TAGAGCTGCGATCCAAGGTT-3'

* MΦ scavenger receptor 1

Table 2.2 Rat Primer Sets

Gene Target	*Forward Primer*	*Reverse Primer*
GAPDH	5'-TGCCACTCAGAAGACTGTGG-3'	5'-TTCAGCTCTGGGATGACCTT-3'
DDR2	5'-ACTACAGTCGGGATGGCAAC-3'	5'-ACACGTTCATGGAGTGGTC-3'
CD68	5'-CAAAAAGGCTGCCACTCTTC-3'	5'-GTGGGAGAAACTGTGGCATT-3'
$S1P_1$	5'-GGCCCCTCTCTTCATCCTAC-3'	5'-GATGATGGGGTTGGTACCTG-3'
$S1P_2$	5'-CCACCCTCAACTCTCTGCTC-3'	5'-GCATATGCAAGCCTCTCTCC-3'
$S1P_3$	5'-TCAGCCTGTCTCCAACAGTG-3'	5'-AGCACATCCCAATCAGAAGG-3'

Amplicon lengths for each primer set were confirmed by gel electrophoretic separation (2% agarose) with ethidium bromide visualization. Samples were subjected to melt curve analyses following amplification. All experimental data were reported relative to GAPDH levels using either the $2^{-\Delta Ct}$ or $2^{-\Delta\Delta Ct}$ calculation methods, which were considered appropriate based on primer set efficiency determinations.[84,103,104]

2.3.6 Statistical Analyses

Results from replicate experiments were averaged and are presented as mean ± standard deviation. Results were analyzed using statistical software programs for

analysis of variance (ANOVA) with Bonferonni t-test post-hoc testing or Student's t-test. Significance was assumed for results with $p<0.05$.

2.4 Results

2.4.1 Detection and Quantification of MΦ Following Routine CFb Isolation Procedures

In previous studies using collagenase-isolated CFb from the ventricules of adult rats and mice, heterogeneous cell phenotypes were observed during phase contrast microscopic examination. Specifically, in addition to the adherent cells having characteristic fibroblast morphology, there were also rounded adherent cells and phase contrast-dense cells of varied cell shape and size (Figures 2.1 and 2.2). Initial screening of these non-fibroblast cell types by qPCR implicated these cells to be monocytes and MΦ based on the relatively high expression of surface antigens CD64 (found predominantly in monocytes, MΦ, activated granulocytes, and dendritic cells), CD68 (found predominantly on tissue MΦ) and relatively low expressions of CD16 (found predominantly in natural killer cells, neutrophils, mast cells, and MΦ) and CD48 (found predominantly in lymphocytes) (data not shown).

To characterize further these non-fibroblast cell types, cultures of mouse and rat CFb were analyzed by immunological staining methods. Antibodies against the highly specific mouse MΦ surface receptor F4/80[5,57,116] demonstrated the presence of MΦ in cultures of CFb (Figure 2.1). Similarly, MΦ were detected in rat CFb isolations using anti-CD68 antibodies (Figure 2.2).

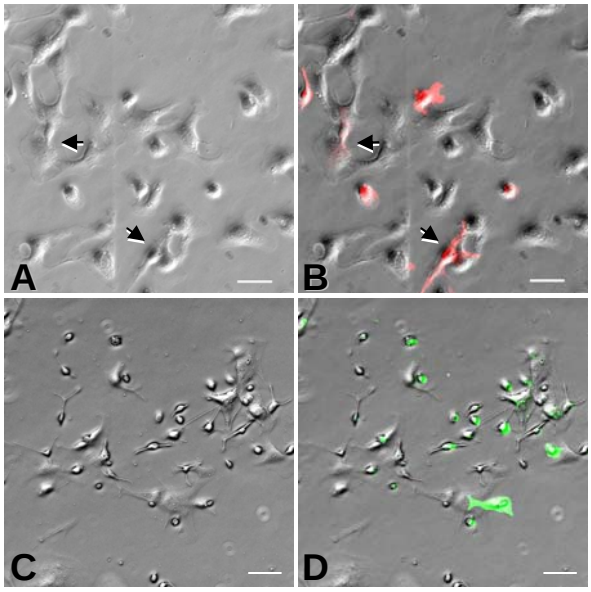

Figure 2.1 Identification of MΦ in Adult Mouse CFb Isolations. MΦ were consistently detected in cultures of adult mouse CFb using anti-F4/80 antibodies. Phase contrast (***A***) and F4/80 overlay (***B***) images of mouse CFb populations with the presence of MΦ (red color). Two MΦ (arrows) can be observed in close association with underlying fibroblast(s). Note several of the MΦ having a fibroblast-like appearance both in shape and size. Phase contrast (***C***) and F4/80 overlay (***D***) images of P1 passaged mouse CFb populations with the continued presence of MΦ (green color). Bar equals 50 μm.

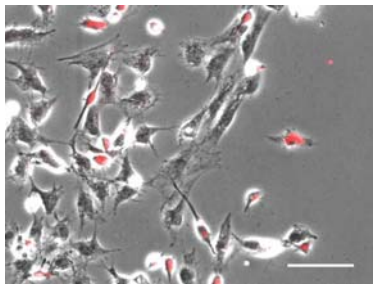

Figure 2.2. Identification of MΦ in Adult Rat CFb Isolations. MΦ were consistently detected in cultures of adult rat CFb using anti-CD68 antibodies. Phase contrast image with CD68 overlay (red) of rat CFb populations with the presence of MΦ. Bar equals 50 μm.

Flow cytometry analysis was employed to quantify the numbers of monocytes/ MΦ present in freshly digested myocardial tissues (Figure 2.3). Adult mouse ventricles

were digested, stained with antibodies against F4/80, and counted. The average percentage of F4/80-positive cells that produced signals which exceeded isotype controls was 7.04 ± 2.61%. Analysis of rat ventricular cell cultures (approximately 2 weeks old) by flow cytometry against CD68 demonstrated that between 0.5 and 10% of the total cells were MΦ. Thus, MΦ are present in both mouse and rat CFb isolations and can constitute up to 10% of total non-myocytes. Further, any meaningful study of CFb therefore requires awareness of this potential problem.

2.4.2 Removal of MΦ by Scavenger Receptor Adherence

Since MΦ are co-isolated during "CFb isolations" from both mouse and rat myocardial tissue,[8] we investigated methods that would augment their removal. Washing CFb cultures the day following initial isolation was found to help remove some monocytes/ MΦ, however this only removed a small subset of the existing contaminants (data not shown). Trypsinization has been employed in other cell isolation methods as a means to help separate MΦ from fibroblasts.[11,100] Consistent with these reports, we found that when CFb cultures were trypsinized within a few days after their initial isolation, MΦ numbers were reduced; that is, many trypsin-resistant MΦ remain adhered to the tissue culture plastic (Figure 2.4). Again, however, this procedure removes only a small subset of contaminating cells (i.e. those adhered to the tissue culture plastic surface). Notably it does not affect MΦ which are adhered to or closely associated with CFb (see Figures 2.1 and 2.2). As such, MΦ could still be detected in unpurified CFb cultures after the first passage (Figure 2.1).

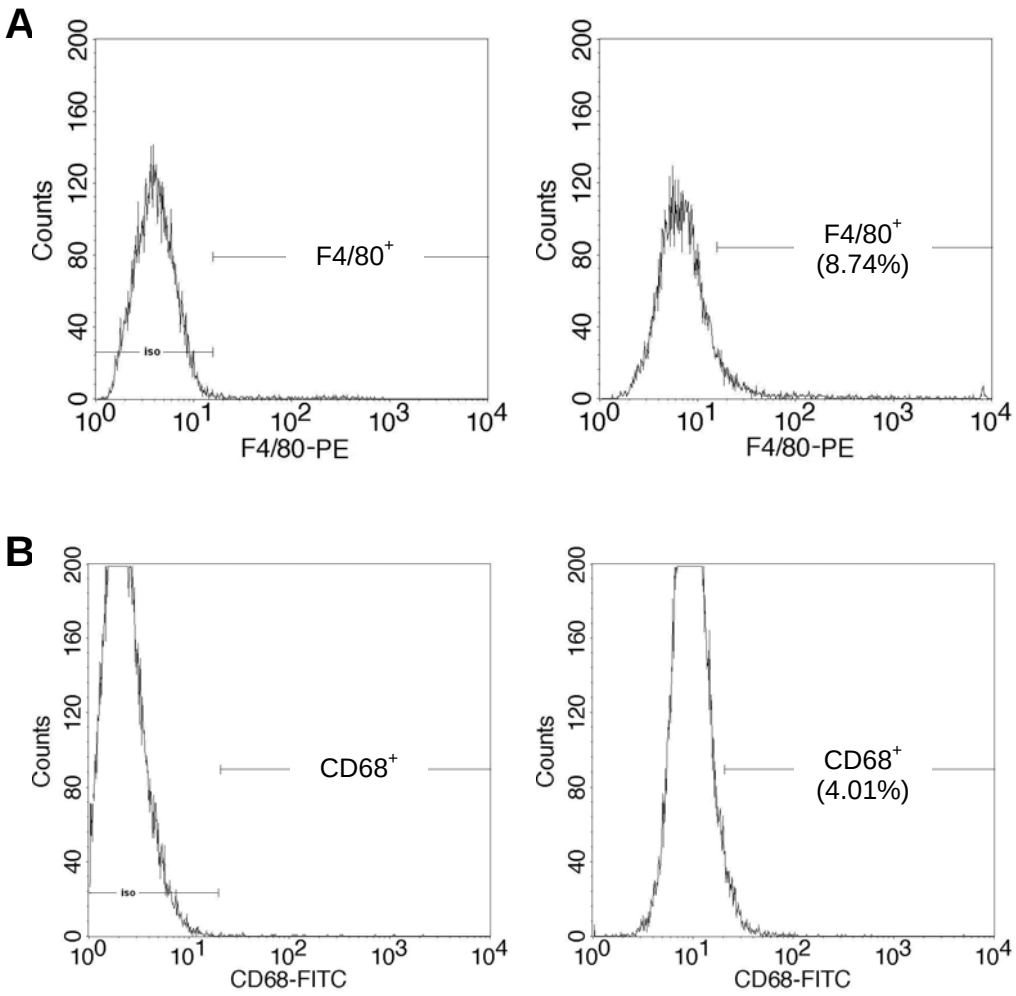

Figure 2.3 Quantification of MΦ in Adult CFb Isolations by Flow Cytometry. ***A.*** Representative histograms for isotype control (left panel) and F4/80$^+$ MΦ (right panel) from adult mouse ventricular myocardial digests after removal of myocytes. Averaged data (n=5) resulted in 7.04 ± 2.61% MΦ detected from non-myocyte cells after gating on isotype control. ***B.*** Representative histograms for isotype control (left panel) and CD68$^+$ MΦ (right panel) from adult rat ventricular CFb cultures after removal of myocytes and culture for 13-17 days. Data (n=4) ranged from 0.5 to 10% MΦ detected from non-myocyte cells after gating on isotype control.

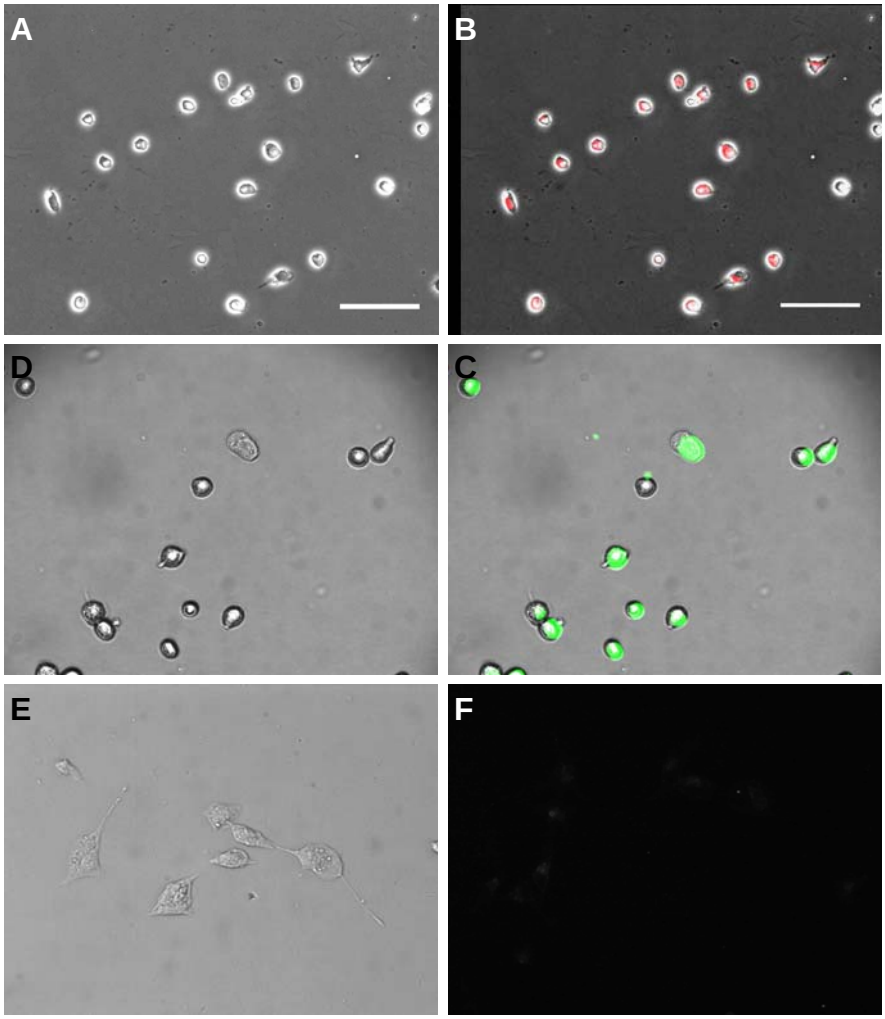

Figure 2.4. Rat Cardiac MΦ Are Resistant to Trypsinization. Positive reactivity to anti-CD68 antibodies and uptake of Ac-LDL (conjugated to Alexa Fluor 488) confirmed that adherent cells after trypsinization were macrophages (MΦ). Phase contrast (***A***) and after CD68 immunostaining (***B***, image overlay) of trypsinized rat MΦ. Phase contrast (***C***) and after exposure to Ac-LDL-AlF488 (***D***, overlay image) of trypsinized rat MΦ. Phase contrast (***E***) and after exposure to Ac-LDL-AlF488 (***F***) of negative control NIH3T3 fibroblasts. Bar equals 50 μm.

Fibroblasts attach to extracellular matrix (ECM) molecules via cell-surface integrin receptors and this process requires divalent cations. In addition to this integrin-mediated attachment, MΦ can attach to culture surfaces in integrin-independent ways

which depend on scavenger receptors.[55] We have taken advantage of this to develop an additional depletion step during the CFb isolation procedure. The MΦ buffer used during our pre-plating step contains no serum (and hence no serum-derived attachment factors such as fibronectin or vitronectin) but does contain BSA to block non-specific protein binding. Addition of EDTA (2 mM) chelates divalent cations. An incubation period of 30 min at 4-8°C was shown to be optimal since shorter time periods yielded fewer MΦ. Incubations for up to 2 hr in this solution failed to allow attachment of NIH3T3 mouse embryonic fibroblasts, used as control cells. NIH3T3 cells remained in the non-adherent fraction (i.e. suspended in the solution) (data not shown).

When freshly digested mouse myocardial isolates were subjected to a MΦ pre-plating step, the percent of F4/80-positive MΦ was significantly reduced from 7.04 ± 2.61% to 1.50 ± 0.017% ($p<0.02$) of total non-myocytes, as determined by flow cytometry (Figure 2.5). Analysis by qPCR of the adherent and non-adherent fractions following the MΦ pre-plating step confirmed that MΦ were significantly enriched in the adherent fraction (i.e. they were able to attach via their scavenger receptors) and that CFb were enriched in the non-adherent fraction (i.e. they were unable to attach and remained suspended in the solution). In mouse myocardial digests, there was a 7-fold increase in MΦ-specific MSR1 expression levels in the adherent fraction and a 20-fold increase in CFb-specific DDR2 in the non-adherent fraction (Figure 2.5). Rat myocardial digests experienced a similar enrichment of MΦ in the adherent fraction as determined by relative expression of CD68 (4.75-fold increase) and an enrichment of CFb in the non-adherent fraction by relative expression of DDR2 (2.5-fold increase) (Figure 2.5).

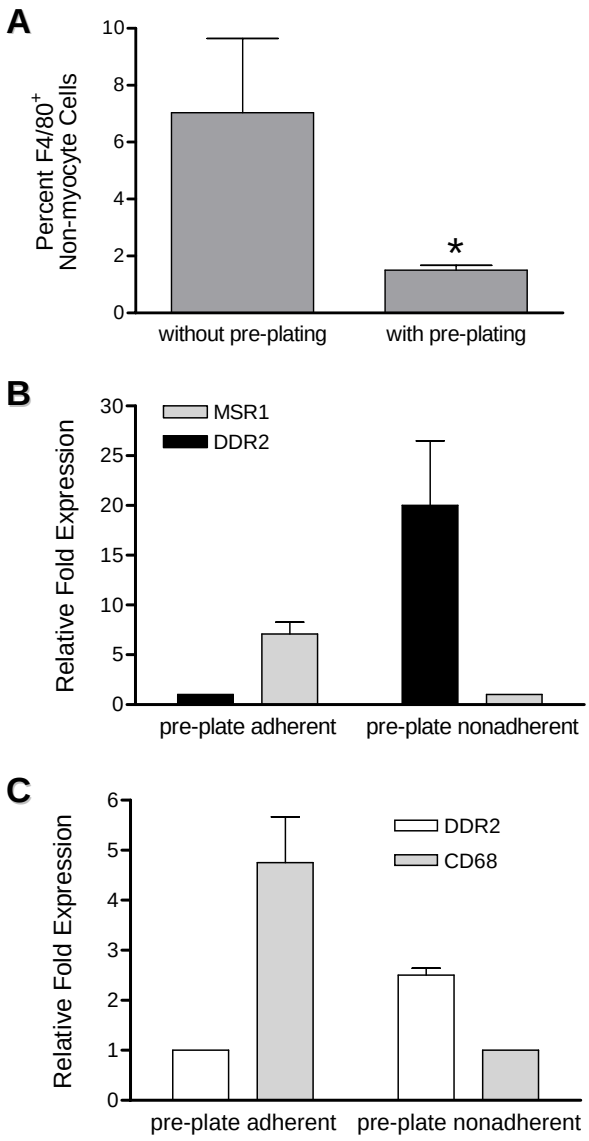

Figure 2.5 Assessment of Pre-plating Procedure for Reducing MΦ. MΦ were removed from ventricular myocardial digests (after removal of myocytes) by incubation in cold MΦ buffer for 30 min on tissue culture plastic surfaces. ***A.*** Pre-plating of adult mouse digests analyzed by flow cytometry demonstrated a significant (*$p<0.02$) reduction of $F4/80^+$ MΦ following pre-plating. ***B, C.*** Analysis by qPCR of cell fractions from mouse (***B***) or rat (***C***) digests after pre-plating showed higher expression of MΦ markers MSR1 and CD68 within the cell populations adhered to the tissue culture plastic surfaces and higher expression of CFb marker DDR2 in the cell populations in the non-adherent fractions.

2.4.3 Antibody-Mediated Separation Can Reduce MΦ Contamination

This MΦ pre-plating step has proven to be straight-forward, cost-effective and easily incorporated into the overall isolation procedure. However, it relies on cells with active scavenger receptors and may therefore be less effective at eliminating monocytes or undifferentiated MΦ. As a result, some non-adherent monocytes/ MΦ may be carried through with the CFb-containing fraction, and then become activated, and eventually adhere to the tissue culture plastic along with the CFb. To address this concern, we utilized magnetic activated cell sorting methods in order to remove monocytes/ MΦ from cells in suspension.

Magnetic particle-conjugated anti-CD11b antibodies were reacted with CFb cultures immediately following the MΦ pre-plating step. After centrifugation to remove excess free antibody, the labeled cells were loaded onto a column containing packed metallic beads under an induced magnetic field (MiniMACS Separator, Miltenyi Biotec). The $CD11b^+$ cells were retained within the column while the $CD11b^-$ cells flowed through and were collected from the reservoir tip. After several washes, the column was removed from the magnet and the bound cells ($CD11b^+$) were eluted. Results of CD11b-sorting experiments are presented in Figure 2.6.

We routinely perform CD11b sorting 1-2 days post-isolation to minimize the potential effect(s) of MΦ co-culture on the CFb (see Figure 2.10 and Chapter 3). Performing the sorting procedure immediately following the initial enzymatic digestion process was shown to be less effective due to dead myocytes and debris interfering with the elution of CFb from the column (data not shown). Furthermore, allowing the CFb to

adhere initially onto tissue culture plastic surfaces takes advantage of differential plating times for minimizing endothelial cell contamination.

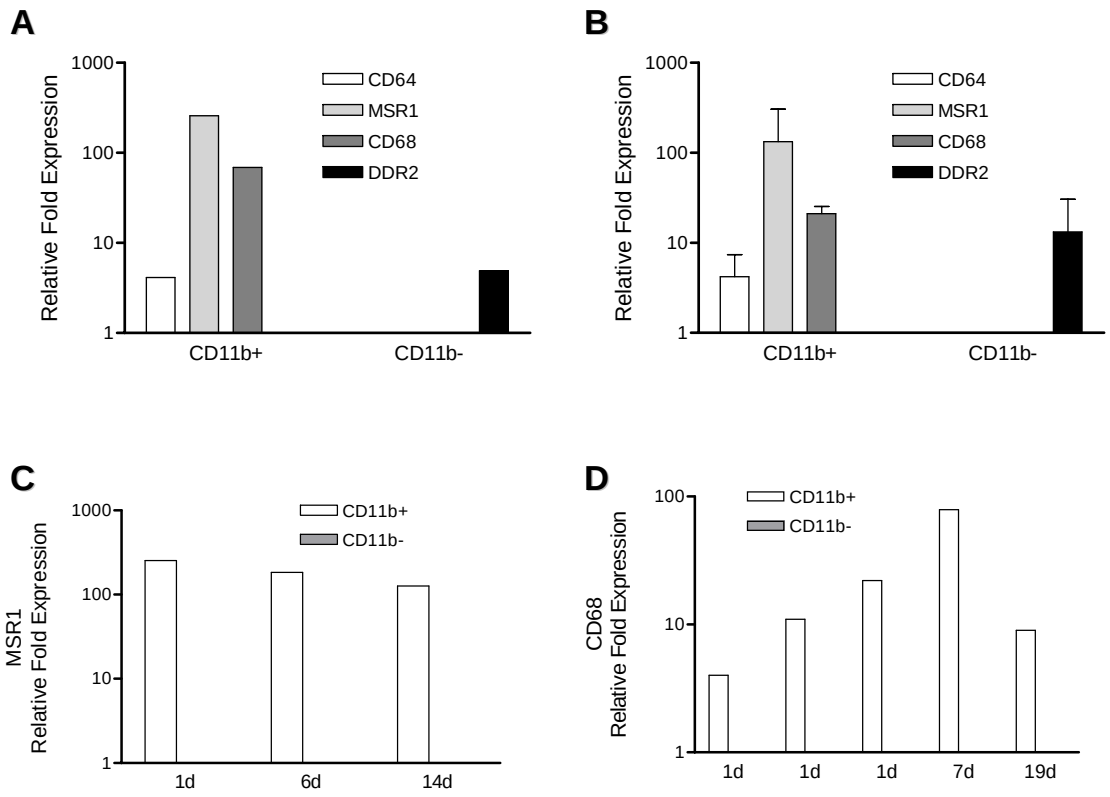

Figure 2.6 Assessment of CD11b Sorting Procedure for Reducing MΦ. Adult mouse CFb populations could be further purified by CD11b sorting even after pre-plating in MΦ buffer. Cell fractions after anti-CD11b magnetic antibody sorting were analyzed by qPCR to determine the effectiveness of this method for removing MΦ. ***A.*** Adult mouse peritoneal MΦ were used as control cells to confirm that expression markers of MΦ (i.e. CD64, MSR1, and CD68) were highest in the $CD11b^+$ fraction and that fibroblasts (i.e. DDR2 expression) were found predominantly in the $CD11b^-$ fraction. ***B.*** Adult mouse CFb populations showed similar expression patterns as peritoneal MΦ control cells, with $CD11b^-$ populations enriched with CFb (DDR2) and depleted of (CD64, MSR1, and CD68). ***C.*** Adult mouse CFb, if not purified by CD11b-sorting shortly after initial isolation, continued to exhibit high expression of MΦ markers in the $CD11b^+$ fractions after several weeks in culture. ***D.*** Adult rat CFb, if not purified by CD11b-sorting shortly after initial isolation, also continued to exhibit high expression of MΦ markers in the $CD11b^+$ fractions after several weeks in culture.

Adult mouse peritoneal MΦ were utilized to validate the CD11b-sorting method initially. As shown in Figure 2.6, strong mRNA expression of MΦ markers CD64, MSR1, and CD68 were found in the $CD11b^+$ fraction. In contrast, very distinct expression of the CFb marker DDR2 was found in the $CD11b^-$ fraction. When adult mouse CFb cultures were sorted, a similar expression profile was obtained. These results demonstrate successful separation of monocytes/ MΦ and CFb in isolations from mouse hearts. To determine whether MΦ can remain in unpurified CFb cultures for extended periods, cultures at various times post-isolation were analyzed by CD11b sorting. As depicted in Figure 2.6, MSR1 continued to be strongly expressed in $CD11b^+$ fractions of adult mouse CFb cultures for up to 14 days (the longest time evaluated). Detection of MΦ expression proteins was assessed by qPCR in these studies, since many of the MΦ have been already removed by the pre-plating step and flow cytometry was not considered sensitive enough for the analysis of this sorting procedure.

Although the anti-CD11b antibodies are generated against antigen from the mouse, we hypothesized that there may be sufficient homology between mouse and rat CD11b that the magnetic antibodies may exhibit cross reactivity. When adult rat CFb cultures were subjected to CD11b sorting (Figure 2.6), CD68 expression levels of the same order of magnitude as those found expressed in mouse cells were noted in $CD11b^+$ fractions. Similar to mouse CFb cultures, rat CFb cultures exhibited strong CD68 expression in the $CD11b^+$ fractions after sorting for up to 19 days (the longest time evaluated), indicating that MΦ were present in those cultures as well. A phase contrast image of $CD11b^-$

mouse CFb in culture after CD11b-sorting is shown in Figure 2.7. It is readily apparent that culture purity has improved.

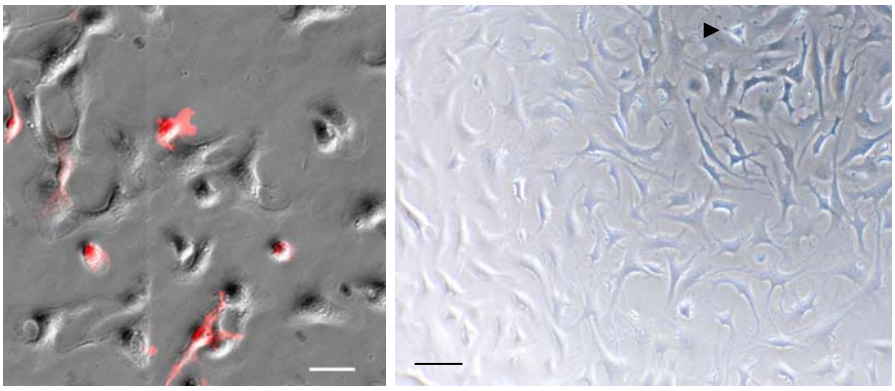

Figure 2.7. Phase Contrast Image of CD11b^{-} Adult Mouse CFb. Unforted culture of CFb (left panel) shows many F4/80-staining MΦ. Another culture of CFb which were isolated as described in Methods and sorted using anti-CD11b antibodies the following day (right panel). This image is of CFb after culture for 3 days. Even with sorting, cells with unrepresentative CFb morphologies (arrow) are sometimes present, albeit at lower frequencies than without sorting. Bar equals 50 μm.

While the pre-plating in MΦ buffer and subsequent CD11b sorting proved the most efficient at reducing MΦ levels in CFb cultures, it should be noted that several other methods were investigated. These included: (i) culture on collagen,[71] on which it is reported that MΦ proliferate poorly; (ii) culture in heat-inactivated serum[15] to reduce complement; (iii) culture in salicylic acid;[13,45,128] and (iv) pre-plating in serum-free medium[120] to allow monocyte/ MΦ to adhere to the plastic ware. All of these methods were demonstrated to be less successful or unsuccessful in reducing MΦ and were not pursued further (data not shown).

In summary, the optimal method we found for significantly removing MΦ from CFb cultures was to pre-plate in cold EDTA buffer after removal of myocytes, then to negatively deplete by magnetic antibody cell sorting using anti-CD11b antibodies.

2.4.4 Immunological Assessment of CFb Markers

Results of immunological assessment of CFb are presented in Figures 2.8 and 2.9. CFb are often identified by positive immunoreactivity for vimentin and smooth muscle α-actin as markers of undifferentiated and differentiated (i.e. myofibroblasts) phenotypes, respectively.[36,132] Vimentin is an intermediate filament which is abundant in migrating cells and co-localizes with several integrins at focal adhesions.[72] In the next set of experiments, CFb were isolated from adult mice and stained with anti-vimentin antibodies. As expected, strong reactivity was observed in all CFb examined and as early as 2 days post-isolation. Similarly, we also observed strong immunoreactivity against smooth muscle α-actin in CFb isolated from adult mice and rats.

However, both vimentin and smooth muscle α-actin have also been reported to be expressed in monocytes/MΦ.[26,52,59,92] When using mouse peritoneal MΦ as a positive control for the MΦ cell type, we consistently observed positive staining for both vimentin and smooth muscle α-actin (Figure 2.8). To further explore this finding, we examined vimentin and smooth muscle α-actin expression in $CD11b^+$ cardiac-isolated MΦ. Dual labeling with antibodies against F4/80 and the cytoskeletal proteins vimentin or smooth muscle α-actin (Figure 2.8) demonstrated co-localization in mouse MΦ which had been isolated from CFb preparations. While the staining in the MΦ was less intense than that observed with CFb, MΦ were, nonetheless, immunoreactive against these proteins which are routine used as selective fibroblast markers. Similarly, rat MΦ were shown to be positive for both CD64 and smooth muscle α-actin (Figure 2.9).

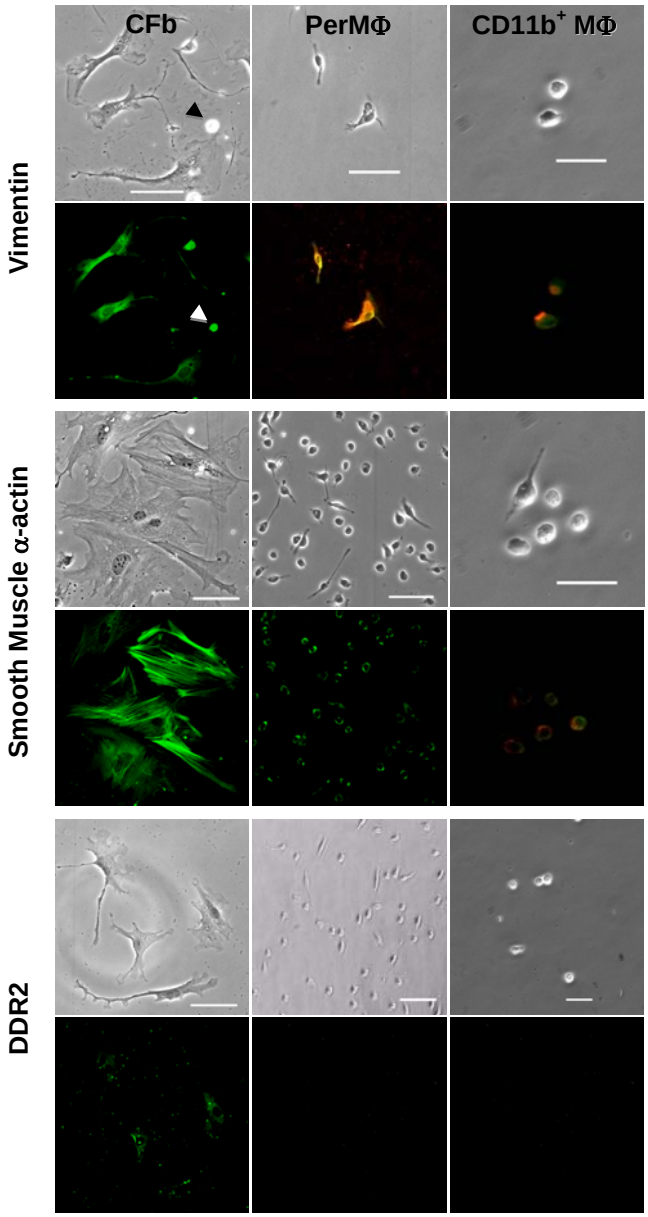

Figure 2.8 Evaluation of Adult Mouse CFb Immunodetection Markers. CFb (left column), peritoneal MΦ (middle column) and CD11b$^+$ MΦ from cardiac digests (right column) of adult mice were evaluated by immunostaining for vimentin (top panel), smooth muscle α-actin (middle panel) and DDR2 (bottom panel). Immunostaining with anti-vimentin antibodies and visualization with FITC-labeled secondary antibody revealed extensive intracellular staining for vimentin (green) in mouse CFb (as expected). A MΦ (arrows) can be observed in the field of view. CFb also stained positive (green color) for smooth muscle α-actin and DDR2 (green color) (as expected). Peritoneal MΦ and CD11b$^+$ MΦ were dual labeled with anti-F4/80 antibodies (red color) and anti-vimentin antibodies (green color) such that co-expression is observed as yellow in the overlay image. Peritoneal MΦ expressed smooth muscle α-actin and CD11b$^+$ MΦ (overlay image) were likewise positive. Neither peritoneal MΦ nor CD11b$^+$ MΦ exhibited immunoreactivity against DDR2. Bar equals 50 μm.

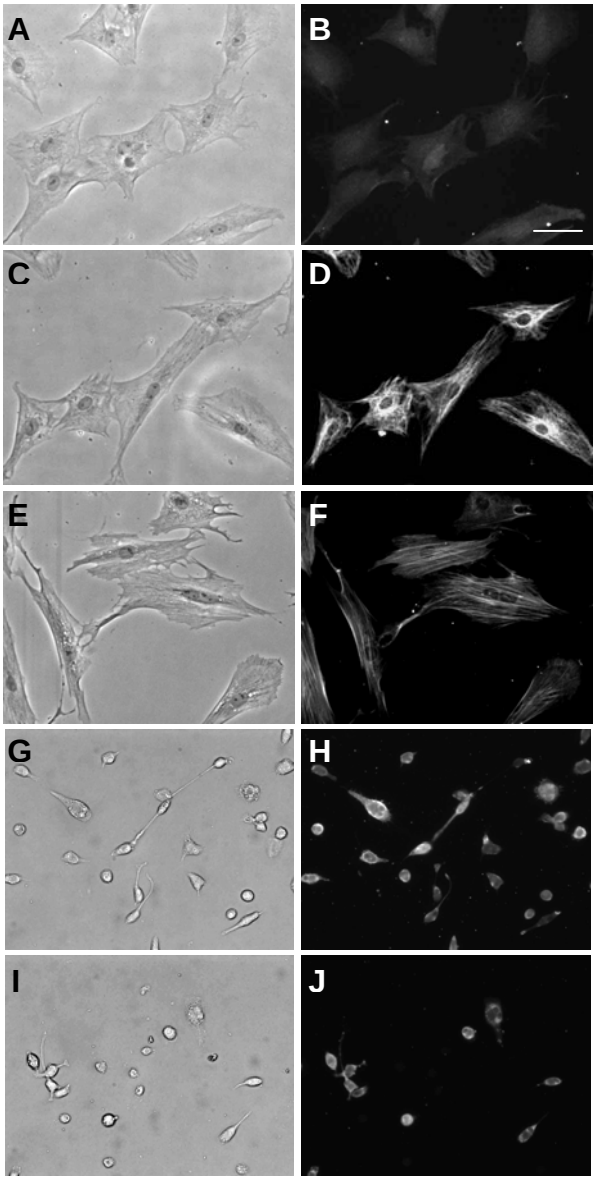

Figure 2.9 Evaluation of Adult Rat CFb Immunodetection Markers. Paired image sets consist of phase contrast images (left column) and images after labeling with FITC-conjugated secondary antibody (right column). As expected, rat CFb reacted positively to immunolabeling for DDR2 (***B***), vimentin (***D***), and smooth muscle α-actin (***F***). Rat MΦ reacted positively to CD64 (***H***), as expected, but also reacted positively to smooth muscle α-actin (***J***). Bar equals 50 μm.

Although CD11b is expressed primarily on monocytes and MΦ, it can also be found on other myeloid-derived cells such as granulocytes (i.e. neutrophils, basophils, eosinophils, and dendritic cells).[121] Thus, the CD11b sorting method employed may be

capable of removing these cell types as well. However, our immunostaining results using F4/80 suggest that the $CD11b^+$ cells were almost exclusively monocytes MΦ.

Recently, in efforts to identify a more specific marker of CFb, researchers have identified the fibrillar collagen receptor DDR2.[51] DDR2 has been reported to be expressed on CFb, but not on endothelial cells, smooth muscle cells, or myocytes within normal cardiac tissue. Based on our observations that MΦ can co-isolate with CFb and that the cited study on DDR2 did not specifically the evaluate MΦ, we characterized both CFb and MΦ for immunoreactivity to DDR2. We also observed positive labeling of adult mice and rat CFb with anti-DDR2 antibodies (Figures 2.8 and 2.9). Importantly, we observed no immunoreactivity of DDR2 towards $CD11b^+$ adult mouse peritoneal MΦ or $CD11b_+$ MΦ from cardiac isolations (Figure 2.8). Thus, DDR2 does appear to be a cardiac-specific immunomarker for the fibroblast population.

2.4.5 MΦ in CFb Cultures Can Bias Results

In some circumstances, having a percentage of monocytes/MΦ within a culture of CFb may not have any significant bearing on the interpretation of experimental findings. This, of course, would depend heavily on the nature of the studies. Our laboratory is interested in electrophysiology and physiological responses in CFb to sphingosine-1-phosphate (S1P). S1P is a lipid agonist that selectively binds to five known G-protein coupled receptors. These receptors, designated $S1P_{1-5}$, are ubiquitously found on many cell types.[21,32,89,107,117] We therefore were interested in investigating whether MΦ express similar S1P receptor isotypes as CFb. As shown in Figure 2.10, acutely isolated adult

mouse ventricular CFb express message primarily for $S1P_1$, $S1P_2$, and $S1P_3$. They have negligible expression of $S1P_4$ or $S1P_5$. Similarly, MΦ isolated either from cardiac tissues or from peritoneal lavage also express these same receptors.

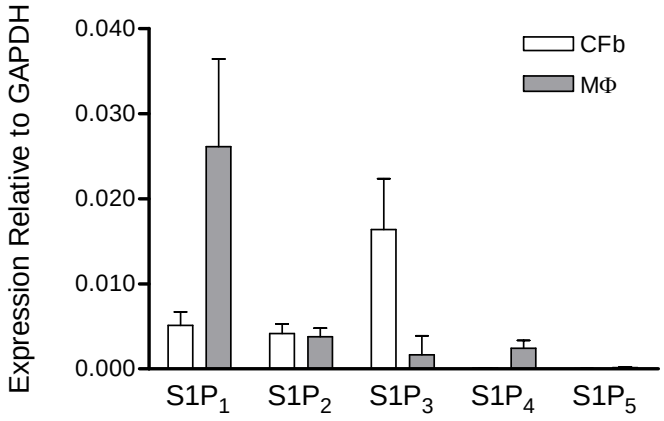

Figure 2.10 Comparison of S1P Receptor Isotypes in CFb and MΦ. CD11b-purified CFb and pre-plate enriched cardiac MΦ were characterized without further culture by qPCR for expression levels of $S1P_{1-5}$ relative to GAPDH.

In another example of how MΦ contamination of CFb cultures can complicate data interpretation, we utilized a functional migration assay. Motile cells are often studied for their ability to exhibit chemotaxis-directed migration towards a concentration gradient of a chemical stimulus. In these experiments, CD11b-sorted or unsorted CFb were seeded onto microporous inserts, "serum starved" overnight, and subjected to either 0.1% or 10% FBS medium for an additional 24 hours. As shown in Figure 2.11, both purified and unpurified CFb cultures migrated towards 10% serum. Since the unpurified cultures (containing MΦ) had a significantly ($p<0.05$) stronger overall response, we performed control experiments using peritoneal MΦ to determine whether MΦ are chemotactic to serum. Our results show that both adult mouse and rat peritoneal MΦ are

capable of migrating in response to 10% serum (Figure 2.11). Compared to their respective controls, both mouse and rat peritoneal MΦ exhibited a significant ($p<0.05$) response when exposed to 10% FBS.

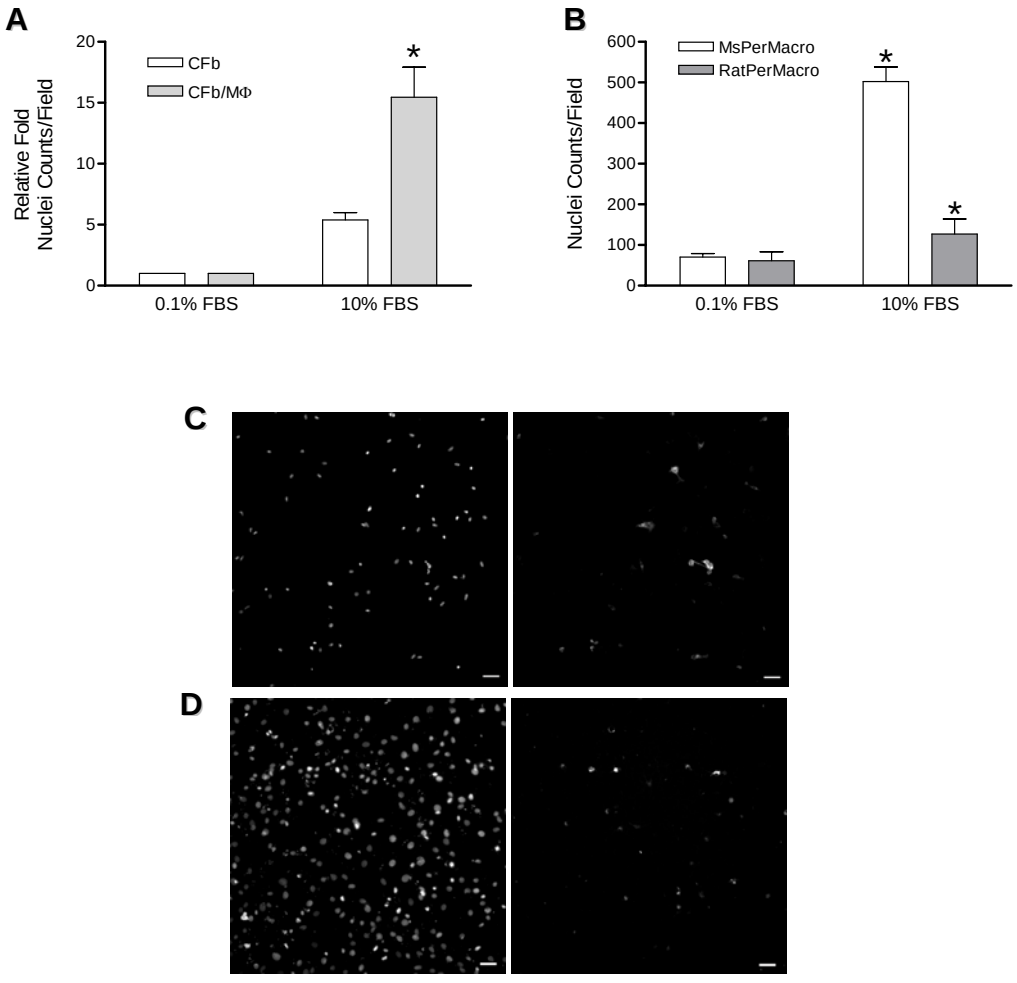

Figure 2.11 Influence of MΦ on Adult CFb Migration Experiments. ***A.*** Unpurified cultured of rat CFb containing MΦ contaminants (CFb/MΦ) have a stronger migratory response to mitogenic stimuli (10% FBS) than purified CFb. *$p<0.05$ vs CFb. ***B.*** Both adult mouse and adult rat peritoneal macrophages (MΦ) migrate in response to 10% FBS. $p<0.05$ vs 0.1% FBS controls. ***C.*** Migration chambers stained with anti-F4/80 antibodies (right panel) show that MΦ from unpurified adult mouse CFb cultures also migrate in response to 10% FBS. Total migrating cells were visualized after staining nuclei with DAPI (left panel). ***D.*** Migration chambers of unpurified adult rat CFb cultures stained with anti-CD68 antibodies (right panel) and DAPI (left panel) also demonstrate migration of MΦ in response to 10% FBS.

To demonstrate that MΦ might be contributing to overall assessments of cellular migration, unpurified CFb fibroblast cultures were exposed to 10% FBS and the culture inserts immunostained for MΦ using anti-F4/80 and anti-CD68 antibodies (Figure 2.11). It was clearly evident that many of the cells having migrated were actually MΦ.

Thus, these two examples demonstrate how MΦ contaminants in CFb cultures could complicate or bias experimental results and possibly reduce their overall meaning and significance.

2.5 Discussion

2.5.1 Roles and Identification of CFb and MΦ Within Myocardial Tissue

CFb are an important cell type in normal and pathological myocardium. After myocytes, they are the most plentiful cell type in cardiac tissue, and are found interspersed between myofibers. In addition to providing structural support by secreting and maintaining interstitial collagen types I and III, fibroblasts also secrete a variety of cytokines and growth factors that can have autocrine and paracrine effects.

During wound healing (e.g. following a myocardial infarction event), resident CFb undergo differentiation to a myofibroblast phenotype.[43] This transdifferentiation is regulated by a complex mix of environmental and regulatory factors and is most often associated with increased proliferation and extracellular matrix synthesis. In addition to fibroblast/myofibroblast populations, MΦ are also found in remodeling tissue. As normal residents of cardiac tissue where they perform immunological surveillance, MΦ numbers can increase in injured sites from the differentiation of circulating blood

monocytes. Once there, MΦ can have direct interactions with the fibroblast/myofibroblast populations.

Since monocytes/ MΦ are present in normal cardiac tissue, it is expected that they should regularly be obtained during isolation procedures for CFb. However, the published literature is limited regarding the presence of MΦ in isolated cardiac cultures. Our objective was therefore to quantify and characterize the levels of monocytes/ MΦ present in rodent CFb cultures and to develop methods to aid in their removal. Additionally, because the fibroblast characterization markers most often employed are poor at detecting the presence of MΦ in cardiac cultures, a second objective was to illustrate the importance of culture purity by providing several examples whereby MΦ contamination could significantly complicate the interpretation of data.

Identification of CFb is often based on cell morphology, phenotype, production of extracellular matrix proteins, or by positive immunolabeling to various cytoskeletal proteins. Most assessments of CFb cultures assert a high degree of purity; however, rarely is quantitative data provided. Identification is generally based on phase contrast examination and immunostaining. Vimentin is the most frequently cited marker for identifying CFb and smooth muscle α-actin is the most frequently cited marker for identifying myofibroblasts. However, vimentin and/or smooth muscle α-actin are expressed by a number of other cell types including smooth muscle cells, dendritic cells, peripheral blood mononuclear cells, and MΦ.[26,44,86,92] We demonstrate that vimentin and smooth muscle α-actin are expressed by both MΦ and CFb and, thus, other more specific markers should be considered so as not to cause misidentification.

The plasmalemmal receptor DDR2, a non-integrin tyrosine kinase receptor that binds to fibrillar collagen (primarily types I and III), has been proposed as a specific marker for the identification of CFb.[51] It is reportedly present in embryonic through adult hearts and absent in smooth muscle cells, endothelial cells, and myocytes. Furthermore, MΦ are reported to only express DDR1.[61] In our studies on CFb and MΦ, we have found that message for DDR2 was enriched in the $CD11b^-$ fractions, and that CFb demonstrated immunoreactivity to anti-DDR2 antibodies. Our results with DDR2 immunoreactivity and MΦ (i.e. $CD11b^+$ peritoneal MΦ and $CD11b^+$ cardiac MΦ) demonstrated no immunoreactivity. Because MΦ have Fc receptors on their surfaces that can nonspecifically bind antibodies, we utilized several controls to ensure that the results obtained were accurate. We pre-incubated the MΦ with an anti-FcγIII/II receptor (CD16/CD32) blocking antibody prior to addition of primary antibody, and we compared staining intensity to the isotype control samples (as with the CFb cultures). Additionally, we evaluated various concentrations of serum blocking with or without Fc receptor blocking in the absence or presence of DDR2 primary antibody. In no case (even with no blocking) did MΦ express positive signal in the absence of primary antibody. Thus, we conclude that the immunostaining signals observed for the MΦ were true and not simply non-selective reaction with the FITC-conjugated secondary antibody. We therefore concur that DDR2 be considered instead of or in conjunction with the traditional cytoskeletal proteins (i.e. vimentin) used to identify CFb.

In our studies, we show that MΦ comprised between 3 and 10% of non-myocyte cells in freshly digested mouse ventricular myocardium and between 0.5 and 10% in 2-

week-old rat CFb cultures. Monocytes reside in the peripheral blood and can become activated and differentiate into MΦ after migrating to tissue sites. Insufficient removal of peripheral blood monocytes could provide a source of MΦ observed in our cultures. However, it is doubtful that the entirety of MΦ observed in our cultures originated from peripheral blood, since MΦ have been reported within the myocardium.[94]

We propose several potential mechanisms that might cause monocyte/MΦ activation during the course of the CFb isolation procedure. The first is the likelihood of endotoxin contaminants within collagenase preparations. The collagenase used in our preparations, and which is often cited, was Worthington type 2, a crude preparation from the bacterium *Clostridium histolyticum*. Others have shown that less-purified collagenases can contain variable levels of endotoxin depending on manufacturer and lot number.[60,83,126] MΦ express the endotoxin-binding toll-like receptor CD14.[68] Thus, exposure to endotoxin from our collagenase was likely to have induced various cytokines and inflammatory agents, as has been shown with other collagenases which were found to induce IL-1α, IL-1β, TNFα, and IL-6.[60,126] It may be that use of more highly purified collagenase/protease preparations (e.g. Liberase Blendzymes from Roche) could help minimize monocyte activation due to their lowered endotoxin levels.[49]

Secondly, it has been shown that protease peptide fragments, also referred to as matricryptic peptides,[29] can activate neutrophils, especially when exposed to digests from cardiac tissue.[130] Other investigators have found that alveolar MΦ become activated upon exposure to collagen peptides as evidenced by increased chemotactic migration and release of ROS (e.g. superoxide anion and hydrogen peroxide) and other matrix

metalloproteases (e.g. elastase and gelatinase).[78] We postulate that peripheral blood monocytes and cardiac tissue MΦ might similarly become activated after exposure to collagenase-digested peptides.

Lastly, it is proposed that monocytes/ MΦ might become activated by exposure to cell debris during the isolation procedure. Even with carefully optimized isolation procedures, some level of cell death is expected, especially within the myocyte population. MΦ have been shown to equally engulf apoptotic and necrotic cells,[23] although they respond more proinflammatory in response to necrotic cells.[17,28]

Thus, there are several potential entry points for monocyte/MΦ activation in standard CFb isolation protocols.

2.5.2 Significance of MΦ in CFb Cultures

Why should investigators be concerned with MΦ contamination of their CFb cultures? First, it was been shown that MΦ can survive for several passages when co-cultured with fibroblasts,[120] most likely due to reciprocal feedback of various cytokines and growth factors. Therefore, once a CFb culture becomes contaminated, it is likely that the MΦ will persist for extended periods unless proactive steps are undertaken to eradicate them.

Second, both CFb and MΦ secrete a number of factors that influence wound healing and remodeling. Activated MΦ can induce secretion of TGFβ1 (as can activated peripheral blood monocytes[4]), TNFα, granulocyte MΦ colony stimulating factor (GM-CSF), adrenomedullin (AM), angiontensin II (AngII), and S1P.[4,80,91,95,110,123,124] TNFα

stimulates ceramide levels and can lead to cell apoptosis[97] and AM, in turn, can increase TNFα production.[75,98] GM-CSF can serve as a recruiting and differentiation factor for additional MΦ and is also secreted by certain types of fibroblasts.[39,63,99,99] MΦ can participate in TGFβ1 pathways via membrane-bound angiotensin-converting enzyme (ACE) and Ang II.[62,102,133,133] As previously stated, TGFβ1 is an important inducer of myofibroblast differentiation[80,131] and can regulate collagenesis, increase stress fiber formation, increase atrial natriuretic peptide (ANP) levels, induce sphingosine kinase synthesis, and induce connective tissue growth factor (CTGF).[20,77,79,81,82,122,127,135] S1P, which can be secreted by MΦ, has been shown to induce myofibroblast differentiation in lung fibroblasts.[125] Lastly, fibroblasts co-cultured with monocytes or MΦ have shown increased matrix metaloprotease (MMP) activity[31,56,138] and increased collagen gel contraction.[139] Therefore, since MΦ may modulate myo/fibroblast phenotyope and/or differentiation, their presence in CFb cultures may complicate the interpretation of studies of CFb function.

Third, as has been shown with vimentin and smooth muscle α-actin cytoskeletal proteins, MΦ may express proteins in common with CFb. An example of interest in our laboratory are the S1P receptors. S1P is a cell membrane-associated sphingolipid that is secreted by activated platelets,[136] mast cells,[2] and MΦ[91] which binds with high affinity to five distinct G protein coupled receptors (GPCR).[22] S1P receptors are found ubiquitously on many cell types, including both CFb and MΦ.[87] The downstream responses of S1P receptor activation can affect proliferation, motility, intracellular calcium regulation, cell survival, and ion channel activation depending on the cell type, the complement of S1P

receptor expression, and the associated G proteins (reviewed in [41,42,107,110,115]). Thus, a clear understanding of S1P-mediated responses in CFb requires highly purified cultures, free of contaminating cell types that may co-express similar receptor subtypes.

Fourth, we have shown that MΦ contamination can obscure results of functional assays. Both CFb and MΦ were capable of migrating towards a serum stimulus. However, it was shown that MΦ directly contributed to the numbers of total migrating cell in mixed cultures. In addition to directly interfering with accurate migration estimations, it can also be suggested that paracrine signaling between MΦ and CFb may result in pro- or anti-migratory signals, depending on the factors secreted. For example, TNFα has been shown to affect cell migration. In studies utilizing mouse embryonic fibroblasts, TNFα had both inducing and inhibitory actions over time.[46] We, however, did not observe an overall reduction in migrating cells in our assays using mixed CFb and MΦ which might be due to differences between cell types or due to the more complicated paracrine milieu of our system.

Lastly, the presence of contaminating cells may have implications in the context of fibroblast-based regenerative medicine. Fibroblasts have been experimentally utilized in preclinical studies to block atrioventricular node conduction for management of atrial fibrillation.[19] The basis of those studies was that fibroblasts are able to electrically couple to myocytes through gap-junctional intracellular communication.[9,37,109] Taking further advantage of fibroblast-myocyte cell coupling, investigators[38] have also explored using transfected fibroblasts as carriers of voltage-gated potassium channels (e.g. Kv1.3) to impose conduction delays and conduction blocks. Fibroblasts and myocytes can form

gap junctions via connexins (Cx) 43 and 45.[47] Interestingly, MΦ have also been shown to express Cx43 and various K^+ channels, including Kv1.3.[12,30,35,67] Thus, there exists a potential for unwanted cellular connections when using unpurified CFb populations, and it remains unclear how MΦ contaminants may interact and/or affect CFb-myocyte electrotonic interactions.

2.5.3 Removal of MΦ from CFb Cultures

Several methods were initially investigated to reduce the numbers of monocytes/MΦ in CFb cultures. These included: (i) culture on collagen, on which it is reported that MΦ fail to proliferate;[71] (ii) culture in heat-inactivated serum to reduce complement;[15] (iii) culture in salicylic acid;[13,45,128] and (iv) pre-plating in serum-free medium to allow monocytes/MΦ to adhere to the plastic ware.[120] While the first three methods were unsuccessful in our hands in adequately preventing or reducing MΦ (data not shown), pre-plating showed considerable promise and was therefore pursued further with modifications. Others have noted the ability of MΦ to adhere to tissue culture plastic within 30 min.[98] It should be also noted that routine trypsinization during cell passage may aid in the removal of MΦ as they are relatively resistant to dissociation from tissue culture plastic surfaces by trypsin.[40] Our own results with both mouse and rat CFb cultures confirmed that the remaining trypsin-resistant cells were MΦ as identified by F4/80 and CD68 immunostaining, respectively.

As mentioned, F4/80 is a highly specific marker of murine MΦ. It is a 150,000-kDa extracellular membrane glycoprotein.[116] CD68 is also widely used for detection of

MΦ. It is localized both extracellularly, but predominantly intracellularly within lysosomal membranes.[76] It should be noted that dendritic cells, which are also monocyte-derived,[101] have been reported to display negative expression of CD68 in human cardiac tissue.[137] Furthermore, there have been reports that fibroblasts (from synovium of arthritis patients) may cross-react with CD68.[76] We, however, have not observed any such cross-reactivity in our studies on CFb which may reflect differences in anatomical location or associations with disease status.

Pre-plating CFb enzymatic digests in cold cation-chelated buffer for 30 min resulted in significant increases in MSR1 and CD68 expression levels in the adherent fraction, indicating that MΦ were effectively attaching and being removed from the non-adherent cell fraction containing CFb. This pre-plating step is cost-effective and simple to perform. It takes advantage of MΦ ability to rapidly bind to tissue culture plastic and to attach by calcium- and integrin-independent mechanisms via class A scavenger receptors. CFb, on the other hand, require calcium for cation-mediated integrin binding and are less likely to adhere to the plates (although the possibility that some fibroblasts adhere to the plates cannot be entirely excluded).[50] Other immune cell types such as lymphocytes should not attach to plastic (although their presence has been shown to increase monocyte attachment),[16] and neutrophils have reduced adherence at cold temperatures,[108] in Mg^{++}-free medium,[34,70] and when exposed to albumin.[27,70,108] CFb cultures that utilize a 1-2 hr pre-plating step to minimize endothelial attachment would be expected to have monocyte and MΦ attachment also. Monocytes have been shown to

adhere within 1 hr in PBS alone and MΦ readily plate out in 10% serum-containing medium within 1 hr.[74]

Whereas pre-plating cell digests in cold calcium- and magnesium-free buffer containing EDTA reduced MΦ numbers to approximately 1.5% of total non-myocytes, it did not completely remove all of the MΦ. Thus, magnetic activated cell sorting was employed to more effectively deplete MΦ and enrich CFb. It should be noted that anti-CD11b antibodies could be utilized in flow-activated cell sorting; we chose, however, to utilize magnetic activated cell sorting for its ease of use and accessibility/availability to most labs.

CD11b is the complement C3b receptor expressed on monocytes and MΦ. CD11b is also found on other myeloid-derived cells such as granulocytes (i.e. neutrophils, basophils, and eosinophils)[111] and dendritic cells,[6] thus the CD11b sorting method employed may be capable of removing these cell types as well. Our immunostaining results using F4/80 would however suggest that the $CD11b^+$ cells were almost exclusively monocytes/ MΦ. The primary disadvantage of CD11b sorting is that it is a negative depletion method, and as such, may not completely remove all unwanted cells. Hence, MΦ can periodically be detected, albeit at very low frequencies, in $CD11b^-$ fractions upon further culture; and vice versa, occasional fibroblasts can be seen in $CD11b^+$ fractions.

In our studies, we found that magnetic CD11b sorting was able to reduce the number of CD68-positive cells from CFb isolations. While it may be likely that the CD11b antibodies, though produced against mouse antigen, are also capable of cross-

reacting with rat antigen, an alternative explanation may be that the rat monocytes/MΦ are simply reacting to the antibody through Fc surface receptors. Therefore, rat cells may be reacting to the anti-CD11b antibodies in a less specific manner. Regardless of the mechanism, these data demonstrate that this procedure has applicability in removing monocytes/MΦ from both mouse and rat CFb cultures.

A potentially more suitable method would be positive selection of CFb using a fibroblast-specific surface marker. One possible candidate would be DDR2. Our initial attempts at biotinylating DDR2 antibodies and using an anti-biotin secondary approach for magnetic sorting were not successful. This is still an area of future consideration, but will require additional development as directly conjugated magnetized anti-DDR2 antibodies are not commercially available and DDR2 protein expression in cultured CFb was weakly expressed.

2.5.4 Concluding Remarks

In summary, MΦ are a significant contaminating cell type frequently found in CFb cultures and are often undetected or overlooked during culture characterization. Their presence was shown in our studies to alter the characteristics of CFb S1P receptor expression and to affect migration assay results. Unwanted or contaminating cells have been reported to interfere with experimental interpretation involving other cell types. In studies of neutrophils,[112] monocyte contamination has been suspected to account for variations in neutrophil activation and apoptosis rates, as the results varied when highly purified populations of neutrophils were used. Similarly, we propose caution in the interpretation of experimental results from cultures that have not been adequately

characterized and screened for MΦ contamination. We further suggest that fibroblasts isolated from other tissues may also experience similar types of MΦ contamination and propose that the findings presented herein may thus have broader implications beyond those studies involving cardiac cells.

2.6 Chapter acknowledgement

This chapter was modified from the following manuscript: Landeen L.K., Aroonsakool N., Haga J.H., Hu B.S., Giles W.R., Sphingosine-1-Phosphate Receptor Expression in Cardiac Fibroblast Cells is Modulated by in vitro Culture Conditions, *American Journal of Physiology: Heart and Circulatory Physiology*, 2007 (in press). The Dissertation author (LL) was the principal investigator/author of this paper.

We would like to sincerely thank Dr. Masahiko Hoshijima and Dr. Shu Chien of the University of California, San Diego for allowing us to use their qPCR machines for S1P receptor expression assays.

This work was supported in part by a grant from the American Heart Association Western States Affiliate Program. Lee Landeen was supported by a graduate research fellowship from the National Science Foundation.

2.7 References

1. Agocha,A.E. & Eghbali-Webb,M. A simple method for preparation of cultured cardiac fibroblasts from adult human ventricular tissue. *Mol. Cell Biochem.* 172, 195-198 (1997).

2. Artuc,M., Hermes,B., Steckelings,U.M., Grutzkau,A. & Henz,B.M. Mast cells and their mediators in cutaneous wound healing--active participants or innocent bystanders? *Exp. Dermatol.* 8, 1-16 (1999).

3. Arya,M. *et al.* Basic principles of real-time quantitative PCR. *Expert. Rev. Mol. Diagn.* 5, 209-219 (2005).

4. Assoian,R.K. *et al.* Expression and secretion of type beta transforming growth factor by activated human macrophages. *Proc. Natl. Acad. Sci. U. S. A.* 84, 6020-6024 (1987).

5. Austyn,J.M. & Gordon,S. F4/80, a monoclonal antibody directed specifically against the mouse macrophage. *Eur. J. Immunol.* 11, 805-815 (1981).

6. Austyn,J.M. *et al.* Isolation and characterization of dendritic cells from mouse heart and kidney. *J. Immunol.* 152, 2401-2410 (1994).

7. Azzawi,M. *et al.* The distribution of cardiac macrophages in myocardial ischaemia and cardiomyopathy. *Histopathology* 46, 314-319 (2005).

8. Balogh,J. *et al.* Phospholipase C and cAMP-dependent positive inotropic effects of ATP in mouse cardiomyocytes via P2Y11-like receptors. *J. Mol. Cell Cardiol.* 39, 223-230 (2005).

9. Baudino,T., Carver,W., Giles,W.R. & Borg,T.K. Cardiac Fibroblasts: friend or foe? *Am. J. Physiol Heart Circ. Physiol.* 293, H1015-H1026 (2006).

10. Benhaiem-Sigaux,N. *et al.* Characterization of human pericardial macrophages. *J. Leukoc. Biol.* 38, 709-721 (1985).

11. Bertrand,S., Godoy,M., Semal,P. & Van Gansen,P. Transdifferentiation of macrophages into fibroblasts as a result of Schistosoma mansoni infection. *Int. J. Dev. Biol.* 36, 179-184 (1992).

12. Beyer,E.C. & Steinberg,T.H. Evidence that the gap junction protein connexin-43 is the ATP-induced pore of mouse macrophages. *J. Biol. Chem.* 266, 7971-7974 (1991).

13. Borel,J.F. & Feurer,C. Chemotaxis of rabbit macrophages in vitro: inhibition by drugs. *Experientia* 31, 1437-1439 (1975).

14. Brixius,K. & Schwinger,R.H. Modulation of cross-bridge interaction by 2,3-butanedione monoxime in human ventricular myocardium. *Naunyn Schmiedebergs Arch. Pharmacol.* 361, 440-444 (2000).

15. Brodbeck,W.G., Colton,E. & Anderson,J.M. Effects of adsorbed heat labile serum proteins and fibrinogen on adhesion and apoptosis of monocytes/macrophages on biomaterials. *J. Mater. Sci. Mater. Med.* 14, 671-675 (2003).

16. Brodbeck,W.G., Macewan,M., Colton,E., Meyerson,H. & Anderson,J.M. Lymphocytes and the foreign body response: lymphocyte enhancement of macrophage adhesion and fusion. *J. Biomed. Mater. Res. A* 74, 222-229 (2005).

17. Brouckaert,G. *et al.* Phagocytosis of necrotic cells by macrophages is phosphatidylserine dependent and does not induce inflammatory cytokine production. *Mol. Biol. Cell.* 15, 1089-1100 (2004).

18. Brouty-Boye,D., Kolonias,D., Savaraj,N. & Lampidis,T.J. Alpha-smooth muscle actin expression in cultured cardiac fibroblasts of newborn rat. *In Vitro Cell Dev. Biol.* 28A, 293-296 (1992).

19. Bunch,T.J. *et al.* Impact of transforming growth factor-beta1 on atrioventricular node conduction modification by injected autologous fibroblasts in the canine heart. *Circulation.* 113, 2485-2494 (2006).

20. Cameron,V.A. *et al.* Atrial (ANP) and brain natriuretic peptide (BNP) expression after myocardial infarction in sheep: ANP is synthesized by fibroblasts infiltrating the infarct. *Endocrinology* 141, 4690-4697 (2000).

21. Chae,S.S., Proia,R.L. & Hla,T. Constitutive expression of the $S1P_1$ receptor in adult tissues. *Prostaglandins Other Lipid Mediat.* 73, 141-150 (2004).

22. Chun,J. *et al.* International Union of Pharmacology. XXXIV. Lysophospholipid receptor nomenclature. *Pharmacol. Rev.* 54, 265-269 (2002).

23. Cocco,R.E. & Ucker,D.S. Distinct modes of macrophage recognition for apoptotic and necrotic cells are not specified exclusively by phosphatidylserine exposure. *Mol. Biol. Cell.* 12, 919-930 (2001).

24. Colston,J.T., Chandrasekar,B. & Freeman,G.L. A novel peroxide-induced calcium transient regulates interleukin-6 expression in cardiac-derived fibroblasts. *J. Biol. Chem.* 277, 23477-23483 (2002).

25. Colston,J.T., de la Rosa,S.D., Strader,J.R., Anderson,M.A. & Freeman,G.L. H2O2 activates Nox4 through PLA2-dependent arachidonic acid production in adult cardiac fibroblasts. *FEBS Lett.* 579, 2533-2540 (2005).

26. Correia,I., Chu,D., Chou,Y.H., Goldman,R.D. & Matsudaira,P. Integrating the actin and vimentin cytoskeletons. adhesion-dependent formation of fimbrin-vimentin complexes in macrophages. *J. Cell Biol.* 146, 831-842 (1999).

27. Curtis,A.S. & Forrester,J.V. The competitive effects of serum proteins on cell adhesion. *J. Cell Sci.* 71:17-35., 17-35 (1984).

28. Cvetanovic,M. & Ucker,D.S. Innate immune discrimination of apoptotic cells: repression of proinflammatory macrophage transcription is coupled directly to specific recognition. *J. Immunol.* 172, 880-889 (2004).

29. Davis,G.E., Bayless,K.J., Davis,M.J. & Meininger,G.A. Regulation of tissue injury responses by the exposure of matricryptic sites within extracellular matrix molecules. *Am. J. Pathol.* 156, 1489-1498 (2000).

30. DeCoursey,T.E., Kim,S.Y., Silver,M.R. & Quandt,F.N. Ion channel expression in PMA-differentiated human THP-1 macrophages. *J. Membr. Biol.* 152, 141-157 (1996).

31. Domeij,H., Yucel-Lindberg,T. & Modeer,T. Cell interactions between human gingival fibroblasts and monocytes stimulate the production of matrix metalloproteinase-1 in gingival fibroblasts. *J. Periodontal Res.* 41, 108-117 (2006).

32. Duong,C.Q. *et al.* Expression of the lysophospholipid receptor family and investigation of lysophospholipid-mediated responses in human macrophages. *Biochim. Biophys. Acta* 1682, 112-119 (2004).

33. Eghbali,M. *et al.* Collagen chain mRNAs in isolated heart cells from young and adult rats. *J. Mol. Cell Cardiol.* 20, 267-276 (1988).

34. English,D. & Gabig,T.G. Differentiation of cellular processes involved in the induction and maintenance of stimulated neutrophil adherence. *Blood* 67, 1314-1322 (1986).

35. Eugenin,E.A., Branes,M.C., Berman,J.W. & Saez,J.C. TNF-alpha plus IFN-gamma induce connexin43 expression and formation of gap junctions between human monocytes/macrophages that enhance physiological responses. *J. Immunol.* 170, 1320-1328 (2003).

36. Eyden,B. The myofibroblast: an assessment of controversial issues and a definition useful in diagnosis and research. *Ultrastruct. Pathol.* 25, 39-50 (2001).

37. Fast,V.G., Darrow,B.J., Saffitz,J.E. & Kleber,A.G. Anisotropic activation spread in heart cell monolayers assessed by high-resolution optical mapping. Role of tissue discontinuities. *Circ. Res.* 79, 115-127 (1996).

38. Feld,Y. *et al.* Electrophysiological modulation of cardiomyocytic tissue by transfected fibroblasts expressing potassium channels: a novel strategy to manipulate excitability. *Circulation* 105, 522-529 (2002).

39. Fitzgerald,S.M. *et al.* GM-CSF induction in human lung fibroblasts by IL-1beta, TNF-alpha, and macrophage contact. *J. Interferon Cytokine Res.* 23, 57-65 (2003).

40. Freshney,R.I. Culture of animal cells. Wiley-Liss, New York (2005).

41. Fukushima,N., Ishii,I., Contos,J.J., Weiner,J.A. & Chun,J. Lysophospholipid receptors. *Annu. Rev. Pharmacol. Toxicol.* 41:507-34., 507-534 (2001).

42. Futerman,A.H. & Hannun,Y.A. The complex life of simple sphingolipids. *Eur. Mol. Biol. Organization* 5, 777-782 (2004).

43. Gabbiani,G. The myofibroblast in wound healing and fibrocontractive diseases. *J. Pathol.* 200, 500-503 (2003).

44. Gabbiani,G. *et al.* Vascular smooth muscle cells differ from other smooth muscle cells: predominance of vimentin filaments and a specific alpha-type actin. *Proc. Natl. Acad. Sci. U. S. A* 78, 298-302 (1981).

45. Gabourel,J.D., Moore,M.A., Bagby,G.C., Jr. & Davies,G.H. Effect of sodium salicylate on human and mouse granulopoiesis in vitro. *Arthritis Rheum.* 20, 59-64 (1977).

46. Gadea,G. *et al.* TNFalpha induces sequential activation of Cdc42- and p38/p53-dependent pathways that antagonistically regulate filopodia formation. *J. Cell Sci.* 117, 6355-6364 (2004).

47. Gaudesius,G., Miragoli,M., Thomas,S.P. & Rohr,S. Coupling of cardiac electrical activity over extended distances by fibroblasts of cardiac origin. *Circ. Res.* 93, 421-428 (2003).

48. Gaur,U. & Aggarwal,B.B. Regulation of proliferation, survival and apoptosis by members of the TNF superfamily. *Biochem. Pharmacol.* 66, 1403-1408 (2003).

49. Gill,J.F. *et al.* Safety testing of Liberase, a purified enzyme blend for human islet isolation. *Transplant. Proc.* 27, 3276-3277 (1995).

50. Godoy,M., Geuskens,M., Van Marck,E.A., Borojevic,R. & Van Gansen,P. Schistosomiasis and in vitro transdifferentiation of murine peritoneal macrophages into fibroblastic cells. *Parasitol. Res.* 76, 150-161 (1989).

51. Goldsmith,E.C. *et al.* Organization of fibroblasts in the heart. *Dev. Dyn.* 230, 787-794 (2004).

52. Heidenthal,A.K., Weber,P.C., Lottspeich,F. & Hrboticky,N. The binding in vitro of modified LDL to the intermediate filament protein vimentin. *Biochem. Biophys. Res. Commun.* 267, 49-53 (2000).

53. Hewett,P.W. & Murray,J.C. Human microvessel endothelial cells: isolation, culture and characterization. *In Vitro Cell Dev. Biol. Anim.* 29A, 823-830 (1993).

54. Hoffmann,S. *et al.* Rapid isolation of choriocapillary endothelial cells by Lycopersicon esculentum-coated Dynabeads. *Graefes Arch. Clin. Exp. Ophthalmol.* 236, 779-784 (1998).

55. Hughes,D.A., Fraser,I.P. & Gordon,S. Murine M phi scavenger receptor: adhesion function and expression. *Immunol. Lett.* 43, 7-14 (1994).

56. Huybrechts-Godin,G., Hauser,P. & Vaes,G. Macrophage-fibroblast interactions in collagenase production and cartilage degradation. *Biochem. J.* 184, 643-650 (1979).

57. Inoue,T., Plieth,D., Venkov,C.D., Xu,C. & Neilson,E.G. Antibodies against macrophages that overlap in specificity with fibroblasts. *Kidney Int.* 67, 2488-2493 (2005).

58. Iwasaki,H., Isayama,T., Ichiki,T. & Kikuchi,M. Intermediate filaments of myofibroblasts. Immunochemical and immunocytochemical analyses. *Pathol. Res. Pract.* 182, 248-254 (1987).

59. Jabs,A., Moncada,G.A., Nichols,C.E., Waller,E.K. & Wilcox,J.N. Peripheral blood mononuclear cells acquire myofibroblast characteristics in granulation tissue. *J. Vasc. Res.* 42, 174-180 (2005).

60. Jahr,H., Pfeiffer,G., Hering,B.J., Federlin,K. & Bretzel,R.G. Endotoxin-mediated activation of cytokine production in human PBMCs by collagenase and Ficoll. *J. Mol. Med.* 77, 118-120 (1999).

61. Kamohara,H., Yamashiro,S., Galligan,C. & Yoshimura,T. Discoidin domain receptor 1 isoform-a (DDR1alpha) promotes migration of leukocytes in three-dimensional collagen lattices. *FASEB J.* 15, 2724-2726 (2001).

62. Katoh,M. *et al.* Cardiac angiotensin II receptors are upregulated by long-term inhibition of nitric oxide synthesis in rats. *Circ. Res.* 83, 743-751 (1998).

63. Kaushansky,K., Lopez,J.A. & Brown,C.B. Role of carbohydrate modification in the production and secretion of human granulocyte macrophage colony-stimulating factor in genetically engineered and normal mesenchymal cells. *Biochemistry* 31, 1881-1886 (1992).

64. Kern,S., Robertson,S.A., Mau,V.J. & Maddocks,S. Cytokine secretion by macrophages in the rat testis. *Biol. Reprod.* 53, 1407-1416 (1995).

65. Kim,J.G., Keshava,C., Murphy,A.A., Pitas,R.E. & Parthasarathy,S. Fresh mouse peritoneal macrophages have low scavenger receptor activity. *J. Lipid Res.* 38, 2207-2215 (1997).

66. Kim,N.N., Villarreal,F.J., Printz,M.P., Lee,A.A. & Dillmann,W.H. Trophic effects of angiotensin II on neonatal rat cardiac myocytes are mediated by cardiac fibroblasts. *Am. J. Physiol* 269, E426-E437 (1995).

67. Kim,S.Y., Silver,M.R. & DeCoursey,T.E. Ion channels in human THP-1 monocytes. *J. Membr. Biol.* 152, 117-130 (1996).

68. Kitchens,R.L. Role of CD14 in cellular recognition of bacterial lipopolysaccharides. *Chem. Immunol.* 74:61-82., 61-82 (2000).

69. Kohn,F.R. & Klingemann,H.G. Regulation of fibronectin receptor (alpha 5 beta 1) mRNA expression in human monocytes and monocyte-derived macrophages by activation/differentiation signals. *Exp. Hematol.* 19, 653-658 (1991).

70. Kownatzki,E., Weil,B. & Uhrich,S. The effects of bovine serum albumin and the chemotactic peptide formyl-methionyl-leucyl-phenylalanine on the adherence of guinea pig polymorphonuclear leukocytes to nylon fiber columns. *Immunobiology* 159, 392-401 (1981).

71. Koyama,Y. *et al.* Type I collagen is a non-adhesive extracellular matrix for macrophages. *Arch. Histol. Cytol.* 63, 71-79 (2000).

72. Kreis,S., Schonfeld,H.J., Melchior,C., Steiner,B. & Kieffer,N. The intermediate filament protein vimentin binds specifically to a recombinant integrin alpha2/beta1 cytoplasmic tail complex and co-localizes with native alpha2/beta1 in endothelial cell focal adhesions. *Exp. Cell Res.* 305, 110-121 (2005).

73. Krutzik,S.R. *et al.* TLR activation triggers the rapid differentiation of monocytes into macrophages and dendritic cells. *Nat. Med.* 11, 653-660 (2005).

74. Kubo,A. *et al.* C-type natriuretic peptide is synthesized and secreted from leukemia cell lines, peripheral blood cells, and peritoneal macrophages. *Exp. Hematol.* 29, 609-615 (2001).

75. Kubo,A. *et al.* Production of adrenomedullin in macrophage cell line and peritoneal macrophage. *J. Biol. Chem.* 273, 16730-16738 (1998).

76. Kunisch,E. *et al.* Macrophage specificity of three anti-CD68 monoclonal antibodies (KP1, EBM11, and PGM1) widely used for immunohistochemistry and flow cytometry. *Ann. Rheum. Dis.* 63, 774-784 (2004).

77. Kunz-Schughart,L.A., Wenninger,S., Neumeier,T., Seidl,P. & Knuechel,R. Three-dimensional tissue structure affects sensitivity of fibroblasts to TGF-beta 1. *Am. J. Physiol Cell Physiol* 284, C209-C219 (2003).

78. Laskin,D.L., Soltys,R.A., Berg,R.A. & Riley,D.J. Activation of alveolar macrophages by native and synthetic collagen-like polypeptides. *Am. J. Respir. Cell Mol. Biol.* 10, 58-64 (1994).

79. Leask,A., Holmes,A. & Abraham,D.J. Connective tissue growth factor: a new and important player in the pathogenesis of fibrosis. *Curr. Rheumatol. Rep.* 4, 136-142 (2002).

80. Li,M.O., Wan,Y.Y., Sanjabi,S., Robertson,A.K. & Flavell,R.A. Transforming growth factor-beta regulation of immune responses. *Annu. Rev. Immunol.* 24, 99-146 (2006).

81. Lijnen,P., Petrov,V. & Fagard,R. Transforming growth factor-beta 1-mediated collagen gel contraction by cardiac fibroblasts. *J. Renin. Angiotensin. Aldosterone. Syst.* 4, 113-118 (2003).

82. Lijnen,P., Petrov,V., Rumilla,K. & Fagard,R. Transforming growth factor-beta 1 promotes contraction of collagen gel by cardiac fibroblasts through their differentiation into Myofibroblasts. *Methods Find. Exp. Clin. Pharmacol.* 25, 79-86 (2003).

83. Linetsky,E., Inverardi,L., Kenyon,N.S., Alejandro,R. & Ricordi,C. Endotoxin contamination of reagents used during isolation and purification of human pancreatic islets. *Transplant. Proc.* 30, 345-346 (1998).

84. Livak,K.J. & Schmittgen,T.D. Analysis of relative gene expression data using real-time quantitative PCR and the 2(-Delta Delta C(T)) Method. *Methods* 25, 402-408 (2001).

85. Lucas,M., Stuart,L.M., Savill,J. & Lacy-Hulbert,A. Apoptotic cells and innate immune stimuli combine to regulate macrophage cytokine secretion. *J. Immunol.* 171, 2610-2615 (2003).

86. Martinez-Gonzalez,J., Berrozpe,M., Varela,O. & Badimon,L. Heterogeneity of smooth muscle cells in advanced human atherosclerotic plaques: intimal smooth muscle cells expressing a fibroblast surface protein are highly activated by platelet-released products. *Eur. J. Clin. Invest* 31, 939-949 (2001).

87. Martino,A. *et al.* Sphingosine 1-Phosphate Interferes on the Differentiation of Human Monocytes into Competent Dendritic Cells. *Scand. J. Immunol.* 65, 84-91 (2007).

88. Matsuyama,W., Wang,L., Farrar,W.L., Faure,M. & Yoshimura,T. Activation of discoidin domain receptor 1 isoform b with collagen up-regulates chemokine production in human macrophages: role of p38 mitogen-activated protein kinase and NF-kappa B. *J. Immunol.* 172, 2332-2340 (2004).

89. Mazurais,D. *et al.* Cell type-specific localization of human cardiac S1P receptors. *J. Histochem. Cytochem.* 50, 661-670 (2002).

90. McCann,F.V., Cole,J.J., Guyre,P.M. & Russell,J.A. Action potentials in macrophages derived from human monocytes. *Science* 219, 991-993 (1983).

91. Melendez,A.J. & Ibrahim,F.B. Antisense knockdown of sphingosine kinase 1 in human macrophages inhibits C5a receptor-dependent signal transduction, Ca^{2+} signals, enzyme release, cytokine production, and chemotaxis. *J. Immunol.* 173, 1596-1603 (2004).

92. Mor-Vaknin,N., Punturieri,A., Sitwala,K. & Markovitz,D.M. Vimentin is secreted by activated macrophages. *Nat. Cell Biol.* 5, 59-63 (2003).

93. Morales,M.O., Price,R.L. & Goldsmith,E.C. Expression of Discoidin Domain Receptor 2 (DDR2) in the developing heart. *Microsc. Microanal.* 11, 260-267 (2005).

94. Nag,A.C. Study of non-muscle cells of the adult mammalian heart: a fine structural analysis and distribution. *Cytobios* 28, 41-61 (1980).

95. Okamura,A. *et al.* Upregulation of renin-angiotensin system during differentiation of monocytes to macrophages. *J. Hypertens.* 17, 537-545 (1999).

96. Olivera,A. & Spiegel,S. Sphingosine-1-phosphate as second messenger in cell proliferation induced by PDGF and FCS mitogens. *Nature* 365, 557-560 (1993).

97. Osawa,Y. *et al.* Roles for C16-ceramide and sphingosine 1-phosphate in regulating hepatocyte apoptosis in response to tumor necrosis factor-alpha. *J. Biol. Chem.* 280, 27879-27887 (2005).

98. Paine,R., III *et al.* Impaired functional activity of alveolar macrophages from GM-CSF-deficient mice. *Am. J. Physiol Lung Cell Mol. Physiol* 281, L1210-L1218 (2001).

99. Patil,R.R. & Borch,R.F. Granulocyte-macrophage colony-stimulating factor expression by human fibroblasts is both upregulated and subsequently downregulated by interleukin-1. *Blood* 85, 80-86 (1995).

100. Pearlstein,E., Dienstman,S.R. & Defendi,V. Identification of macrophage external membrane proteins and their possible role in cell adhesion. *J. Cell Biol.* 79, 263-267 (1978).

101. Peters,J.H., Ruhl,S. & Friedrichs,D. Veiled accessory cells deduced from monocytes. *Immunobiology.* 176, 154-166 (1987).

102. Petrov,V.V., Fagard,R.H. & Lijnen,P.J. Transforming growth factor-beta(1) induces angiotensin-converting enzyme synthesis in rat cardiac fibroblasts during their differentiation to myofibroblasts. *J. Renin. Angiotensin. Aldosterone. Syst.* 1, 342-352 (2000).

103. Pfaffl,M.W. A new mathematical model for relative quantification in real-time RT-PCR. *Nucleic Acids Res.* 29, e45 (2001).

104. Pfaffl,M.W., Horgan,G.W. & Dempfle,L. Relative expression software tool (REST) for group-wise comparison and statistical analysis of relative expression results in real-time PCR. *Nucleic Acids Res.* 30, e36 (2002).

105. Phillips,R.M. & Altschuld,R.A. 2,3-Butanedione 2-monoxime (BDM) induces calcium release from canine cardiac sarcoplasmic reticulum. *Biochem. Biophys. Res. Commun.* 229, 154-157 (1996).

106. Pollice,A.A. *et al.* Sequential paraformaldehyde and methanol fixation for simultaneous flow cytometric analysis of DNA, cell surface proteins, and intracellular proteins. *Cytometry* 13, 432-444 (1992).

107. Pyne,S. & Pyne,N.J. Sphingosine 1-phosphate signalling in mammalian cells. *Biochem. J.* 349, 385-402 (2000).

108. Rainard,P. Adherence, spreading, and locomotion of bovine polymorphs: effect of proteins and metabolic inhibitors. *Vet. Immunol. Immunopathol.* 18, 129-137 (1988).

109. Rook,M.B. *et al.* Differences in gap junction channels between cardiac myocytes, fibroblasts, and heterologous pairs. *Am. J. Physiol* 263, C959-C977 (1992).

110. Rosen,H. & Goetzl,E.J. Sphingosine 1-phosphate and its receptors: an autocrine and paracrine network. *Nat. Rev. Immunol.* 5, 560-570 (2005).

111. Rosmarin,A.G. *et al.* Differential expression of CD11b/CD18 (Mo1) and myeloperoxidase genes during myeloid differentiation. *Blood.* 73, 131-136 (1989).

112. Sabroe,I. *et al.* What can we learn from highly purified neutrophils? *Biochem. Soc. Trans.* 32, 468-469 (2004).

113. Savikko,J. & von Willebrand,E. Coexpression of platelet-derived growth factors AA and BB and their receptors during monocytic differentiation. *Transplant. Proc.* 33, 2307-2308 (2001).

114. Song,E. *et al.* Influence of alternatively and classically activated macrophages on fibrogenic activities of human fibroblasts. *Cell Immunol.* 204, 19-28 (2000).

115. Spiegel,S. & Milstien,S. Sphingosine-1-phosphate: an enigmatic signalling lipid. *Nat. Rev. Mol. Cell Biol.* 4, 397-407 (2003).

116. Starkey,P.M., Turley,L. & Gordon,S. The mouse macrophage-specific glycoprotein defined by monoclonal antibody F4/80: characterization, biosynthesis and demonstration of a rat analogue. *Immunology.* 60, 117-122 (1987).

117. Taha,T.A., Argraves,K.M. & Obeid,L.M. Sphingosine-1-phosphate receptors: receptor specificity versus functional redundancy. *Biochim. Biophys. Acta* 1682, 48-55 (2004).

118. Takahashi,K. *et al.* Taurine renders the cell resistant to ischemia-induced injury in cultured neonatal rat cardiomyocytes. *J. Cardiovasc. Pharmacol.* 41, 726-733 (2003).

119. Takatani,T. *et al.* Taurine prevents the ischemia-induced apoptosis in cultured neonatal rat cardiomyocytes through Akt/caspase-9 pathway. *Biochem. Biophys. Res. Commun.* 316, 484-489 (2004).

120. Talbot,N.C., Paape,M., Sohn,E.J. & Garrett,W.M. Macrophage population dynamics within fetal mouse fibroblast cultures derived from C57BL/6, CD-1, CF-1 mice and interleukin-6 and granulocyte colony stimulating factor knockout mice. *In Vitro Cell Dev. Biol. Anim* 40, 196-210 (2004).

121. Terstappen,L.W., Hollander,Z., Meiners,H. & Loken,M.R. Quantitative comparison of myeloid antigens on five lineages of mature peripheral blood cells. *J. Leukoc. Biol.* 48, 138-148 (1990).

122. Thibault,G. *et al.* Upregulation of alpha(8)beta(1)-integrin in cardiac fibroblast by angiotensin II and transforming growth factor-beta1. *Am. J. Physiol Cell Physiol* 281, C1457-C1467 (2001).

123. Tomoda,Y., Isumi,Y., Katafuchi,T. & Minamino,N. Regulation of adrenomedullin secretion from cultured cells. *Peptides* 22, 1783-1794 (2001).

124. Tsai,V., Firestein,G.S., Arend,W. & Zvaifler,N.J. Cytokine-induced differentiation of cultured nonadherent macrophages. *Cell Immunol.* 144, 203-216 (1992).

125. Urata,Y., Nishimura,Y., Hirase,T. & Yokoyama,M. Sphingosine 1-phosphate induces alpha-smooth muscle actin expression in lung fibroblasts via Rho-kinase. *Kobe J. Med. Sci.* 51, 17-27 (2005).

126. Vargas,F. *et al.* Endotoxin contamination may be responsible for the unexplained failure of human pancreatic islet transplantation. *Transplantation.* 65, 722-727 (1998).

127. Vaughan,M.B., Howard,E.W. & Tomasek,J.J. Transforming growth factor-beta1 promotes the morphological and functional differentiation of the myofibroblast. *Exp. Cell Res.* 257, 180-189 (2000).

128. Viken,K.E. Effect of sodium-salicylate on the function of cultured, human mononuclear cells. *Acta Pathol. Microbiol. Scand. [C.]* 84C, 465-470 (1976).

129. Villarreal,F.J., Kim,N.N., Ungab,G.D., Printz,M.P. & Dillmann,W.H. Identification of functional angiotensin II receptors on rat cardiac fibroblasts. *Circulation* 88, 2849-2861 (1993).

130. Waldo,S.W., Rosario,H.S., Penn,A.H. & Schmid-Schonbein,G.W. Pancreatic digestive enzymes are potent generators of mediators for leukocyte activation and mortality. *Shock.* 20, 138-143 (2003).

131. Wang,J., Chen,H., Seth,A. & McCulloch,C.A. Mechanical force regulation of myofibroblast differentiation in cardiac fibroblasts. *Am. J. Physiol Heart Circ. Physiol* 285, H1871-H1881 (2003).

132. Wang,J., Lukse,E., Seth,A. & McCulloch,C.A. Use of conditionally immortalized mouse cardiac fibroblasts to examine the effect of mechanical stretch on alpha-smooth muscle actin. *Tissue Cell* 33, 86-96 (2001).

133. Weber,K.T. & Sun,Y. Recruitable ACE and tissue repair in the infarcted heart. *J. Renin. Angiotensin. Aldosterone. Syst.* 1, 295-303 (2000).

134. Xu,K. *et al.* Strong red fluorescent probes suitable for detecting hydrogen peroxide generated by mice peritoneal macrophages. *Chem. Commun. (Camb.).* 5974-5976 (2005).

135. Yamanaka,M. *et al.* Sphingosine kinase 1 (SPHK1) is induced by transforming growth factor-beta and mediates TIMP-1 up-regulation. *J. Biol. Chem.* 279, 53994-54001 (2004).

136. Yatomi,Y., Ruan,F., Hakomori,S. & Igarashi,Y. Sphingosine-1-phosphate: a platelet-activating sphingolipid released from agonist-stimulated human platelets. *Blood* 86, 193-202 (1995).

137. Yokoyama,H. *et al.* Cardiac dendritic cells and acute myocarditis in the human heart. *Jpn. Circ. J.* 64, 57-64 (2000).

138. Zhu,Y. *et al.* Collaborative interactions between neutrophil elastase and metalloproteinases in extracellular matrix degradation in three-dimensional collagen gels. *Respir. Res.* 2, 300-305 (2001).

139. Zhu,Y. *et al.* Fibroblasts and monocyte macrophages contract and degrade three-dimensional collagen gels in extended co-culture. *Respir. Res.* 2, 295-299 (2001).

CHAPTER 3

MODULATION OF SPHINGOSINE-1-PHOSPHATE RECEPTOR EXPRESSION IN CARDIAC FIBROBLASTS

3.1 Abstract

The bioactive molecule sphingosine-1-phosphate (S1P) binds with high affinity to five recognized receptors ($S1P_{1-5}$) which are ubiquitously expressed on various mammalian cell types. S1P receptors are coupled to G-proteins, and activation of specific isoforms (subtypes) can affect such cellular behaviors as intracellular calcium concentrations, differentiation, and migration. We investigated the expression of S1P receptor isoforms on ventricular fibroblasts acutely isolated from the adult mouse and after exposure to various in vitro culture conditions to understand parameters that can modulate specific isoforms. In particular, we focused on factors that may be derived from macrophages (MΦ) and factors that could affect cardiac fibroblast (CFb) migration.

Our results demonstrate that primary isolated, purified CFb express predominantly $S1P_{1-3}$; however, the relative levels of these receptor subtypes are modulated with time and by culture conditions. In co-culture experiments, MΦ altered CFb S1P receptor levels relative to controls. Further investigations using known MΦ-secreted factors showed that S1P and hydrogen peroxide (H_2O_2) had minimal effects on CFb $S1P_{1-3}$ expression, whereas transforming growth factor beta-1 (TFGβ1), tumor necrosis factor alpha (TNFα), and platelet-derived growth factor BB (PDGF-BB) significantly altered all S1P receptor subtypes. Lowering fetal bovine serum (FBS)

concentrations from 10% to 0.1% increased $S1P_2$, whereas supplementation with either PDGF-BB or the Rho-associated protein kinase inhibitor Y-27632 significantly elevated $S1P_3$ levels. Similarly, an inhibitor of Rac 1 decreased levels of $S1P_3$. $S1P_2$ and $S1P_3$ receptors are known to regulate cell migration. Using cells isolated from either wild-type or $S1P_3$-null mice, we demonstrate that $S1P_3$ is important and necessary for CFb migration, but not so for MΦ migration. These results highlight the relationships between S1P receptor isoforms and migration and the ability of multiple factors to alter expression levels. Since several factors secreted by MΦ were capable of altering S1P receptor isoforms, this may have implications towards studies with unknown CFb culture purity and may also suggest response mechanisms within normal and compromised myocardium.

3.2 Introduction

Sphingosine-1-phosphate (S1P) is a biologically active, cell membrane-associated sphingolipid that is secreted by various cells upon activation. S1P binds with high affinity to five distinct G protein-coupled receptors (GPCR), also referred to as endothelial differentiation gene (EDG) receptors. S1P receptors are ubiquitously expressed on mammalian cells and can affect such cellular behaviors as proliferation, differentiation, and migration (reviewed in [1,7,8,33,35,42]). In order to characterize accurately S1P regulation, it is therefore necessary to have pure populations of cells.

We previously reported on methods for consistently obtaining highly purified cultures of cardiac fibroblasts (CFb), which do not include any significant contaminating cell types (see Chapter 2). The findings of those studies demonstrated that macrophages

(MΦ) are frequently found to co-isolate with CFb. MΦ are known to secrete a number of paracrine factors that are capable of rapidly changing target cell behavior and phenotype (e.g. interleukins, cytokines, and growth factors),[3,10,15,22,25,26,31,39,40,51] In addition, MΦ are also a source of S1P.[27] We therefore investigated whether certain of these factors, either by direct-co-culture with MΦ or through addition of purified sources, could alter CFb phenotype by altering expression levels of S1P receptors. This has relevance not only for better understanding of paracrine signaling in native tissue, where CFb and MΦ are in close approximation,[28] but also in conditions of wound healing (e.g. granulation tissue or infracted myocardium) where MΦ play a prominent role.[6,29,45]

S1P receptor isoforms couple to overlapping and unique G-proteins. $S1P_1$ is exclusively coupled to G_i and is involved in migration of several cell types, including embryonic fibroblasts, endothelial cells, lymphocytes, and smooth muscle cells.[17,24,30,32,38,49] $S1P_2$ and $S1P_3$ can also couple to G_i. In addition, each can couple to either G_q, or $G_{12/13}$.[44,50] Activation of $S1P_2$ and $S1P_3$ can signal Rho and Rac pathways, respectively, via $G_{12/13}$.[21,44] Rho and Rac are important effector molecules involved in directed cell motion.[21,30,38,46] We investigated the consequences of interfering with Rho and Rac signaling pathways by using selective inhibitors. Lastly, we investigated the contributions of $S1P_2$ and $S1P_3$ receptor levels towards migration of CFb using culture conditions to modulate S1P receptor expression levels and through the use of CFb isolated from $S1P_3$-null mice.

3.3 Methods

3.3.1 Cell Isolation

Hearts from heparinized adult C57Bl/6 or $S1P_3$-null mice[19] were isolated under isoflurane anesthesia in accordance with protocols approved by the Institutional Animal Care and Use Committee and adhered to *Guidelines for the Care and Use of Laboratory Animals* (©1996). Isolated hearts were placed in calcium-free Tyrodes buffer (130 mM NaCl, 5.4 mM KCl, 0.3 mM Na_2HPO_4, 1 mM $MgCl_2$, 10 mM HEPES, 5.5 mM glucose, pH 7.2-7.4). After cannulation of the aorta with a blunted 21G needle, the heart was retrograde perfused with Tyrodes buffer to clear the coronary arteries. Each heart was then placed on a Langendorff apparatus and perfused at 3-5 ml/min for 5 min with oxygenated, 37°C Tyrodes buffer. After an additional 10-15 min of enzymatic digestion in Tyrodes buffer containing collagenase type 2 (1 mg/ml, Worthington Biochemical Corporation, Lakewood, NJ) and 40 μM $CaCl_2$, the ventricles were removed, gently triturated and filtered through 100-μm nylon mesh into modified Krebs-Henseleit buffer (100 mM K-glutamate, 10 mM K-aspartate, 25 mM KCl, 10 mM KH_2PO_4, 2 mM $MgSO_4$, 0.5 mM EGTA, 5 mM HEPES, 1% BSA, 20 mM glucose, 20 mM taurine, and 5 mM creatine; pH 7.2-7.4). Myocyte populations were removed by mild centrifugation (1 min, 50 x g, repeated twice). The CFb-containing supernatant was pelleted (5 min, 750 x g), resuspended, and pelleted again through a density gradient (4% BSA in Tyrodes buffer) to remove debris. The CFb-containing pellet was resuspended in 37°C culture medium (Dulbecco's Modified Eagles Medium supplemented with 10% FBS, L-glutamine, sodium pyruvate, and antibiotic-antimycotic), plated onto tissue culture plastic, and

allowed to incubate for 1-2 hr in a humidified, 5% CO_2 incubator at 37°C. After this attachment period, non-adherent cells were removed by aspiration, remaining cells were gently washed twice with calcium- and magnesium-free PBS (Ca^{++}/Mg^{++}-free PBS), and the cells were incubated with fresh culture medium.

Peritoneal MΦ were isolated from anesthetized adult mice by intraperitoneal lavage with MΦ buffer (Ca^{++}/Mg^{++}-free PBS containing 2 mM EDTA and 0.5% BSA) and gentle abdominal massage for 1 min, similar to methods previously described.[16]

3.3.2 MΦ Removal

The CFb-containing pellet was resuspended in ice-cold MΦ buffer and incubated on tissue culture plastic for 30 min at 4-8°C. The non-adherent cells (containing CFb) were collected and layered onto the 4% BSA density gradient. Cells were pelleted and resuspended in cold MΦ buffer and reacted with anti-CD11b antibodies for removal of MΦ via magnetic particle cell sorting (Miltenyi Biotech, Auburn, CA).

3.3.3 PCR

Cells were lysed, total RNA was isolated by silica-gel columns using RNeasy kits (QIAGEN, Valencia, CA) and eluted in water, and cDNA was reverse transcribed from mRNA by oligo-dT priming and Omniscript reverse transcriptase (QIAGEN). Expression levels of gene targets were characterized by SYBR Green[2] quantitative real-time PCR (qPCR) of cDNA using specific primer sets for GAPDH (5'-AACTTTGGCATTGTGGAAGG-3', 5'-ACACATTGGGGGTAGGAACA-3'), $S1P_4$

(5'-GGCTACTGGCAGCTATCCTG-3', 5'-AAGGCCACCAAGATCATCAG-3'), and $S1P_5$ (5'-GATCCCTTCCTGGGTCTAGC-3', 5'-TAGAGCTGCGATCCAAGGTT-3'). Expression levels of other S1P receptors were performed using Applied Biosystems (Foster City, CA) TaqMan® primer/probe sets as follows: $S1P_1$ (Mm00514644_m1), $S1P_2$ (Mm01177794_m1), $S1P_3$ (Mm00515669_m1), and GAPDH (Mm99999915_g1).

Primer sets for genotyping $S1P_3$-null mice were as previously reported[19] and are listed in Table 3.1.

Table 3.I $S1P_3$ Mouse Genotyping Primers

Allele	*Forward (5' – 3')*	*Reverse (5' – 3')*
+	TCAGTATCTTCACCGCCATT	AATCACTACGGTCCGCAGAA
–	GTGCAATCCATCTTGTTCAAT	AATCACTACGGTCCGCAGAA

Amplicon lengths for each primer set were confirmed by gel electrophoretic separation (2% agarose) with ethidium bromide visualization. All experimental data were reported relative to GAPDH levels using the $2^{-\Delta Ct}$ or $2^{-\Delta\Delta Ct}$ calculation methods, which were considered appropriate based on primer set efficiency determinations.[23]

3.3.4 Electrophoresis and Immunoblotting

NIH3T3 embryonic fibroblasts were lysed in ice-cold RIPA buffer consisting of 10 mM Tris, 50 mM NaCl, 1% Triton X-100, 30 nM sodium pyrophosphate, 50 mM NaF, 10% glycerol, and protease inhibitors (1:100 Protease Inhibitor Cocktail, Sigma). Whole cell lysates were clarified by centrifugation (13,000 xg, 10 min, 4°C) and the supernatants measured for total protein using the Bradford assay against a standard curve

of bovine serum albumin (BSA) in water. Protein concentrations were normalized to each other and equal amounts of protein were added to 4X Laemli loading buffer (200 mM Tris, 400 mM dithiothreitol, 8% sodium dodecyl sulfate, 40% glycerol, and 0.4% bromphenol blue). The samples were boiled for 5 min before loading onto 12% polyacrylamide gels and separated by electrophoresis (i.e. SDS-PAGE). Proteins were transferred from the gels to nitrocellulose membranes, blocked with 5% BSA, and incubated in appropriate, diluted primary antibodies for $S1P_1$ (Santa Cruz Biotechnology, Santa Cruz, CA; Abcam, Inc., Cambridge, MA). Detection and visualization of bands was accomplished using species-specific horseradish peroxidase (HRP)-conjugated secondary antibodies (Pierce, Rockford, IL) and chemiluminescence (Amersham ECL or Pierce Pico West ECL). Films were scanned for densitometry measurements using Scion Iimage software (Frederick, MD).

3.3.5 S1P Expression Experiments

Adult mouse CFb were purified based on CD11b sorting the day following isolation and plated at sub-confluent densities to multi-well plates in 10% FBS DMEM culture medium. In separate wells, cardiac MΦ (either CD11b-purified or as mixed CFb cultures) were seeded onto microporous cell culture inserts (BD Falcon, Bedford, MA; Corning Costar, Acton, MA; or Nalge Nunc, Rochester, NY) and allowed to attach. After this attachment period, the inserts were transferred to wells containing CFb and fresh culture medium was supplied. The cells were co-cultured for an additional 3 days at which time they were washed in PBS and collected for PCR.

Alternatively, CD11b-purified CFb were seeded to multi-well plates, allowed to adhere, then dosed with various substances for 48 – 72 hr. These included TGFβ1 (Sigma), TNFα (Sigma), S1P (Avanti Polar Lipids, Alabaster, AL), H_2O_2 (Rite Aid, Harrisburg, PA), PDGF-BB (Sigma), IGF-I (Sigma), the Rho-associated protein kinase inhibitor Y-27632 (Sigma), or a Rac 1 inhibitor (Calbiochem, La Jolla, CA).

3.3.6 Migration Assay

Selected cell populations were seeded at relatively high density to 8-μm pore size modified Boyden migration chambers (BD Falcon or Corning Costar) and allowed to attach. The cells were then washed with PBS and "serum-starved" by overnight culture in 0.1% FBS DMEM culture medium. The medium was replaced with either 0.1% FBS DMEM control medium or treatment medium in the lower chamber (to establish a concentration gradient) and the cells were cultured for an additional 24 hr. These preparations were then fixed and stained for MΦ (anti-F4/80), counterstained with DAPI, and the non-migrating cells on the upper membrane surface were removed by physical abrasion using a cotton swab. The surface of the lower membrane of the migration chamber was then analyzed using epifluorescent microscopy as described previously. In addition, captured images of cell nuclei were counted using ImagePro Plus software.

3.3.7 Statistical Analyses

Results from replicate experiments were averaged and are presented as mean and standard deviation (SD). Results were analyzed for ANOVA (with Bonferonni t-test

post-hoc testing) or Student's t-test. Significant differences were accepted for results with $p<0.05$.

3.4 Results

3.4.1 Expression of S1P Receptor Subtypes in Isolated CFb

Primary isolated CFb from adult mice were characterized after purification and were found to express predominantly $S1P_1$, $S1P_2$, and $S1P_3$ receptor subtypes (Figure 3.1). Expression levels of $S1P_4$ and $S1P_5$ were approximately 50-fold and 150-fold lower, respectively, than either $S1P_{1-3}$ (see Figure 2.10 for $S1P_4$ and $S1P_5$ expression data). Accordingly, $S1P_4$ and $S1P_5$ levels were omitted from analysis in the studies reported here. The relative S1P receptor expression levels for 1-day-old CFb, when normalized to $S1P_1$, showed that $S1P_3$ was most abundant and that $S1P_2$ was expressed the least (Figure 3.1). With extended time in culture (4 days), however, the levels of $S1P_2$ and $S1P_3$ (relative to $S1P_1$) changed. $S1P_2$ was noted to increase whereas $S1P_3$ was noted to decrease slightly with time.

3.4.2 Modulation of S1P Receptor Expression in CFb by Direct MΦ Co-Culture

The nature of these CFb studies necessitated the use of qPCR to assess changes in S1P receptor isoform expression levels due to limited numbers of available cells and the lack of high quality, commercially available antibodies. To address whether changes in receptor message expression actually reflect changes in protein expression, NIH3T3 fibroblasts were exposed to 10% or 1% FBS for 2 days and analyzed by qPCR and Western blotting for expression of $S1P_1$. As shown in Figure 3.2, 1% FBS induced an

increase in both message and protein levels of $S1P_1$ in NIH3T3 cells. Hereafter, the term "expression" is explicitly made in reference to expression levels of mRNA.

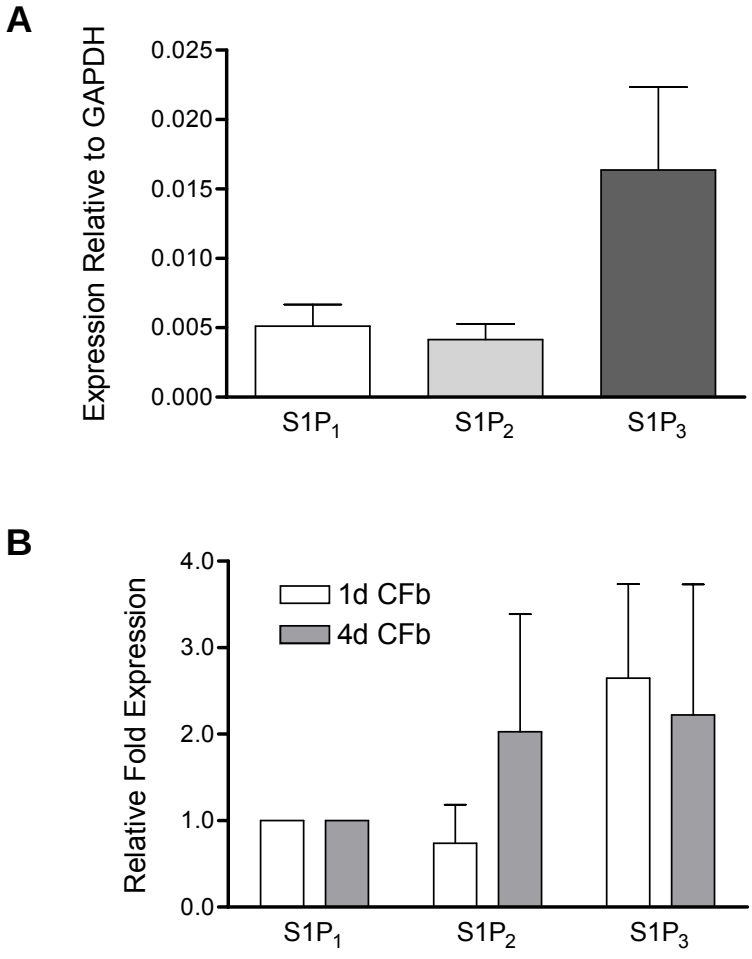

Figure 3.1 S1P Receptor Expression in Adult CFb. Adult mouse CFb express predominantly $S1P_{1\text{-}3}$. ***A.*** Purified CFb analyzed by qPCR the day following isolation (i.e. 1 day old) express $S1P_3$ mRNA levels the highest. $S1P_1$ and $S1P_2$ expression levels were comparable. ***B.*** One-day-old $CD11b^-$ CFb exhibit greater expression levels of $S1P_3$ relative to $S1P_1$. In these acutely isolated cells, $S1P_2$ is expressed the least of the three subtypes. S1P expression changes with in vitro culture. By the fourth day post-isolation/purification, CFb are observed to have increasing $S1P_2$ levels.

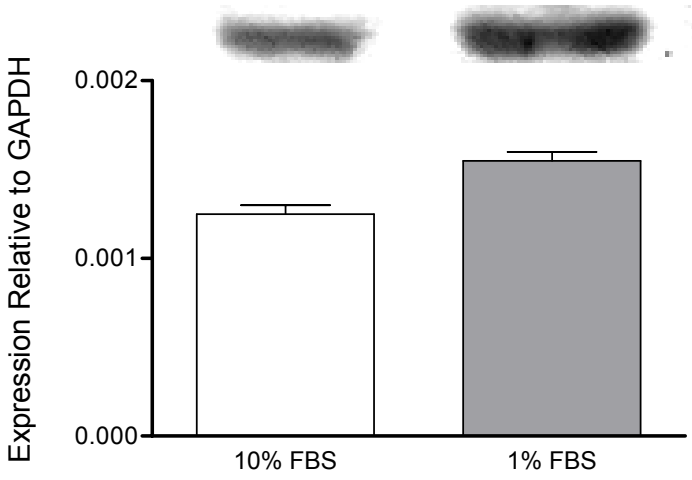

Figure 3.2 Expression Levels of $S1P_1$ in NIH3T3 Fibroblasts. $S1P_1$ mRNA expression levels were increased after culture in 1% FBS-containing medium for 2 days. Images of Western blot analysis are shown for each condition above the respective qPCR data. HUVEC lysates (which highly express $S1P_1$) were used as positive controls to verify reactivity at appropriately sized proteins masses (~42 kDa).

In some experimental settings, having a percentage of monocytes/MΦ within a culture of CFb may not have any significant bearing on the interpretation of experimental findings. However, this must depend heavily on the objective of those studies. A representative case can be based on our interest in physiological responses of CFb to S1P. S1P receptors are ubiquitously found on many cell types and exhibit differing cellular responses depending on the specific receptor subtype(s) expressed. We therefore investigated whether the presence of MΦ in CFb cultures can significantly affect the measurement of the expression of S1P receptor isoforms on CFb.

We first examined the effect of co-culturing MΦ with CFb on S1P receptor expression (Figure 3.3). Unpurified (CFb/MΦ) or purified ($CD11b^+$ MΦ) cultures of mouse cardiac MΦ were seeded into separate microporous inserts, allowed to attach, then placed into wells pre-plated with purified mouse CFb and co-cultured for 3 days. When

CFb were exposed to mixed CFb/MΦ populations, $S1P_3$ levels decreased and $S1P_1$ levels increased. These changes were shown to be significantly different from each other ($p<0.05$). However, when MΦ were first purified (by CD11b sorting) and then allowed to co-culture with CFb, $S1P_2$ experienced decreased expression whereas $S1P_1$ and $S1P_3$ exhibited slight increases in expression levels. Thus, MΦ were shown to have the capacity to alter S1P receptor expression levels in CFb by co-culture experiments.

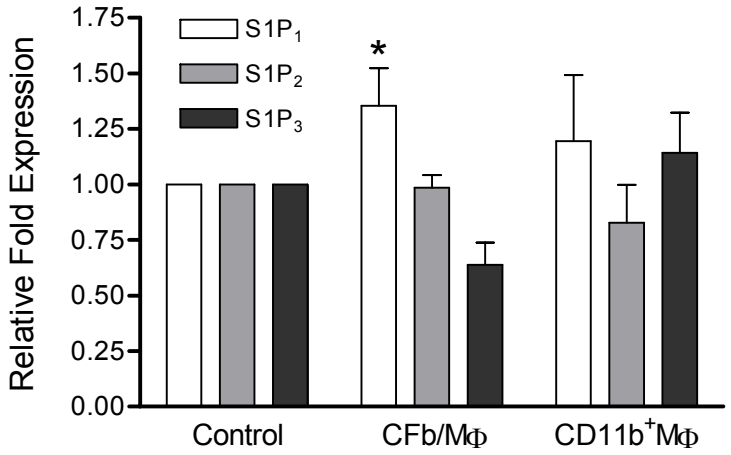

Figure 3.3 Influence of MΦ on Adult CFb S1P Receptor Expression. S1P receptor subtype expression levels in adult mouse CFb are affected by co-culture with MΦ. $CD11b^-$ CFb showed decreased $S1P_3$ levels relative to untreated controls when co-cultured for 3 days with mixed CFb/ MΦ populations. However, when co-cultured with purified ($CD11b^+$) MΦ, CFb expression of $S1P_2$ decreased. Additionally, $S1P_1$ and $S1P_3$ showed moderate increases in receptor expression levels when co-cultured with $CD11b^+$ MΦ.

3.4.3 Modulation of S1P Receptor Expression in CFb by Known MΦ-Secreted Factors

MΦ can secrete various paracrine factors including interleukins, cytokines and growth factors and often reside in close approximation with fibroblasts. To investigate whether such MΦ-secreted factors could cause alterations of S1P receptor expression in

CFb, the effects of a number of purified factors were studied one at a time. Since MΦ have been identified as a source of S1P,[27] we were interested in knowing whether exposure to S1P would alter subsequent S1P receptor isoform expression patterns. Exposure to physiologically relevant concentrations of the bioactive molecule S1P (0.1 μM in DMEM with 10% FBS) failed to alter S1P receptor expression levels in CFb (Figure 3.4). Increasing the S1P dosing concentration 10-fold noted only a slight increase in $S1P_1$ expression, but this was not significant. Our S1P results agree with published reports[24] on the absence of an effect of S1P on $S1P_1$ expression in mouse embryonic fibroblasts. Similarly, exposure of CFb to H_2O_2 (0.1 – 1 μM) failed to alter S1P receptor expression levels compared to control cells (data not shown).

We next evaluated the effects of TGFβ1. Purified CFb were seeded to multi-well dishes and incubated in standard culture medium (DMEM with 10% FBS) or in culture medium supplemented with TGFβ1 (5 ng/ml) for 48-72 hr. TGFβ1 reduced the relative expression levels (versus normalized control values) of all three S1P receptor subtypes (Figure 3.5). However, when TNFα, another MΦ-secreted factor, was supplemented at either 0.1 or 1 ng/ml (Figure 3.5), all three S1P receptor subtype expression levels increased relative to normalized control levels. Furthermore, there was a reproducible and significant rank-ordering of the changes. After TNFα treatment, $S1P_3$ showed significant increases ($p<0.05$) compared to $S1P_1$ and $S1P_2$ levels, which exhibited slight increases. Lastly, TGFβ1 and TNFα were co-administered to CFb. The presence of TGFβ1 abolished the observed upregulation by TNFα, and S1P receptor levels approximated those of TGFβ1 alone (Figure 3.5).

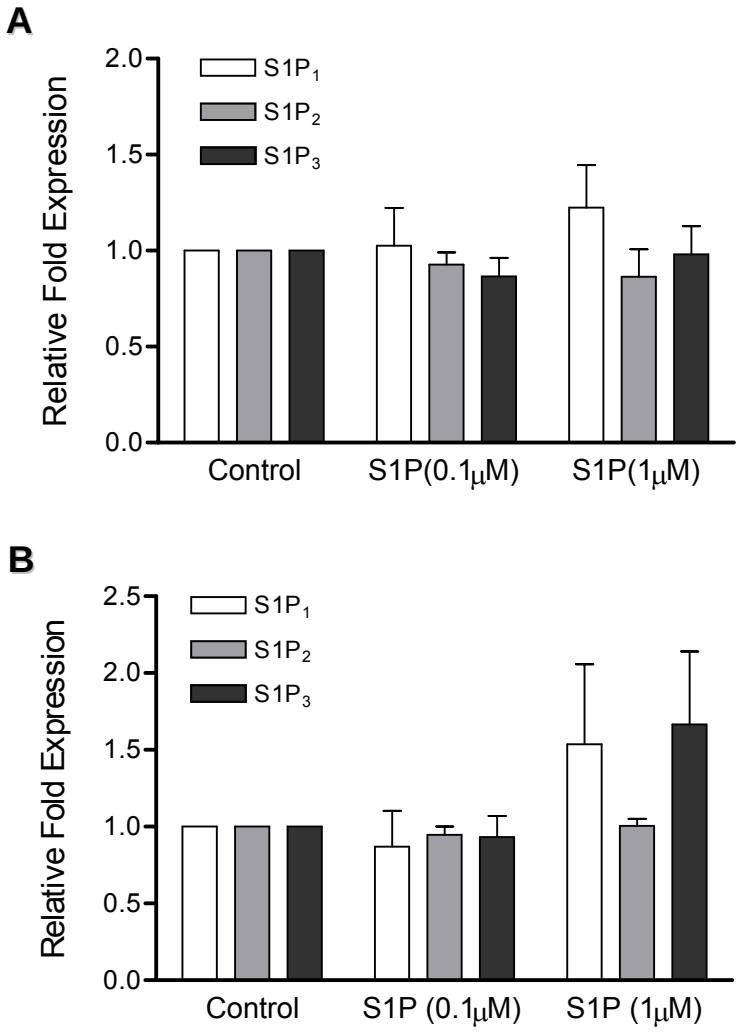

Figure 3.4 Influence of S1P on Adult CFb S1P Receptor Expression. ***A.*** S1P itself (0.1 or 1 μM) failed to modulate significantly S1P receptor expression in CFb when applied in the presence of 10% FBS-containing medium. ***B.*** When S1P was administered in 0.1% FBS-containing medium, a stronger increase in $S1P_1$ and $S1P_3$ receptor isotype mRNA expression was noted, but this was still not significant.

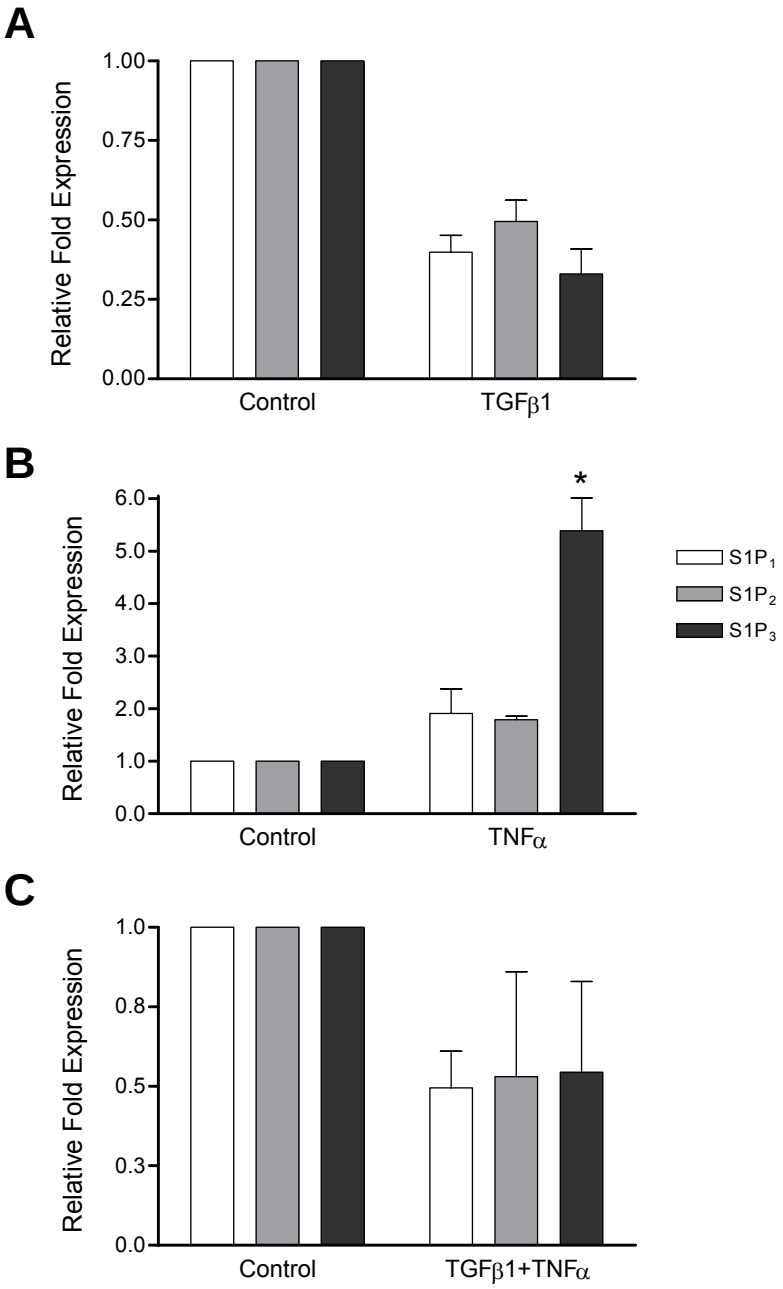

Figure 3.5 Influence of TGFβ1 and TNFα on Adult CFb S1P Receptor Expression. S1P receptor subtype mRNA expression in adult mouse CFb was influenced by treatment with known MΦ-secreted factors compared to control cells cultured in 10% FBS-containing medium. ***A.*** CFb treated with TGFβ1 (5 ng/ml) for 2-3 days showed reduced expression levels of all three S1P receptor subtypes relative to control cells. ***B.*** In contrast, CFb treated with TNFα (1 ng/ml) exhibited increased expression levels for all three S1P receptor subtypes relative to controls, with $S1P_3$ having the greatest increase ($p<0.05$ vs. $S1P_1$ or $S1P_2$). ***C.*** Co-administration of TGFβ1 and TNFα resulted in expression profiles resembling those of TGFβ1 treatment alone.

PDGF-BB was selected as a candidate for supplementation because it has been shown to cross-activate with S1P signaling pathways.[4] PDGF-BB (50 ng/ml in DMEM with 10% FBS) resulted in a significant increase in $S1P_1$ ($p<0.05$) and a moderate increase in $S1P_3$ (Figure 3.6). Whereas mouse embryonic fibroblasts have been reported not to respond to an increase in $S1P_1$ upon exposure to PDGF,[24] our results using adult mouse cardiac fibroblasts demonstrated a significant increase in $S1P_1$.

In summary, we demonstrate that several factors which are produced by MΦ can affect CFb S1P receptor expression when investigated in purified form. Since MΦ are a frequent contaminating cell type in CFb isolations, our results presented here emphasize the necessity for having pure CFb populations.

3.4.4 Modulation of S1P Receptor Expression in CFb Cultured in Low Serum Conditions

Many experimental procedures include a serum withdrawal/deprivation step prior to initiating treatment. For example, this is routinely performed before addition of a chemotactic agent in migration-based assays or before addition of a mitogenic factor in proliferation-based assays. We therefore wanted to determine whether S1P receptor expression levels would be affected during such pre-treatment steps. To our surprise, when CFb were exposed to culture medium containing only 0.1% FBS, $S1P_2$ expression was increased over 2.5-fold relative to control cells cultured in 10% FBS-containing medium ($p<0.05$ vs. $S1P_1$ or $S1P_3$) (Figure 3.7). In addition, $S1P_3$ levels were reduced to less than one-fourth that of control cells and $S1P_1$ was diminished by approximately 50% to that of control levels.

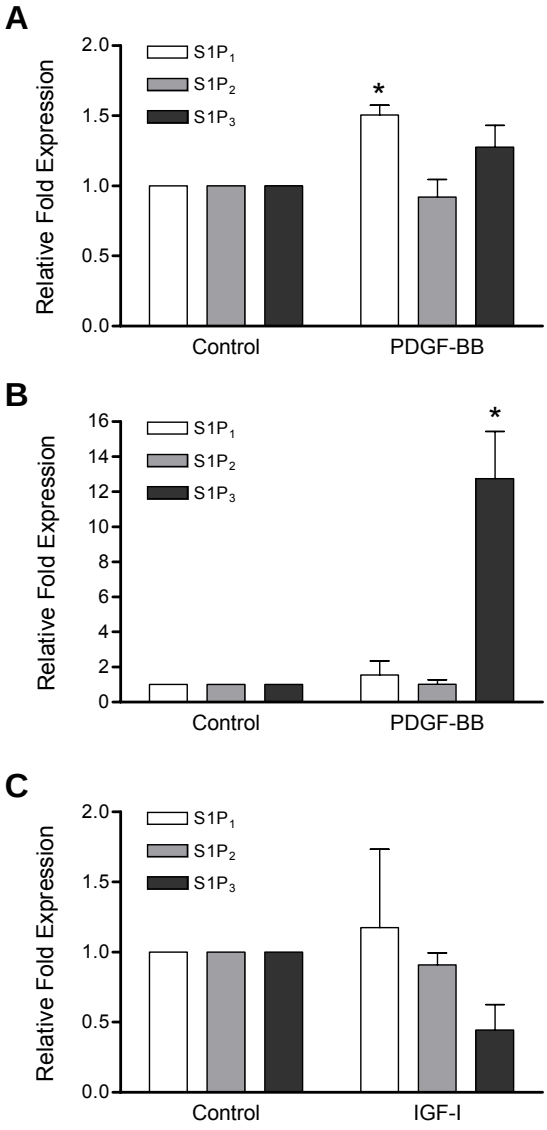

Figure 3.6 Influence of PDGF-BB and IGF-I on Adult CFb S1P Receptor Expression. ***A.*** Treatment of CFb with PDGF-BB (50 ng/ml) exhibited significant enhancement in $S1P_1$ and moderate increase in $S1P_3$ receptor expression when compared to control cells cultured in 10%-FBS containing medium ($p<0.05$ vs. $S1P_2$). ***B.*** When cultured in 0.1% FBS-containing medium, PDGF-BB (50 ng/ml) significantly increased $S1P_3$ expression levels compared to control cells and relative to $S1P_1$ and $S1P_2$ ($p<0.05$). ***C.*** IGF-I, conversely, down-regulated $S1P_3$ expression.

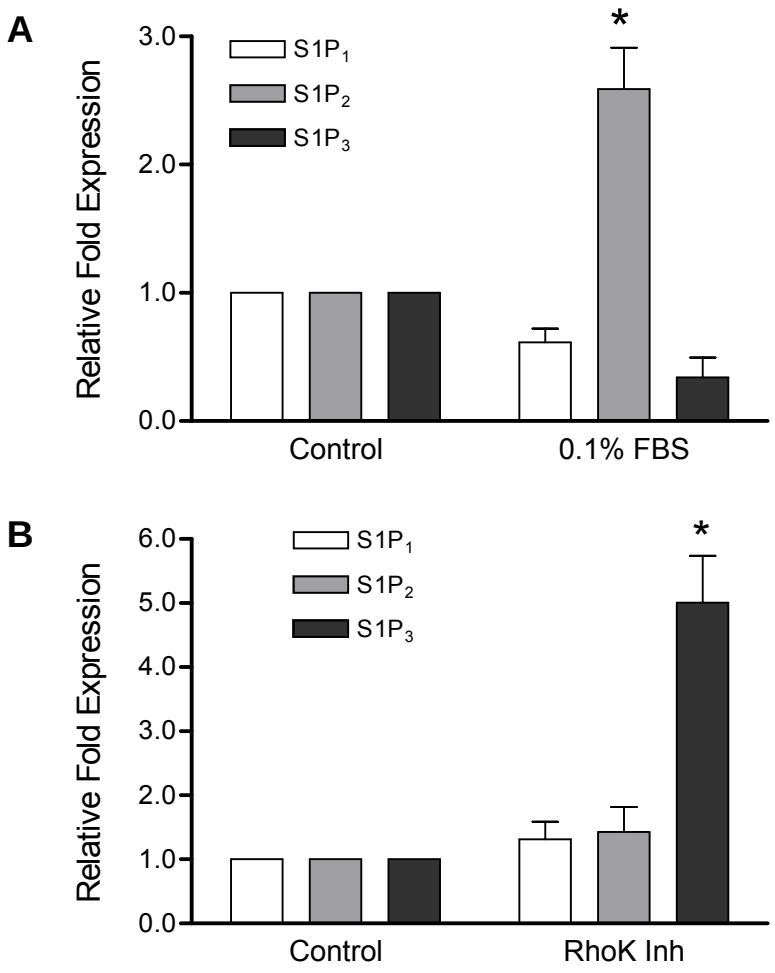

Figure 3.7 Modulation of CFb $S1P_2$ and $S1P_3$ Receptor Expression by Culture in Low Serum and a Rho Pathway Inhibitor. ***A.*** $S1P_2$ receptor isotype expression in adult mouse CFb was significantly increased when cells were cultured in 0.1% FBS-containing medium for 2-3 days ($p<0.05$ vs. $S1P_1$ or $S1P_3$ expression). $S1P_3$ expression levels were slightly decreased. ***B.*** CFb cultured in 0.1% FBS (shown in ***A*** to increase $S1P_2$ and to decrease $S1P_3$) and treated with the Rho-associated protein kinase inhibitor Y-27632 (70 μM) blunted the effects of low serum on $S1P_2$ expression and significantly increased $S1P_3$ expression levels ($p<0.05$ vs $S1P_1$ or $S1P_2$).

CFb were exposed to S1P under conditions of serum-deprivation. As before, S1P at low concentrations (0.1 μM) failed to influence significantly S1P receptor subtype

expression in CFb, whereas S1P at higher concentrations (1 μM) had a slightly stronger effect (i.e. slight increases) on $S1P_1$ and $S1P_3$ (Figure 3.4).

However, when serum-deprived (i.e. cultured in 0.1% FBS) CFb were compared to serum-deprived CFb supplemented with PDGF-BB (50 ng/ml), the expression level of $S1P_3$ was over 12-fold higher ($p<0.05$ vs. $S1P_1$ or $S1P_2$) (Figure 3.6). This response was the most dramatic of any of the evaluated factors. In order to determine whether this increase was specific to PDGF-BB, we evaluated the response of CFb to IGF-I, another known tyrosine kinase receptor. IGF-I was also unable to up-regulate $S1P_3$ expression, and in fact, caused a slight reduction in expression levels (Figure 3.6).

Because the relative levels of $S1P_2$ and $S1P_3$ have been associated with negative and positive, respectively, influences on cell migration,[46] we investigated potential agents that could either reduce or minimize the increases observed in $S1P_2$ levels or, alternatively, increase levels of $S1P_3$ when exposed to reduced serum concentrations. $S1P_2$ has a signaling pathway through $G_{12/13}$ that activates Rho. Therefore, we investigated whether this pathway could be interrupted using the Rho-associated protein kinase inhibitor Y-27632 This inhibitor was selected since it had been shown previously to inhibit $S1P_2$-mediated Rho-dependent stress fiber formation in transfected CHO cells.[43] Whereas there was a significant increase in $S1P_2$ in CFb cultured in 0.1% FBS only, treatment of CFb under these serum concentrations and in the presence of the Rho kinase inhibitor failed to show a similar increase in $S1P_2$ expression levels (relative to control cells). Furthermore, a significant increase in $S1P_3$ was noted in the Y-27632-treated cells ($p<0.05$ vs. $S1P_1$ or $S1P_2$) (Figure 3.7).

Since interfering with the $S1P_2$ signaling pathway using a Rho-associated protein kinase inhibitor resulted in a decrease in $S1P_2$ expression, we investigated whether interfering with the $S1P_3$ signaling pathway might induce similar down-regulation. PDGF-BB was used as a positive modulator of $S1P_3$ expression under conditions of low serum (see Figure 3.6). When CFb were co-incubated with PDGF-BB and a Rac 1 inhibitor, $S1P_3$ expression levels were reduced to those of controls ($p<0.05$) (Figure 3.8). Thus, it appears that downstream interference of S1P receptor pathways can alter expression of the very same isoforms in CFb.

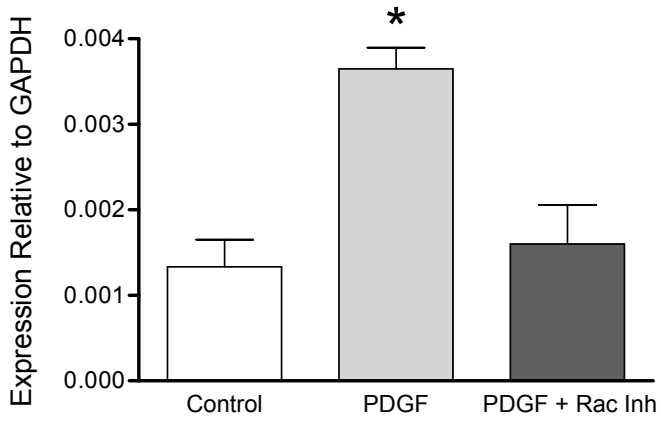

Figure 3.8 Modulation of CFb $S1P_3$ Receptor Expression by a Rac Pathway Inhibitor. Treatment of adult mouse CFb with PDGF-BB (50 ng/ml) in 0.1% FBS-containing medium upregulated $S1P_3$ mRNA expression levels. However, this was significantly reduced ($p<0.05$) to control levels (i.e. cells without PDGF-BB) when a Rac 1 inhibitor (100 μM) was co-administered.

3.4.5 Modulation of S1P Receptor Expression in $S1P_3$-null CFb

$S1P_3$ has been shown to positively influence cell migration via G_i signaling.[43] Because we planned to conduct comparative migration studies using CFb from normal

and $S1P_3$-null mice, we characterized $S1P_3$-null CFb to determine how they would respond to several of the S1P receptor modulations that had been demonstrated in normal CFb. First, we confirmed the genotype of $S1P_3$-null mice (Figure 3.9). Next, we exposed CFb isolated from these mice to PDGF-BB (50 ng/ml) or to 0.1% FBS for 2-3 days. Similar to normal CFb (see Figures 3.6 and 3.7), $S1P_3$-null CFb increased expression of $S1P_1$ in response to PDGF-BB and increased $S1P_2$ in response to reduced serum (Figure 3.9). Compared to control $S1P_3$-null cells cultured in 0.1% FBS-containing medium, $S1P_3$-null cells exhibited attenuated $S1P_2$ expression levels when cultured in 0.1% FBS supplemented with the Rho-associated protein kinase inhibitor Y-27632 or PDGF-BB (Figure 3.9). These results agree with the responses obtained in normal CFb under similar conditions (see Figure 3.7 and 3.6).

3.4.6 S1P Chemotaxis in Adult CFb

S1P can have stimulatory or inhibitory effects on cell migration depending on S1P concentration, cell type, and relative levels of S1P receptor subtypes. Since the literature is lacking with regards to the effects of S1P on CFb migration, we performed experiments on the migratory response of CFb to S1P. Purified adult mouse CFb (4 d old) were seeded to migration chambers, serum-deprived for 24 hr and exposed to S1P (0.05 – 1 μM). Compared to cells receiving only 0.1% FBS, S1P failed to elicit any fold-change above these controls (Figure 3.10). However, additional chambers containing PDGF-BB (50 ng/ml) elicited a positive migratory response, thus ensuring that the evaluated CFb populations were not defective in this regard (Figure 3.10).

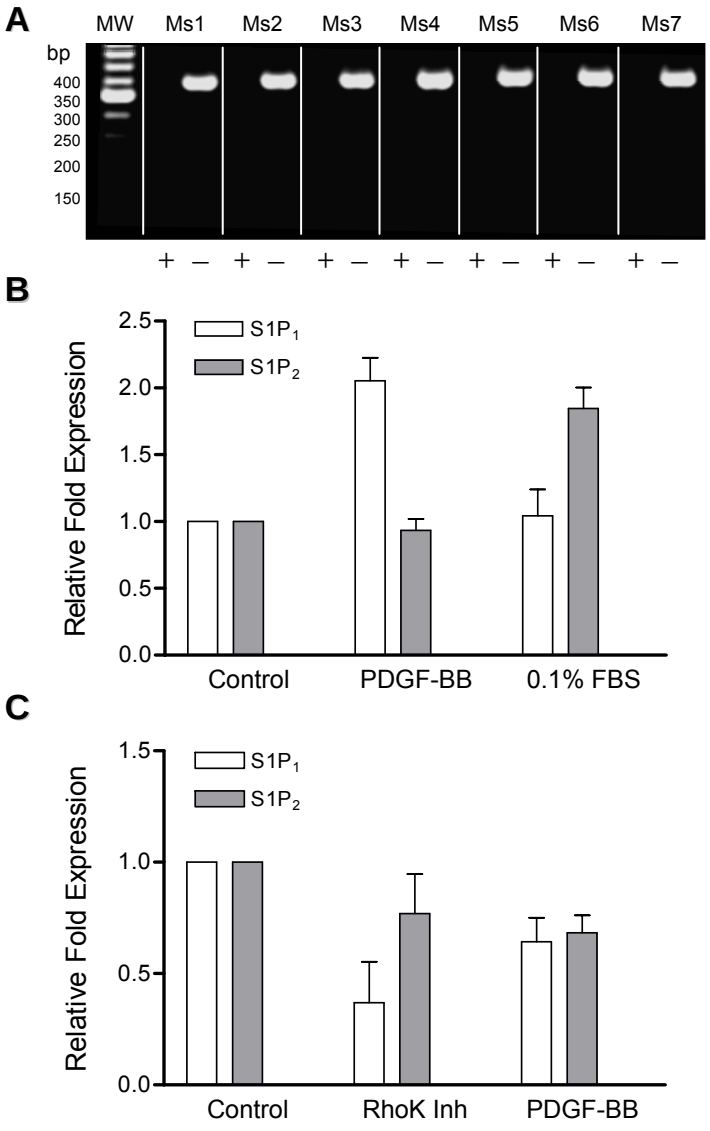

Figure 3.9 Modulation of S1P Receptor Expression in $S1P_3$-null CFb. Similar to CFb isolated from normal mice, S1P receptor expression in CFb isolated from $S1P_3$-null mice was affected by culture conditions. ***A.*** Specific primers against the wild-type $S1P_3$ allele (+, 130 bp) and the targeted/knock-out allele (–, 380 bp) were reacted with DNA isolated from tail snips and visualized by agarose gel electrophoresis. All offspring (and parental mice) were confirmed to be homozygous $S1P_3^{-/-}$ (i.e. $S1P_3$-null). ***B.*** Similar to wild-type CFb, $S1P_3$-null CFb exhibited an increase in $S1P_1$ in response to PDGF-BB (50 ng/ml) when cultured in 10% FBS-containing medium and an increase in $S1P_2$ after culture in 0.1% FBS-containing medium. ***C.*** However, lacking the $S1P_3$ receptor, these $S1P_3$-null CFb failed to respond in a similar manner as wild-type CFb when exposed to 0.1% FBS-containing medium supplemented with either the Rho-associated protein kinase inhibitor Y-27632 (70 μM) or PDGF-BB (50 ng/ml).

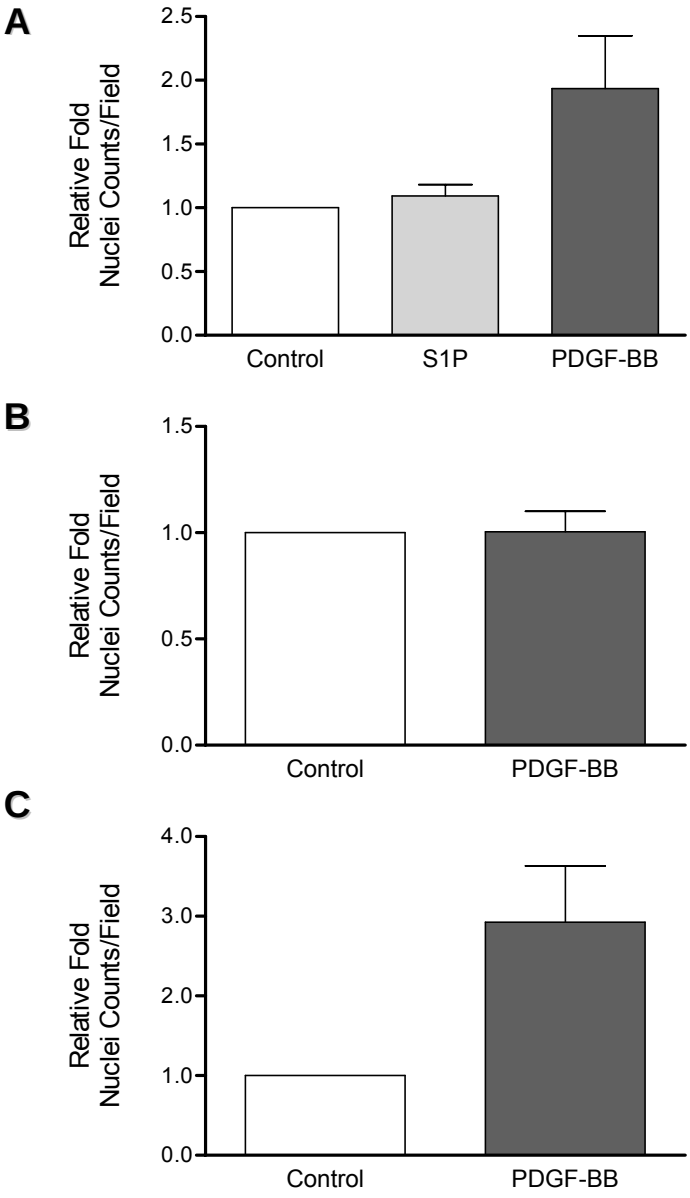

Figure 3.10 Assessment of Migration in Cells Isolated From Normal and $S1P_3$-null Mice. ***A.*** Adult mouse CFb exhibited no chemotactic response towards S1P (0.05 – 1 μM) compared to control cells (incubated in 0.1% FBS). However, CFb did migrate in response to PDGF-BB (50 ng/ml). ***B.*** In contrast, CFb isolated from $S1P_3$-null mice failed to migrate in response to PDGF-BB. ***C.*** Peritoneal MΦ lacking the $S1P_3$ receptor (i.e. isolated from $S1P_3$-null mice) still remained capable of migrating towards PDGF-BB.

3.4.7 Involvement of $S1P_3$ Receptors in CFb Chemotaxis

To ascertain the involvement of $S1P_3$ in migration of CFb, we isolated CFb from $S1P_3$-null mice and performed migration assays using PDGF-BB as the stimulus. In contrast with normal CFb (which were capable of migrating towards PDGF-BB), migration assays using $S1P_3$-null CFb failed to show a similar response (Figure 3.10). To determine whether this was a generalized response in cells lacking $S1P_3$, we isolated peritoneal MΦ from $S1P_3$-null mice and performed migration assays. As shown in Figure 3.10, $S1P_3$-null peritoneal MΦ migrated towards PDGF-BB. Thus, the unresponsiveness towards PDGF-BB observed using CFb appears to be cell type specific. In follow-up studies, peritoneal MΦ were shown to express almost exclusively message for $S1P_1$ (data not shown, but resembled the S1P receptor expression profile of cardiac-isolated MΦ shown in Figure 2.10). Thus, knock-out of the $S1P_3$ gene in peritoneal MΦ had little impact on their migrational capabilities and further illustrates S1P receptor isoform differences and their functional relationship to migration in differing cell types.

3.5 Discussion

3.5.1 Summary of Main Findings

The main objective of this study was to identify the S1P receptor isoforms (subtypes) expressed in cells (CFb) which comprise a significant portion of the working myocardium and to identify factors that can alter relative expression levels of these receptors. Our initial emphasis was on studies of ventricular fibroblasts/myofibroblasts isolated from the adult mouse. Our work shows that CFb can alter their S1P receptor

levels within a few days after initial isolation and in vitro culture. Furthermore, receptor expression levels are sensitive to a variety of culture conditions which can affect both CFb phenotype and interpretation of CFb functional responses.

We demonstrate that exposure of primary isolated CFb to MΦ alters S1P receptor levels in CFb. Further, we demonstrate that exposure to purified factors which are known to be released by MΦ also affects S1P receptor subtype expression. For example, TNFα can increase all S1P receptor subtypes, whereas TGFβ1 can decrease all S1P receptor subtypes evaluated. Furthermore, TGFβ1 can abolish the effects of TNFα when co-administered. Other factors secreted by MΦ such as S1P itself and H_2O_2 had no effect on CFb S1P receptor expression. In other experiments, we show that withdrawal of serum can increase $S1P_2$ levels, but that $S1P_2$ levels are not increased when cells are treated with the Rho-associated protein kinase inhibitor Y-27632. Y-27632, instead altered the relative expression levels in favor of $S1P_3$, similar to increases after exposure to PDGF-BB. This was shown to be specific for PDGF-BB and not a general response by tyrosine kinase receptors since IGF-I was unable to mimic the increases in $S1P_3$. Interfering with $S1P_3$ signaling pathway via a Rac 1 inhibitor reduced $S1P_3$ receptor expression, suggesting that S1P receptor expression levels are regulated respectively by downstream events. Lastly, we demonstrate that CFb do not migrate towards S1P, and that $S1P_3$ is necessary for migration of CFb in response to PDGF-BB. MΦ, however, have naturally low expression levels of $S1P_3$, and migration in this cell type is not affected by the loss of this receptor isoform.

3.5.2 Modulation of S1P Receptor Isoforms in CFb Cultures

S1P receptors are found ubiquitously on many cell types and their downstream responses can affect proliferation, motility, intracellular calcium regulation, cell survival, and ion channel activation depending on the cell type, the complement of S1P receptor expression, and the associated G proteins (reviewed in [7,8,33,35,42]). The literature on S1P receptor expression in CFb is limited. Most studies involving S1P and S1P receptor-mediated responses in fibroblasts utilize mouse embryonic fibroblasts.[13,14,18,24,36,37] It cannot, however, be assumed that these findings are directly transferable to fibroblasts isolated from different anatomical locations or from mice of different ages. Our own unpublished data has demonstrated differences in S1P receptor isoform expression levels between neonatal and adult mouse myocardium. Further, the findings presented in this Chapter demonstrate how receptor expression levels can be altered within the first few days of in vitro culture. Lastly, we have shown that the presence of selected growth factors and cytokines can affect the expression profile of S1P receptors in adult mouse CFb. Thus, it may be that studies measuring downstream signaling events in cells pre-treated with similar factors may be modulating S1P-mediated pathways.

TGFβ1 has been shown in other fibroblasts to alter S1P levels and S1P receptor expression. In dermal fibroblasts, TFBβ1 can both up-regulate sphingosine kinase and down-regulate sphingosine phosphatase to increase overall S1P levels.[52] In lung fibroblasts, exposure to TGFβ1 (2 ng/ml for 3 days) has been shown to modulate S1P receptor expression.[53] In this cell type, TGFβ1 caused $S1P_2$ to increase and $S1P_3$ to decrease. It is also interesting to note that myofibroblasts secrete TGFβ1 at basal levels

greater than cardiac fibroblasts.[5] Thus, myofibroblasts might be altering S1P receptor levels through autocrine or paracrine pathways.

PDGF stimulation of fibroblasts has been shown to induce Rac activation.[34] The Rac1 inhibitor used in these studies has been shown previously to block PGDF-induced Rac1 activation.[9] This may help explain why $S1P_3$ in adult mouse CFb increased upon exposure to PDGF-BB and why the use of a Rac1 inhibitor further reduced $S1P_3$ levels to baseline.

3.5.3 Involvement of $S1P_3$ in Migration of CFb

S1P has been shown to be involved both directly and indirectly in the migration of cells. Endothelial cells migrate in response to S1P, whereas SMC are either not induced or are inhibited to migrate in the presence of S1P.[38,48] It is known that endothelial cells have a relative absence of $S1P_2$ and an abundance of $S1P_1$ and $S1P_3$, whereas cultured SMC have an abundance of $S1P_2$.

$S1P_2$ and $S1P_3$ are involved in Rac- and Rho-mediated migration. While $S1P_2$ and $S1P_3$ both can activate G_i and $G_{12/13}$ signaling pathways, $S1P_2$ largely acts through $G_{12/13}$-Rho. In contrast, $S1P_3$ largely acts through G_i-Rac. Excess levels of $S1P_2$ may therefore inhibit migration not only through positive regulation of Rho but also through negative control of Rac-associated co-factors.[38,43,46]

S1P levels are increased in cells treated with PDGF or serum[31] and S1P has been shown to be involved in cross-communication of PDGF receptors. Cross-communication of PDGF receptors with S1P can have subsequent effects on migration.[4,41] Although there are conflicting studies regarding the necessity of $S1P_1$ on PDGF receptor activation

and PDGF-induced migration,[18,47,48] $S1P_3$ has been shown to have involvement.[4]

We did not observe any positive chemotactic response of CFb to S1P during migration assays. S1P has been shown to mediate migration in endothelial cells, which strongly express $S1P_1$ and $S1P_3$.[11,20] That S1P did not exhibit a similar positive response in CFb may have been due to the combined effects of increased $S1P_2$ (from the serum-deprivation pre-treatment step) and the fact that S1P itself had no effect on altering S1P receptor expression levels. CFb did respond to PDGF-BB as the chemotactic agent, as expected. These results may be explained by a reversal of $S1P_2$ and $S1P_3$ expression levels upon exposure to PDGF-BB (i.e. $S1P_2$ decreases and $S1P_3$ increases after PGDF-BB treatment).

Our results using $S1P_3$-null CFb confirmed that $S1P_2$ is also upregulated in the absence of serum and that these cells respond similarly to treatments that attenuate an increase in $S1P_2$ in normal CFb (e.g. the Rho-associated protein kinase inhibitor Y-27632 and PDGF-BB). Furthermore, $S1P_3$-null CFb did not migrate towards PDGF-BB, demonstrating that $S1P_3$ is involved in PDGF-directed chemotaxis in adult mouse CFb. However, other studies using $S1P_3$-null mouse embryonic fibroblasts[12] have shown positive migration in response to PDGF which was further enhanced upon deletion of $S1P_2$. The discrepancy between these sets of results may be related to age differences (i.e. embryonic vs. adult) or that fibroblasts isolated from different anatomical regions do not behave similarly. Interestingly, our results using $S1P_3$-null MΦ showed that this cell type migrated in response to PDGF-BB, similar to $S1P_3$-null mouse embryonic fibroblasts. Since normal MΦ express negligible levels of $S1P_3$ or $S1P_2$, their migration in response to PDGF-BB is not dependent on $S1P_3$. It is therefore possible that mouse embryonic

fibroblasts are similarly regulated. Alternatively, it is interesting to speculate whether preparations of mouse embryonic fibroblasts yield highly purified cell populations.

In summary, the complex interplay of S1P receptor subtypes with regards to migration and the ability of multiple factors to alter expression levels and ratios not only can complicate interpretation of functional studies using CFb but may suggest complicated response mechanisms within normal and compromised tissues.

3.6 Limitations of Our Work

It should be noted that the conclusions of our studies were largely based on expression levels of mRNA. We performed comparative analysis of mRNA expression levels with protein levels by Western blot to demonstrate that $S1P_1$ is similarly modulated in NIH3T3 fibroblasts. However, it cannot be assumed that protein levels for the specific receptor subtypes would be similarly expressed either in relative quantity or with time in CFb. However, due to the limited sample size (i.e. total cell numbers available from each isolation) and the desire to study S1P receptor expression in early, non-passaged cells, quantitative PCR was considered not only an appropriate methodology, but a necessary methodology. Lastly, signaling pathways of S1P are increasingly being identified. These are complex and can vary between study systems (e.g. cell type, overexpression methods, and concentrations of S1P used). Therefore, alternative explanations for the observed findings may exist.

3.7 Chapter acknowledgement

This chapter was modified from the following manuscript: Landeen L.K., Aroonsakool N., Haga J.H., Hu B.S., Giles W.R., Sphingosine-1-Phosphate Receptor Expression in Cardiac Fibroblast Cells is Modulated by in vitro Culture Conditions, *American Journal of Physiology: Heart and Circulatory Physiology*, 2007 (in press). The Dissertation author (LL) was the principal investigator/author of this paper.

We would like to sincerely thank Dr. Richard L. Proia of the National Institute of Diabetes and Digestive and Kidney Diseases for the use of his S1P transgenic mice and Dr. Masahiko Hoshijima and Ms. Kim Weldy of the University of California, San Diego for maintenance of the $S1P_3$-null breeding colonies. Dr. Hoshijima also was gracious for allowing us to use his ABI qPCR machine for S1P receptor expression assays. We would similarly like to thank Dr. Shu Chien for use of his Bio-Rad qPCR machine for expression assays.

This work was supported in part by a grant from the American Heart Association Western States Affiliate Program. Lee Landeen was supported by a graduate research fellowship from the National Science Foundation.

3.8 References

1. Alewijnse,A.E., Peters,S.L. & Michel,M.C. Cardiovascular effects of sphingosine-1-phosphate and other sphingomyelin metabolites. *Br. J. Pharmacol.* 143, 666-684 (2004).

2. Arya,M. *et al.* Basic principles of real-time quantitative PCR. *Expert. Rev. Mol. Diagn.* 5, 209-219 (2005).

3. Assoian,R.K. *et al.* Expression and secretion of type beta transforming growth factor by activated human macrophages. *Proc. Natl. Acad. Sci. U. S. A.* 84, 6020-6024 (1987).

4. Baudhuin,L.M. *et al.* $S1P_3$-mediated Akt activation and cross-talk with platelet-derived growth factor receptor (PDGFR). *FASEB J.* 18, 341-343 (2004).

5. Campbell,S.E. & Katwa,L.C. Angiotensin II stimulated expression of transforming growth factor-beta1 in cardiac fibroblasts and myofibroblasts. *J. Mol. Cell Cardiol.* 29, 1947-1958 (1997).

6. Cooper,L., Johnson,C., Burslem,F. & Martin,P. Wound healing and inflammation genes revealed by array analysis of 'macrophageless' PU.1 null mice. *Genome Biol.* 6, R5 (2005).

7. Fukushima,N., Ishii,I., Contos,J.J., Weiner,J.A. & Chun,J. Lysophospholipid receptors. *Annu. Rev. Pharmacol. Toxicol.* 41:507-34., 507-534 (2001).

8. Futerman,A.H. & Hannun,Y.A. The complex life of simple sphingolipids. *Eur. Mol. Biol. Organization* 5, 777-782 (2004).

9. Gao,Y., Dickerson,J.B., Guo,F., Zheng,J. & Zheng,Y. Rational design and characterization of a Rac GTPase-specific small molecule inhibitor. *Proc. Natl. Acad. Sci. U. S. A.* 101, 7618-7623 (2004).

10. Gaur,U. & Aggarwal,B.B. Regulation of proliferation, survival and apoptosis by members of the TNF superfamily. *Biochem. Pharmacol.* 66, 1403-1408 (2003).

11. Gonzalez,E., Kou,R. & Michel,T. Rac1 modulates sphingosine 1-phosphate-mediated activation of phosphoinositide 3-kinase/Akt signaling pathways in vascular endothelial cells. *J. Biol. Chem.* 281, 3210-3216 (2006).

12. Goparaju,S.K. *et al.* The $S1P_2$ receptor negatively regulates platelet-derived growth factor-induced motility and proliferation. *Mol. Cell Biol.* 25, 4237-4249 (2005).

13. Ishii,I. *et al.* Selective loss of sphingosine 1-phosphate signaling with no obvious phenotypic abnormality in mice lacking its G protein-coupled receptor, LP(B3)/EDG-3. *J. Biol. Chem.* 276, 33697-33704 (2001).

14. Ishii,I. *et al.* Marked perinatal lethality and cellular signaling deficits in mice null for the two sphingosine 1-phosphate (S1P) receptors, S1P(2)/LP(B2)/EDG-5 and S1P(3)/LP(B3)/EDG-3. *J. Biol. Chem.* 277, 25152-25159 (2002).

15. Kern,S., Robertson,S.A., Mau,V.J. & Maddocks,S. Cytokine secretion by macrophages in the rat testis. *Biol. Reprod.* 53, 1407-1416 (1995).

16. Kim,J.G., Keshava,C., Murphy,A.A., Pitas,R.E. & Parthasarathy,S. Fresh mouse peritoneal macrophages have low scavenger receptor activity. *J. Lipid Res.* 38, 2207-2215 (1997).

17. Kimura,T. *et al.* Sphingosine 1-phosphate stimulates proliferation and migration of human endothelial cells possibly through the lipid receptors, Edg-1 and Edg-3. *Biochemical Journal* 348, 71-76 (2000).

18. Kluk,M.J., Colmont,C., Wu,M.T. & Hla,T. Platelet-derived growth factor (PDGF)-induced chemotaxis does not require the G protein-coupled receptor $S1P_1$ in murine embryonic fibroblasts and vascular smooth muscle cells. *FEBS Lett.* 533, 25-28 (2003).

19. Kono,M. *et al.* The sphingosine-1-phosphate receptors $S1P_1$, $S1P_2$, and $S1P_3$ function coordinately during embryonic angiogenesis. *J. Biol. Chem.* 279, 29367-29373 (2004).

20. Lee,H., Goetzl,E.J. & An,S. Lysophosphatidic acid and sphingosine 1-phosphate stimulate endothelial cell wound healing. *American Journal of Physiology* 278, C612 (2000).

21. Lepley,D., Paik,J.H., Hla,T. & Ferrer,F. The G protein-coupled receptor $S1P_2$ regulates Rho/Rho kinase pathway to inhibit tumor cell migration. *Cancer Res.* 65, 3788-3795 (2005).

22. Li,M.O., Wan,Y.Y., Sanjabi,S., Robertson,A.K. & Flavell,R.A. Transforming growth factor-beta regulation of immune responses. *Annu. Rev. Immunol.* 24, 99-146 (2006).

23. Livak,K.J. & Schmittgen,T.D. Analysis of relative gene expression data using real-time quantitative PCR and the 2(-Delta Delta C(T)) Method. *Methods* 25, 402-408 (2001).

24. Long,J.S., Natarajan,V., Tigyi,G., Pyne,S. & Pyne,N.J. The functional PDGFbeta receptor-$S1P_1$ receptor signaling complex is involved in regulating migration of mouse embryonic fibroblasts in response to platelet derived growth factor. *Prostaglandins Other Lipid Mediat.* 80, 74-80 (2006).

25. Lucas,M., Stuart,L.M., Savill,J. & Lacy-Hulbert,A. Apoptotic cells and innate immune stimuli combine to regulate macrophage cytokine secretion. *J. Immunol.* 171, 2610-2615 (2003).

26. Matsuyama,W., Wang,L., Farrar,W.L., Faure,M. & Yoshimura,T. Activation of discoidin domain receptor 1 isoform b with collagen up-regulates chemokine production in human macrophages: role of p38 mitogen-activated protein kinase and NF-kappa B. *J. Immunol.* 172, 2332-2340 (2004).

27. Melendez,A.J. & Ibrahim,F.B. Antisense knockdown of sphingosine kinase 1 in human macrophages inhibits C5a receptor-dependent signal transduction, Ca^{2+} signals, enzyme release, cytokine production, and chemotaxis. *J. Immunol.* 173, 1596-1603 (2004).

28. Nag,A.C. Study of non-muscle cells of the adult mammalian heart: a fine structural analysis and distribution. *Cytobios* 28, 41-61 (1980).

29. Newton,P.M., Watson,J.A., Wolowacz,R.G. & Wood,E.J. Macrophages restrain contraction of an in vitro wound healing model. *Inflammation* 28, 207-214 (2004).

30. Okamoto,H. *et al.* Inhibitory regulation of Rac activation, membrane ruffling, and cell migration by the G protein-coupled sphingosine-1-phosphate receptor EDG5 but not EDG1 or EDG3. *Mol. Cell Biol.* 20, 9247-9261 (2000).

31. Olivera,A. & Spiegel,S. Sphingosine-1-phosphate as second messenger in cell proliferation induced by PDGF and FCS mitogens. *Nature* 365, 557-560 (1993).

32. Paik,J.H., Chae,S.-S., Lee,M.-J., Thangada,S. & Hla,T. Sphingosine 1-phosphate-induced endothelial cell migration requires the expression of EDG-1 and EDG-3 receptors and Rho-dependent activation of αvβb and β1 containing integrins. *Journal of Biological Chemistry* 276, 11830-11837 (2001).

33. Pyne,S. & Pyne,N.J. Sphingosine 1-phosphate signalling in mammalian cells. *Biochem. J.* 349, 385-402 (2000).

34. Ridley,A.J. Rho family proteins: coordinating cell responses. *Trends Cell Biol.* 11, 471-477 (2001).

35. Rosen,H. & Goetzl,E.J. Sphingosine 1-phosphate and its receptors: an autocrine and paracrine network. *Nat. Rev. Immunol.* 5, 560-570 (2005).

36. Rosenfeldt,H.M. *et al.* EDG-1 links the PDGF receptor to Src and focal adhesion kinase activation leading to lamellipodia formation and cell migration. *FASEB J.* 15, 2649-2659 (2001).

37. Rosenfeldt,H.M., Hobson,J.P., Milstien,S. & Spiegel,S. The sphingosine-1-phosphate receptor EDG-1 is essential for platelet-derived growth factor-induced cell motility. *Biochem. Soc. Trans.* 29, 836-839 (2001).

38. Ryu,Y. *et al.* Sphingosine-1-phosphate, a platelet-derived lysophospholipid mediator, negatively regulates cellular Rac activity and cell migration in vascular smooth muscle cells. *Circ. Res.* 90, 325-332 (2002).

39. Savikko,J. & von Willebrand,E. Coexpression of platelet-derived growth factors AA and BB and their receptors during monocytic differentiation. *Transplant. Proc.* 33, 2307-2308 (2001).

40. Song,E. *et al.* Influence of alternatively and classically activated macrophages on fibrogenic activities of human fibroblasts. *Cell Immunol.* 204, 19-28 (2000).

41. Spiegel,S. & Milstien,S. Sphingosine 1-phosphate, a key cell signaling molecule. *J Biol. Chem.* 277, 25851-25854 (2002).

42. Spiegel,S. & Milstien,S. Sphingosine-1-phosphate: an enigmatic signalling lipid. *Nat. Rev. Mol. Cell Biol.* 4, 397-407 (2003).

43. Sugimoto,N., Takuwa,N., Okamoto,H., Sakurada,S. & Takuwa,Y. Inhibitory and stimulatory regulation of Rac and cell motility by the G12/13-Rho and Gi pathways integrated downstream of a single G protein-coupled sphingosine-1-phosphate receptor isoform. *Mol. Cell Biol.* 23, 1534-1545 (2003).

44. Taha,T.A., Argraves,K.M. & Obeid,L.M. Sphingosine-1-phosphate receptors: receptor specificity versus functional redundancy. *Biochim. Biophys. Acta* 1682, 48-55 (2004).

45. Takemura,G. *et al.* Role of apoptosis in the disappearance of infiltrated and proliferated interstitial cells after myocardial infarction. *Circ. Res.* 82, 1130-1138 (1998).

46. Takuwa,Y. Subtype-specific differential regulation of Rho family G proteins and cell migration by the Edg family sphingosine-1-phosphate receptors. *Biochim. Biophys. Acta.* 1582, 112-120 (2002).

47. Usui,S. *et al.* Blood lipid mediator sphingosine 1-phosphate potently stimulates platelet-derived growth factor-A and -B chain expression through $S1P_1$-Gi-Ras-MAPK-dependent induction of Kruppel-like factor 5. *J. Biol. Chem.* 279, 12300-12311 (2004).

48. Waters,C.M. *et al.* Cell migration activated by platelet-derived growth factor receptor is blocked by an inverse agonist of the sphingosine 1-phosphate receptor-1. *FASEB J.* 20, 509-511 (2006).

49. Wei,S.H. *et al.* Sphingosine 1-phosphate type 1 receptor agonism inhibits transendothelial migration of medullary T cells to lymphatic sinuses. *Nat. Immunol.* 6, 1228-1235 (2005).

50. Windh,R.T. *et al.* Differential coupling of the sphingosine 1-phosphate receptors Edg-1, Edg-3, and H218/Edg-5 to the G(i), G(q), and G(12) families of heterotrimeric G proteins. *J. Biol. Chem.* 274, 27351-27358 (1999).

51. Xu,K. *et al.* Strong red fluorescent probes suitable for detecting hydrogen peroxide generated by mice peritoneal macrophages. *Chem. Commun. (Camb.).* 5974-5976 (2005).

52. Yamanaka,M. *et al.* Sphingosine kinase 1 (SPHK1) is induced by transforming growth factor-beta and mediates TIMP-1 up-regulation. *J. Biol. Chem.* 279, 53994-54001 (2004).

53. Yin,Z. & Watsky,M.A. Chloride channel activity in human lung fibroblasts and myofibroblasts. *Am. J. Physiol Lung Cell Mol. Physiol.* 288, L1110-L1116 (2005).

CHAPTER 4

A COMPARISON OF PATCH-ON-A-CHIP WHOLE-CELL VOLTAGE-CLAMP PLATFORMS FOR ASSESSING FIBROBLAST ELECTROPHYSIOLOGY

4.1 Abstract

Electrophysiological data obtained using intracellular recordings can assist in the characterization of cell type, function, and phenotype, as well as being used to gather useful information regarding cellular responses to drugs and receptor agonists. Efficient, relatively high throughput electrophysiological data gathering using conventional micropipette techniques or whole-cell patch clamp, however, requires specific training, skill and instrumentation. As such, it is seldom available to the research laboratories which are based on Cell Biology, Cell Signaling or Tissue Engineering. Furthermore, single-cell electrophysiological techniques are time-consuming and, therefore, do not lend themselves as readily to high-throughput screening, as would be required by the biotech and pharmaceutical industries. In an effort to reduce the technical barriers and to increase throughput, several technologies are either currently available, as beta-test platforms or under development. These may allow a wider audience the ability to interrogate cells using electrophysiological methods.

This Chapter compares two types of planar chip technologies with conventional micropipette methods in terms of their ability to record whole-cell currents from cardiac fibroblasts (CFb) and to characterize the electrophysiological responses to application of sphingosine-1-phosphate (S1P). It was found that both the Nanion[3] and AVIVA[60] chip

platforms were capable of recording whole-cell potassium (K^+) currents from these cells. These results resembled those from conventional techniques. The AVIVA platform was advantageous in its ability to visualize the cell being patched, whereas the Nanion platform was easier to use and was more space efficient. However, both chip technologies were more sensitive to flow-mediated disturbances than conventional patching and made distinguishing true receptor-activated responses from artifact more difficult. As such, these chip technologies were not as flexible in their capabilities as conventional patching, and an understanding of both cell type and experimental objectives should be considered when deciding on a potential platform to adopt. Hence, experiments investigating the electrophysiological response of CFb to S1P were made using conventional techniques. S1P, when superfused onto adult rat CFb, was shown to activate a conductance with a reversal potential near -30 mV. This activation was time-dependent and resulted in both inward and outward currents. The nature of these currents was consistent with those that are activated by chloride channels or transient receptor potential (TRP) channels.

4.2 Introduction

4.2.1 Ion Channel Biophysics

The phospholipid bilayer, which forms an essential component of all cellular membranes, prevents passive movement of charged molecules either into or out of isolated cells. However, most cells rely on membrane potential signals and changes in ion concentrations to perform many necessary cellular functions. These include initiating action potentials in both nerve and contractile cells, cell migration, secretion and

exocytosis, and some responses to mechanostimulation. To facilitate and control ion transport across the plasma membrane, cells utilize ion channels.[19]

Ion channels are highly involved in regulating cellular activity, and a number of disease states occur as a consequence of abnormal ion channel physiology. Because of their cellular importance, the human genome is estimated to encode for >400 ion channel genes, which represents approximately 1.3% of the entire genome.[57]

Ion channels are multi-unit transmembrane proteins that contain a narrow central pore which confers the ion selectivity. The type of ion that can pass through is regulated by both the size of the pore and the charge of the specific amino acids that line the pore.[20] Ion channels can exist in open, closed, or inactivated states and may be activated by specific types of gating. In voltage-gating, the state of the pore depends on the membrane potential of the cell; in ligand-gating, the state of the pore depends on binding of an agonist to its associated receptor; and in mechanical-gating, the pores are opened by physical deformation (e.g. shear or stretch) of the cellular membrane.

Intracellular and extracellular monovalent cation concentrations are markedly different. For example, in mammals, intracellular potassium ion concentrations are approximately 140 mM, whereas extracellular potassium ion concentrations are approximately 5 mM. Conversely, sodium ion concentrations are in approximately the opposite concentration relative to intracellular and extracellular spaces. This unequal distribution of ions, coupled with selective permeability, creates an ion potential across the plasma membrane. When an ion channel is in an open state, ions freely move through it, driven by both electric and concentration gradients. Up to 100 million ions per second may move through an ion channel during its opened state.[34,49] This creates an ionic

current. The ease with which an ion channel conducts current defines the conductance of the channel, which is inversely related to resistance. In accordance with Ohm's law, voltage is the product of current and resistance. The cell membrane potential (measured in voltage) can therefore be expressed as the summation of each individual ion channel's current and conductance.

The cell membrane can be represented as a simplified electrical circuit that connects the intracellular contents with the extracellular solution (see Figure 4.1).[50] Ion channels are arranged/expressed in parallel with the cell membrane, which has a characteristic capacitance (proportional to surface area) due to the prominent lipid bilayer component of the plasma membrane. The current carried by a population of channels is a function of the ion channel conductance and the probability of an individual channel being in the opened state. This current is in series with the reversal potential of the ions (e.g. the battery) through the particular class of ion channel.

By convention, ion channel currents are classified as either inward or outward with reference to the Nernst potential for the permeant ion. The net quantity of these inward and outward currents strongly modulates the cell membrane potential. For example, voltage-gated potassium channels open when the cell becomes depolarized. Since potassium ion concentration is greater inside the cell, the potassium ions move outward (based on the concentration gradient) and this generates an outward current. Potassium currents can also be inward. For example, there are potassium currents that are observed in greater magnitude as the membrane potential is increasingly hyperpolarized relative to potassium equilibrium potential.

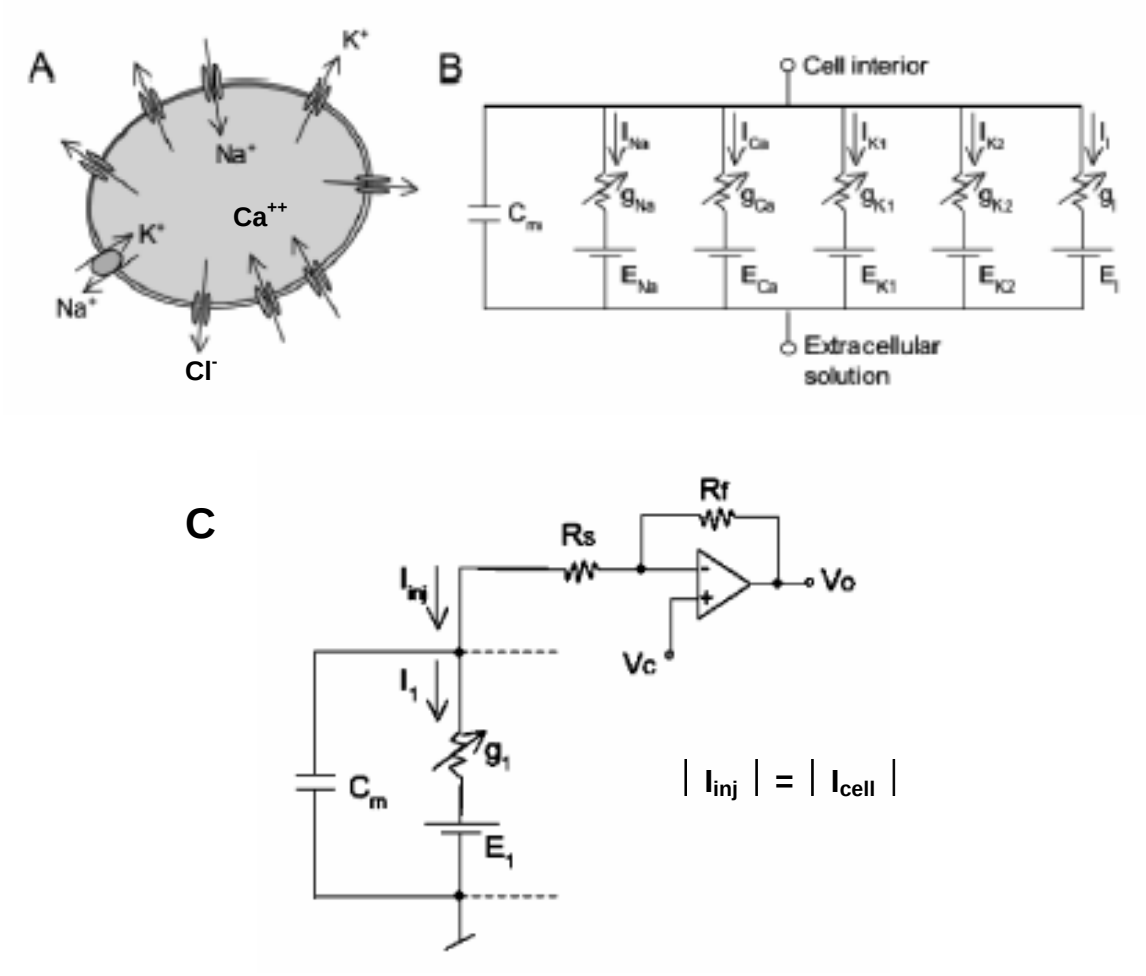

Figure 4.1. Models of Ccellular Electrical Activity. ***A.*** Numerous ion channels and transport proteins are located within the plasma membrane. The total current through these channels (inward or outward) establishes the membrane potential. ***B.*** The cell membrane represented as a simplified electrical circuit. The cell membrane has a capacitance (C_m) of approximately 1 $\mu F/cm^2$. Ion channels are connected in parallel within the cell membrane. The current (I) that moves through a population of ion channels is represented by the ion channel conductance (g) and the fraction of channels open and is in series with the reversal potential of the channel type, represented as a battery (E). ***C.*** Diagram of electrical circuit during voltage-clamp. Injected current (I_{inj}) offsets differences in observed/recorded voltage (V_o) and command voltage (V_c) using negative feedback (R_f) and equals currents moving into and out of the cell (I_{cell}). The electrode series resistance (R_s) and I_{inj} must be accounted to yield the actual membrane potential. Modified from Sigworth and Klemic.[50]

Myocytes, cells from myocardial tissue, express a number of voltage-gated potassium ion channels (Kv) as well as inwardly rectifying potassium ion channels (Kir). Recently, isotypes of both classes of potassium channels have also been identified in cardiac fibroblasts (CFb). In studies of adult rat ventricular CFb by Chilton, et al.[6], message for a number of Kv and Kir ion channel isotypes have been identified.

Both Kv and Kir channels are tetramers, and may be composed of either homomeric or heteromeric subunits.[40] Kv currents open in a sigmoidal fashion, slowly inactivate, and have single channel conductances that vary between 8-27 pS.[15] The membrane potential at which approximately half of the channels open can vary widely depending on isotype and species. For example, mouse Kv1.3 activates at approximately -26 mV whereas rat Kv1.2 activates at more depolarized values (~ 27 mV).[15] Kv channels can be blocked by a number of pharmacological agents and toxins. Concentrations of $\leq$ 0.5 mM 4-aminopyridine (4-AP) have been shown to block peak currents of most Kv channels.[15] Kir channels, however, are relatively insensitive to 4-AP.[40]

Kir channels are largely responsible for maintaining resting membrane potentials near the potassium equilibrium potential.[35] Kir channels are classified into six subfamilies based on similarity of structure and function. Kir2.x channels are ubiquitously expressed in the heart and resemble I_{K1} channels in their time- and voltage-dependent rectification. Kir3.x channels are G-protein-gated, and a relevant example is the acetylcholine-activated potassium channel (K_{Ach}) which is activated also by S1P in cardiac myocytes.[36] Kir4.x and Kir5.x channels are primarily expressed in brain and tissues of the nervous system. Lastly, Kir6.x channels are ATP-gated. Regardless of

subfamily, all are regulated by PIP_2 and are sensitive to blockade by polyamines, and magnesium, barium or cesium ions.[35,40]

Literature regarding the electrophysiological effects of S1P on the CFb is lacking. However, one study using the mouse embryonic fibroblast cell line NIH3T3 has shown that S1P can affect cell resting membrane potential via potassium currents. In the study by Repp, et al.,[41] S1P was shown to increase transiently and rapidly (i.e. within 100 ms) intracellular calcium release from endoplasmic reticulum stores and to activate both hyperpolarizing potassium channels and depolarizing chloride channels. S1P activated a calcium-dependent, voltage-independent K^+ current which caused membrane hyperpolarization of NIH3T3 fibroblasts in a concentration-dependent manner. This current was blocked by charybdotoxin, margatoxin and iberiotoxin, confirming that it was a Ca-dependent K^+ channel (K_{Ca}, a subfamily of Kv ion channels). Additional studies on fetal lung fibroblasts and corneal keratocytes have demonstrated that S1P can activate a chloride channel.[58,63]

4.2.2 Conventional Whole-Cell Voltage-Clamp Methods

Conventional whole-cell patch clamping in this section refers to recording currents or membrane potential of single, isolated cells using a microelectrode fashioned from a small-caliber glass pipette or micropipette (see Figures 4.3 and 4.6).[16,49] This method was first made possible through the efforts of Nobel Prize winners (1991) Erwin Neher and Bert Sakmann in the mid 1970s and further refined to improve the quality of the pipette/cell interactions over the next several years.[34,49] The micropipette can be moved towards the cell membrane from any number of entry angles through the use of

micromanipulators that span all three axes. When the tip of the micropipette encounters the cell membrane, gentle suction is applied to form a seal between the aperture of the micropipette and the cell membrane. This is termed seal resistance. When the resistance of this seal reaches giga-ohm (GΩ) levels (signifying formation of a tight seal that should have minimal leak currents), additional suction is applied to rupture the cell membrane circumscribed by the micropipette aperture. When this occurs, the system is said to be in whole-cell configuration since there is continuity between the micropipette and the intracellular space. Accordingly, the micropipette is usually filled with a solution which resembles the intracellular ionic composition.

Obtaining gigaseals is largely dependent on micropipette design and preparation. The type of glass used, the cleanliness of the glass, selecting a new micropipette for each cell, and using filtered solutions to remove debris all contribute to seal quality.[16,39,50] Background noise level is also reduced after formation of gigaseals. To maintain clean micropipette tip surfaces, slight positive pressure is applied to prevent debris for adhering. HEPES buffer is preferred when patching in the presence of calcium ions since calcium phosphate crystals may form with using phosphate-buffered solutions.[16] It should be noted that calcium and other divalent ions help in formation of glass-membrane seals.[50]

Successful impalement in the whole-cell configuration is characterized by a marked increase in the capacitive current[4] (see Figure 4.2). When recording currents, a second (grounded or reference) electrode is placed in the extracellular bath surrounding the cell. Because the electrodes are separated from each other by the cell membrane, the capacitance of the cell can be measured. This capacitance can be calculated by integration of the capacitive current over time and normalizing to voltage (see Figure 4.2).

The value of the cell capacitance is often used to normalize current measurements (thereafter referred to as current density) since cells may vary in size and cell capacitance is proportional to cell size (e.g. 10-20 pF for a fibroblast, 25-40 pF for a myofibroblast, and 100-150 pF for a myocyte). Typically, the specific membrane capacitance can be approximated by 1 $\mu F/cm^2$ (e.g. 1 pF represents approximately 100 μm^2 of membrane surface area).[4,16,50] This capacitance is offset to zero prior to initiating the voltage-clamp protocol.

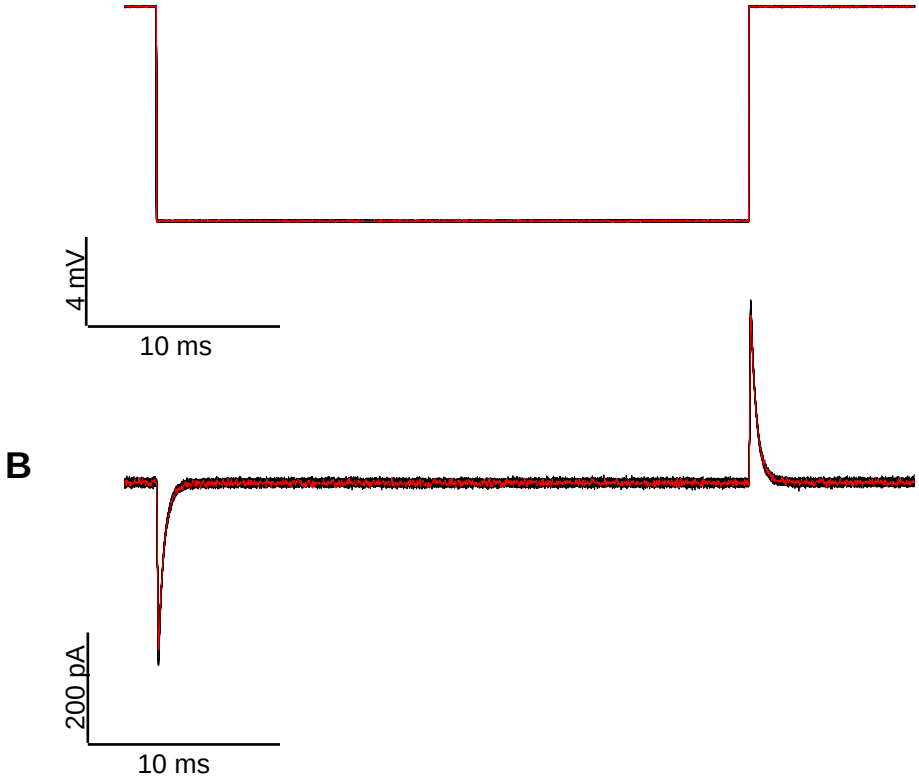

Figure 4.2 Determination of Cell Capacitance. ***A.*** A 10-mV hyperpolarizing voltage step is applied to the cell from its holding potential. ***B.*** The resulting transient currents are due to charging and discharging of the cell capacitor. Each can be integrated over time to yield cell capacitance. The cell membrane capacitance in this example (a rat cardiac fibroblast) was calculated to be 10.32 pF.

Once in whole-cell configuration, the investigator can "clamp" the cell at a specific membrane potential. The voltage clamp circuit/method is designed on a negative feedback principle. The membrane voltage of the cell is measured and compared to the command voltage from the signal generator (see Figure 4.1). The difference between these two voltages is minimized by directly injecting current into the cell. This clamping circuit, in effect, produces a current equal and opposite to the ionic currents of the cell and can be used as a direct measure of ion channel current. Conversely, a cell can also be clamped at a desired current by introducing the appropriate amount of voltage into the cell. This is partially accomplished through the patch clamp headstage, which utilizes capacitive feedback to minimize noise. In both cases, the electrode placed inside the cell serves both the voltage and current recording/passing duties.

Patch clamping has superior temporal resolution and signal-to-noise ratios compared to other methods such as fluorescent-dye methods for measuring membrane potential or changes in ion concentration. Patch clamping is capable of recording currents in the pico-amp range and can be used to study single channel events. However, it is laborious and throughput may be only 10-30 analyzed cells per day.[27,34,61] New strategies that, in principle, can voltage clamp thousands of cells per day are under development.[27] The need for high throughput screening to assay interaction on cardiac ion channels (e.g. the human Kv ion channel hERG) is important to the biotech/pharma industries since this is a requirement of new drugs by the International Conference on Harmonisation.[55]

4.2.3 Recent Alternatives to Whole-Cell Voltage-Clamp Methods

Conventional voltage clamping using micropipettes allows for the measurement of electrical signals by separating two electrolyte-containing compartments (the micropipette-intracellular space and the extracellular space) by an insulating material (the glass micropipette). However, the length of the micropipette contributes to increased series resistance and capacitance. Furthermore, conventional methods are time-consuming and require skilled experimentalists, as well as relatively prolonged training time periods.[34,50,52] In an effort to (i) reduce these factors (and thus increase resolution), (ii) lend itself more to automation and high-throughput screening, and (iii) enable simultaneous microscopic or spectroscopic evaluation, several investigators have explored conjugated planar geometries with associated microelectrodes. Collectively, this is referred to as patch-on-a-chip technology.[11]

Patch chips are planar pieces of thin (approximately 200 μm thickness) glass or silicon nitride covered polyimide films[10,11,52] containing single apertures of ~1 μm diameters (see Figure 4.3). Quartz has been used in several chip designs (because it has been shown to achieve greater signal-to-noise ratios than traditional glass);[29] however, it is not currently widely used in the commercially available chip platforms.

Many such chips utilize etching techniques developed within the semiconductor industry to avoid the difficulties of micromachining at the required dimensions. In one such embodiment,[11] a 5 x 5 mm^2 glass substrate has a 300-500-μm diameter region reduced to 80 μm in thickness by etching in hydrofluoric acid. Bombardment by gold ions creates a nanometer-sized defect which is further etched in hydrofluoric acid until

breakthrough is achieved. The resulting aperture is smooth, circular and can range in diameter from < 1 μm to 50 μm.

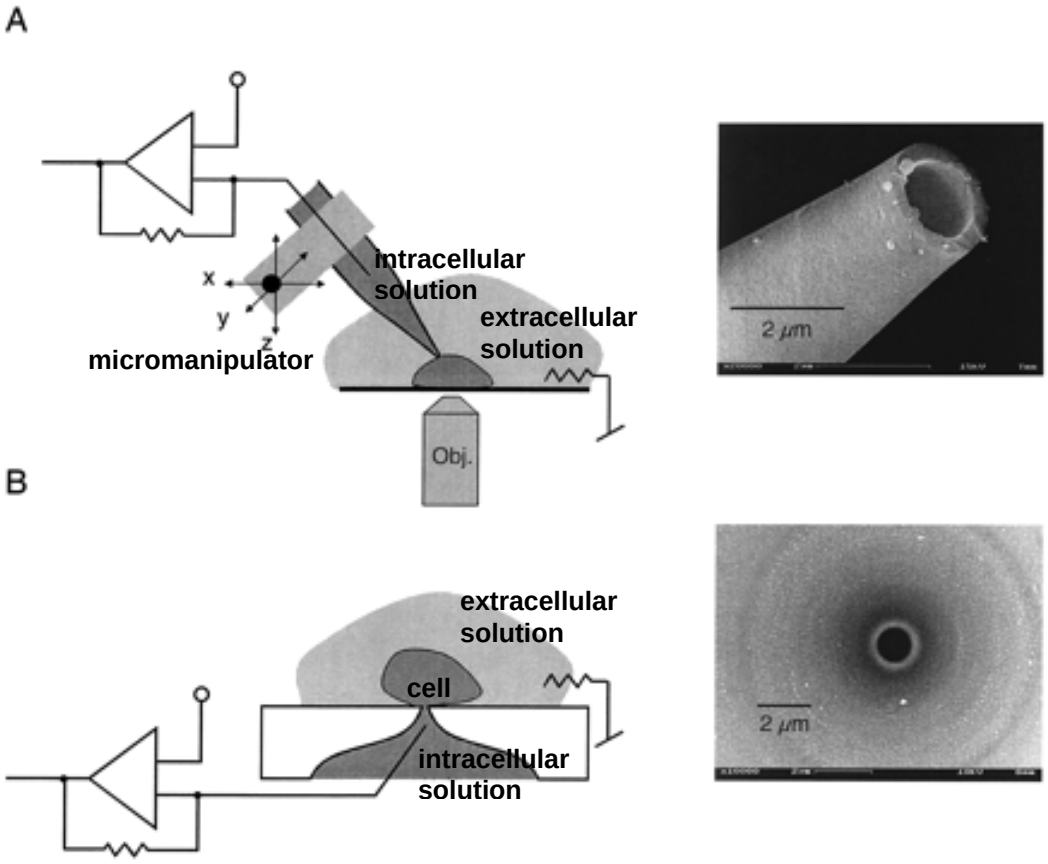

Figure 4.3 Comparison of Conventional Microelectrode and Chip Patching Technologies. ***A.*** Diagram of microelectrode access of cells, controlled by a three-axis micromanipulator, and the electrical equivalent circuitry (left). Visual examination is achieved using an inverted microscope. Scanning electron micrograph of conventional micropipette (right). ***B.*** Diagram of patch chip access of cells and electrical equivalent circuitry (left). Visual examination is possible in some chip configurations which are designed to mount to an inverted microscope. Scanning electron micrograph of a patch chip showing aperture of comparable dimensions as bore of micropipette (right). Modified from Fertig, et al.[10]

Aperture shape and physical chemistry have been shown to influence cell sealing significantly. Plasma-enhanced chemical vapor deposition of SiO_2 is a process that has been incorporated into certain chip designs to provide a hydrophilic surface, reduce aperture diameter and yield an hourglass pore shape. These factors taken together result in less aperture resistance, lower chip capacitance (which results in less electrical noise), increased cell sealing rates, and higher cell seal resistances.[50,51]

A diagrammatic comparison between conventional and chip patching is presented in Figure 4.3. It is readily observable that, although the entry or access point into the cell differs, the electrical circuits of the patching systems remain equivalent. It is also further evident that the apertures of the micropipette and planar chip are similarly sized.

Whole-cell recordings using patch chips were reported in 2002 by Fertig, et al.[10] In this initial report, calcium currents and calcium-activated potassium currents were recorded from cell lines. While patch chips have been used most commonly on cell lines (e.g. Chinese hamster ovary cells and or human embryonic kidney cells) transfected with specific ion channels, they have also been used with freshly isolated cardiac myocytes.[52]

A schematic of a generic "patch chip" and its operation are shown in Figure 4.4. Cells are positioned over the aperture and sealed onto the chip through the use of negative pressure. Other methods for positioning cells over the aperture can include electrophoresis, dielectrophoresis, and directed fluidic flow.[60] The AVIVA chips used in the experiments described herein are chemically treated (a proprietary process) to facilitate cell membrane interactions with the glass substrate.[60] Once a cell is in place over the aperture, suction is applied to help stabilize the seal and break through to achieve the whole-cell recording configuration. In other applications, cells are added or cultured

onto substrates containing micro-apertures and access is gained through the addition of membrane-penetrating ionophores.[27]

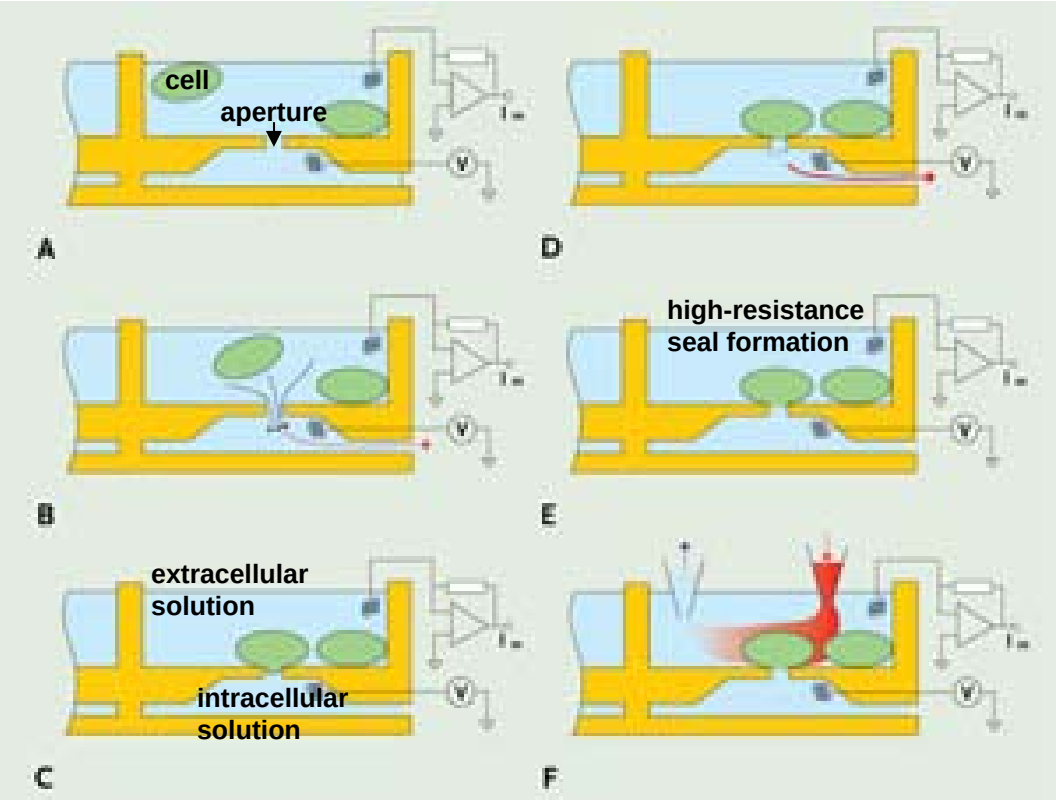

Figure 4.4 Schematic of Steps Involved in Chip Patching Technologies and Electrical Circuitry. ***A.*** Cells added to patch chip chamber. ***B.*** Individual cell positioned towards aperture via negative pressure. ***C.*** Initial seal formed. ***D.*** Seal resistance is then increased by applying graded amounts of negative pressure (typically up to -50 mBar). ***E.*** Whole-cell configuration achieved. ***F.*** Administration of test compounds. Modified from Heyman, et al.[18]

Most chip platforms have a single aperture within each isolated well and may have up to 16 of such wells assembled together in a row. There are additional formats that have up to 384 apertures per chip array. The IonWorks systems (Essen Instruments, Molecular Devices) are examples of a planar array patch clamp technology that can measure ionic current as the aggregate average of up to 64 contributing cells, with an

overall patch-clamping success rate of approximately 60-80%.[12,44] However, the seal resistance obtained is typically only in the 100-MΩ range. This type of platform is often referred to as population patch clamping and differs from other planar chip technologies in that multiple apertures within a single well share common internal and external electrical circuits. As noted, one disadvantage of these "population patch clamp" systems is the lower seal resistances (≤ 200 MΩ) which contribute to leak currents larger than conventional micropipette patching (with gigaseals). However, digital leak subtraction methods and the ability to average large numbers of cells reduces variability due to cell heterogeneity, improves the signal-to-noise ratio and improves the coefficient of variation for the assay when determining dose-response curves. In addition, the system is capable of evaluating approximately 2,000 compounds per day.[12,22]

Microelectrode arrays (MEAs) are another technology platform developed to record single-cell electrophysiology. MEAs, however, have not been favored for high throughput screening because they rely predominantly on passive cell attachment to the surfaces containing the electrodes and do not rely on negative pressure to ensure tighter seals. Thus, the low seal resistances (~ 1 MΩ) result in *extracellular recordings* of two orders of magnitude less than those achieved with gigaseal methods.[52]

A number of different resistances must be monitored during voltage clamping (see Figure 4.5) in order to properly interpret the resulting data set. These include membrane resistance (R_m), cell resistance (R_{cell}), electrode resistance (R_e), current resistance (R_i), and leak resistance (R_{leak}). The sum of these gives the total resistance of the system. Access resistance (R_a) is the sum of R_{cell} and R_e. The values of R_m and R_a

are indications of seal quality, with higher R_m values (e.g. >200 MΩ) and lower R_a values (e.g. <15 MΩ) providing improved recording quality.[60]

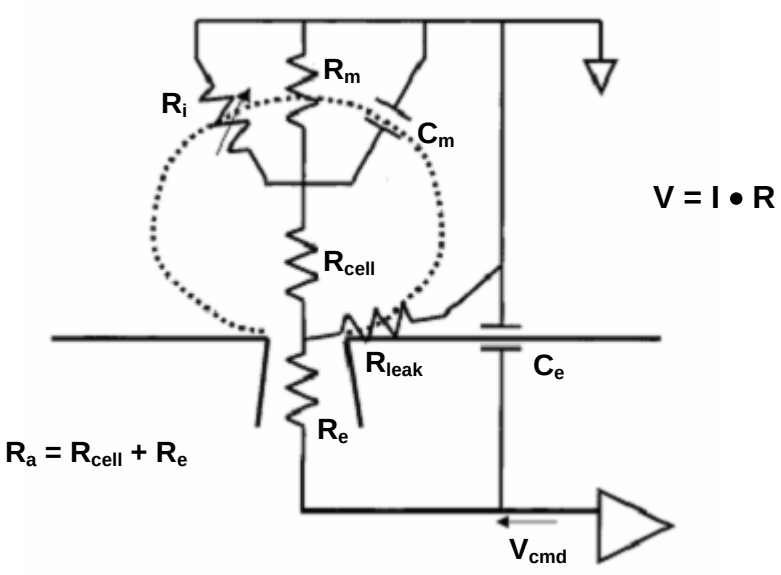

Figure 4.5 Diagram of the resistance (R) parameters which regulate seal quality and recording accuracy. R_i (ion current), R_m (membrane), R_a (access), R_e (electrode), C_e (electrode capacitance), C_m (membrane capacitance), V_{cmd} (voltage command input). Currents and resistances follow Ohm's law (V=I·R). Modified from Xu, et al.[60]

Compared to conventional micropipettes, patch chips have smaller capacitances (generally < 1 pF) and more than ten times less series resistance. Chip resistances are measured using Ohmic principles (V=I·R) by applying a pre-determined potential difference (e.g. a 10-mV square-wave voltage-clamp pulse) across the aperture and measuring current flow.[60] Although the patch chips have greater surface area for cellular membrane attachment, it has been shown that application of negative pressure and drawing the membrane inside the pore walls produces the high seal resistances.[52]

The patch chip technologies evaluated in this project included those from Nanion Technologies (Munich, Germany) and AVIVA Biosciences (San Diego, CA). However,

it should be noted that there are a number of other companies advancing this technology as an alternative to conventional micropipette patching. These include Cellectricon (Gaithersburg, MD), flyion (Tübingen, Germany), Molecular Devices (Sunnyvale, CA), Multi Channel Systems (Reutlingen, Germany), Cytion (Lausanne, Switzerland), Sophion Bioscience (Ballerup, Denmark), Genion (Hamburg, Germany), and Essen Instruments (Ann Arbor, MI).[3,18,28,34,50,61]

4.3 Methods

4.3.1 Cells

Adult mouse CFb were isolated as previously described (see Chapter 2) and utilized approximately 3-5 days later. Adult rat CFb were isolated using similar enzymatic digestion protocols and utilized at approximately 1-2 weeks of age. NIH3T3 mouse embryonic fibroblasts were obtained from the American Type Culture Collection (ATCC Number CRL-1658). Cells were cultured in DMEM supplemented with 10% FBS at 37°C in a humidified incubator regulated with 5% CO_2.

4.3.2 Quantitative PCR

SYBR Green qPCR was performed as previously described to characterize various ion channels in both mouse and rat CFb and NIH3T3 cells. Table 4.1 lists the primer sets used for mouse mRNA. Primer sets used for rat mRNA were generously provided by S. Ohya[6] (Nagoya City University, Nagoya, Japan) and are listed in Table 4.2.

Table 4.1 Mouse Primer Sets for SYBR Green qPCR of Ion Channels

Gene	*Forward (5'-3')*	*Reverse (5'-3')*
Kv1.2	CCCAAGAAACGGATGAGGTA	TCATCCTCCCGAAACATCTC
Kv1.3	TTTCCGCATCTTCAAGCTCT	TGACCCCAATGAAGAGGAAG
Kv1.4	GCTTCGAAACCCAAATGAAA	GCCCTGTCCTCCTCTTCTCT
Kv1.6	ACTTCGCAGAGGCTGATGAT	CATGTCCCCATAACCTACCG
Kir2.1	ATGAGGGATGGCAAACTCTG	TGCGGTCAATTCCACTATCA
Kir3.1	ACCCTGGTGGATCTCAAGTG	GGGAGTGTAGTTGCCGACAT
Kir3.4	AAGATCAGCCAGCCAAAGAA	GGAGATGATGAGTGGGGAGA
Kir6.1	TTCGGAGGGAGAATGATGAC	CGTGGTTTTCTTGACCACCT
TRPM4	GAGAGGATCATGACCCGAAA	GTCATTCAGCAGAGCATCCA
TRPM7	GCTCCATGGGGAGTGATAGA	ATCAAAGCCACCACAGGAAC
TRPV2	TGATGAAGGCTGTGCTGAAC	CACCACAGGCTCCTCTTCTC

Table 4.2 Rat Primer Sets for SYBR Green qPCR of Potassium Channels[6]

Gene	*GenBank Accession Number*
Kv1.1	NM_173095
Kv1.2	NM_012970
Kv1.5	NM_012972
Kv1.6	AJ276137
Kir1.1	NM_017023
Kir2.1	NM_017296
Kir2.2	NM_053981
Kir2.3	NM_053870
Kir2.4	NM_170718
Kir3.1	NM_031610
Kir6.1	NM_017099
Kir6.2	NM_031358
GAPDH	NM_017008

4.3.3 Conventional Patch Clamping

Freshly dissociated cells were allowed to settle to the bottom surface of a perfusion flow chamber (1-2 ml volume) which was positioned on the stage of a Nikon Diaphot inverted microscope configured for phase contrast optics. Microelectrodes were made from borosilicate glass tubes (World Precision Instruments, Sarasota, Florida) using a P-87 Flaming/Browning pipette puller (Sutter Instruments, Novato, CA) and were polished (Narishige Scientific Instrument Lab microforge). Microelectrodes had

resistances between 6-12 MΩ when filled with internal solution. Clampex software (Version 8.1) (Axon Instruments, Sunnyvale, CA) was used to generate and apply voltage clamp protocols through an EPC7 amplifier (ListElectronic, Darmstadt, Germany) interfaced with a Digidata 1322A data-acquisition system (Axon Instruments). The system used is depicted in Figure 4.6.

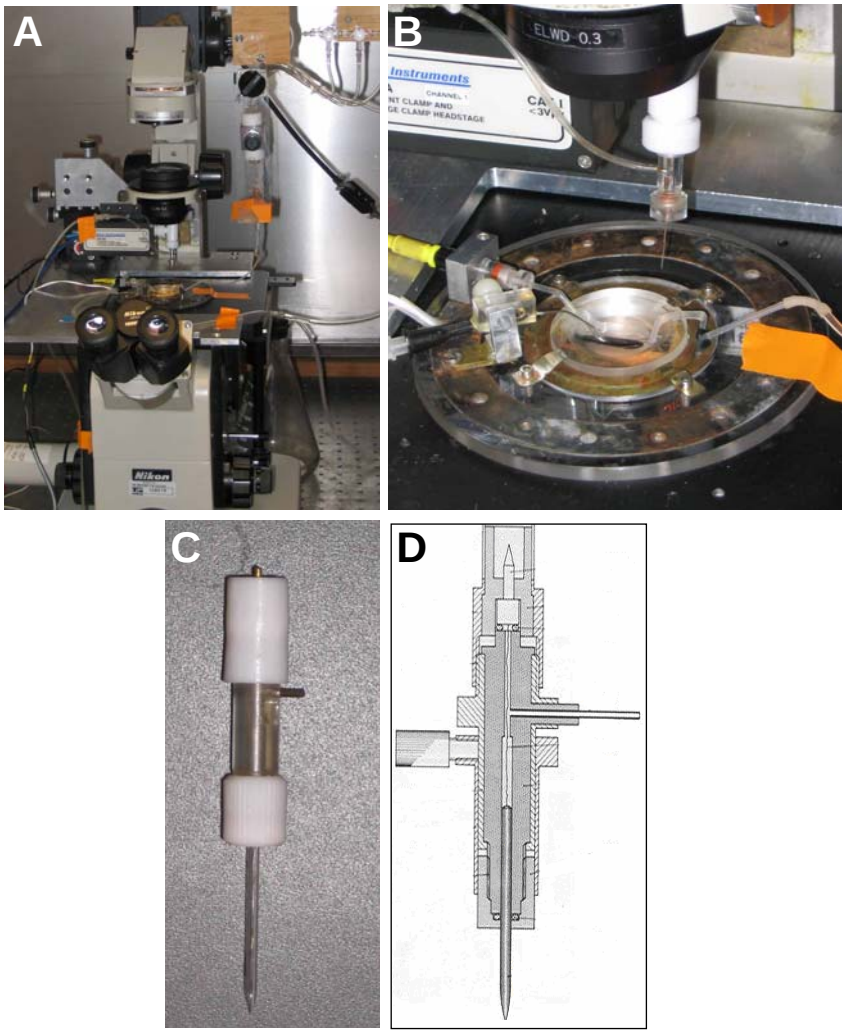

Figure 4.6 Conventional Patch Clamping System. ***A.*** Inverted microscope with stage-mounted micromanipulator and perfusion system. ***B.*** Close-up of perfusion chamber. ***C.*** Close-up of microelectrode. ***D.*** Schematic of microelectrode components in cut-away view.

Whole-cell current-voltage (I-V) relationships were obtained using a protocol which consisted of 300- or 500-ms, 10-mV steps from a holding potential of -50 mV between -130 mV and 60 mV. Current records were analyzed using pCLAMP and Clampfit software (Axon Instruments) and plotted using Prism (GraphPad, San Diego, CA). Currents were measured as maximal inward or outward currents at fixed times. Total measured current is the summation of current passing through the membrane (e.g. ion channel current) and current passing through the cell seal (e.g. leak current). This leak current can be subtracted from total current to reveal transmembrane ionic current. When appropriate, I-V relationships were corrected for leak currents by subtracting this linear current.[6]

4.3.4 Nanion Patch Clamping

Electrophysiological assessments made using the Port-a-Patch© NPC©-1 instrument (Nanion Technologies, München, Germany) were carried out according to the recommendations of this manufacturer. Briefly, 5 μl of internal solution was added to the underside of the patch clamp chip and the chip was then tightly screwed onto the mounting station. The chips are made from borosilicate glass (100 μm thickness), thinned to ~20 μm in the region where the aperture is made (~1 μm diameter). Chip resistances are reported at ~6 MΩ with capacitances of < 1pF.[3] The "shield" cover was then placed over the chip, and the PatchControl software program initiated. After addition of 5 μl of external solution to the top of the chip, a background chip resistance was collected (2-5 MΩ). Both the internal and external solutions are required to contain

chloride ions to function as the conducting ions.[3] A small aliquot (~ 5 µl) of concentrated cell suspension was added and the experiment was initiated. The custom software automatically controls negative pressure (measured in mBar) to draw a cell towards the opening and to initiate cell/chip contact. When a 5-MΩ or large seal resistance has been detected, the program assumes contact with a cell has been made and begins additional negative pressure to improve seal resistance. When the cell seal resistance reached approximately 50-100 MΩ, it was necessary to add 20 µl of a proprietary "Seal Enhancer" solution in order for the cell to progress to giga-ohm seals. The Seal Enhancer solution was washed off using external solution after whole-cell access was achieved. Chips were used only once and discarded after each patching attempt. The Nanion system and solution/cell loading steps are depicted in Figure 4.7.

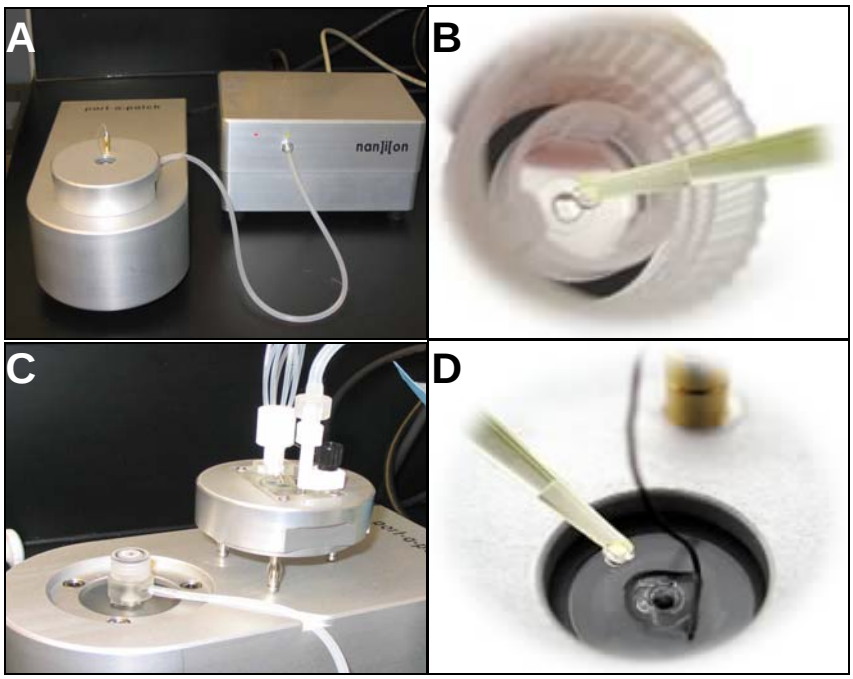

Figure 4.7 Nanion Patch Clamping System. ***A.*** Assembled device showing shielded testing chamber (left) and pressure control unit (right). ***B.*** Chip within screw cap with internal solution being applied. ***C.*** Chip/cap in place with perfusion flow shielding cover removed. ***D.*** Shielding cover in place with external solution being applied.

Data acquisition was via an EPC10 amplifier (HEKA Electronic, Mahone Bay, Nova Scotia, Canada) and PatchMaster (v2.11) software (HEKA Electronic). Raw data were visualized in real-time on the monitor to assess current tracings and current-voltage relationships. Data was then saved and exported into MatLab for extraction and use by other data processing and graphing software. Leak subtraction was performed as previously described, when appropriate.

4.3.5 AVIVA Biosciences Patch Clamping

Whole-cell patch clamp recordings made on site at AVIVA Biosciences utilized a beta prototype system containing 16 individual wells per chip. The chip was fastened into a holder with a gasket underneath and grounding electrodes were positioned in each well. Internal solution was pipetted under each well of the chip through a series of tubes and the tubes subsequently clamped. The assembled chip was positioned onto the stage of a Nikon Eclipse TE 2000-U inverted microscope (on an air-suspension table, housed within a shielded Faraday cage) and connected to the grounding electrode (Ag/AgCl wire) and input electrode (Ag/AgCl wire) (via a CV-7A Axon headstage). Data acquisition was performed using MultiClamp 700 and Digidata 1322 A data acquisition system (Axon) and controlled using ClampEx software (Axon).

After focusing the well over the precision-made chip aperture (visualized by CCD camera export to both a monitor and to an on-screen window), external solution (~ 50 μl) was added to the well and the chip resistance was measured. Cells were loaded into the well and negative pressure (via a syringe connected to the internal solution port) was used to bring an individual cell in contact with the aperture. Sealing and break-through

negative pressures were controlled manually using a syringe with magnitude displayed on a digital pressure monitor. Fluid exchange was handled by pipetting directly into the well. Recordings of a single cell were made within each well, and the chip was replaced with a new one after all 16 wells had been used. Although flow-through chip designs are available (with a single cell per chip), they were not utilized in these experiments. Data files were recorded using Clampex software (Axon Instruments) and processed using Clampfit software (Axon Instruments) to determine I-V curves. Leak subtraction was performed as previously described, when necessary. The AVIVA system used is shown in Figure 4.8.

4.3.6 Patch Clamp Solutions

The patch clamp solutions utilized are listed in Tables 4.3. All solutions were used at room temperature and were filter-sterilzed before use. Internal solutions are generally 10% more hypo-osmolar than the external solutions since this has been found to assist in giga-seal development.[16] Internal A and External A solutions are the solutions recommended by Nanion for patching of potassium channels, whereas Internal B and External B solutions are the patching solutions used with conventional micropipette patching.[6] Internal C and External C solutions are reported AVIVA solution formulations.[60]

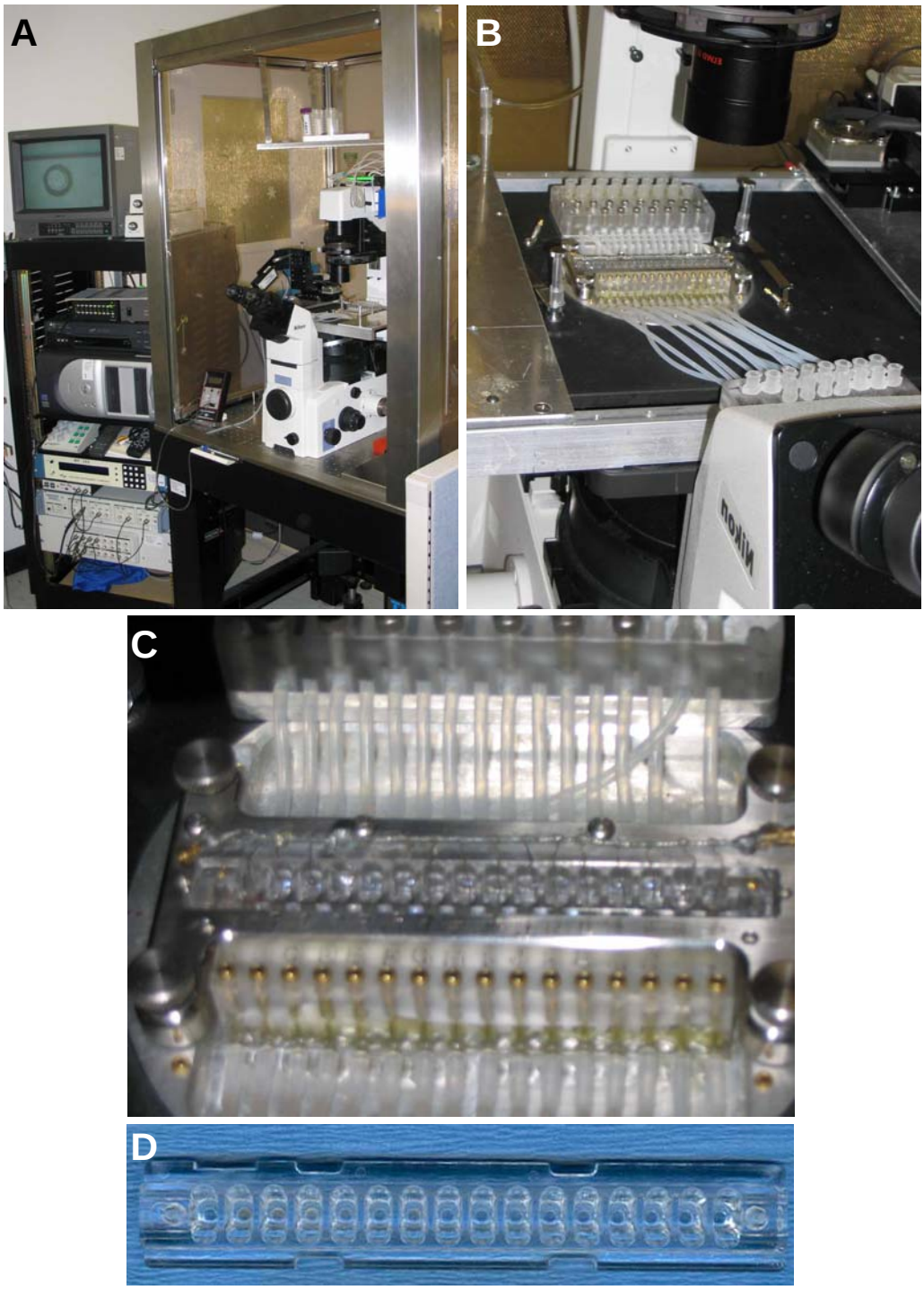

Figure 4.8 AVIVA Patch Clamping System. ***A.*** Patch clamp system with imaging capabilities. The chip aperture area is in view on the monitor. ***B.*** Assembled chip in place on inverted microscope. ***C.*** Close-up of chip showing 16-well design with ground and input electrodes. ***D.*** Close-up of chip itself.

Table 4.3 Patch Clamp Solutions (in mM)

Internal A	*Internal B*	*Internal C*	*External A*	*External B*	*External C*
KCl (75)	NaCl (12)	KCl (20)	NaCl (160)	NaCl (140)	NaCl (138)
NaCl (10)	KCl (20)	K-glutamate	KCl (4.5)	KCl (5.4)	KCl (2.67)
KF (70)	K-aspartate (110)	(110)	$MgCl_2$ (1)	$CaCl_2$ (1)	$MgCl_2$ (0.5)
$MgCl_2$ (2)	$CaCl_2$ (1)	NaCl (8)	$CaCl_2$ (2)	$MgCl_2$ (1)	$CaCl_2$ (0.9)
EGTA (10)	$MgCl_2$ (1)	$MgCl_2$ (1)	glucose (5)	HEPES (10)	glucose (5.6)
HEPES (10)	K_2ATP (4)	Mg-ATP (4)	HEPES (10)	glucose (5.5)	Na-pyruvate
pH 7.2 (KOH)	EGTA (10)	EGTA (10)	pH 7.4 (NaOH)	mannitol	(0.33)
	HEPES (10)	HEPES (10)		(7.14)	KH_2PO_4 (1.47)
	pH 7.2 (KOH)	pH 7.2 (KOH)		pH 7.4	Na_2HPO_4 (8.1)
				(NaOH)	pH 7.4 (NaOH)

4.4 Results

4.4.1 AVIVA Whole-Cell Patching

Results from the AVIVA system were more difficult to interpret, partly because this was the first technology attempted using the adult mouse CFb, and partly because solution formulations and clamping protocols had not yet been standardized. Nevertheless, sufficient data was obtained to address feasibility.

It was noted consistently that adult mouse CFb were difficult to patch using the AVIVA system. The precise reasons for this difficulty were not determined, but approximately only 1 out of every 10 cells which were attempted formed a stable seal. The results of three successful recordings are shown in Figure 4.9. Although the signals were noisy and relatively small, the current tracings exhibited slow activation kinetics at the more depolarized potentials, and a sigmoidal isochronal I-V relationship. The reversal potential was approximately -10 mV, which is more depolarized than would be expected of CFb[6] and may be due to current adjustment from the on-line leak subtraction protocol employed. There were no observed currents from inwardly rectifying potassium channels (Kir) in these cells, even though mouse CFb were shown to express

various Kir isoforms (see Figure 4.22). Kir currents in rat CFb (see Figure 4.10 and Chilton, et al.[6]) are observed at membrane potentials less than -80 mV. Therefore, the lack of Kir in mouse CFb was most likely due to the fact that the voltage clamp protocol in these experiments did not step below -70 mV.

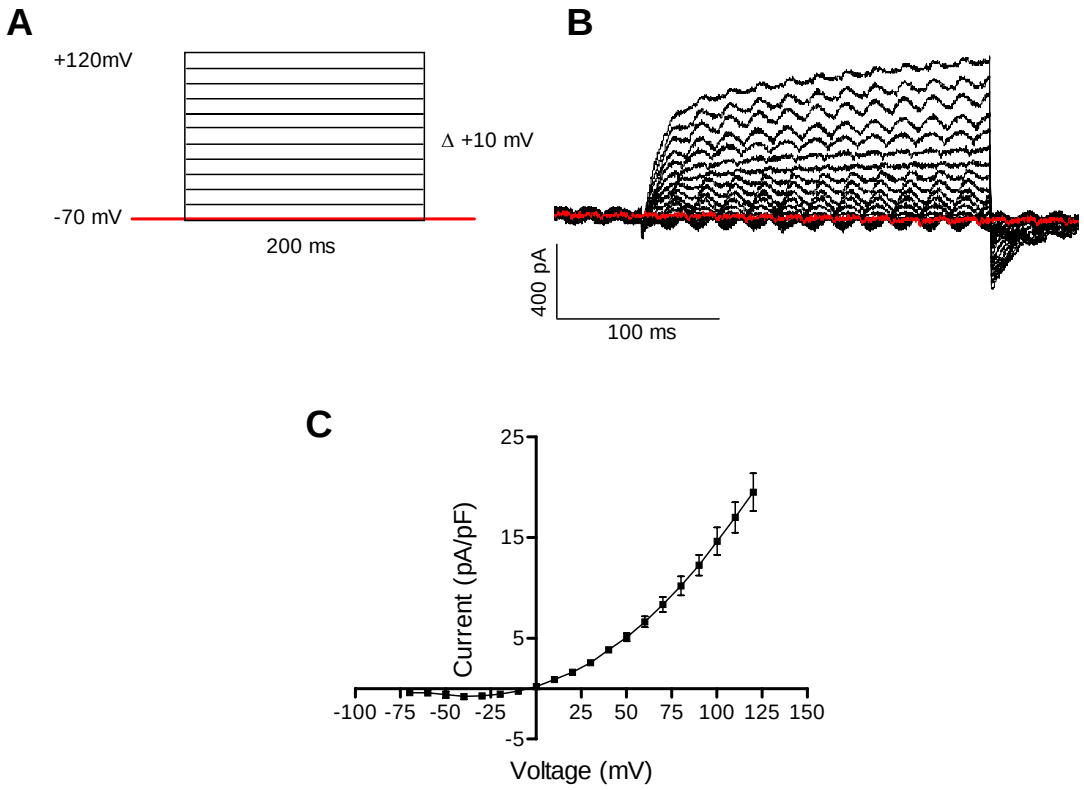

Figure 4.9 Voltage-clamp Measurements on an Adult Mouse CFb Using the AVIVA Chip System. ***A.*** Voltage-clamp protocol consisting of a 200-msec, 10-mV steps from a holding potential of -70 mV to a maximum potential of +120 mV. ***B.*** Representative family of currents. ***C.*** Isochronal I-V relationship, obtained by plotting peak inward or outward currents at the end of the 200-msec clamp step, reported as mean ± sd. Cell capacitance was estimated at 30 pF.

A representative family of currents generated from rat CFb using the AVIVA patch system is shown in Figure 4.10. Again, these currents exhibited graded time- and voltage-dependent onset kinetics. The magnitudes of the fibroblast current densities over comparable voltage potentials were similar for the mouse and the rat (compare Figures

4.9 and 4.10). Furthermore, the I-V relationship of the cells tested with the AVIVA chip mimic the shape of reported I-V relationships for rat ventricular fibroblasts.[6] However, the AVIVA current densities were approximately 3-fold lower in magnitude than those published.

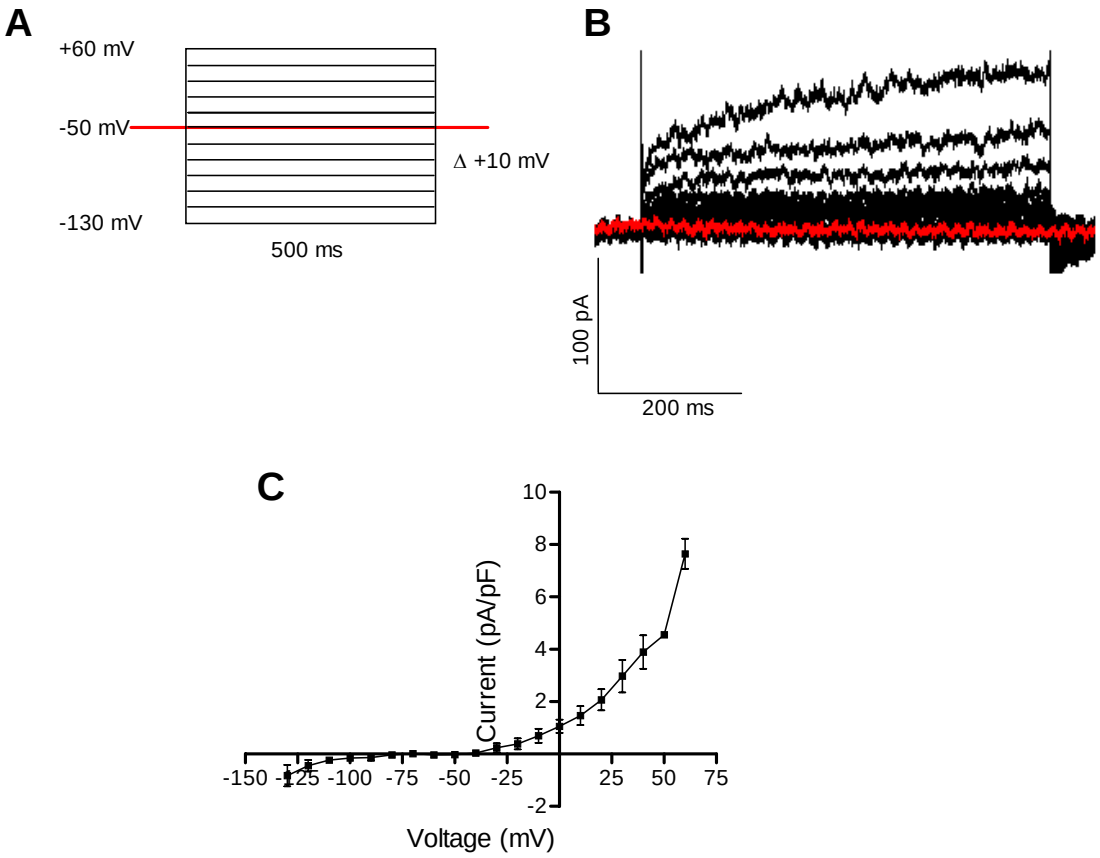

Figure 4.10 Voltage-clamp Measurements on an Adult Rat CFb Using the AVIVA Chip System. ***A.*** Voltage-clamp protocol consisting of a holding potential of -50 mV with 500-msec, 10-mV steps from -130 mV to +60 mV. ***B.*** Representative family of currents. ***C.*** Isochronal I-V relationship of peak currents at the end of the clamp step, reported as mean ± sd. Cell capacitance averaged 30 pF.

In a third set of experiments, an assessment of NIH3T3 cells was made. These cells were difficult to break through into whole-cell configuration. Repeated voltage

pulses (approximately 10 total, 20 ms in duration and +1.3 V in magnitude), which transiently weaken the plasma membrane, had to be applied before whole cell was achieved. The result of one successful patch experiment is presented in Figure 4.11. Again, there is similarity in the shape and magnitudes of the I-V relationship between NIH3T3 fibroblasts and primary isolated mouse and rat ventricular fibroblasts.

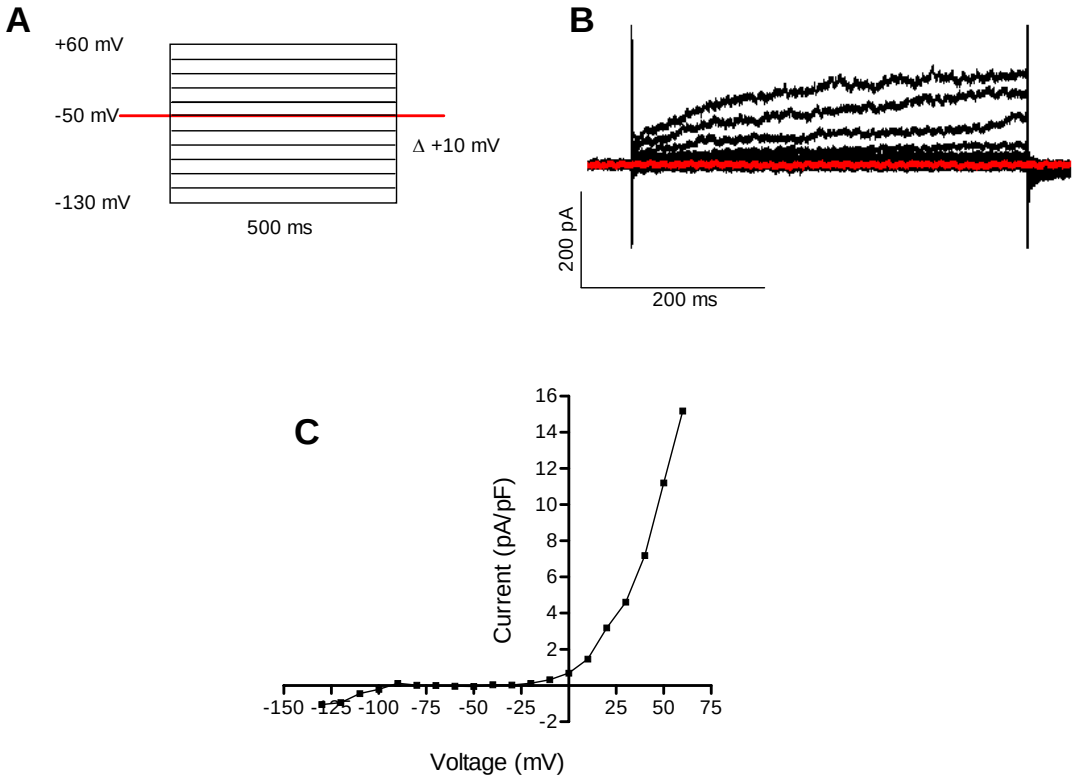

Figure 4.11 Voltage-clamp Measurements on an NIH3T3 Embryonic Mouse Fibroblast Using the AVIVA Chip System. ***A.*** Voltage-clamp protocol consisting of a holding potential of -50 mV with 500-msec, 10-mV steps from -130 mV to +60 mV. ***B.*** Representative family of currents. ***C.*** Isochronal I-V relationship of peak currents at the end of the clamp step of a single cell with capacitance of 20 pF.

Ion channel activation and inactivation probabilities can be influenced by holding potential and polarity of the steps (i.e. depolarizing or hyperpolarizing), so a comparison of two different voltage-step protocols was made. These two protocols differed in their holding potentials (-15 mV vs. -70 mV), minimum potentials (-105 mV vs. -70 mV), and maximum potentials (+185 mV vs. +120 mV), and were equivalent only for pulse length (200 ms). Regardless, these I-V relationships were in reasonable agreement over the defined voltage ranges of each (data not shown).

To begin to evaluate whether these outward currents in the fibroblast I-V relationships are carried in part by specific Kv ion channels, an adult mouse CFb was patched and recorded pre- and post-application of 4-aminopyridine (4-AP), which is a known blocker of Kv channels in the heart. As shown in Figure 4.12, application of 4-AP (5 mM) reduced outward current density (measured at +50 mV), but did not affect inward current density (measured at -80 mV). A similar reduction in outward current was also observed in rat CFb exposed to 4-AP (Figure 4.12).

In summary, the AVIVA chip system was capable of whole-cell patching of both mouse and rat CFb and, to a lesser extent, NIH3T3 fibroblasts. Further, the system was able to distinguish 4-AP blockade of Kv currents from baseline controls. Unfortunately, because of scheduling limitations and availability of the system, an evaluation of S1P was not conducted. In addition, because of the noted success rates in patching mouse CFb and because of the much higher cell yields needed for the chip technologies, further comparative experiments using the Nanion system focused primarily on rat CFb.

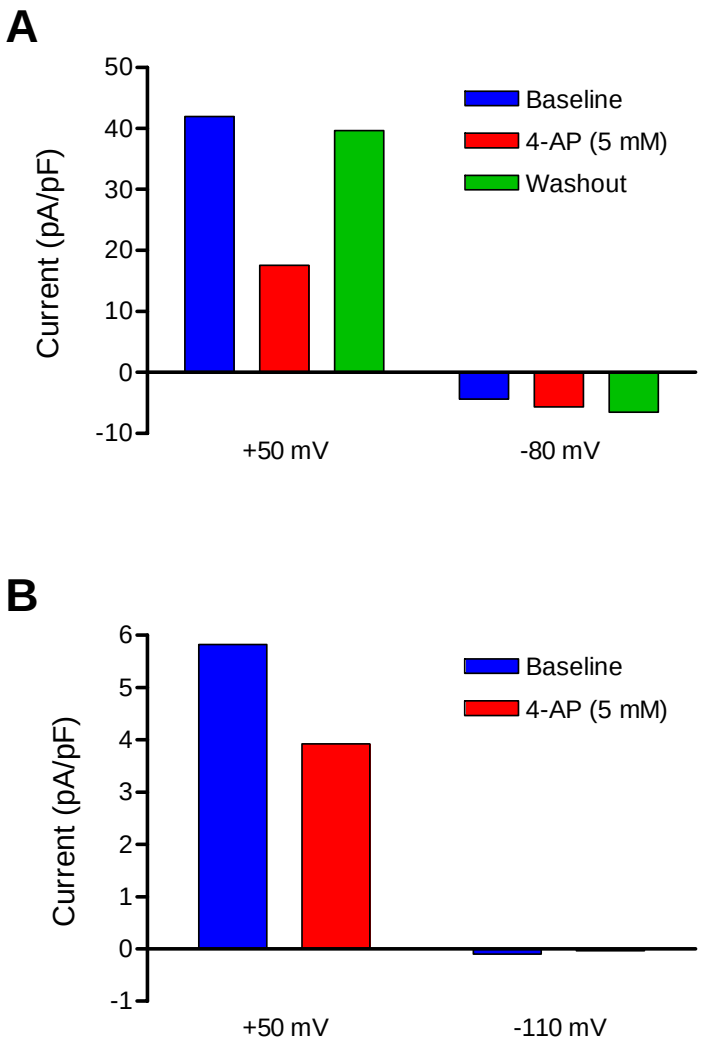

Figure 4.12 Response of Adult CFb to 4-AP Using the AVIVA Chip System. ***A.*** A single mouse CFb was patched using a voltage-ramp protocol of -80 mV holding potential and decreasing voltages from +60 to -130 mV over a 500-msec period. Outward current densities at +50 mV and inward current densities at -80 mV were measured at baseline, after 4-AP (5 mM) application, and following a washout period. Cell capacitance was 35 pF. ***B.*** A single rat CFb was patched using a voltage-step protocol of -50 mV holding potential and 500-msec, 10-mV steps from -130 to + 60 mV. Outward currents at +50 mV and -110 mV were measured at baseline and after 4-AP (5 mM) application. The cell seal was lost before washout could be completed. Cell capacitance was 32 pF.

4.4.2 Nanion Whole-Cell Patching

Adult rat CFb were patch clamped in the whole-cell configuration using the Nanion chip system. It was necessary to add seal enhancer solution each time in order for this recording paradigm to progress past mega-ohm (MΩ) seals to giga-ohm seals. Without the seal enhancer solution, seal resistances rarely progressed past 100 MΩ. A rationale for this necessity, based on solution composition, has not yet been adequately determined. However, no cells were observed to progress to giga-ohm seal levels in its absence.

A summary of the I-V relationships obtained from rat CFb is shown in Figure 4.13. The cells exhibited a reversal potential of approximately -40 mV and displayed prominent time- and voltage-dependent outward currents and smaller inward currents. Note that a similar shaped I-V relationship was obtained using the Nanion system as with the AVIVA system and that rat CFb again exhibited expected reductions in outward currents when treated with 4-AP[48] (Figure 4.14). It was noted, however, that the current densities obtained with the Nanion chip system were much greater (at least 10 times greater) in magnitude than those obtained with the AVIVA chip system or by conventional micropipettes (refer to Figures 4.10, 4.13, and 4.18).

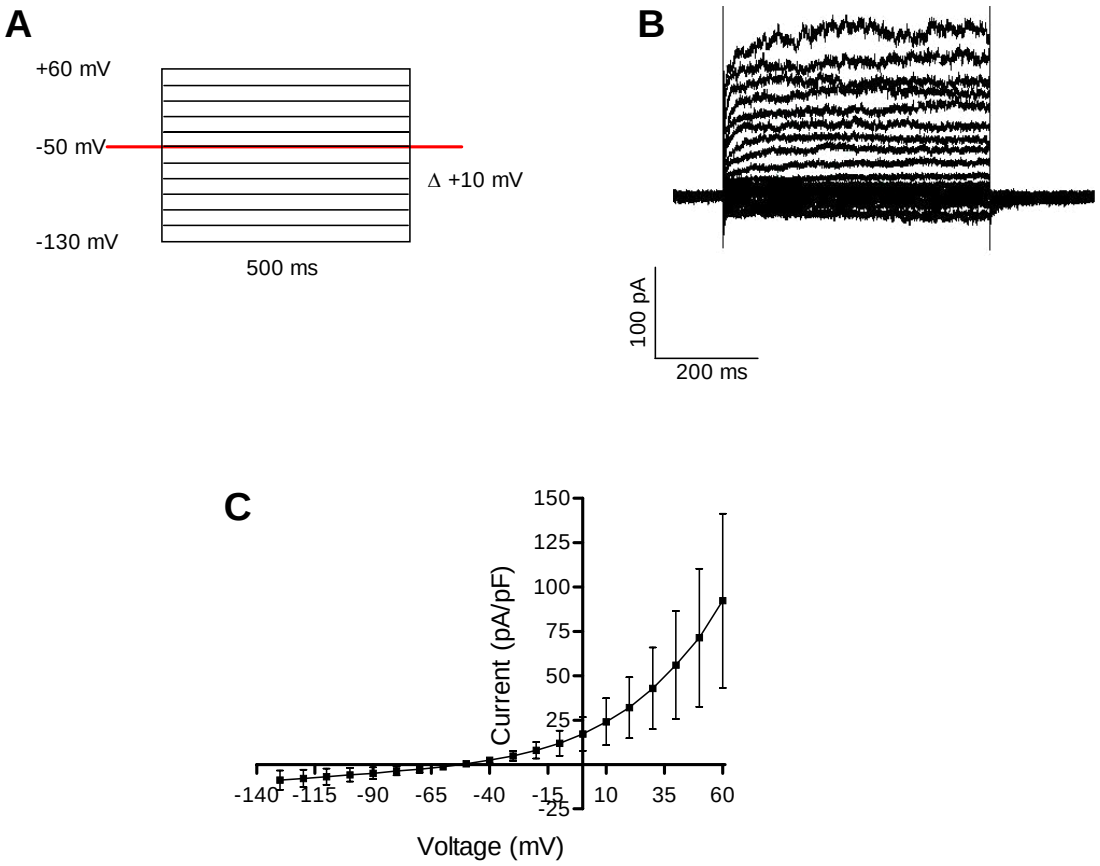

Figure 4.13 Voltage-clamp Measurements on an Adult Rat CFb Using the Nanion Chip System. ***A.*** Voltage-clamp protocol consisting of a holding potential of -50 mV with 500-msec, 10-mV steps from -130 mV to +60 mV. ***B.*** Representative family of currents. ***C.*** Isochronal I-V relationships of peak currents at the end of the clamp step from 12 cells, reported as mean ± sd.

The Nanion system controls pressure automatically to help maintain seal resistance. However, the user may override the set points. To determine if the pressure maintenance level can affect the density of currents recorded, a repetition of voltage-step clamping protocols were carried out while slowly increasing the magnitude of negative pressure. As shown in Figure 4.15, the application of greater negative pressures (e.g. -300 vs. -50 mBar) augmented the current density particularly at membrane potentials

which were relatively far from the reversal potential of approximately -50 mV. This was confirmed by performing correlation coefficients of the current densities over the pressure range evaluated. Increased pressure likely improved seal quality and thereby increased the signal-to-noise ratio of the measured currents. It is unlikely that this was due to increasing leak currents. Leak current is characterized by a depolarizing shift in the reversal potential and currents that have a linear I-V relationship. Since the reversal potential remained consistently near -50 mV over the pressure range evaluated, leak currents were unlikely to have been the source of the increased current.

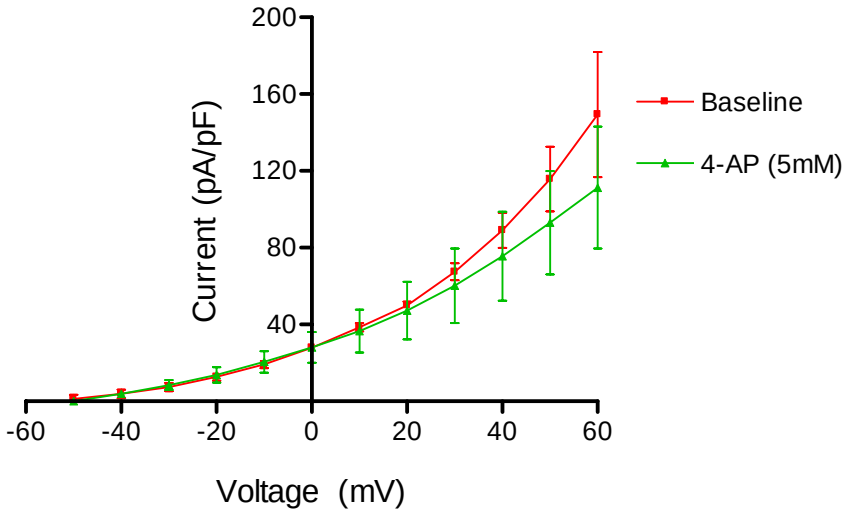

Figure 4.14 Response of Adult Rat CFb to 4-AP Using the Nanion Chip System. Cells were voltage-clamped from a holding potential of -50-mV using 500-msec, 10-mV steps from -130 to +60 mV. The outward current densities from 3 cells (mean ± sd) are shown at baseline and after 4-AP (5 mM) application.

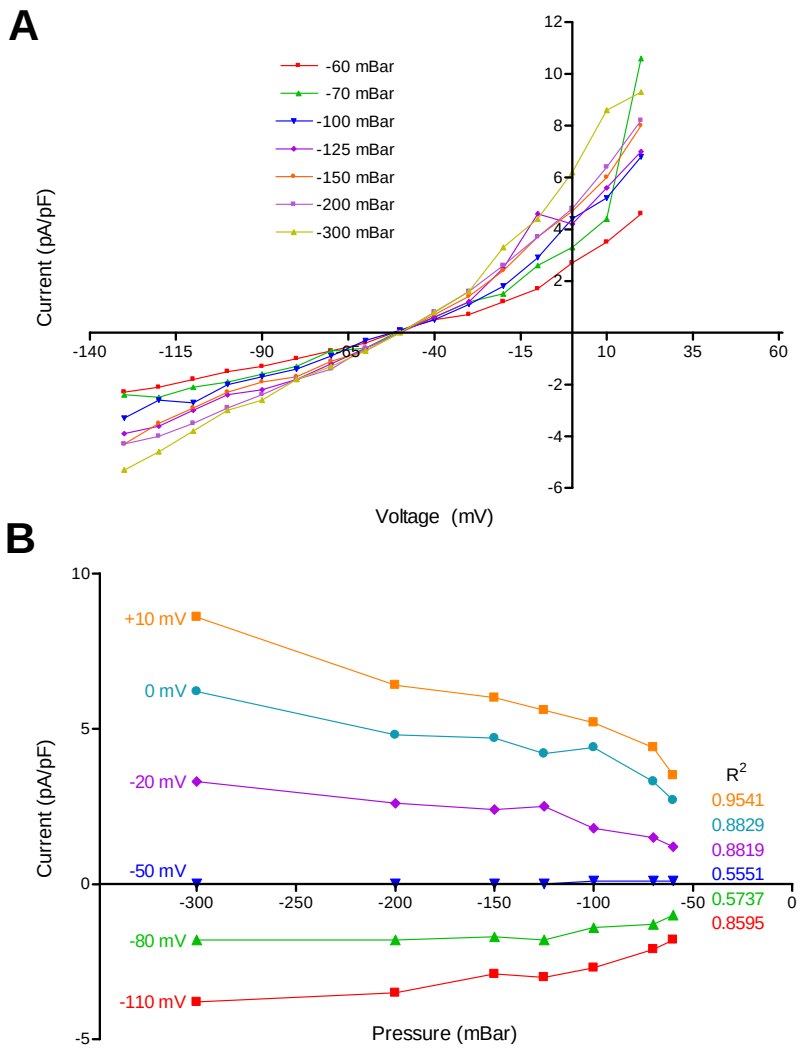

Figure 4.15 Response of an Adult Rat CFb to Changes in Negative Pressure Using the Nanion Chip System. A single cell was voltage-clamped from a holding potential of -50-mV using 500-msec, 10-mV steps from -130 to +60 mV. ***A.*** Isochronal I-V relationships at increasingly negative pressures. ***B.*** The current densities at selected membrane potentials are shown over the range of pressures evaluated. Correlation coefficients (R^2) of the pressure-current relationships are reported.

With the Nanion design, test solutions are applied to the surface of the chip, directly onto the patched cell. To exchange solutions (e.g. application of test compounds or washout), one must pipette onto the chip, wait for the incoming solution to mix with

the existing solution, and then remove an equivalent volume. In our experiment, this was repeated at least three times to result in an adequate solution exchange. It was noted that currents tended to slowly decline over time following this procedure. It was hypothesized that the pipetting might be weakening the seal or triggering a stretch-activated current due to shear stress. To address this concern, a patched cell was analyzed before, immediately after, and 5 min after performing a sham fluid exchange of pipetting the existing solution up and down three times. This simple test suggested that pipetting action could result in increased current measurements that were sustained even after 5 minutes (Figure 4.16). The increases in current were not believed to be due to increased leak current, again because the reversal potential during the pipetting experiment remained near -50 mV. The current increases were therefore attributed to activation of mechanosensitive receptors or channels.

To further test the effect of shear stress on patched cells, the Nanion system was evaluated using its perfusion flow system. This component of the device (see Figure 4.7) is substituted for the standard shield cover after the cell has reached whole-cell configuration. The perfusion flow system is gravity-fed and the incoming fluid dispenses directly on top of the patched cell. As seen in Figure 4.16, fluid shear stress from the perfusion flow system caused marked changes in the current densities. Upon cessation of perfusion flow and return to static flow, the I-V relationship returned to baseline values.

Thus, it was difficult to ascertain true agonist responses (e.g. such as S1P) from fluid shear stress responses when using the Nanion system. This is most likely a consequence of the reduced volumes needed in this system. The results of these tests using the Nanion system also place the results of the AVIVA system under speculation

since fluids were administered in a similar manner (i.e. repeated pipetting/removal). However, it should be noted that the fluid volumes contained in the wells of the Nanion system were approximately 2-3 fold less than those of the AVIVA system, and so motion artifacts may be more exaggerated in the Nanion system.

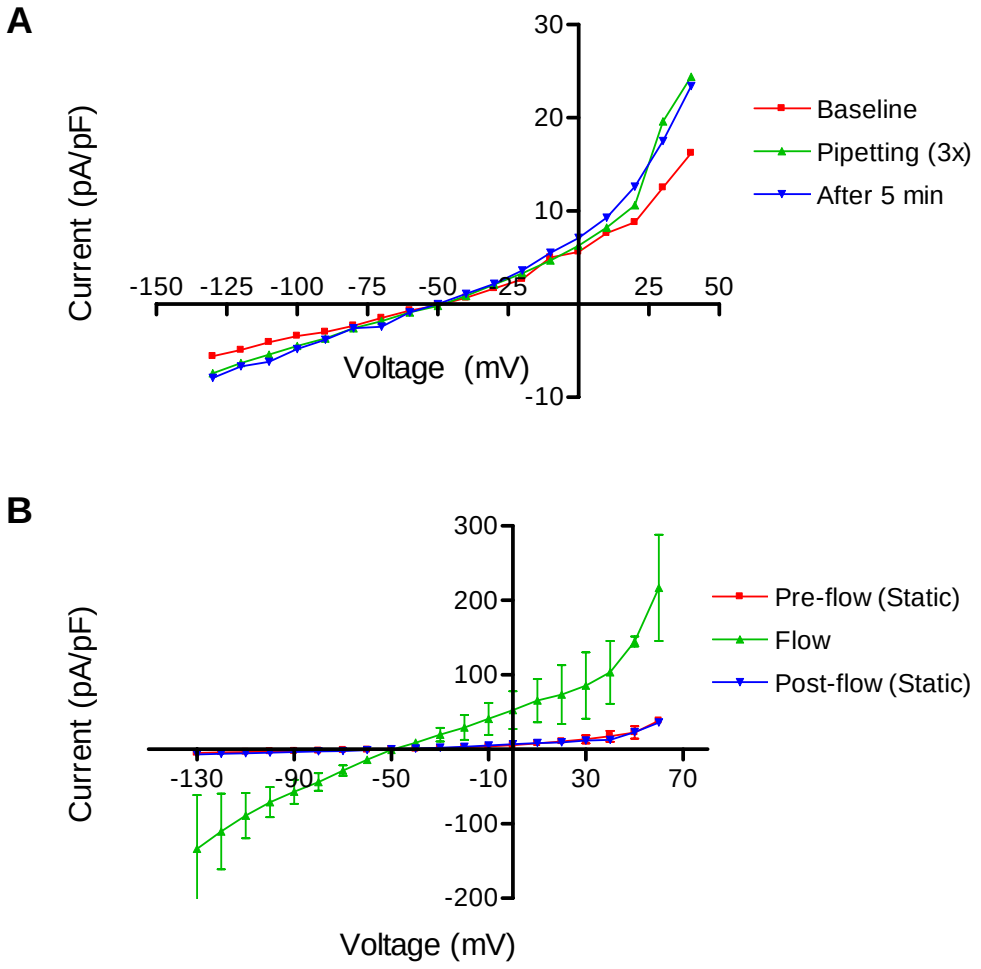

Figure 4.16 Response of an Adult Rat CFb to Fluid Perturbations Using the Nanion Chip System. Cells were voltage-clamped from a -50-mV holding potential using 500-msec, 10-mV steps from -130 to +60 mV. ***A.*** Isochronal I-V relationship at baseline, after pipetting the solution three times (to induce fluid shear stress), and after leaving the solution undisturbed for an additional 5 min. ***B.*** Isochronal I-V relationships before, during, and after the application of perfusion flow, reported as mean ± sd. The I-V curves have not been leak corrected to better illustrate their differences.

In summary, the Nanion system generated qualitatively similar, but quantitatively different I-V relationships than were obtained with the AVIVA system. That is, the current density of the K^+ currents measured differed very substantially (see Figures 4.10 and 4.13). The Nanion system is sensitive to fluid motion artifacts, and because it lacks the capabilities of visualizing the cells under investigation, it is difficult to know whether the cells are undergoing any morphological changes during their examination.

4.4.3 Conventional Whole-Cell Patching

As stated earlier, there were considerable difficulties in patching NIH3T3 fibroblasts when using either the AVIVA or Nanion platforms. To determine if this was a compatibility issue with this particular cell line and the chip technologies, comparison whole-cell patchings were made in NIH3T3 fibroblasts by conventional techniques. Although four cells were successfully patched, it was noted that achieving whole-cell configuration was indeed difficult (data not shown). Additionally, some "blebbing" or distention of the outer membrane from the main cell body was noted in two of the cells examined.

Rat CFb were also examined by conventional whole-cell patching. It was noted that smaller current densities were recorded using conventional patching than had been recorded using the Nanion system, even when using identical stocks of rat CFb. Aside from the differences in technology platforms (i.e. chip vs. pipette), the Nanion system recommends the use of internal and external solutions that differ in composition from those solutions used by Chilton, et al.[6] and utilizes a "seal enhancer" to assist with gigaseal formation. Nanion solutions (Internal/External A) and conventional patching

solutions (Internal/External B) were as listed in Table 4.3. To determine whether the solutions could account for differences in the current densities recorded, rat CFb (from another source, tested on another day) were evaluated using the Nanion solutions. As shown in Figure 4.17, it appears that the Nanion solutions result in much larger current changes to be recorded. Thus, the differences noted previously between the Nanion system and conventional patching can be attributed more to differences in solution formulations, and less due to differences between microelectrode/chip platforms.

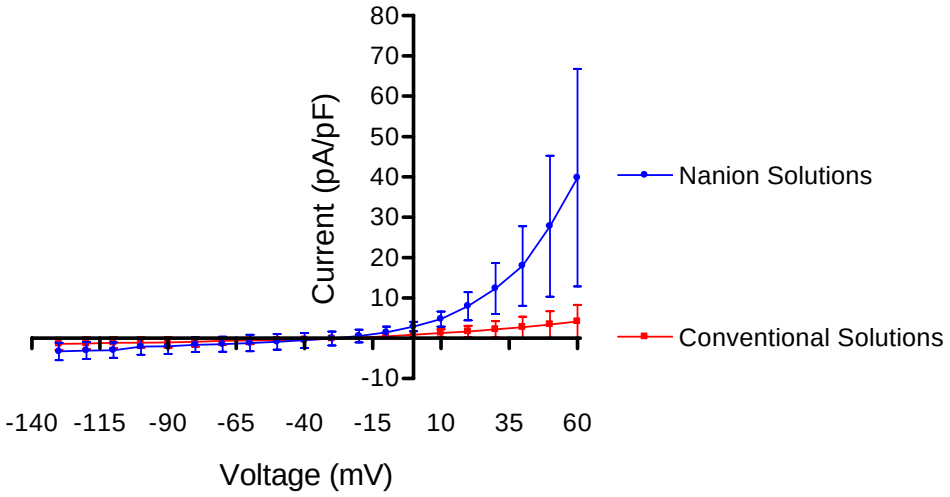

Figure 4.17 Comparison of Solutions Using Conventional Voltage-clamp Patching of Adult Rat CFb. Cells were voltage-clamped using a protocol consisting of a holding potential of -50 mV with 500-msec, 10-mV steps from -130 mV to +60 mV. Isochronal I-V relationships of cells with either conventional or Nanion solutions are shown, reported as mean ± sd.

A summary of the current densities recorded in each platform and those from the literature are presented in Table 4.4. It should be noted that while AVIVA and conventional current densities were similar, the values obtained on rat CFb by conventional patch clamping during these recording sessions were much lower than those previously reported on rat CFb.[6] An explanation for these differences is not readily

evident except to state that the ages of the cells evaluated during these recordings were slightly younger than those used by Chilton, et al.[6] and that age/differentiation differences had been observed in those studies.

Table 4.4 Summary of Adult Rat CFb Current Density Recordings

Voltage (mV)	*AVIVA (pA/pF)*	*Nanion (pA/pF)*	*Conventional (pA/pF)*	*Chilton, et al.[6] (pA/pF)**
-100	-0.16	-5.79	-1.09	-1.5
-70	0.02	-2.56	-0.68	-0.25
-40	0.04	2.43	-0.386	1.5
0	1.06	17.22	0.83	9.25
+30	2.98	42.94	2.16	13.0
+60	7.65	92.26	4.11	not available

*estimates from published data on myofibroblasts

During conventional patching, several rat CFb were observed to form surface blebs. Cell blebbing is a physical separation of the plasma membrane from the underlying cytoskeleton that results in protrusion of the membrane from the cell body.[5,17,26,32] In some cases, blebbing increased during the time-course of the study. To determine what effects blebbing had on the I-V relationship, those cells that were noticed to bleb were compared to those cells that remained stable in their morphology (Figure 4.18). Only those recordings during the baseline period were used, to minimize potential changes over time in the I-V relationships. A consistent observation is that blebbed cells have increased inward and outward currents. Furthermore, blebbed cells appear to have undergone a slight depolarized shift in their reversal potential, which may indicate that leak currents were more pronounced in cells experiencing this phenomenon. Blebbing occurred in cells whether they were in conventional or Nanion solutions, and seemed to

be based more on the particular batch of cells (i.e. cells on a given day were either prone to blebbing or not).

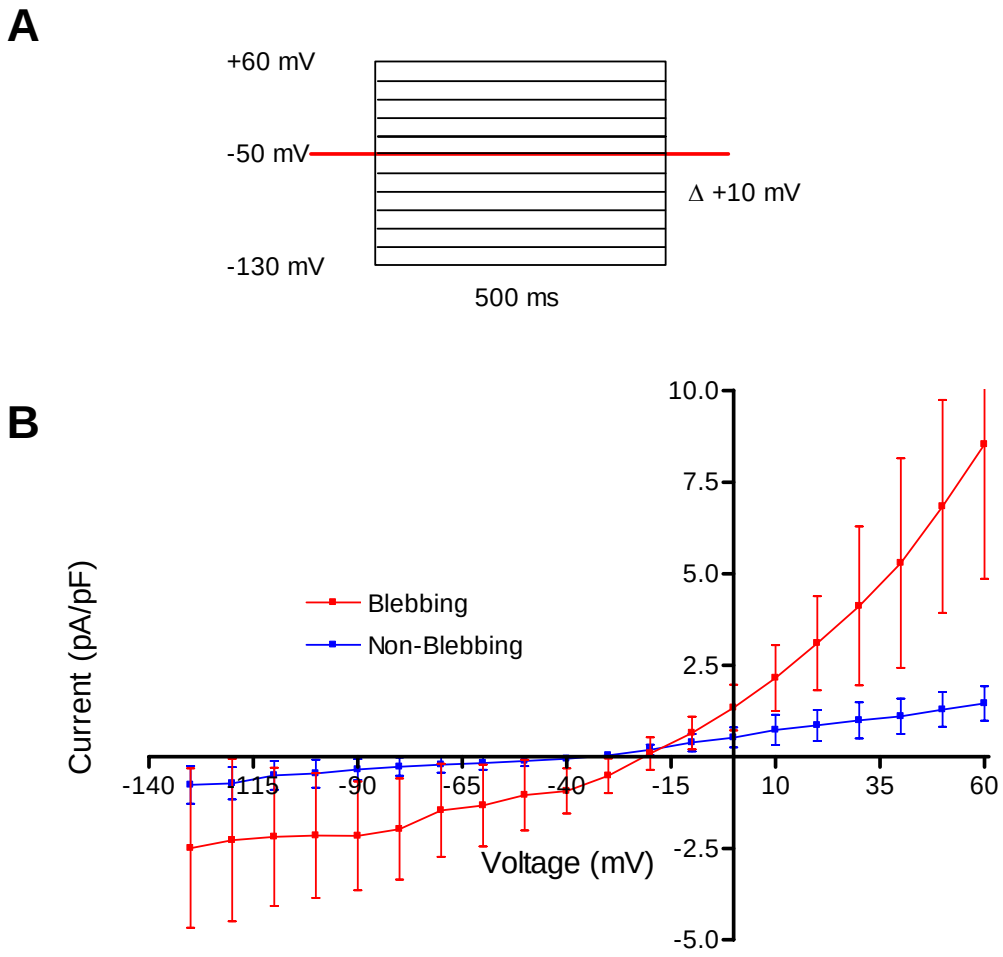

Figure 4.18 Evaluation of the Electrophysiological Effects of Cell Blebbing by Conventional **V**oltage-clamp Methods Applied to Individual Rat CFb. ***A.*** Voltage-clamp protocol consisting of a holding potential of -50 mV with 500-msec, 10-mV steps from -130 mV to +60 mV. ***B.*** Isochronal I-V relationships of cells with observed blebbing or non-blebbing during baseline recordings. The I-V curves, reported as mean ± sd, have not been leak corrected to better illustrate their differences.

In summary, conventional patching still remains the standard platform for electrophysiologists and those studying biophysical properties of ion channels. It is a more suitable technique for cells of limited quantity (e.g. a single cell may be easily

located for patching) or to assess cells in a more characteristic architecture (i.e. adherent to an underlying substrate). Lastly, conventional patching is less sensitive to motion artifacts. This is primarily because the cells are slowly perfused in the chamber bath and the fluid level and flow rates can be controlled to achieve sufficient fluid exchange without inducing mechanical disturbances on the cell.

4.4.4 Electrophysiology of Rat CFb After Application of S1P

S1P is known to activate a number of ionic currents in various cell types such as fibroblasts, myocytes, and endothelial cells.[33,36,41,58,63] These include K_{Ca}, K_{ACh}, Cl^-, and nonselective cation (Na^+, K^+, and Cs^+) currents. Preliminary electrophysiological studies conducted by this laboratory had demonstrated that acutely isolated rat CFb respond to application of 50 nM S1P by activating inward and outward currents (Figure 4.19) (Rose and Giles, unpublished results). The experimental design eliminated contribution of K^+ (by pretreatment with tetraethylammonium and 4-aminopyridine) and Cl^- (by anion substitution with aspartate) currents, suggesting that transient receptor potential (TRP) ion channel(s), which have been shown in other cell types to be activated by S1P,[62] may have been involved.

The response of cultured rat CFb to S1P was evaluated by conventional patching. In the first example, a freshly trypsinized rat CFb (approximately 2 weeks post-isolation) was evaluated. After obtaining stable baseline current recordings, S1P (100 nM) was added to the perfusate. Upon initial exposure to S1P, the cell exhibited a modest increase in its isochronal I-V relationship. With continued time, the inward and outward current

peaked (after approximately 10-12 min), and then returned to baseline values (over the next 3-4 minutes) (Figure 4.20).

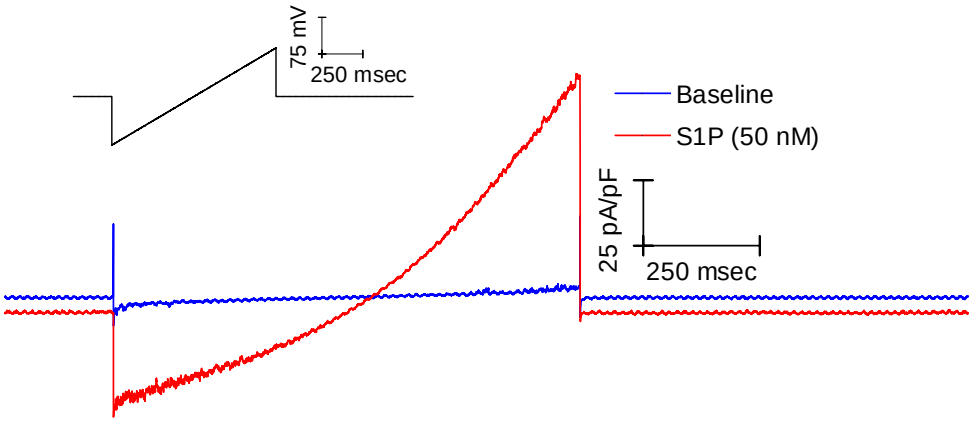

Figure 4.19 Evaluation of Currents Activated by S1P in Acutely Isolated Adult Rat CFb Recorded by Conventional Voltage-clamp Methods. S1P (50 nM) strongly activates currents in the absence of Cl^- and in the presence of K^+ channel blockers. Voltage-ramp protocol is shown in insert (0-mV holding potential). (Rose and Giles, unpublished results).

Because of the concern of blebbing in trypsinized rat CFb and the potential for blebbing artifacts to obscure any true S1P ligand response, a series of additional studies were conducted using non-trypsinized rat CFb. In these next experiments, rat CFb (approximately 17-18 days old) were patched in their flattened, adherent state. The cells were exposed first to 10 nM S1P and then to 100 nM S1P. The results are presented in Figure 4.21. The voltage-ramp protocol results of Figures 4.19 and 4.21 agree qualitatively in that S1P caused both inward and outward current increases above baseline in rat CFb. Furthermore, there was a dose-dependent response with 100 nM S1P activating currents more strongly than 10 nM S1P.

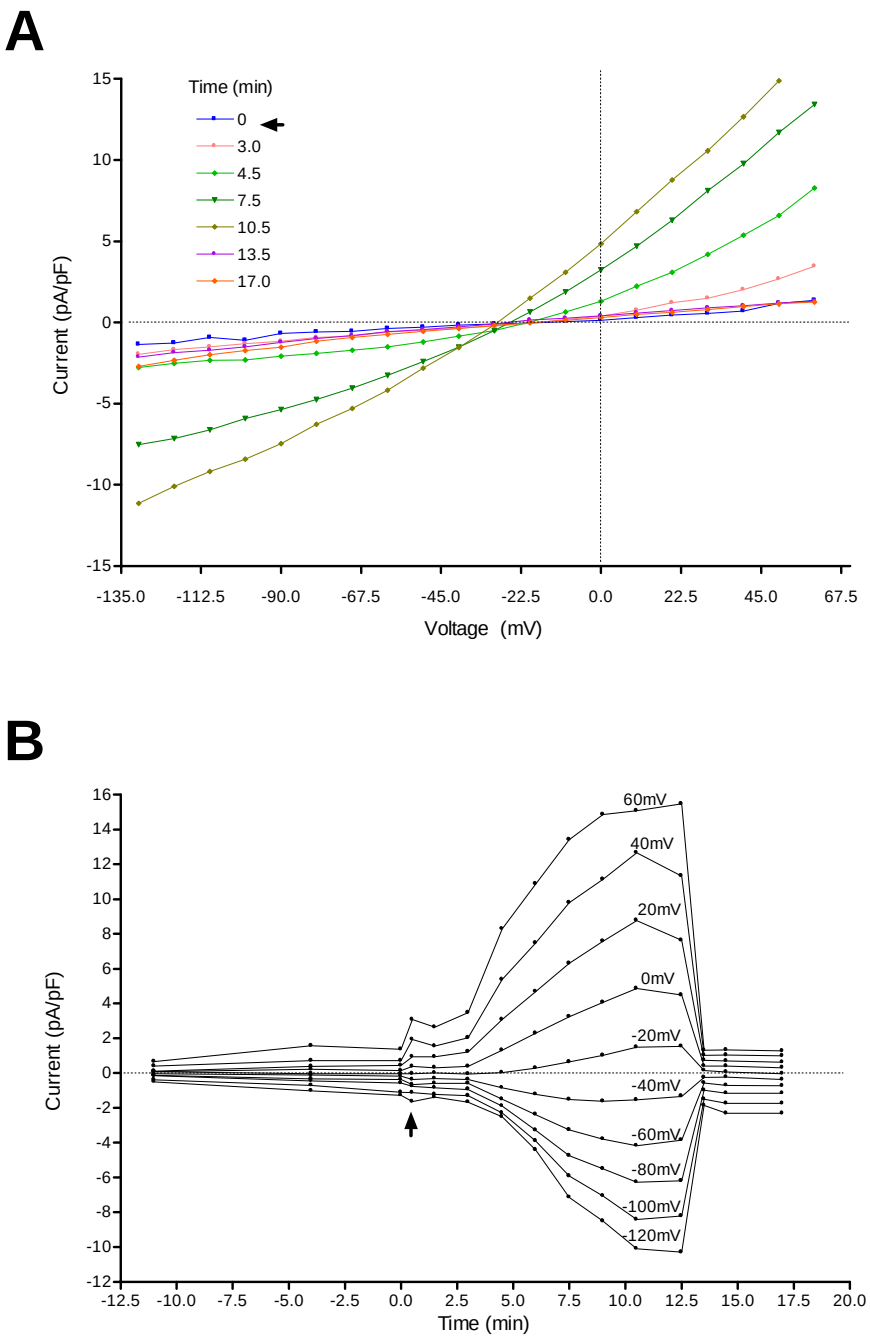

Figure 4.20 Response of Adult Rat CFb to Administration of S1P Recorded by Conventional Voltage-clamp Methods. ***A.*** Isochronal I-V relationships of peak currents at the end of the clamp step of a single cell was voltage-clamped from a holding potential of -50 mV using 500-msec, 10-mV steps from -130 mV to +60 mV. The administration of S1P (100 nM) is indicated by the arrow head. ***B.*** Current densities for voltage steps, plotted as a function of time. The administration of S1P (100 nM) is indicated by the arrow head.

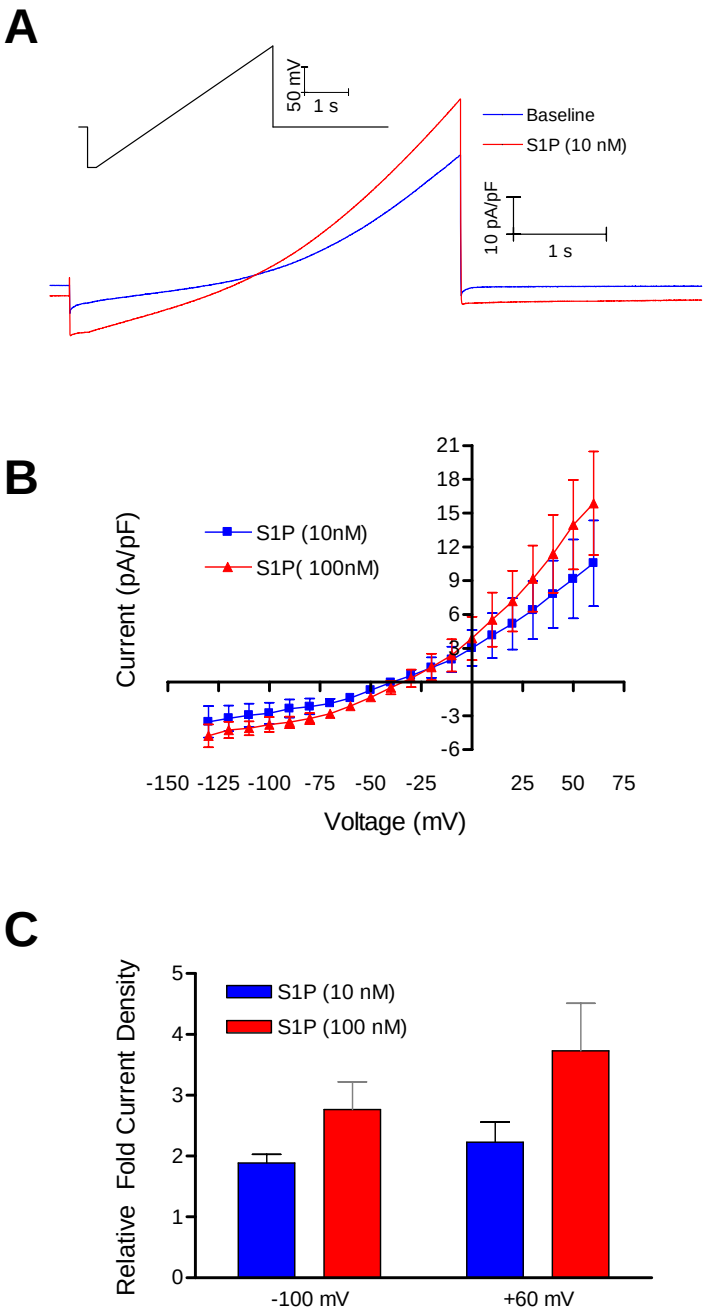

Figure 4.21 Evaluation of Currents Activated by S1P in Adherent Adult Rat CFb Recorded by Conventional Voltage-clamp Methods. ***A.*** S1P (10 nM) activates currents using voltage-ramp protocol (see insert; -60 mV holding potential). ***B.*** Isochronal I-V relationships of peak currents after application of either 10 nM or 100 nM S1P. The I-V curves, reported as mean ± sd, have had baseline values subtracted. ***C.*** Comparison of fold-changes (relative to baseline values) in current densities at -100 mV and +60 mV after application of S1P (10 or 100 nM). (Chilton and Giles, unpublished results).

Thus, S1P causes a dose- and time-dependent activation of inward and outward currents in both trypsinized and adherent rat CFb. In these experiments, 10 mM EGTA was included in the pipette filling solution, resulting in a cytosolic free Ca^{++} concentration of approximately 10 nM. This level of $[Ca^{++}]_i$ was estimated to have been too small to activate K_{Ca} ion channels effectively[59] even if intracellular stores were activated by S1P signaling pathways.[21,41] Therefore, it implicates either Cl^- or TRP channels.

4.4.5 Ion Channel Characterization by qPCR

The significant block of outward currents by 4-AP (5 mM) suggested that Kv channels are expressed in CFb. To explore which of the Kv family isoforms might be responsible for these voltage-gated outward currents, SYBR Green qPCR was performed. As shown in Figure 4.22, several Kv isoforms were detectable in both adult mouse and rat CFb. For the mouse, Kv1.3 and Kv1.6 were the most highly expressed of the isoforms evaluated. For the rat, Kv1.6 was expressed at the highest levels, with Kv1.2 showing the next greatest expression level. Several Kir isoforms were also detectable in mouse and rat CFb (Figure 4.22) which would agree with the Kir components of the I-V curves identified for each species. Analysis of mouse CFb by qPCR also demonstrated TRPM4, TRPM7, TRPV2, and K_{Ca} at expression levels similar to many of the Kir and Kv ion channel isoforms (Figure 4.22).

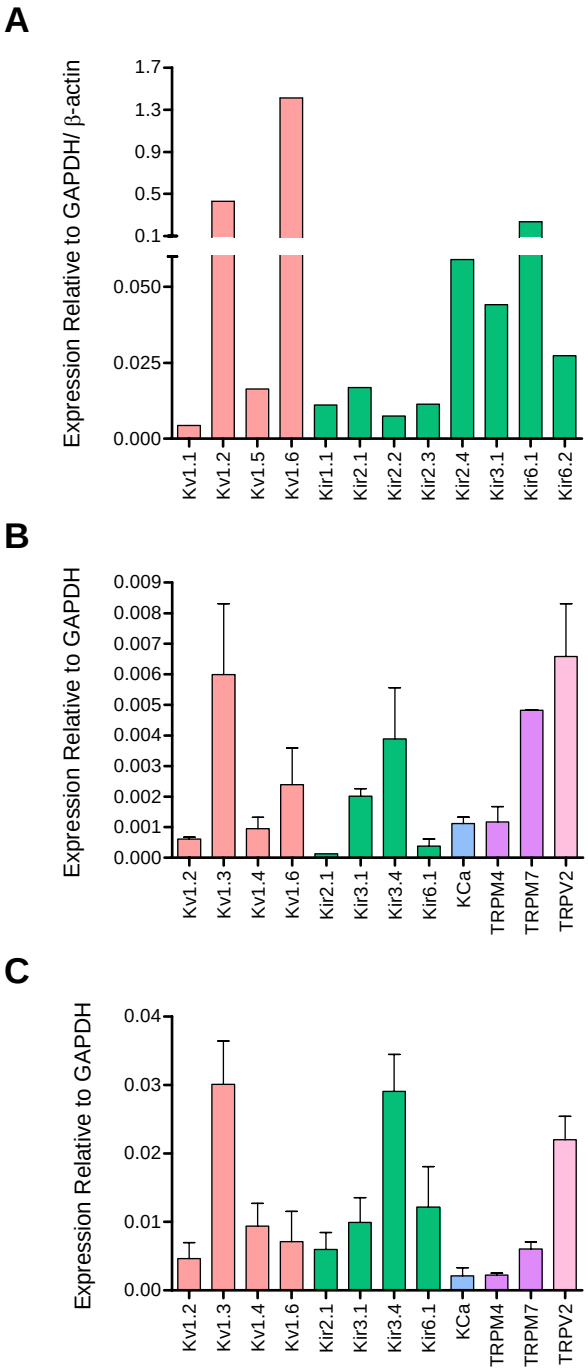

Figure 4.22 SYBR Green qPCR Analysis of Expression Levels for Several Ion Channel Isotypes. ***A.*** Adult rat cardiac fibroblasts ***B.*** Adult mouse cardiac fibroblasts, mean ± sd. ***C.*** Adult mouse cardiac macrophages, mean ± sd. Note differences in scaling of ordinate axes.

As discussed in Chapter 2, CFb cultures were routinely found to include non-fibroblast cell types. Macrophages (MΦ) isolated from mouse ventricular myocardium were therefore collected and analyzed by qPCR to determine whether they shared expression for any of the Kv or Kir ion channel isotypes identified in CFb. Importantly, not only did MΦ express all Kv, Kir, K_{Ca} and TRP isotypes found in CFb, but they were generally expressed at higher expression levels (Figure 4.22). Thus, the importance of having purified cultures is also relevant when conducting electrophysiological analyses to avoid mistakenly attributing currents to the "wrong" cell. Further, this exemplifies how patching systems that allow visual examination of the cells being interrogated have a greater advantage over alternative systems since morphological evaluation is possible or cells may be immunolabeled to help identify cell type.

4.5 Discussion

4.5.1 Summary of Major Findings

The experiments summarized in this Chapter compare two whole-cell patch-clamping technology platforms with the standard approach for obtaining electrophysiological data from isolated, single fibroblasts. We conclude that such electrophysiological data can complement the overall phenotypic characterization of a given cell type, and may be accessible to a range of scientific disciplines. The main goal of this Chapter was not to complete a detailed characterization of ion channel properties in CFb. However, several benchmark observations were attempted to familiarize our Group with this technology and to assess its applicability for measuring K^+ currents in CFb.

In both mouse and rat adult CFb, voltage-gated potassium ion currents (I_{Kv}) were activated in response to depolarization from the holding potential. As a confirmation, several Kv ion channel isotypes were identified by qPCR in both mouse and rat ventricular fibroblasts. In rat CFb, application of S1P caused ion channel activation that resulted in increased outward and inward currents compared to baseline values. Although the identity of the underlying ion channels was not further explored, the data support that TRP ion channels may have partially responsible.

Lastly, it was noted that the chip systems were more prone to activation of mechanically sensitive ion channels due to pipetting of solutions in close proximity to the sealed cell. Thus, for investigations in which mechanosensitive channels may carry similar currents as the ion channel currents of interest, these technology platforms may be limiting in this regard.

4.5.2 Comparisons of Two Technology Platforms

It is certainly the case that the chip-based systems are simpler to use than conventional whole-cell patching. They require less preparation and do not require skill in forming high giga-ohm seals. However, these patch chip technologies may have significant limitations. These can include: (i) a high incidence of unsuccessful sealing of the cell due to debris, bubble(s) blocking the aperture, or the health of the cell itself; (ii) failure to resolve currents that are too small due to a minimal expression level of the ion channels; or (iii) the absence of stable currents over time which prevents quantitative assessment of pre- and post-treatment(s).[12]

It is also the case that planar chip systems require greater numbers of cells (up to several million per milliliter) since the positioning of a cell to the aperture is dependent on cell density. In contrast, conventional patching can be performed theoretically with just a single cell added to the chamber bath. Thus, the emerging planar chip technologies may be better suited for cell lines in which ion channels have been transfected, rather than for primary cell isolates or cells of limited numbers. Also, in the patch-on-a-chip systems in which there are no visual observation capabilities, it is unknown whether recordings are being made from a single cell or a cell coupled to any number of other cells. If these cells are coupled through gap junctions, then the measured cellular capacitance should reveal this. However, lack of direct visualization presents a potential limitation in studies where single-cell determinations are assumed.

Of the two systems, the Nanion system was the simplest to use. The Nanion chips were the quickest and easiest to assemble, largely due to their design. The chip is glued to the inside of a small screw cap containing an o-ring; assembly therefore consists of simply tightening the cap onto the electrode holder. Although it was not evaluated during these studies, the Nanion chip cap can be removed to exchange with alternative internal solutions after the cell has been sealed.[3] Also, the Nanion system has a smaller footprint and does not require a suspension table or Faraday cage. The suggested protocol was simple (requiring the least oversight by the user), and it utilized the least amount of cells and reagents. We noted that the Nanion protocol utilizes specially formulated solutions (see Table 4.3) that are designed to increase seal resistance and increase stability of the recorded currents. A detailed comparison of formulations identified some differences in internal solutions that might help explain the differences noted in current magnitudes.

For example, the Nanion internal solution (Internal A, Table 4.3) contains no ATP and derives nearly half of its anions from fluoride. Fluoride is a known strong activator of a number of enzymes including adenylyl cyclase.[1,23]

One drawback of the Nanion system was that its automatic software program settings would often progress to the next stage after a specified period of time, regardless of whether the seal resistance was appropriate. For example, even cells with seal resistances of less than 100 MΩ would be advanced to the whole-cell recording stage before giga-ohm seals were formed (and would be pronounced to be in whole-cell configuration after another timed period). Alternatively, some cells would progress through the various stages in the Nanion system to reach whole-cell configuration much faster than the allocated program set times, while still achieving high seal strengths. These cells most likely had true stable membrane-substrate interactions, since this is indicative of fast seal times.[60]

However, the greatest detraction of the Nanion system was its inability to microscopically examine the cell under investigation. This proved important in later studies when cells were observed to undergo blebbing and discovered how this can affect the electrophysiological recordings.

One important benefit of the patch chip technologies is that they require only very small volumes of extracellular fluid. The Nanion system required a minimum of 10 µl (5 µl external fluid to close circuit and 5 µl of cell suspension), but was generally operated with ~30 µl total volume. The AVIVA system required approximately 50-60 µl. These small volumes are beneficial for the evaluation of limited or expensive compounds and also permit rapid equilibration with the target cell. Our conventional system, on the other

hand, required a chamber bath volume of approximately 1-2 ml. However, with this benefit comes a price. The small volumes used in this system make it more sensitive to fluid shear effects which can impact cell sealing strength and can induce mechanosensitive currents.

The AVIVA chip prototype used in these experiments contained 16 wells. Fertig, et al.[10] have described successful prototyping of a 16-well patch chip in 2002. The 16-well *Seal*Chip™ has been successfully used in an automated high throughput system (PatchXpress®) marketed by Molecular Devices Corporation (Union City, CA).[8] Although flow-through single-chip AVIVA prototypes have been developed, these were not used in these assessments.

Patch chips have reported capacitances of approximately 1 pF.[10] Patch chip seal resistances are approximately 2 MΩ[10] to 100-200 MΩ.[27] In contrast, micropipettes have reported capacitances of approximately 50 pF and allow formation of seal resistances to GΩ levels.[27] In side-by-side comparisons, Fertig, et al.[10] found identical characteristics between conventional and chip patching, although the micropipette recordings were of better quality owing to the increased seal resistances. AVIVA reports that its high throughput chip (*Seal*Chip™) can achieve GΩ seals with membrane resistances above 200 MΩ, access resistances below 15 MΩ and whole-cell access for up to 15 min. Their overall success rate is reported at >75% with their technology.[60]

As in conventional patching, debris in the superfusate proved to be a problem with the chip systems. Quite frequently, the system was unable to form seals upon addition of cells due to debris from dead cells and/or secreted cell proteins. Cell debris

has been previously noted as interfering with patch chips. In one study by Fertig, et al.,[10] a 30-50% success rate in achieving whole cell recordings was noted using NIE-115 mouse neuroblastoma or CHO cell lines. My experience with the Nanion system was estimated to yield 60-70% success when using primary isolated rat CFb. This was slightly lower for the AVIVA system. These values may have been influenced by a learning curve and might be expected to improve with further experience. The success rate for conventional patching of CFb was higher (approximately 90%), but these studies were conducted by an experienced, highly skilled researcher.

Using these approaches to patch adult mouse CFb was more difficult than for the adult rat. In addition, NIH3T3 fibroblasts were the most difficult. In fact, the NIH3T3 cells had to be subjected to repeated "zaps" (short, high voltage pulses to weaken the membrane) to break in (note: zapping was not attempted with the Nanion system, because this function was unknown at the time of those studies). The reasons for this are not clearly understood. It may be due to differences between species or may be related to age of donor or age of the isolated cells in culture. For example, the rat CFb were used between 1-2 weeks in culture, whereas the mouse CFb were used at less than 1 week in culture. Within the mouse, the CFb were isolated from adult donors, whereas the NIH3T3 fibroblasts originated from an embryonic source. Alternatively, the type of glass used in the micropipettes or chips could have affected the sealing success rate, as certain types of glass are known anecdotally to seal particular types of cells better than others.[39]

In summary, patch chip technologies seem most useful and practical for high-throughput screening and when using a uniform population of cells with moderate- to high-expression levels of the targeted ion channel. As they currently exist, they are not

intended to replace conventional micropipette techniques for studying the subtler biophysical characteristics of ion channel electrophysiology.[12]

4.5.3 Mechanically Activated Ion Channels in CFb

Mechanically activated ion channels have been noted in cells that are subjected to mechanical load. For example, in chondrocytes (freshly isolated primary cells or chondrosarcoma cell lines), blockade of stretch-activated ion channels (with gadolinium, Gd^{3+}) can cause a phenotypic shift from a rounded cell shape with few actin stress fibers to a more fibroblastic morphology with prominent actin stress fibers, focal adhesions, reassembly of microtubles within the cytoplasm.[38] These phenotypic shifts were not observed in chondrosarcoma cells with other more specific ion channel blockers (e.g. nifedipine/calcium, tetrodotoxin/sodium, 4-AP/potassium, or amiloride/sodium). Thus, it was concluded that they were dependent on non-selective cation, stretch-activated ion channel currents.

CFb have been shown to express stretch-activated non-selective ion channels. In experiments by Kamkin, et al.,[24,25] compression of atrial fibroblasts caused a depolarization from a resting membrane potential of -37 mV to -10 mV, whereas stretch caused a hyperpolarization to -61 mV.

Lastly, human skin fibroblasts have also been shown to express a stretch-activated ion channel that can be activated by as little as 10 mmHg (13.3 mBar) suction.[53] These channels were permeable to sodium and also potassium and were not found to be voltage-sensitive.[14,53] Interestingly, the open probability for the channels was increased with increasing suction.

The data regarding human fibroblasts and their sensitivity to suction,[53] supports the data generated with the Nanion system (refer to Figure 4.15) in which increasingly negative pressures resulted in increased inward currents. This suggests that the inward currents were carried by stretch-activated ion channels. The cell membrane experiences surface tension due to forces exerted upon it. Since surface tension is one-half the product of pressure and radius of the affected area (i.e. the membrane circumscribed by the aperture), the stretch-activated channels described in human skin fibroblasts[53] would be expected to open at approximately $7x10^{-4}$ N/m. In contrast, the holding pressure of the Nanion system is -50 mBar, which equals $2.5x10^{-3}$ N/m of surface tension, or approximately 3.5 times that needed to activate the channels.

It was observed that a waiting period during Nanion baseline recordings was beneficial to achieve a more stable recording. This was because current magnitudes tended to decrease with time after washout of the "seal enhancer" solution. Similarly, with the AVIVA system, it was noted that the cells appeared to exhibit a substantial current activation immediately following fluid exchange. Thus, it is conceivable that stretching or fluid shear stress due to the need to pipette solutions in close proximity to the sealed cells could activate mechanosensitive ion channels.

TRP ion channels are involved in many aspects of mechanosensation.[2,7] For example, an inwardly rectifying, non-selective, cation ion channel was recently been shown to be identical to a TRP channel (TRPC1).[30] These mechanosensitive channels were blocked by Gd^{3+} and were found to be gated by membrane tension. During our characterization of K^+ channel isotypes in fibroblasts, the expression of TRP channel isotypes was also investigated. It was found that adult mouse CFb and NIH3T3

fibroblasts were each found to express message for several TRP channel proteins including TRPM4, TRPM7 and TRPV2 (the only ones evaluated) in the range of expression levels found for Kv and Kir ion channels (see Figure 4.22 for CFb data; data for NIH3T3 cells not shown). Whereas TRPC1 is inwardly rectifying,[30] TRPM4 and TRPM7, on the other hand, have been shown to activate at positive potentials.[43,56] Thus, it is not unreasonable to assume that various TRP channels may have contributed to currents due to mechanical shear or during blebbing.

4.5.4 Possible Consequences of Ion Channel Activation in Blebbing Cells

Blebbing is a protrusion of the plasma membrane from the main cell body. Membrane blebs are rapidly forming (within seconds), and are thought to be caused by destabilization of the cytoskeleton (actin filaments or microtubules). This destabilization allows the membrane to separate from the underlying cortex, thereby allowing cytoplasmic pressure to push the membrane outward.[5,17,26,32] Blebbing can be a frequent occurrence during patch clamping. During the course of these studies, it was noted on several occasions when working with rat CFb and was shown to affect I-V relationships. The occurrence of blebbing appeared to be batch dependent (i.e. cells of a particular isolation/trypsinization procedure). Blebs can also form in cells exposed to suction pipettes, generally at end opposite to the suction.[26] This could be a mechanical tearing at the opposite end from the cytoskeleton being pulled into the pipette. Thus, the very process of obtaining gigaseals by negative pressure might introduce blebbing in cells with unstable cytoskeletal architecture or if excessive suction is applied.[17] Excessive negative pressure has also been shown to alter activity of mechanosensitive ion channels.[17] It is of

interest to note that the holding pressure in the Nanion system is just below that shown to cause membrane detachment in certain type of mammalian cells.[17]

Destabilization of the actin network can increase inward currents.[13] Inward currents in actin-destabilized cells may be carried through stretch-activated or other mechanosensitive ion channels. These currents would likely be carried by cations as they enter the cell. Cells can also activate chloride currents when they experience changes in volume. Thus, during blebbing, currents that react in response to the increased intracellular pressure caused by cell swelling might also be activated. Currents activated by cell swelling are outward rectifying are carried by chloride ions. These volume-regulated outward currents (VROC) have been identified in a number of cells, including various types of fibroblasts, and have been associated with transition of fibroblasts to a myofibroblast phenotype.[42,63] Since the rat CFb were likely of a myofibroblastic phenotype (based on their age in culture and reported changes in smooth muscle α-actin)[6], it is highly likely that such outward currents were active in visibly swelling/blebbing cells. The increased currents observed with blebbed cells were not likely due to leak currents, since leak currents are typified by reversal potential migration towards 0 mV and having a more linear I-V relationship. Such changes in reversal potential were not noted.

The cells used in these studies were almost exclusively from freshly trypsinized cultures (except the adherent cell reported in Figure 4.21). Trypsinization of fibroblasts releases them from the substratum (by disrupting focal adhesions) to assume a spherical shape. If the trypsinization were slightly over-aggressive or if the cells had poor quality membranes, it may be that the internal actin/microtubule structures were mechanically altered in such as way as to separate membrane from underlying actin cortex or as to

activate stretch-activated ion channels.[46] Alternatively, disruption of integrins on the cell surface could trigger Rho activation, which has been shown to be involved with cell blebbing.[5,26,32]

Lastly, blebbing is often observed during cellular apoptosis.[32,37] Thus, its occurrence during whole-cell patching should be of concern since this may be an indication that the cells are unhealthy and may therefore be generating unreliable electrophysiological data.

4.5.5 Activation of Currents in CFb by S1P

As was previously discussed, electrophysiological data on the effects of S1P on CFb was not attempted with the AVIVA system and was unattainable with the Nanion system. Therefore, conventional patch clamping techniques were employed. S1P application (10-100 nM) was shown to activate a conductance with a reversal potential near -31 mV. This resulted in both inward and outward currents in adult rat CFb (see Figures 4.19 – 4.21). Although subsequent investigations were not pursued to identify further the nature of these currents, there are several possible types that might be contributing. S1P has been shown to activate K_{Ca} in NIH3T3 fibroblasts.[41] The mechanism was believed to be through increased $[Ca^{++}]_i$ as a result of S1P receptor activation. Expression of K_{Ca} mRNA has been detected in adult mouse CFb (data not shown), so it is highly likely that adult rat CFb also express K_{Ca}. The addition of EGTA to the pipette filling solution (which would buffer free Ca^{++}), however, would lessen the likelihood of the observed currents being from K_{Ca}.

S1P has also been shown to activate Cl^- currents in corneal keratocytes (fibroblasts).[58] While the data in Figure 4.19 demonstrates that S1P was activating a non-Cl^-, non-K^+ current in adult rat CFb, the data in Figures 4.20 and 4.21 did not use anion substitution. Therefore, Cl^- may have been a plausible contributing current in those sets of data.

Lastly, all data sets on rat CFb seem generally consistent with the hypothesis that TRP channels may be activated by S1P. TRP channels are ion channels with mechanosensitive properties. S1P has been shown in bone marrow-derived stromal cells to induce rapid (within minutes) assembly of actin stress fibers, to redistribute paxillin to the cell periphery, and to phosphorylate focal adhesion kinase (FAK).[31] Combined with the fact that $S1P_2$ expression increases in cultured CFb (see Figure 3.1) and that $S1P_2$ is associated with Rho signaling pathways[54], activation of $S1P_2$ by S1P could activate Rho-associated changes in the cytoskeleton[45] and thereby impart deformations within the plasma membrane. Such mechanical stresses could potentially activate stretch-activated ion channels, such as those which are members of the TRP family. Further, TRPM7, which exhibits an outwardly rectifying non-selective cation current, has been shown to be inhibited by PLC through reduction of PIP_2.[43] Since $S1P_2$ can couple to several G-proteins including G_q and $G_{12/13}$,[54] activation through G_q-PLC pathways might reduce TRPM7 whereas activation through $G_{12/13}$-Rho pathways might further enhance TRPM7.

Since these currents all have an outward component, the current(s) measured in these studies using conventional patch clamping techniques could be due to any one or combination thereof. Moreover, they may have been identified by conventional patching more easily for other reasons described previously.

4.5.6 Potassium Ion Channels in CFb

As shown previously, potassium currents are expressed in CFb.[6,47] Kv currents activate (open probability 0.95 or greater) at membrane potentials ≥ -20 mV.[9] Inactivation is voltage-sensitive, with enhanced steady-state inactivation at depolarizing potentials. Hence, the more hyperpolarizing the holding potential, the fewer Kv channels will be inactivated and the greater would be the signal to noise ratio for records obtained in response to transient, depolarizing voltage-clamp steps. We examined Kv channel currents in several types of fibroblasts using the AVIVA system. This analysis was not platform-dependent. However, since the AVIVA system was the first to be evaluated, a complete data set between the various types of fibroblasts was available. Additional examination of rat CFb using the Nanion system complemented the AVIVA data regarding the presence of Kv channels.

It was observed that the Kv current densities in mouse CFb, rat CFb, and NIH3T3 fibroblasts (see Figures 4.9-4.11) were similar in magnitude. This was true, despite the small differences in holding potentials (e.g. -70 and -50 mV). This was interesting given that rat CFb had much greater expression of Kv isoforms in general than mouse CFb (see Figure 4.22) or NIH3T3 fibroblasts (data not shown). The confirmation of the identity of these outward currents as belonging to the Kv family was made using the Kv- blocker 4-AP (see Figures 4.12 and 4.14).

A comprehensive analysis of potassium ion currents in rat CFb has been published by our laboratory. Chilton, et al.[6] and Shibukawa, et al.[47] found that the cells exhibited resting membrane potentials (E_{rest}) of approximately -60 mV. These cells exhibited Kir currents that were activated at membrane potentials (E_m) less than -70 mV,

could be enhanced by altering the extracellular potassium ion concentrations, and were sensitive to application of $BaCl_2$. Furthermore, these Kir currents were larger in rat fibroblasts having adopted a myofibroblastic phenotype. Kv currents in rat CFb/myofibroblasts were activated at $E_m > -40$ mV and were shown to be slowly activating and inactivating. A number of Kv and Kir ion channel isotypes were identified by PCR in rat CFb. Among Kv isotypes, Kv1.1, Kv1.2, Kv1.5 and Kv1.6 were all detectable, with Kv1.6 having the highest expression. Expression levels for Kir were smaller, in general, than those for Kv. While Kir1.1, Kir2.1-2.4, Kir3.1 and Kir6.1-6.2 were all detectable, Kir2.1 and Kir6.1 were expressed the greatest amount.

The rat qPCR results presented in this Chapter agreed qualitatively with results by Chilton, et al.[6] Kv1.6 was the most prominent Kv isotype and Kir6.1 was the most prominent Kir isotype. It was interesting to note that the Kv and Kir expression levels differed between mouse and rat CFb. However, this may be attributed to differences in either species or age, as the mouse fibroblasts were less than one week old whereas the rat fibroblasts were closer to two weeks old when evaluated. NIH3T3 fibroblasts had negligible IKir, but expressed measurable IKv signals. This would be in agreement with qPCR results in which Kir expression levels were on average 83% lower than Kv expressions for the isotypes evaluated (data not shown). NIH3T3 have been used in other studies of potassium channel electrophysiology because of their reported lack of endogenous Kv1.3 expression.[15] However, Kv1.3 was detectable by qPCR in my studies (data not shown).

4.5.7 Concluding Remarks

The main objective of this Chapter was to generate feasibility data on various ionic currents expressed in CFb at baseline and after application of S1P. In an effort to reduce the technical hurdles posed by conventional patch clamping, two patch-on-a-chip technology platforms were investigated. While the AVIVA and Nanion systems were each capable of patching rat CFb relatively easily for the novice electrophysiologist, neither system was capable, in their evaluated configurations, of generating clean data on the actions of S1P. This was largely due to both the AVIVA and Nanion systems to react strongly to mechanical perturbations. Because ligand-receptor activation of ion channels is such an important component of any meaningful electrophysiological evaluation of a cell, these systems would require redesign considerations before being more fully useful.

In particular, the Nanion flow system should be modified to reduce the flow rate. This is probably more critical in this format than for the AVIVA format because of the reduced volumes retained on the Nanion chip cap. Further, the flow inlet should be repositioned farther away from the aperture of the chip. The current Nanion design subjects the patched cell to direct assault of fluid shear forces since the inlet is placed directly over the aperture.

Similarly, the AVIVA system would benefit from having flow volumes that are commensurate with the chip well volumes. A gravity-fed flow system was utilized for a few recordings, but the additional noise generated made the gathered data unusable. The depth of the chip well in the AVIVA system presents a concern for achieving adequate mixing without having to place the inlet and outlet in close proximity to the patched cell/aperture. As previously mentioned, a fluid-flow prototype chip has been designed by

AVIVA, but this was not evaluated. However, having only a single aperture, the high throughput benefits of using patch-on-a-chip platforms would have been lost using this flow-through chip.

Thus, for now, conventional patch clamping still remains the gold standard by which these other platforms will be compared. However, as the industry develops and becomes more readily adopted in the marketplace, further refinements and improvements to the design features and capabilities are sure to improve.

4.6 Chapter Acknowledgements

This work was done in collaboration with AVIVA Biosciences (San Diego, CA) at their industrial site under the supervision of Dr. Victor Panchenko. Additional studies were performed at the University of Calgary (Calgary, Alberta, CAN) with the collaboration of Drs. Lisa Chilton and Robert Clark and Mr. Ricardo Goméz García. Rat primers for Kv and Kir isoforms were generously provided by Dr. Susumu Ohya (Haga City University).

4.7 References

1. Adamek,E., Pawlowska-Goral,K. & Bober,K. In vitro and in vivo effects of fluoride ions on enzyme activity. *Ann. Acad. Med. Stetinensis* 51, 69-85 (2005).

2. Barritt,G. & Rychkov,G. TRPs as mechanosensitive channels. *Nature (Cell Biol.)* 7, 105-107 (2005).

3. Bruggemann,A. *et al.* High quality ion channel analysis on a chip with the NPC technology. *Assay. Drug Dev. Technol.* 1, 665-673 (2003).

4. Cahalan,M. & Neher,E. Patch clamp techniques: an overview. *Methods Enzymol.* 207:3-14., 3-14 (1992).

5. Charras,G.T., Hu,C.K., Coughlin,M. & Mitchison,T.J. Reassembly of contractile actin cortex in cell blebs. *J. Cell Biol.* 175, 477-490 (2006).

6. Chilton,L. *et al.* K^+ currents regulate the resting membrane potential, proliferation, and contractile responses in ventricular fibroblasts and myofibroblasts. *Am. J. Physiol Heart Circ. Physiol* 288, H2931-H2939 (2005).

7. Clapham,D.E. TRP channels as cellular sensors. *Nature* 426, 517-524 (2003).

8. Dubin,A.E. *et al.* Identifying modulators of hERG channel activity using the PatchXpress planar patch clamp. *J. Biomol. Screen.* 10, 168-181 (2005).

9. Fedida,D. & Hesketh,J.C. Gating of voltage-dependent potassium channels. *Prog. Biophys. Mol. Biol.* 75, 165-199 (2001).

10. Fertig,N., Blick,R.H. & Behrends,J.C. Whole cell patch clamp recording performed on a planar glass chip. *Biophys. J.* 82, 3056-3062 (2002).

11. Fertig,N., Meyer,C., Blick,R.H., Trautmann,C. & Behrends,J.C. Microstructured glass chip for ion-channel electrophysiology. *Phys. Rev. E. Stat. Nonlin. Soft. Matter Phys.* 64, 040901 (2001).

12. Finkel,A. *et al.* Population patch clamp improves data consistency and success rates in the measurement of ionic currents. *J. Biomol. Screen.* 11, 488-496 (2006).

13. Formigli,L. *et al.* Sphingosine 1-phosphate induces cytoskeletal reorganization in C2C12 myoblasts: physiological relevance for stress fibres in the modulation of ion current through stretch-activated channels. *J. Cell Sci.* 118, 1161-1171 (2005).

14. Galietta,L.J., Mastrocola,T. & Nobile,M. A class of non-selective cation channels in human fibroblasts. *FEBS Lett.* 253, 43-46 (1989).

15. Grissmer,S. *et al.* Pharmacological characterization of five cloned voltage-gated K^+ channels, types Kv1.1, 1.2, 1.3, 1.5, and 3.1, stably expressed in mammalian cell lines. *Mol. Pharmacol.* 45, 1227-1234 (1994).

16. Hamill,O.P., Marty,A., Neher,E., Sakmann,B. & Sigworth,F.J. Improved patch-clamp techniques for high-resolution current recording from cells and cell-free membrane patches. *Pflugers Arch.* 391, 85-100 (1981).

17. Hamill,O.P. & McBride,D.W., Jr. Induced membrane hypo/hyper-mechanosensitivity: a limitation of patch-clamp recording. *Annu. Rev. Physiol.* 59:621-31., 621-631 (1997).

18. Heyman,K. The patch clamp goes planar. *The Scientist* 19, 18-22 (2005).

19. Hille,B. The Sharpey-Schafer Lecture. Ionic channels: evolutionary origins and modern roles. *Q. J. Exp. Physiol.* 74, 785-804 (1989).

20. Imoto,K. Ion channels: molecular basis of ion selectivity. *FEBS Lett.* 325, 100-103 (1993).

21. Ishii,I. *et al.* Marked perinatal lethality and cellular signaling deficits in mice null for the two sphingosine 1-phosphate (S1P) receptors, S1P(2)/LP(B2)/EDG-5 and S1P(3)/LP(B3)/EDG-3. *J. Biol. Chem.* 277, 25152-25159 (2002).

22. John,V.H. *et al.* Novel 384-well population patch clamp electrophysiology assays for Ca^{2+}-activated K^+ channels. *J. Biomol. Screen.* ., (2006).

23. Judes,C., Helwig,J.J., Bollack,C. & Mandel,P. Isoproterenol-sensitive adenylate cyclase in glomeruli isolated from young and adult rat renal cortex. *Gen. Pharmacol.* 16, 205-210 (1985).

24. Kamkin,A., Kiseleva,I. & Isenberg,G. Activation and inactivation of a non-selective cation conductance by local mechanical deformation of acutely isolated cardiac fibroblasts. *Cardiovasc. Res.* 57, 793-803 (2003).

25. Kamkin,A. *et al.* Cardiac fibroblasts and the mechano-electric feedback mechanism in healthy and diseased hearts. *Prog. Biophys. Mol. Biol.* 82, 111-120 (2003).

26. Keller,H., Rentsch,P. & Hagmann,J. Differences in cortical actin structure and dynamics document that different types of blebs are formed by distinct mechanisms. *Exp. Cell Res.* 277, 161-172 (2002).

27. Kiss,L. *et al.* High throughput ion-channel pharmacology: planar-array-based voltage clamp. *Assay. Drug Dev. Technol.* 1, 127-135 (2003).

28. Kutchinsky,J. *et al.* Characterization of potassium channel modulators with QPatch automated patch-clamp technology: system characteristics and performance. *Assay. Drug Dev. Technol.* 1, 685-693 (2003).

29. Levis,R.A. & Rae,J.L. The use of quartz patch pipettes for low noise single channel recording. *Biophys. J.* 65, 1666-1677 (1993).

30. Maroto,R. *et al.* TRPC1 forms the stretch-activated cation channel in vertebrate cells. *Nature Cell Biol.* 7, 179-185 (2005).

31. Meriane,M., Duhamel,S., Lejeune,L., Galipeau,J. & Annabi,B. Cooperation of matrix metalloproteinases with the RhoA/Rho kinase and mitogen-activated protein kinase kinase-1/extracellular signal-regulated kinase signaling pathways is required for the sphingosine-1-phosphate-induced mobilization of marrow-derived stromal cells. *Stem Cells.* 24, 2557-2565 (2006).

32. Mills,J.C., Stone,N.L., Erhardt,J. & Pittman,R.N. Apoptotic membrane blebbing is regulated by myosin light chain phosphorylation. *J. Cell Biol.* 140, 627-636 (1998).

33. Muraki,K. & Imaizumi,Y. A novel function of sphingosine-1-phosphate to activate a non-selective cation channel in human endothelial cells. *J. Physiol* 537, 431-441 (2001).

34. Neubert,H.J. Patch clamping moves to chips. *Anal. Chem.* 76, 327A-330A (2004).

35. Nichols,C.G. & Lopatin,A.N. Inward rectifier potassium channels. *Annu. Rev. Physiol.* 59:171-91., 171-191 (1997).

36. Ochi,R., Momose,Y., Oyama,K. & Giles,W.R. Sphingosine-1-phosphate effects on guinea pig atrial myocytes: Alterations in action potentials and K^+ currents. *Cardiovasc. Res.* 70, 88-96 (2006).

37. Orlando,K.A., Stone,N.L. & Pittman,R.N. Rho kinase regulates fragmentation and phagocytosis of apoptotic cells. *Exp. Cell Res.* 312, 5-15 (2006).

38. Perkins,G.L., Derfoul,A., Ast,A. & Hall,D.J. An inhibitor of the stretch-activated cation receptor exerts a potent effect on chondrocyte phenotype. *Differentiation.* 73, 199-211 (2005).

39. Rae,J.L. & Levis,R.A. Glass technology for patch clamp electrodes. *Methods Enzymol.* 207:66-92., 66-92 (1992).

40. Reimann,F. & Ashcroft,F.M. Inwardly rectifying potassium channels. *Curr. Opin. Cell Biol.* 11, 503-508 (1999).

41. Repp,H., Birringer,J., Koschinski,A. & Dreyer,F. Activation of a Ca^{2+}-dependent K^+ current in mouse fibroblasts by sphingosine-1-phosphate involves the protein tyrosine kinase c-Src. *Naunyn Schmiedebergs Arch. Pharmacol.* 363, 295-301 (2001).

42. Ronnov-Jessen,L., Villadsen,R., Edwards,J.C. & Petersen,O.W. Differential expression of a chloride intracellular channel gene, CLIC4, in transforming growth factor-beta1-mediated conversion of fibroblasts to myofibroblasts. *Am. J. Pathol.* 161, 471-480 (2002).

43. Runnels,L.W., Yue,L. & Clapham,D.E. The TRPM7 channel is inactivated by PIP(2) hydrolysis. *Nature Cell Biol.* 4, 329-336 (2002).

44. Schroeder,K., Neagle,B., Trezise,D.J. & Worley,J. Ionworks HT: a new high-throughput electrophysiology measurement platform. *J. Biomol. Screen.* 8, 50-64 (2003).

45. Schwartz,M.A. & Shattil,S.J. Signaling networks linking integrins and rho family GTPases. *Trends Biochem. Sci.* 25, 388-391 (2000).

46. Sheetz,M.P., Sable,J.E. & Dobereiner,H.G. Continuous membrane-cytoskeleton adhesion requires continuous accommodation to lipid and cytoskeleton dynamics. *Annu. Rev. Biophys. Biomol. Struct.* 35:417-34., 417-434 (2006).

47. Shibukawa,Y., Chilton,E.L., Maccannell,K.A., Clark,R.B. & Giles,W.R. K^+ currents activated by depolarization in cardiac fibroblasts. *Biophys. J.* 88, 3924-3935 (2005).

48. Shumilina,E. *et al.* Deranged Kv channel regulation in fibroblasts from mice lacking the serum and glucocorticoid inducible kinase SGK1. *J. Cell Physiol.* 204, 87-98 (2005).

49. Sigworth,F.J. The patch clamp is more useful than anyone had expected. *Fed. Proc.* 45, 2673-2677 (1986).

50. Sigworth,F.J. & Klemic,K.G. Microchip technology in ion-channel research. *IEEE Trans. Nanobioscience.* 4, 121-127 (2005).

51. Sordel,T. *et al.* Hourglass SiO2 coating increases the performance of planar patch-clamp. *J. Biotechnol.* 20;125, 142-154 (2006).

52. Stett,A., Bucher,V., Burkhardt,C., Weber,U. & Nisch,W. Patch-clamping of primary cardiac cells with micro-openings in polyimide films. *Med. Biol. Eng Comput.* 41, 233-240 (2003).

53. Stockbridge,L.L. & French,A.S. Stretch-activated cation channels in human fibroblasts. *Biophys. J.* 54, 187-190 (1988).

54. Taha,T.A., Argraves,K.M. & Obeid,L.M. Sphingosine-1-phosphate receptors: receptor specificity versus functional redundancy. *Biochim. Biophys. Acta* 1682, 48-55 (2004).

55. U.S.Department of Health and Human Services, Food and Drug Administration, Center for Drug Evaluation and Research (CDER) & Center for Biologics Evaluation and Research (CBER). Guidance for Industry S7B Nonclinical Evaluation of the Potential for Delayed Ventricular Repolarization (QT Interval Prolongation) by Human Pharmaceuticals. 1-13. 2005. Rockville, MD , Center for Biologics Evaluation and Research.

56. Ullrich,N.D. *et al.* Comparison of functional properties of the Ca^{2+}-activated cation channels TRPM4 and TRPM5 from mice. *Cell Calcium* 37, 267-278 (2005).

57. Venter,J.C. *et al.* The sequence of the human genome. *Science.* 291, 1304-1351 (2001).

58. Wang,J., Carbone,L.D. & Watsky,M.A. Receptor-mediated activation of a Cl(-) current by LPA and S1P in cultured corneal keratocytes. *Invest Ophthalmol. Vis. Sci.* 43, 3202-3208 (2002).

59. Wang,Y.J., Lin,M.W., Wu,S.N. & Sung,R.J. The activation by estrogen receptor agonists of the BK(Ca)-channel in human cardiac fibroblasts. *Biochem. Pharmacol.* ., (2006).

60. Xu,J. *et al.* A benchmark study with sealchip planar patch-clamp technology. *Assay. Drug Dev. Technol.* 1, 675-684 (2003).

61. Xu,J. *et al.* Ion-channel assay technologies: quo vadis? *Drug Discov. Today.* 6, 1278-1287 (2001).

62. Xu,S.Z. *et al.* A Sphingosine-1-Phosphate-Activated Calcium Channel Controlling Vascular Smooth Muscle Cell Motility. *Circ. Res.* 98, 1381-1389 (2006).

63. Yin,Z. & Watsky,M.A. Chloride channel activity in human lung fibroblasts and myofibroblasts. *Am. J. Physiol Lung Cell Mol. Physiol.* 288, L1110-L1116 (2005).

CHAPTER 5

EFFECTS OF SPHINOGINE-1-PHOSPHATE ON MYOCYTE CONTRACTILITY

5.1 Abstract

Calcium regulation is an essential mechanism for maintaining contraction stability in cardiac myocytes. In the mammalian heart, calcium homeostasis is tightly coupled to excitation in both intact myocardium and isolated cells. In myocytes, calcium entry through voltage-gated L-type calcium channels induces the release of calcium from intracellular stores through ryanodine receptors located in close apposition to the sarcoplasmic reticulum. Once released, calcium binds to several regulatory proteins including calmodulin and troponin C to induce sarcomeric shortening. The strength of contraction of each myocyte is controlled largely by intracellular calcium concentration $[Ca^{++}]_i$. $[Ca^{++}]_i$ can be modulated by several known ligand-gated G protein-coupled receptors (GPCR) located within the sarcolemmal membrane. Muscarinic receptors (e.g. M_2, which binds to carbachol) and β-adrenergic receptors (e.g. β1AR, which binds to isoproteronol) are well established GPCR which can decrease or increase, respectively, $[Ca^{++}]_i$. These two GPCR act through G_i and G_s, respectively, to regulate adenylyl cyclase production of cAMP. Protein kinase A (PKA) activation by cAMP can then regulate calcium via L-type calcium channels (I_{CaL}).

In common with these receptors is the GPCR for sphingosine-1-phosphate (S1P). S1P is a bioactive molecule that binds with high affinity to five known receptors ($S1P_{1-5}$) to significantly modulate cellular responses in a variety of tissues including myocardium. S1P activates an inwardly rectifying potassium (K^+) current, similar to that of

acetylcholine (I_{KAch}) to shorten action potential duration (APD). S1P can also induce a transient bradycardia in mammalian hearts through action on sino-atrial node cells.

In our experiments, the actions of S1P on S1P receptors expressed in the adult mouse ventricular myocyte (predominantly $S1P_1$ and $S1P_3$) were evaluated in terms of a surrogate of cardiac contractility: unloaded shortening of single enzymatically isolated myocytes. Application of isoproterenol (100 nM) and carbamoylcholine/carbachol (100 nM) were used as controls to increase and decrease, respectively, cell shortening. S1P (10-100 nM) was shown to reduce cell shortening by approximately 25% compared to untreated controls in field-stimulated (1-2 Hz, 22-25°C) myocytes. The $S1P_1$-selective agonist SEW2871 (100-1,000 nM) showed a similar negative inotropy, as did S1P when applied to myocytes isolated from $S1P_3$-null mice. These results show that $S1P_1$ is at least partially responsible for reducing cell shortening in isolated adult mouse ventricular myocytes. However, by using the $S1P_1$ antagonist VPC23019, we have also shown that S1P, acting through $S1P_3$, can also significantly reduce shortening.

$S1P_1$ activates G_i exclusively, whereas $S1P_3$ can activate both G_i and G_q. The data generated using SEW2871 and $S1P_3$-null myocytes strongly suggest involvement of G_i pathways in reduced cell shortening, following exposure to S1P. The data generated using VPC23019 further suggests the involvement of G_i activation through $S1P_3$ upon exposure to S1P since G_q is reportedly less active in mouse myocytes.[23]

Experiments using the I_{KAch} blocker tertiapin[18,30] further demonstrate that I_{KAch} contributes (in addition to I_{CaL}) to the negative inotropy induced by S1P. It is well established that the $\beta\gamma$ subunits of G_i are capable of activating I_{KAch}, resulting in APD decreases. In this work, mathematical modeling was used to demonstrate how changes in

APD can affect I_{CaL} and $[Ca^{++}]_i$. These modeling results help to illustrate that a reduction in APD (e.g. induced by I_{KAch}) can lower $[Ca^{++}]_i$ and contribute to the observed negative inotropic effects of S1P.

In summary, these findings illustrate the consequences of S1P through $S1P_1$ and $S1P_3$ activation of G_i in adult mouse ventricular myocytes. They also suggest a mechanism for the observed negative inotropy that includes both inactivation of I_{CaL} and activation of I_{KAch}.

5.2 Introduction

Excitation-contraction coupling is tightly regulated in the adult cardiac myocyte and depends largely on intracellular calcium concentrations during systole and diastole[7,8] (see Figure 5.1). Due to the initial rapid depolarization of the myocyte by influx of sodium ions, L-type calcium channels are activated. Calcium then enters via L-type calcium ion channels (also called dihydropyridine receptors, DHPR) located on the sarcolemma and along the T-tubules. The close proximity of these latter ion channels to ryanodine receptors (RyR) on the sarcoplasmic reticulum (SR) induces a subsequent and very large release of calcium (nearly 100-fold above global $[Ca^{++}]_i$),[7] termed calcium-induced calcium release (CICR). This dramatically increases intracellular calcium concentration $[Ca^{++}]_i$. The initial phase of CICR is a positive feedback mechanism and, thus, L-type calcium currents (I_{CaL}) are important triggers for excitation-contraction coupling. Re-uptake of calcium into the SR via ATP-consuming pumps (i.e. sarcoplasmic/endoplasmic reticulum calcium ATP-ase pump [SERCA]) and extrusion through calcium exchangers (e.g. sodium-calcium exchanger [NCX]) on the sarcolemma,

lowers $[Ca^{++}]_i$. In the mouse, greater than 90% of $[Ca^{++}]_i$ is removed by SERCA, whereas less than 10% is removed by NCX.[37]

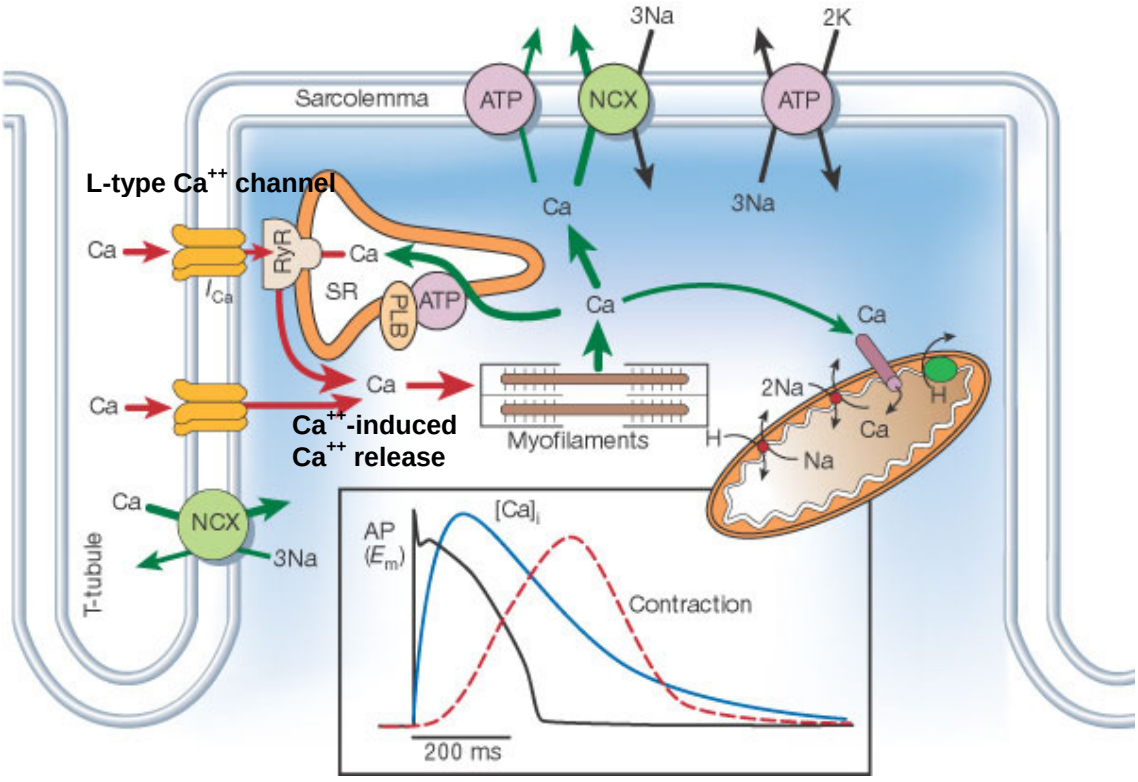

Figure 5.1 Schematic Diagram of Excitation-Contraction Coupling and Calcium Regulation in a Model Ventricular Myocyte. Calcium entry from L-type channels (I_{Ca}) triggers sarcoplasmic reticulum (SR) release through ryanodine receptors (RyR). This is also referred to as calcium-induced calcium releasae (CICR). Additional calcium ions may enter from ion channel leak or the sodium-calcium exchanger (NCX). Calcium binding to myofilaments induces filament shortening and cell contraction. Calcium is returned to the SR via the sarcoplasmic reticulum calcium ATP-ase pump and its associated regulating protein phospholamban (PLB) or the extracellular space via the NCX or other calcium pumps. (Insert) Intracellular calcium concentrations $[Ca^{++}]_i$ are coupled to the action potential (AP) and myocyte contraction. Phase 2 (plateau) of the AP regulates $[Ca^{++}]_i$ and allows initiation of myofilament contraction. As free calcium is removed from the intracellular space, relaxation of the myofilaments occurs. Modified rom Bers 2002.[8]

The contraction-relaxation cycle is rapid and efficient. Calcium is an essential co-factor for initiating actin-myosin myofilament contraction. This effect is mediated by

intermediate calcium-binding proteins (e.g. troponin C and calmodulin) and their associated kinases. Calmodulin, for example, can affect RyR regulation and calmodulin kinase II can affect I_{CaL}.[7] This same enzyme also assists in Ca^{++} reuptake by the SR through interactions with phospholamban (PLB), a regulatory protein that blocks Ca^{++} reentry in its inactivated/non-phosphorylated state. $[Ca^{++}]_i$ and contraction are therefore tightly coupled, and contraction kinetics can be used as an estimation of $[Ca^{++}]_i$.

There are several signaling pathways that can modulate calcium handling within the myocyte (see Figure 5.2). Many of these act through G-protein coupled receptors (GPCR). For example, isoproterenol (Iso) is a ligand for β_1-adrenergic receptor (β_1AR), a GCPR which couples to G_s. Carbamoylcholine or carbachol (CCh) is a ligand for the M_2 muscarinic receptor (M_2R) which couples to G_i. Activation of β_1AR by Iso stimulates cAMP formation, which activates protein kinase A (PKA). PKA, in turn, phosphorylates L-type calcium ion channels to augment extracellular entry of Ca^{++}. PKA can also cause direct release of Ca^{++} from the SR. This increase in $[Ca^{++}]_i$ results in increased contraction (inotropy). PKA also contributes to increased lusitropy (relaxation) by phosphorylating PLB. Conversely, activation of M_2R by CCh inhibits cAMP formation, reduces cAMP-mediated calcium increase, and diminishes contraction strength.

S1P is another example of a GPCR ligand. S1P is a biologically active, cell membrane-associated sphingolipid that binds with high affinity to five distinct receptor isoforms ($S1P_{1-5}$). $S1P_1$ has been detected in abundance in neonatal rat cardiomyocytes.[45] In these cells, exposure to S1P (500 nM) results in negative inotropy (reduction of systolic calcium), calcium overload (increased diastolic calcium), and full cessation of

contractility. In isolated atrial myocytes, S1P has been shown to (i) activate a weakly inwardly rectifying potassium (K^+) current, which was later shown to be similar to the K^+ current activated by acetylcholine (I_{KACh}); (ii) to shorten APD; (iii) to inhibit excitability by reducing sodium current (I_{Na}); and (iv) to increase the minimum stimulus current needed to generate an AP.[13,25,42,49] In whole animals, S1P activation can induce a transient bradycardia.[55]

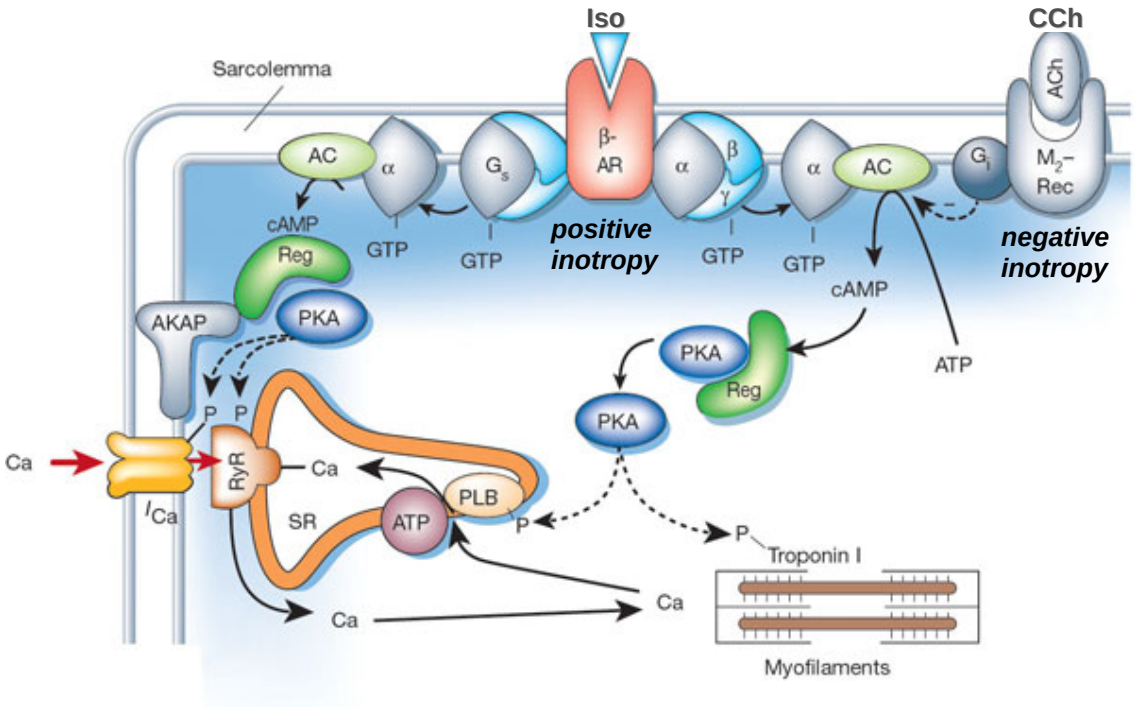

Figure 5.2 Schematic Diagram of β Adrenergic Receptor and Muscarinic Receptor Modulation of Calcium Pathways in the Adult Myocyte. Isoproterenol (Iso) activation of G_s-coupled β1 andrenergic receptors (βAR) releases $G_{s\alpha}$ to induce formation of cAMP from adenylyl cyclase (AC). This further stimulates protein kinase A (PKA). PKA can activate L-type calcium ion channels and ryanodine receptors (RyR) to increase $[Ca^{++}]_i$ in the cytosol or phosphorylate phospholamban (PLB) to allow Ca^{++} reentry into the sarcoplasmic reticulum (SR). Further, PKA can activate calcium-binding proteins such as troponin I. Negative inotropic molecules such as acetylcholine (Ach) and carbachol (CCh) bind to G_i-coupled M_2 muscarinic receptors to inhibit cAMP formation. Modified from Bers.[6]

S1P receptor coupling to G proteins can activate various pathways of calcium handling (see Figure 5.3). $S1P_1$ couples exclusively via G_i, whereas $S1P_2$ and $S1P_3$ have been shown to couple to either G_i, G_q, or $G_{12/13}$.[60] G_i can inhibit cAMP-mediated L-type calcium channel entry, whereas G_q, can cause $[Ca^{++}]_i$ to increase through phospholipase C (PLC) pathways.

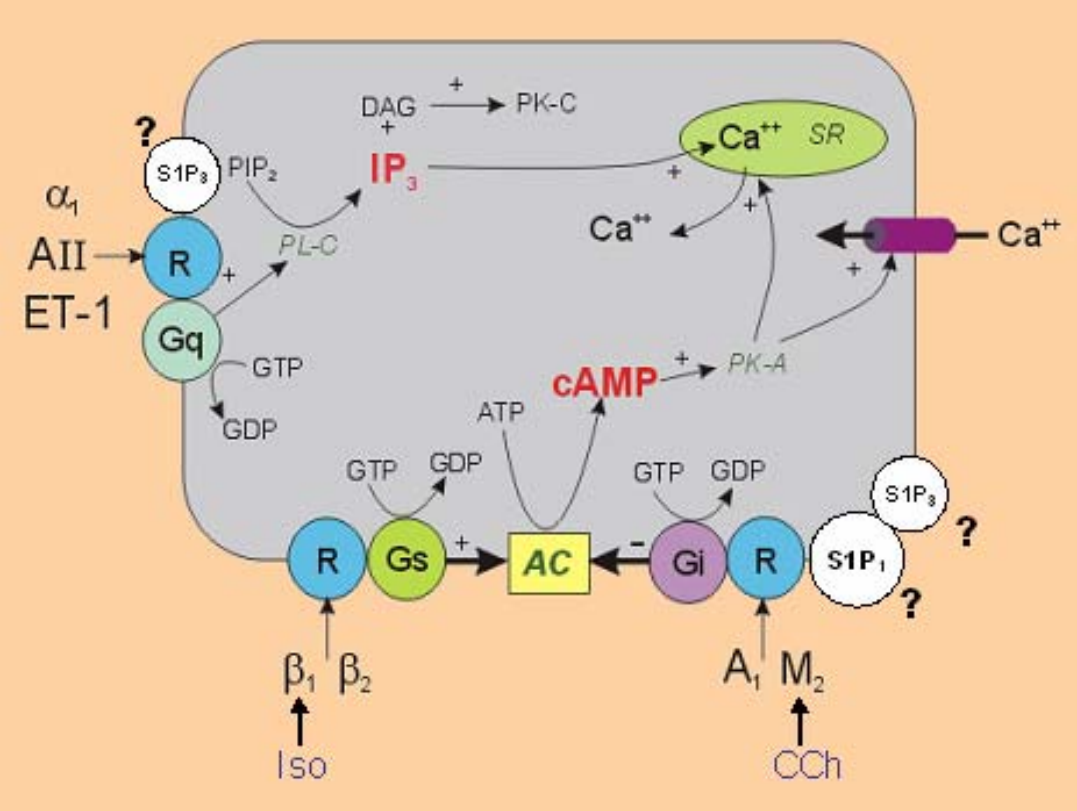

Figure 5.3 Schematic Diagram of Several GPCR Signaling Pathways That Can Regulate $[Ca^{++}]_i$ and Affect Myocyte Inotropy and Cell Shortening. Positive inotropic molecules such as isoproterenol (Iso) bind to Gs-coupled β1 andrenergic receptors and induce formation of cAMP from adenylyl cyclase (AC). This further stimulates protein kinase A (PKA) to activate L-type calcium ion channels. Negative inotropic molecules such as carbachol (CCh) bind to G_i-coupled M_2 muscarinic receptors to inhibit cAMP formation. Both $S1P_1$ and $S1P_3$ can couple via G_i, and $S1P_3$ can couple to G_q as well. G_q signaling (e.g. from α1 adrenoreceptors, angiotensin II [AII] receptors, or edothelin 1 [ET-1] receptors) can activate phospholipase C (PLC) signaling with subsequent increases in inositol 1,4,5-triphosphate (IP_3) and Ca^{++} release from sarcomeric reticulum (SR) stores. Mofidied from Klabunde.[31]

The main objectives of the experiments summarized in this Chapter were to study the possibility that S1P can modulate myocyte contractility, and to gain information concerning signaling pathways that might be involved through action on S1P receptors. Our efforts concentrated on known or putative G_i-coupled pathways, since G_q-coupling is less prominent in the mouse.[23] Our results demonstrate that $S1P_1$ is the most highly expressed S1P receptor subtype on adult mouse ventricular myocytes. As such, $S1P_1$ is considered the primary contributor to negative inotropic actions by S1P. However, $S1P_3$ was also shown to contribute to decreased cell contractility. We further demonstrated (through experimental blockade of K_{ACh} channels and through mathematical modeling of the adult mouse ventricular myocyte action potentials) how activation of I_{KACh} by S1P to reduce APD might contribute to the sustained decrease in observed cell shortening secondary to changes in available $[Ca^{++}]_I$ in the myoplasm.

5.3 Methods

5.3.1 Cell Isolation

Hearts from heparinized adult C57Bl/6 or $S1P_3$-null mice[32] were isolated under isoflurane anesthesia in accordance with protocols approved by the Institutional Animal Care and Use Committee and adhered to *Guidelines for the Care and Use of Laboratory Animals* (©1996). Isolated hearts were placed in Ca^{++}-free Tyrodes buffer (130 mM NaCl, 5.4 mM KCl, 0.3 mM Na_2HPO_4, 1 mM $MgCl_2$, 10 mM HEPES, 5.5 mM glucose, pH 7.2-7.4). After cannulation of the aorta with a blunted 21G needle, the heart was retrograde perfused with Tyrodes buffer to clear the coronary arteries. Each heart was then secured on a Langendorff apparatus and perfused at 3-5 ml/min for 5 min with

oxygenated, 37°C Tyrodes buffer. After an additional 8 min of enzymatic digestion in Tyrodes buffer containing Liberase Blenzyme IV (a mixture of highly purified collaganse and protease) (125-250 μg/ml, Roche, Indianapolis, IN) and 50 μM $CaCl_2$, the ventricles were removed, gently separated and shaken into modified Krebs-Henseleit buffer (100 mM K-glutamate, 10 mM K-aspartate, 25 mM KCl, 10 mM KH_2PO_4, 2 mM $MgSO_4$, 0.5 mM EGTA, 5 mM HEPES, 1% BSA, 20 mM glucose, 20 mM taurine, and 5 mM creatine; pH 7.2-7.4) to liberate myocytes from the myocardium. Individual myocyte populations were removed by filtering through 100-μm nylon mesh and mild centrifugation (1 min, 50 x g). Pelleted myocytes were refreshed with Krebs-Henseleit buffer and stored at 4-8°C for 1 hour before use.

5.3.2 Cell Shortening Measurements

All cell shortening measurements were conducted at room temperature. Isolated ventricular myocytes were adhered to laminin-coated (25 μg/ml) glass slides and superfused (0.5 ml/min) in a flow chamber with calcium-free Tyrodes buffer to ensure attachment. Tyrodes buffer containing 1 mM $CaCl_2$ (or 1.8 mM in selected experiments) was superfused for approximately 5 min, at which time field stimulation was initiated using a custom-designed probe (Crescent Electronics, Sandy, UT) (see Figure 5.4). The cells were stimulated with 5-ms current pulses (approximately 10-20% above threshold) using a pulse generator. The stimulus consisted of a 5-ms square waveform with a 20-ms delay. The stimulus frequency (1-2 Hz) did not alter myocyte baseline or response cell shortening (data not shown).

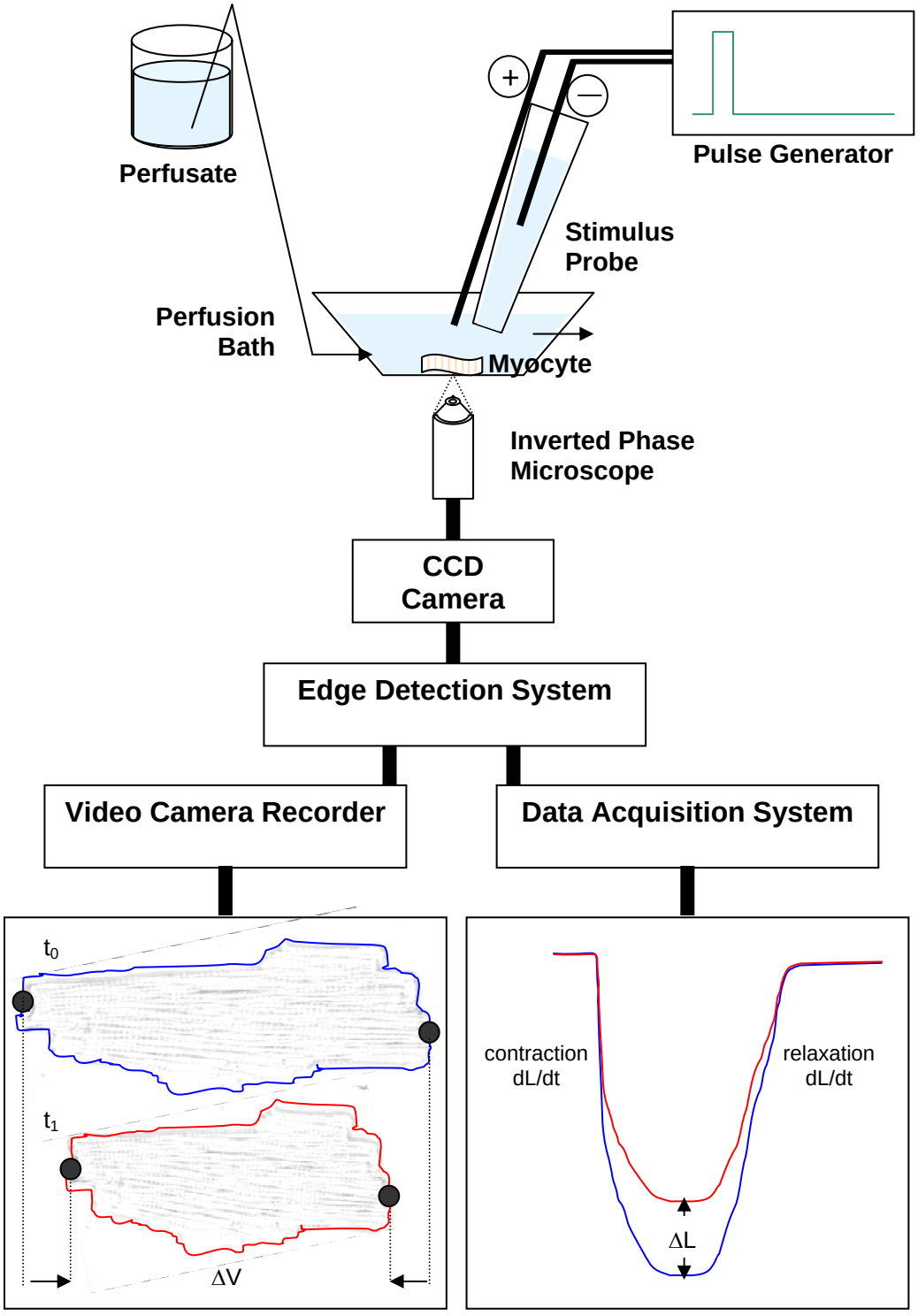

Figure 5.4 Schematic Illustration of System Used to Stimulate Isolated Myocytes and Measure Cell Shortening and Rates of Contraction and Relaxation.

Myocyte shortening was recorded using an edge-detection device (Model VED-205, Crescent Electronics) and a CCD camera (model FTM800NH/HGI, Phillips, Atlanta, GA). The output of this edge detector was linear over a range of 0-110 μm (R^2 = 1.0, 1 V = 17.43 μm). Signals were acquired through a Digidata 1322A 16-bit (Axon Instruments, Sunnyvale, CA) or MP150 (BioPac, Goleta, CA) data acquisition system using either Clampex software (Axon) (10-kHz sampling rate) or Acknowledge software (BioPac) (2-kHz sampling rate), respectively. After >5 min equilibration under field stimulation, baseline measurements were collected. Only those cells which exhibited rod-shaped morphology, clearly defined sarcomere striations, and stable and steady-state baseline cell shortening (≥ 5% of resting length, for ≥ 5 min) were used in data analysis. Positive and negative control responses to Iso (100 nM) and CCh (100 nM),[62] respectively, were obtained from selected cells, followed by wash-out and return to baseline. Data collected using the BioPac system was analyzed by Acknowledge software for signal data averaging of maximal shortening values; contraction rates were analyzed by Kaleidograph (Synergy Software, Reading, PA). Data collected by the Digidata system was analyzed by Clampfit software (Axon) and saved as text files. Text files were imported into MatLab 7 (MathWorks, Natick, MA) and analyzed using a program specifically written to calculate contractility parameters over time.

5.3.3 Materials

S1P (Avanti Polar Lipids, Alabaster, AL) was dissolved in dimethyl sulfoxide (DMSO) to 1-10 mM and applied at 1-1,000 nM. Isoproterenol (Iso; Sigma-Aldrich, St. Louis, MO) and carbamoylcholine/carbachol (CCh; Sigma) were each dissolved in Ca^{++}-

Tyrodes buffer to 500 μM and applied at 50-200 nM. SEW2871 (Calbiochem, La Jolla, CA) was dissolved in DMSO to 1 mM and applied at 10-1,000 nM. VPC23019 (Avanti Polar Lipids) was dissolved in DMSO:1N HCl (95:5 v/v) to 1 mM and applied at 100 nM. Tertiapin (Peptides International, Louisville, KY) was dissolved in water to 100 μM and used at 100 nM. All stock reagents were kept as frozen (-20°) aliquots before use and dissolved to working concentrations in Ca^{++}-containing Tyrodes buffer.

5.3.4 PCR

Cells were lysed, total RNA was isolated by silica-gel columns using RNeasy kits (QIAGEN, Valencia, CA) and eluted in water, and cDNA was reverse transcribed from mRNA by oligo-dT priming and Omniscript reverse transcriptase (QIAGEN). Expression levels of gene targets were characterized by SYBR Green[3] quantitative real-time PCR (qPCR) of cDNA using specific primer sets for GAPDH (5'-AACTTTGGCATTGTGGAAGG-3', 5'-ACACATTGGGGGTAGGAACA-3'), $S1P_4$ (5'-GGCTACTGGCAGCTATCCTG-3', 5'-AAGGCCACCAAGATCATCAG-3'), and $S1P_5$ (5'-GATCCCTTCCTGGGTCTAGC-3', 5'-TAGAGCTGCGATCCAAGGTT-3'). Expression levels of other S1P receptors were performed using Applied Biosystems (Foster City, CA) TaqMan® primer/probe sets as follows: $S1P_1$ (Mm00514644_m1), $S1P_2$ (Mm01177794_m1), $S1P_3$ (Mm00515669_m1), and GAPDH (Mm99999915_g1). Primer sets for genotyping $S1P_3$-null mice were as previously reported.[32]

Amplicon lengths for each primer set were confirmed by gel electrophoretic separation (2% agarose) with ethidium bromide visualization, and all SYBR Green experimental samples were subjected to melt curve analyses following amplification. All

experimental data were reported relative to GAPDH levels using the $2^{-\Delta\Delta Ct}$ calculation methods, which was considered appropriate based on primer set efficiency determinations.[40]

5.3.5 Mathematical Modeling

A published mathematical model of the mouse ventricular myocyte action potential[10] was modified in our laboratory (Dederko and Giles, in preparation) to provide a comprehensive means of studying the mechanisms for repolarization in myocytes from right ventricle versus left ventricle. This software tool was used to explore the relationship between APD and calcium handling. This model uses a non-distributed equivalent electrical circuit with subcellular compartmental spaces and Markov models of ion channel gating states for Na^+, Ca^{++}, and K^+ channels. The findings from these simulations were then utilized to help interpret experimental data, i.e. the effects of S1P on contraction.

5.3.6 Statistical Analyses

Results from replicate experiments involving cells from multiple animals were averaged and are presented as arithmetic means and standard deviations (SD). Results were analyzed for ANOVA (with Bonferonni t-test post-hoc testing), Student's t-test, or paired t-test using statistical software packages (Primer of Biostatistics, McGraw-Hill, New York, NW; GraphPad Prism, San Diego, CA). Significant differences were accepted for results with $p<0.05$.

5.4 Results

5.4.1 Extracellular Ca^{++} and I_{CaL} Regulate Cell Shortening

In murine ventricular myocytes, CICR from L-type calcium ion channel and RyR activation is the predominant mechanism for altering $[Ca^{++}]_{i.}$ These changes in $[Ca^{++}]_i$, in turn, alter contraction rate and strength. The magnitude of I_{CaL} is dependent on the number of L-type calcium channels which open, their open time, and their conductance. Since conductance is a function of membrane potential, experiments were conducted to validate the relationship between extracellular calcium concentration ($[Ca^{++}]_o$) and cell shortening in adult mouse ventricular myocytes. Baseline values were recorded during exposure to 1.8 mM $[Ca^{++}]_o$ in the superfusate. Next, $[Ca^{++}]_o$ in the superfusate was lowered to 1.0 mM and cell shortening was recorded again. After subsequent exposure to 0.5 mM ($[Ca^{++}]_o$, the cells were returned to 1.8 mM ($[Ca^{++}]_o$ in the superfusate. The results of this regimen on both wild-type and $S1P_3$-null myocytes are presented in Figure 5.5. It is evident that changes in $[Ca^{++}]_o$ cause changes in the extent of cell shortening. This relationship is further demonstrated by the strong correlation coefficients (R^2>0.99) that were calculated for both wild-type and $S1P_3$-null myocytes. Similarly, strong correlation coefficients (R^2>0.93) were calculated between cell shortening and calcium electrical equilibrium potential (using the Nernst equation).

To alter conductance and, therefore, calcium flux through L-type channels, experiments were conducted using the L-type calcium channel inhibitor verapamil.[46,63] In these experiments, measurements were made on contracting myocytes at baseline, after application of verapamil (5 μM), and also after a 10-minute washout period. Verapamil effectively blocks I_{CaL} and results in a significant decrease in cell shortening

(Figure 5.5). This was true for myocytes isolated from both wild-type and $S1P_3$-null mice. Washout recovered approximately 70-80% of peak contraction values.

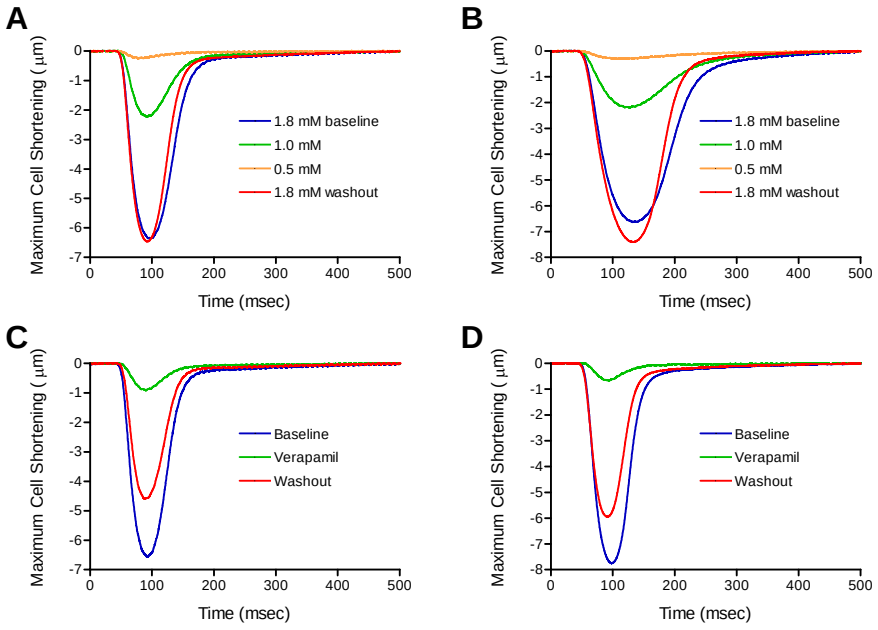

Figure 5.5 Extracellular Calcium and L-type Calcium Channels Affect Cell Shortening in Adult Mouse Ventricular Myocytes. ***A, B.*** Measurements of peak (maximum) cell shortening made on individual, field-stimulated (2 Hz, 22-25°C) wild-type (***A***) or $S1P_3$-null (***B***) myocytes superfused with various concentrations of extracellular calcium $[Ca^{++}]_o$. ***C, D.*** Measurements of peak (maximum) cell shortening made on individual, field-stimulated (2 Hz, 22-25°C) wild-type (***C***) or $S1P_3$-null (***D***) myocytes superfused with 1.8 mM $[Ca^{++}]_o$ in the presence or absence of verapamil (5 μM), a known blocker of I_{CaL}. Representative contraction curves (n=2 each condition).

Additional experiments conducted were performed in which I_{CaL} and cell shortening were measured simultaneously in the same myocyte (Figure 5.6). In these experiments, inotropy was positively and negatively modulated by application of the well-established compounds Iso and CCh, respectively. In order to emphasize I_{CaL} effects, K^+ currents were blocked by $CsCl_2$. From these experiments it is evident that Iso increased I_{CaL} and cell shortening and that CCh reduced the positive-inotropy caused by

Iso. Using peak I_{CaL} and average cell shortening, a strong correlation (R^2>0.99) was established.

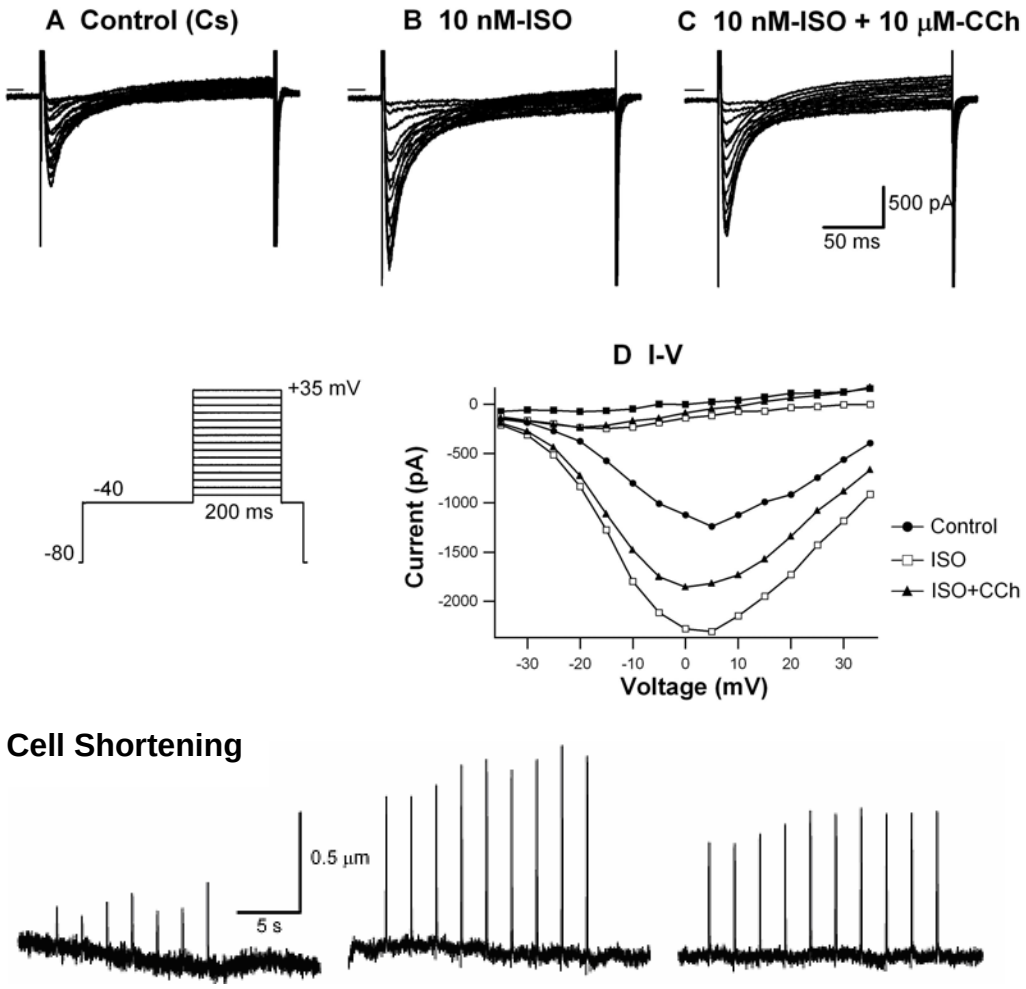

Figure 5.6 Antagonistic Effects of Isoproterenol (Iso) and Carbachol (CCh) on I_{CaL} and Cell Shortening in Adult Mouse Ventricular Myocytes. ***A-C.*** Whole-cell voltage clamp measurements of peak currents during depolarizing step voltages with Cs^+ in patch pipette solution to block K^+ currents. ***D.*** I-V isochronal relationship of peak inward (lower curve set) and outward (upper curve set) from representative family of currents shown in panels A-C. ***E.*** Concurrent cell shortening measurements made on cells depicted above in panels A-C. (Ochi and Giles, unpublished results).

These data collectively demonstrate that cell shortening in adult mouse ventricular myocytes is regulated by changes in $[Ca^{++}]_i$ and that this is further regulated by both $[Ca^{++}]_o$ and L-type calcium channel activity. Furthermore, these findings establish that

G-protein activation (e.g. via Iso-G_s) and inactivation (e.g. via CCh-G_i) of L-type calcium channels are fully functional in ventricular myocytes from the mouse.

5.4.2 S1P Receptor Isoforms Expressed in Myocytes

Isolated myocytes from adult mouse myocardium were analyzed by qPCR for relative expression levels of S1P receptor isoforms 1-3 (Figure 5.7). These results demonstrate that the $S1P_1$ receptor isoform is expressed at the highest level. This was true for myocytes isolated from either the left or the right ventricle. Additional measurements showed that $S1P_3$ expression levels were approximately half of those observed for $S1P_1$, irrespective of the ventricle from which they were isolated. Importantly, $S1P_2$ expression levels were negligible. Myocytes from both ventricles showed a similar pattern of S1P receptor expression. As a result, subsequent experiments did not differentiate between ventricles, and both the left and right ventricles were pooled.

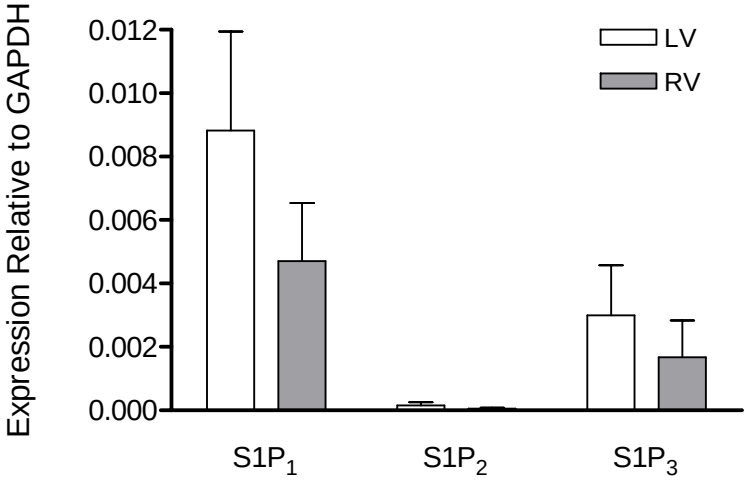

Figure 5.7 Characterization of S1P Receptor mRNA Expression in Adult Mouse Ventricular Myocytes by qPCR. Expression levels of $S1P_1$ in both the left ventricle (LV) and right ventricle (RV) were approximately 2-fold greater than expression levels of $S1P_3$. Expression levels of $S1P_2$ were negligible in both left and right ventricles. Mean ± SD (n=3).

In the experiments which examined the effects of S1P receptor subtype contributions to myocyte contractility measurements, $S1P_3$-null mice were utilized.[32] Myocytes isolated from $S1P_3$-null mice were also characterized for S1P receptor expression levels. As depicted in Figure 5.8, $S1P_3$ positive alleles were absent in $S1P_3$-null mice. As expected, expression of $S1P_3$ mRNA was undetectable by qPCR. $S1P_2$ expression levels did not increase in the $S1P_3$-null mice, and were as negligible as those seen in wild-type mice. Thus, $S1P_3$-null mice essentially have only $S1P_1$ expression and are therefore a useful tool for characterizing S1P signaling pathways via $S1P_1$.

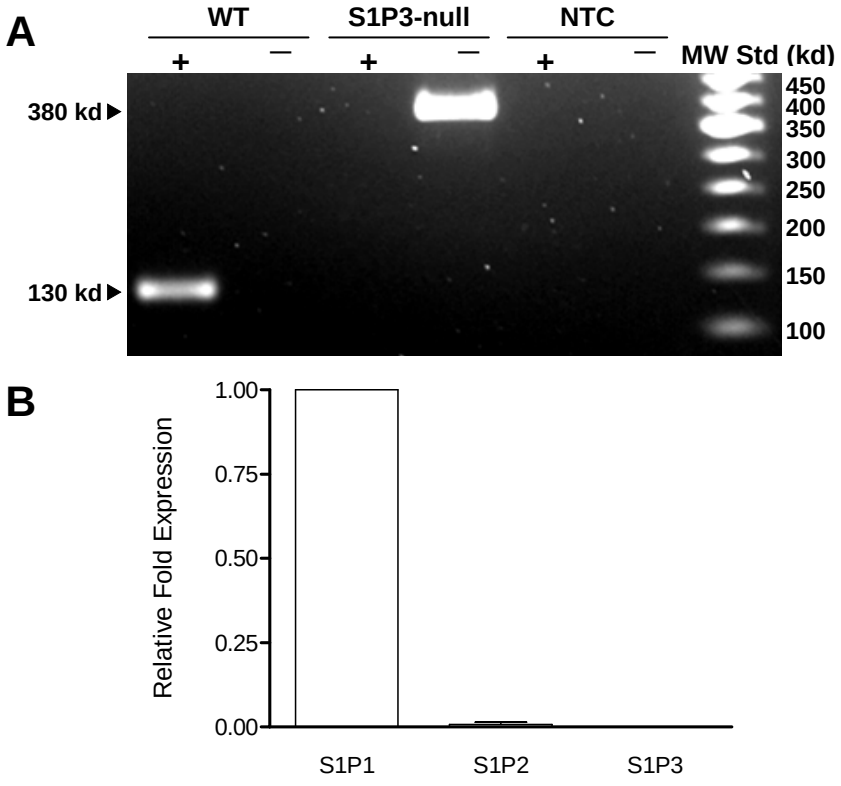

Figure 5.8 Characterization of S1P Receptor Expression in $S1P_3$-null Adult Mouse Ventricular Myocytes. ***A.*** Genotyping of $S1P_3$-null mice demonstrate a single band (predicted 380 kd) of the deleted $S1P_3^-$ allele after amplification by PCR, separation by agarose electrophoresis, and visualization by ethidium bromide. Amplified gene products from wild-type (WT) mice demonstrate a single band (predicted 130 kd) for the intact $S1P_3^+$ allele. No template controls (NTC) are absent of either band. ***B.*** Analysis of $S1P_3$-null myocytes by qPCR demonstrate a total absence of $S1P_3$ mRNA expression and extremely low levels of expression for $S1P_2$. Mean ± SD (n=3).

Therefore, based on qPCR and Western blotting data, $S1P_1$ and $S1P_3$ are the dominant isoforms in adult mouse ventricular myocytes. The contributions of these receptors and associated signaling pathways to regulating myocyte contractility were examined both collectively and separately.

5.4.3 S1P Attenuates Cell Shortening via $S1P_1$ and G_i

When S1P was added to field-stimulated (1-2 Hz, 22-25°C), isolated adult mouse ventricular myocytes, significant decreases in cell shortening were observed consistently (Figure 5.9). The average change in myocyte length in cells during baseline recordings was 8.0 ± 0.7 μm. After application of S1P (100 nM), the average change in myocyte length during a field-stimulated contraction decreased to 6.0 ± 0.5 μm. Thus, S1P-treated myocytes contract at 70.7 ± 15.4% of baseline control values and this was found to be highly statistically significant ($p<0.0001$). Differences were also noted between baseline and S1P-treated myocytes for contraction ($p=0.06$) and relaxation rates ($p<0.001$). S1P has a reported k_d for $S1P_1$ of 8 nM.[36] When S1P was evaluated at lower concentrations (e.g. 10 nM), a similar pattern of findings was observed, with cells contracting at 77.0 ± 13.1% of baseline values (n=4, data not shown). Thus, S1P at physiological concentrations can induce reduced cell contractility.

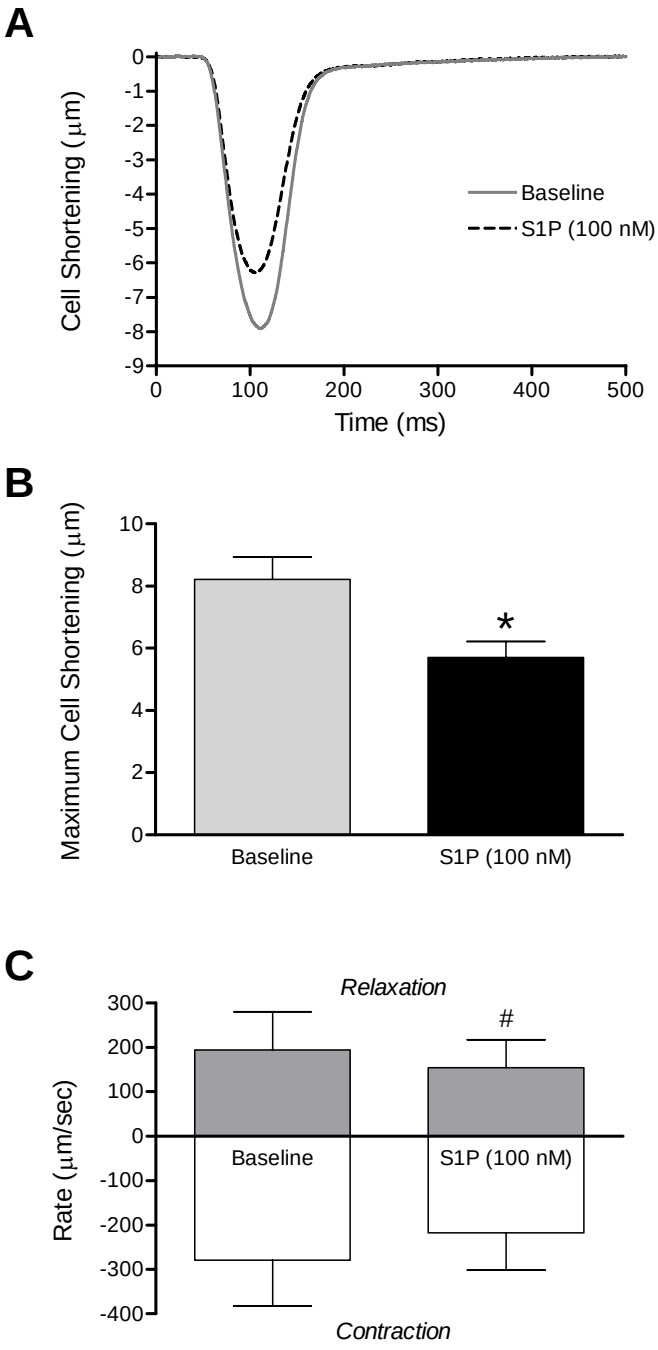

Figure 5.9 S1P Decreases Cell Shortening in Adult Mouse Ventricular Myocytes. Measurements of peak (maximum) cell shortening were made on individual, field-stimulated (1-2 Hz, 22-25°C) myocytes before and after application of S1P (100 nM). ***A.*** Representative contraction curves for each condition. ***B.*** Cell shortening data. *p<0.0001. ***C.*** Contraction/relaxation rates. #p<0.001. Data presented as mean ± SD (n=18).

Iso and CCh are well-known inotropic agents which modulate cAMP concentrations mediated by changes in adenylyl cyclase (AC). Accordingly, these compounds were used as positive and negative controls, respectively, to alter cell shortening in isolated myocytes (Figure 5.10). Compared to control values (100%), Iso (100 nM) increased maximal cell shortening by 89.8 ± 4.3%, whereas CCh (100 nM) decreased cell shortening by 20.6 ± 4.6% when applied to naive myocytes. These differences were found to be statistically significant ($p<0.001$). Similar to CCh, S1P decreased cell shortening by 29.3% when applied to naive myocytes. This was not significantly different than CCh.

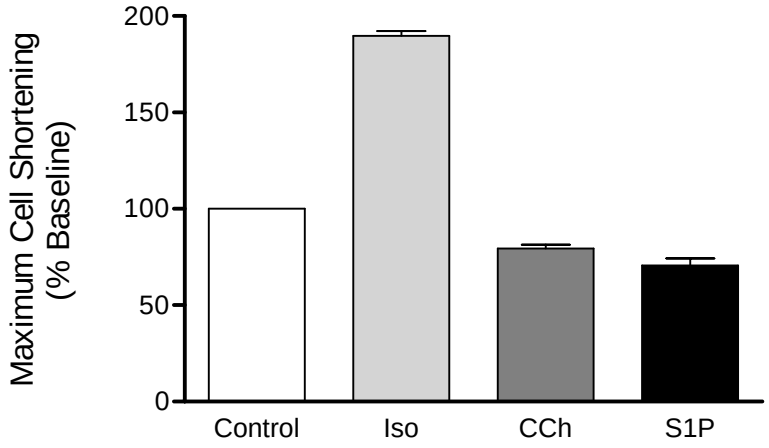

Figure 5.10 Comparison of Positive and Negative Inotropic Agents to S1P in Terms of Effect on Cell Shortening in Adult Mouse Ventricular Myocytes. Measurements of peak (maximum) cell shortening were made on individual, field-stimulated (1-2 Hz, 22-25°C) myocytes before and after application of isoproterenol (Iso, 100 nM, n=3), carbachol (CCh, 100 nM, n=5) or S1P (100 nM, n=18). The effects of S1P were not significantly different than CCh, but both were significantly different than Iso ($p<0.001$). Additionally, each treatment was significantly different than its paired control values ($p=0.0134$ for Iso, $p=0.0301$ for CCh, and $p<0.0001$ for S1P). Data presented as mean ± SD.

Stimulation of the β1AR by Iso activates G_s to induce cAMP formation and positively regulate I_{CaL}. Agonists which activate G_i-coupled receptors, in contrast, inhibit cAMP formation. To determine whether S1P might be antagonistic to Iso, myocytes were first exposed to Iso. After reaching an approximate two-fold increase in cell shortening, cells were superfused with Iso and S1P (100 nM). The addition of S1P reduced cell shortening (Figure 5.11), indicating that S1P can oppose the positive inotropic effects of Iso. Conversely, a separate population of myocytes was pre-treated with S1P (100 nM), and sufficient time was allowed for their contractility to reduce. Iso (in the presence of S1P) was then administered to these myocytes. This maneuver was found to reverse the negative inotropy induced by S1P. Thus, these experiments suggest that a signaling pattern via G_i is involved in the negative inotropy observed after administration of S1P.

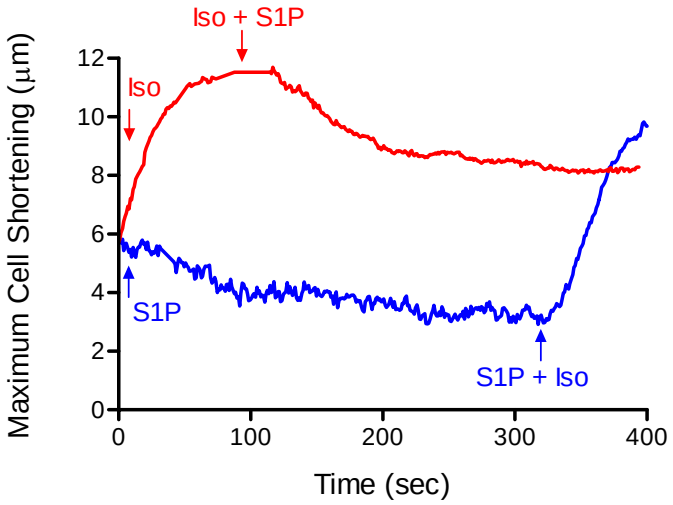

Figure 5.11 Antagonistic Inotropic Effects of S1P and Iso on Cell Shortening in Adult Mouse Ventricular Myocytes. Measurements of peak (maximum) cell shortening were made on individual, field-stimulated (1-2 Hz, 22-25°C) myocytes. In the first protocol (red), cells were first given Iso (100 nM) before administering Iso in the presence of S1P (100 nM). In the second protocol (blue), cells were first given S1P before administering S1P in the presence of Iso. Representative time course for each protocol.

Both $S1P_1$ and $S1P_3$ can signal through G_i. However, $S1P_3$ can also activate other G-proteins. To determine the contributions of $S1P_1$ exclusively (and G_i partially) to decreased myocyte contractility, further experiments were conducted using the $S1P_1$-selective agonist SEW2871. SEW2871 has a reported EC_{50} that is approximately 10-fold higher than S1P.[55] SEW2871 was therefore evaluated at concentrations similar to, and also 10-fold higher to those observed with S1P to have a negative inotropic effect. When SEW2871 (0.1 μM) was applied to myocytes, cell shortening was reduced to 72.0 ± 19.4% of baseline values (Figure 5.12). SEW2871 administered at 1 μM was also effective at reducing cell shortening, and produced a similar steady-state negative inotropy (77.0 ± 15.7% of baseline values). The results of SEW2871 at 0.1 or 1 μM were not significantly different from each other or from the values obtained after S1P treatment. Moreover, additional experiments, which examined the ability of Iso to overcome the reduced contractility caused by SEW2871, yielded a very similar pattern of results to those reported in Figure 5.11 (data not shown).

Since SEW2871 is an $S1P_1$-selective agonist, these results suggest that $S1P_1$ is at least partially, if not fully, the main receptor subtype responsible for the observed decreases in contraction strength. Further, since $S1P_1$ signals exclusively through G_i, these results strongly suggest that G_i is involved in S1P-mediated reductions in cell shortening. The contributions of $S1P_1$ to decreased cell shortening were further confirmed using $S1P_3$-null mice. Figure 5.13 demonstrates that myocytes isolated from these genetically altered mice exhibited a decrease of 23.53% compared to untreated controls after application of S1P (100 nM). Increases in cell shortening by Iso and decreases in cell shortening by CCh in $S1P_3$-null mice were similar to those results

observed with wild-type mice (see Figure 5.10), indicating that AC-cAMP signaling was intact and functioning normally in both genotypes.

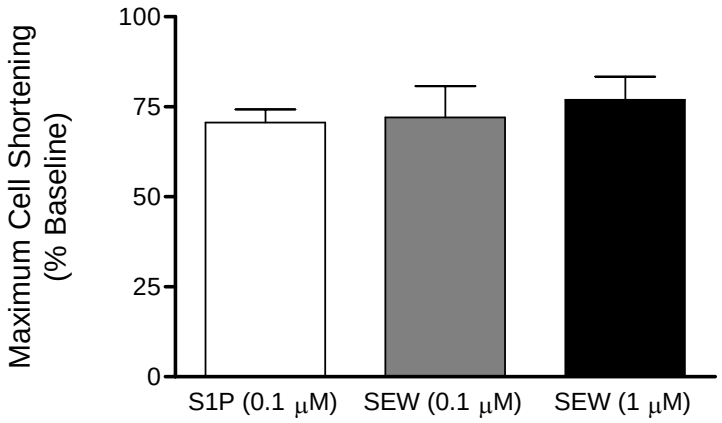

Figure 5.12 The Negative **I**notropic Effect of S1P on Adult Mouse Ventricular Myocytes is Similar to the Effect of the $S1P_1$-selective Agonist SEW2871. There were no significant differences in cell shortening detected after application of S1P (n=18), 0.1 μM SEW (n=5), or 1 μM SEW (n=6) on individual, field-stimulated (1-2 Hz, 22-25°C) myocytes. Each treatment was significantly different than its paired control values ($p<0.0001$ for S1P, $p=0.0166$ for SEW 0.1 μM, and $p=0.0021$ for SEW 1 μM). Data presented as mean ± SD.

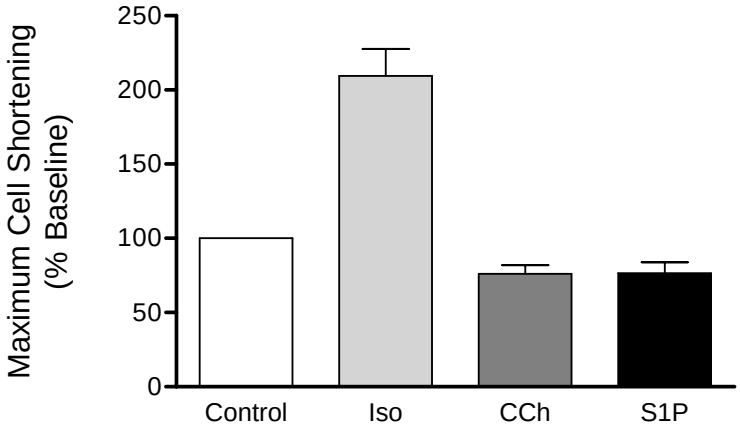

Figure 5.13 The Negative Effect of S1P on Cell Shortening is Reproduced in Ventricular Myocytes from $S1P_3$-null Adult Mice. Measurements of peak (maximum) cell shortening were made on individual, field-stimulated (1-2 Hz, 22-25°C) myocytes before and after application of isoproterenol (Iso, 100 nM, n=3), carbochol (CCh**,** 100 nM, n=4) or S1P (100 nM, n=10). S1P was not significantly different than CCh, but both were significantly different than Iso ($p<0.001$). Additionally, Iso and S1P treatments were significantly different than their paired control values ($p=0.0030$ for Iso, $p=0.0098$ for CCh, and $p=0.0055$ for S1P). Data presented as mean ± SD.

Collectively, the experiments using SEW2871 and $S1P_3$-null mice demonstrate that $S1P_1$ is an important and significant signaling pathway for S1P-induced negative inotropy.

5.4.4 S1P Can Also Attenuate Cell Shortening by Activating $S1P_3$ Receptors

$S1P_3$ receptor expression is approximately 50% that of $S1P_1$ (see Figure 5.7). It was therefore important to examine the effects of S1P mediated by $S1P_3$ receptors on myocyte contractility. Unfortunately, the use of genetically manipulated mice is not an option for these types of studies, as knock-out of $S1P_1$ is embryonically lethal.[39] Therefore, the population of $S1P_1$ receptors in adult mouse ventricular myocytes were blocked by pre-treatment with the antagonist VPC23019[17] in wild-type mice. Subsequent application of S1P was used to study the contributions of $S1P_3$ to cell shortening.

We first evaluated the effectiveness of VPC23019 as an $S1P_1$ antagonist. $S1P_3$-null mice have receptor isoforms limited to $S1P_1$ (almost exclusively, due to knock-out of $S1P_3$ and negligible expression of $S1P_2$). If pre-treatment with VPC23019 effectively prevents S1P from activating $S1P_1$ receptors, then cell shortening in myocytes isolated from $S1P_3$-null mice and pre-treated with VPC23019 should be comparable, prior to and after, application of S1P. As expected, S1P (100 nM) application to $S1P_3$-null myocytes pre-treated with VPC23019 (100 nM, 5 min) resulted in average cell shortenings that were 95.5 ± 5.0% that of baseline values (data not shown). This small decrease was shown to be not significant ($p=0.243$, $n=4$). Therefore, VPC23019 appears to be an effective antagonist against $S1P_1$. On this basis, it was used as a pharmacological tool with which to study $S1P_3$ signaling effects in normal mice.

Pre-treatment of wild-type myocytes with VPC23019 (100 nM) did not affect baseline contractions. Maximal cell shortening was 5.8 ± 0.3 μm, which fell within the normal range of baseline values observed during these experiments. Application of S1P (100 nM) in the continued presence of VPC23019 reduced cell shortening to 3.9 ± 0.4 μm, or 32.5% below baseline values (p=0.0547, n=3) (Figure 5.14). Thus, these results suggest that activation of $S1P_3$ is also capable of reducing myocyte contractility.

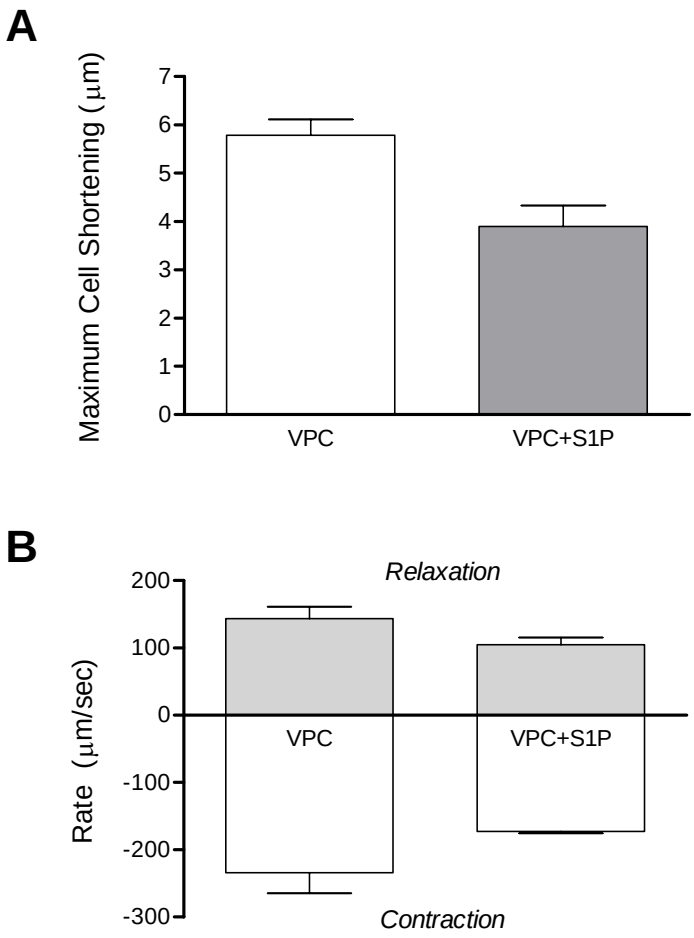

Figure 5.14 Application of S1P to Adult Mouse Ventricular Myocytes After Pre-treatment with the $S1P_1$-selective Antagonist VPC23019 Results in Decreased Cell Shortening. Measurements were made on individual, field-stimulated (1-2 Hz, 22-25°C) myocytes in the presence of VPC (100 nM), with and without concurrent application of S1P (100 nM). ***A.*** Peak (maximum) cell shortening. ***B.*** Contraction and relaxation rates. Data presented as mean ± SD (n=3).

5.4.5 I_{KAch} Contributes to S1P-mediated Cell Shortening via G_i

S1P is known to activate I_{KAch}, which would be expected to reduce action potential duration in mammalian myocytes (see Figure 5.15).[13,49] In an effort to isolate the contributions of I_{KAch} from those due to I_{CaL} in decreasing cell shortening following application of S1P, a series of experiments were conducted using the I_{KAch}-blocking peptide tertiapin.[18,30] To further restrict the potential effects to $S1P_1$ and G_i, myocytes isolated from $S1P_3$-null mice were used in these experiments. After pre-treatment with tertiapin (100 nM) for 5 min, baseline values were recorded. Next, S1P (100 nM) was applied (in the continued presence of tertiapin) and the myocyte pattern of field-stimulus-induced shortening was recorded. Following blockage of I_{KAch} with tertiapin, S1P activation of $S1P_1$ caused a 12.5% reduction from baseline (Figure 5.16). This reduction in cell shortening was significant ($p=0.0067$), as was the reduction in contraction rate ($p=0.0079$). Furthermore, the changes from baseline values observed in $S1P_3$-null myocytes subjected to I_{KAch} blockade were less (12.5%) than those changes observed without blockade (23.5%, see Figure 5.13). These results suggest that, at the concentrations of agents used, I_{KAch} contributes approximately equal to I_{CaL} to the negative inotropy following S1P activation of $S1P_1$.

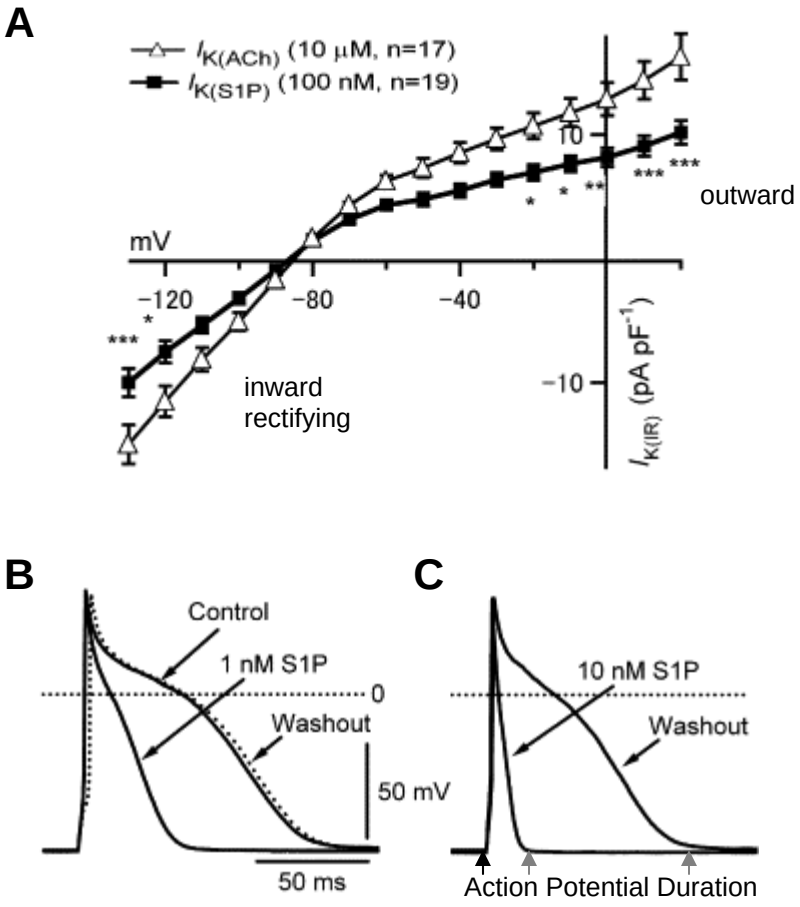

Figure 5.15 Activation of K_{ACh}-like current by S1P in Guinea Pig Atrial Myocytes Reduces APD. ***A.*** Comparison of isochronal current voltage (I-V) relationships between currents activated by Ach or S1P demonstrate that they are both carried by K^+ (based on reversal potential) and that they are both weakly inwardly rectifying. ***B.*** Application of S1P (1 nM) decreases APD. ***C.*** Increasing S1P application to 10 nM results in a further decrease of APD. Modified from Ochi and Giles, et al.[49]

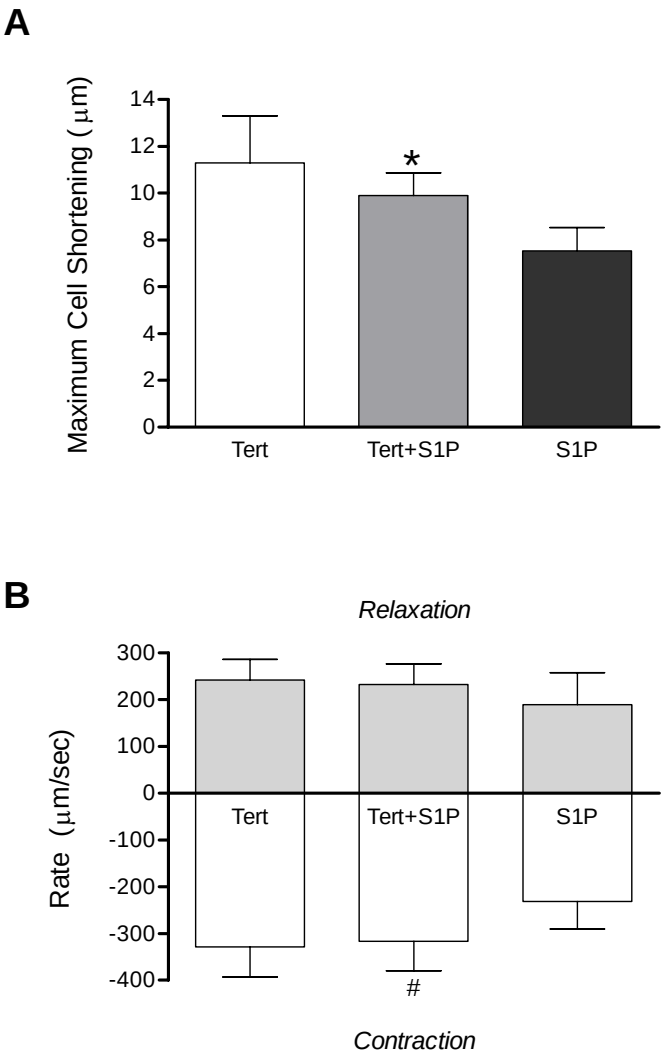

Figure 5.16 Contribution of the S1P-activated I_{KACh} on Cell Shortening in $S1P_3$-null Adult Mouse Ventricular Myocytes. After pre-treatment with the I_{KAch}-selective blocking peptide tertiapin (Tert), measurements were made on individual, field-stimulated (1-2 Hz, 22-25°C) myocytes in the continued presence of Tert (100 nM) with or without concurrent application of 100 nM S1P (Tert+S1P). The S1P data (S1P) was not included in the statistical analysis since these data were not paired measurements with either of the other treatments. The S1P measurements are presented instead to illustrate that tertiapin-treatment appears only to partially account for S1P-mediated negative inotropy. ***A.*** Peak (maximum) cell shortening. *p=0.0067 vs. Tert. ***B.*** Contraction and relaxation rates. $^{\#}$p=0.0079 vs. Tert. Data presented as mean ± SD.

5.4.6 Mathematical modeling predicts I_{KACh}-mediated alterations in $[Ca^{++}]_i$

It is well established that S1P can shorten APD in mammalian atrial myocytes (see Figure 5.15).[49] Further, it has also been established that shortening APD in rat ventricular myocytes can reduce $[Ca^{++}]_i$ and lessen cell shortening (see Figure 5.17).[11] In an attempt to relate these experimental findings to experimental results presented in this Chapter, we utilized a mathematical model of the mouse ventricular myocyte.[10] Our working hypothesis was that activation of an outward K^+ current at depolarized membrane potentials by S1P-mediated I_{KACh} would promote repolarization, leading to decreased APD at smaller $[Ca^{++}]_i$ transients and lowered $[Ca^{++}]_i$. It was further hypothesized that these changes, in addition to inhibition of I_{CaL}, would contribute to the functional changes observed in myocyte cell shortening.

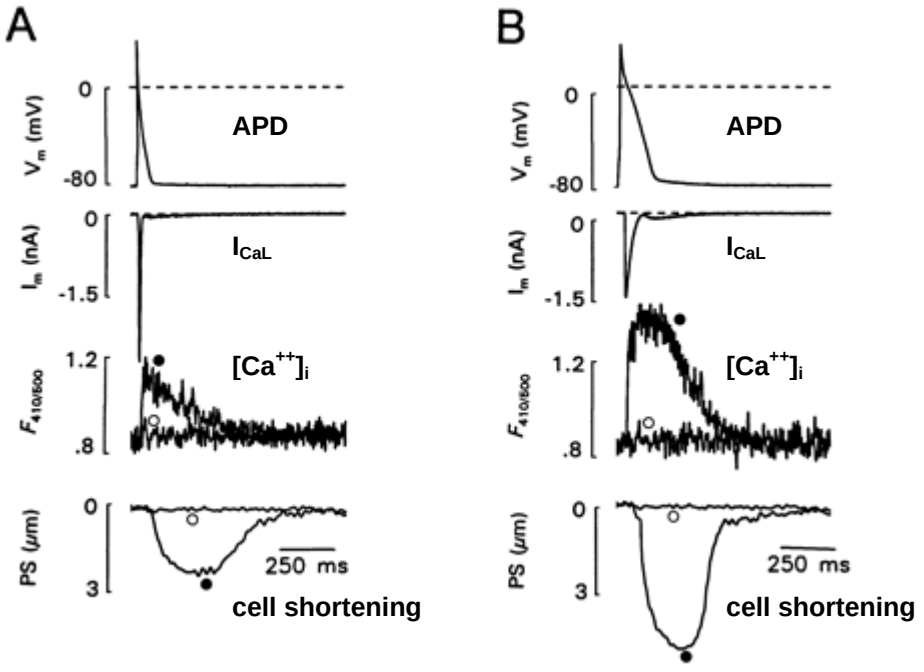

Figure 5.17 Comparison of APD Effects on Calcium Handling and Cell Shortening in Adult Rat Ventricular Myocytes. Voltage clamp protocols (top row) were used to simulate either short (***A***) or long (***B***) APD. Simultaneous recordings of I_{CaL}, $[Ca^{++}]_i$, and cell shortening were made. V_m (command voltage), I_m (current), $F_{410/500}$ (Indo fluorescent ratio), and PS (peak cell shortening). Modified from Bouchard, Clark and Giles.[11]

Upon stimulation, the "myocyte" in this model will initiate an AP that resembles experimentally derived AP (using whole-cell clamping techniques). To begin to evaluate the utility of this approach, we first assessed the robustness of this model by evaluating an *in silico* myocyte that had been exposed to a simulated dose of Iso. Iso acts via G_s to increase I_{CaL}.[47,65] Accordingly, we increased I_{CaL} in the model parameters to 2X that of baseline values (since we observed nearly a 2-fold increase in cell shortening with Iso; see Figures 5.10 and 5.13) and then stimulated the cell to initiate an AP. As shown in Figure 5.18, increasing I_{CaL} predictably results in extension of the "plateau" phase, and alters the rate of repolarization while also increasing APD. Similarly, when I_{CaL} was decreased to 75% that of baseline values (to simulate reductions in cell shortening upon treatment with CCh; see Figures 5.10 and 5.13), APD was decreased.

Next, stimulation with Iso or CCh was used to evaluate changes in I_{CaL} and $[Ca^{++}]_i$ in the *in silico* myocyte. As expected, Iso predictably yielded an approximate 2-fold increase in I_{CaL} and CCh was approximately 25% less than baseline (Figure 5.18). This pattern of computational results helped establish the validity of the model and illustrate the relationship between APD and I_{CaL} under these conditions. Peak $[Ca^{++}]_i$ values also were increased and decreased, respectively, with Iso and CCh in this model.

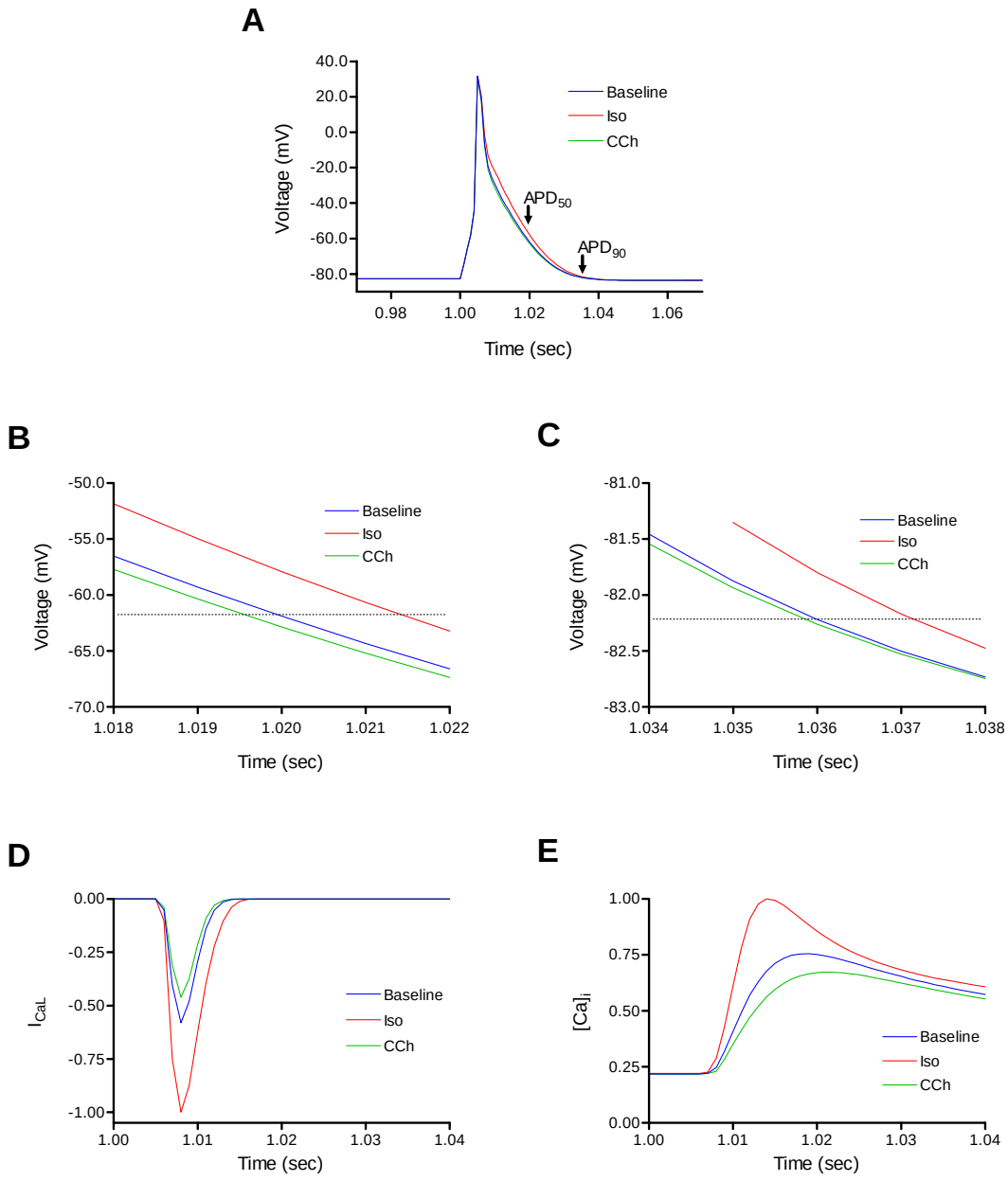

Figure 5.18 Mathematical Modeling of Adult Mouse Ventricular Myocyte AP. Increasing I_{CaL} input parameters to 200% or 75% that of baseline values was used to simulate application of Iso and CCh, respectively. ***A.*** Stimulation of the model cell was initiated and the resulting AP were determined. ***B.*** Examination of AP near baseline APD_{50}. ***C.*** Examination of AP near baseline APD_{90}. ***D.*** Comparison of I_{CaL}. ***E.*** Comparison of intracellular calcium ion concentrations. (Dederko, Landeen and Giles, unpublished data)

Having established this relationship between APD, I_{CaL} and $[Ca^{++}]_i$ with the model using simulated positive and negative inotropic agents, we next explored how changes in APD could effect calcium handling, and ultimately cell contraction. Triangular voltage commands (which simulate the shape of the AP in actual adult mouse ventricular myocytes) were used to "voltage clamp" the in silico myocyte. The rate of repolarization was adjusted to generate APD between of 40 and 5 ms. These ranges of APD were used because they approximated experimental data which has been shown to effect calcium (see Figure 5.17) and to be involved with S1P application (see Figure 5.15), respectively. It was first established that a single voltage command or a train of 10 voltage commands showed no time-dependent changes in either APD, I_{CaL}, or $[Ca^{++}]_i$ (data not shown). Thereafter, a single voltage command was utilized. As shown in Figure 5.19, decreasing the APD from 40 ms to 5 ms resulted in alterations in I_{CaL}. Changes were also noted in $[Ca^{++}]_i$ (data not shown).

Contraction strength is responsive to changes in I_{CaL} (see Figures 5.6 and 5.17) and can be modulated by altering amplitude or duration of the calcium transient.[6,11] We therefore explored the relationship between APD and I_{CaL} using the model of the adult mouse ventricular myocyte to tie together the relationships between S1P, APD, I_{CaL}, $[Ca^{++}]_i$ and cell shortening. As shown in Figure 5.19, there was a strong correlation (R^2>0.92) between APD and total I_{CaL} flux.

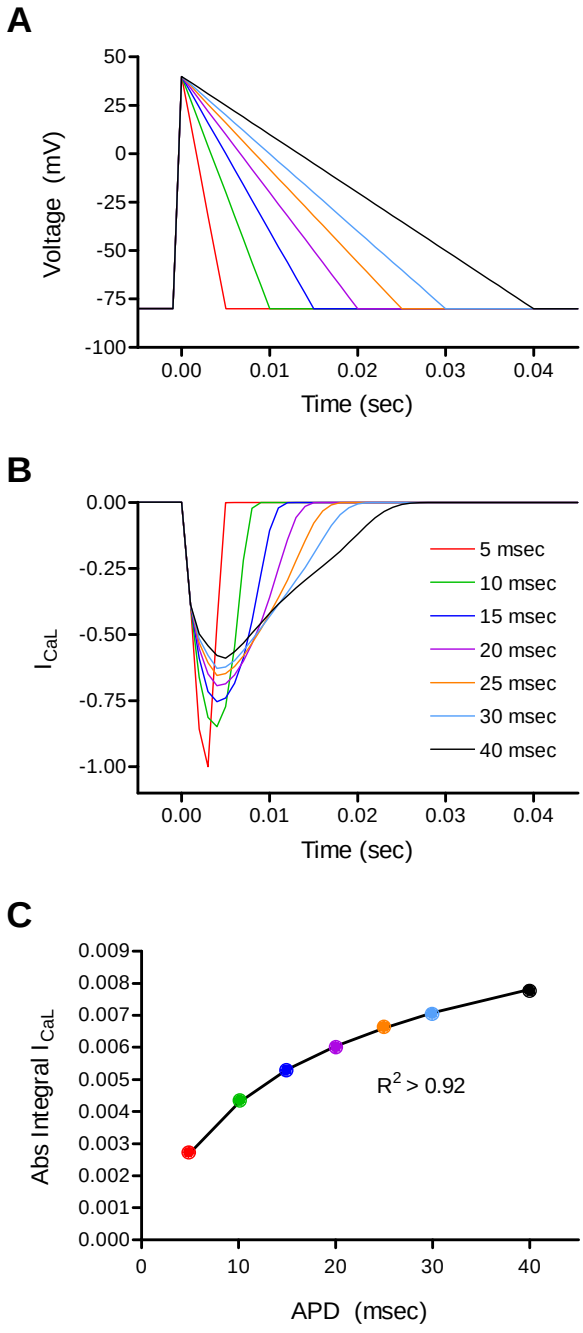

Figure 5.19 Relationship Between APD and I_{CaL} Using a Mathematical Model of the Mouse Ventricular Myocyte. ***A.*** APD were varied between 5 and 40 ms using a triangular-shaped action potential (holding potential of -80 mV, depolarization step to +40 mV, then ramped to -80 mV over APD). ***B.*** Normalized I_{CaL} time-course for each APD. ***C.*** Relationship between the absolute integral of I_{CaL} and APD. (Dederko, Landeen and Giles, unpublished data).

In summary, our experimental findings, direct and related mathematical modeling, illustrate that S1P activation of G_i-coupled S1P receptor isoforms (i.e. $S1P_1$ and $S1P_3$) can decrease cell shortening by both inhibiting I_{CaL} and activating I_{KAch}. Although these mechanisms are distinct and activated by separate G-protein subunits,[35] they contribute nearly equally to the negative inotropy induced by S1P activation of S1P receptors in the adult mouse ventricular myocyte.

5.5 Discussion

5.5.1 Summary of Major Findings

These studies were initiated to investigate the effects and reveal some aspects of the signaling pathways of S1P-mediated negative inotropy in adult mouse ventricular myocytes. Quantitative PCR and immunoblotting demonstrated that adult mouse ventricular myocytes express primarily $S1P_1$ and $S1P_3$ receptor isoforms. Both of these receptor isoforms are coupled to G_i. G_i-coupled receptors, for example M_2 receptors responsive to CCh, are known to inhibit cAMP-mediated I_{CaL}, to reduce cell shortening, and to shorten APD.[13,16,23,25,66] We therefore investigated responses in cell shortening in field-stimulated adult mouse ventricular myocytes after application of S1P.

S1P (10 – 100 nM) caused a negative inotropy within several minutes after application. This response was partially alleviated by the G_s-coupled β1AR agonist Iso. Positive inotropy by Iso stimulation was reduced by S1P, similar to what has been observed with CCh.[16] Using the $S1P_1$-selective agonist SEW2871, the $S1P_1$-selective antagonist VPC23019, and/or myocytes isolated from $S1P_3$-null mice, we demonstrated that S1P-mediated negative inotropy is through activation of both $S1P_1$ and $S1P_3$ receptor

isoforms. In addition, using the I_{KAch}-selective inhibitor tertiapin,[30] we demonstrated that activation of I_{KAch} may account for nearly half of the negative inotropy observed upon exposure to S1P.

To further explore the significance of these experimental findings, we used a mathematical model of the adult mouse ventricular myocyte. Results of the positive and negative inotropic responses to Iso and CCh in myocytes were used to adjust the initial I_{CaL} model parameters to reflect the observed changes in cell shortening. Specifically, the model illustrated that Iso can lengthen APD, whereas CCh results in a decrease in APD. These changes in APD resulted in either an increased or decreased calcium flux through I_{CaL}, respectively. When APD were "voltage clamped" between 40 and 5 ms, a strong correlation between APD and total I_{CaL} was observed. I_{CaL} is largely responsible for initiating CICR and altering $[Ca^{++}]_i$. Further, $[Ca^{++}]_i$ and contraction are tightly coupled in mammalian myocytes.[6,7] These findings therefore suggest that shortening of the APD through direct activation of I_{KAch} or through G_i-coupled inhibition of I_{CaL} are collectively mechanisms which regulate negative inotropy by S1P in adult mouse ventricular myocytes.

5.5.2 Modulation of $[Ca^{++}]_i$ and Contraction in the Mouse Myocyte

In the adult mouse myocyte, $[Ca^{++}]_i$ is tightly coupled to contraction and regulated by CICR which is initiated through L-type calcium channel activation and the corresponding Ca^{++} influx.[6,7] The contributions of calcium through T-type calcium channels, however, is negligible in ventricular myocytes.[6] It takes very few L-type

calcium channels to open to activate a RyR cluster and initiate CICR. Hence, this positive feedback system is highly efficient. We observed a strong correlation between $[Ca^{++}]_o$ and contraction strength (see Figure 5.5).

Calcium removal from the cytosol occurs during relaxation and can be mediated through SERCA, sodium/calcium exchangers (NCX), sarcolemmal Ca^{++} pumps, or mitrochondrial Ca^{++} pumps. In the mouse, 90.3% of cytosolic Ca^{++} is removed via SERCA, with 9.2% removed by NCX, and the remainder via Ca^{++} pumps.[37] Studies on ventricular myocytes isolated from adult NCX-null mice have demonstrated unchanged Ca^{++} dynamics,[53] suggesting that NCX may be less important during the adult mouse ventricular myocyte AP than in other mammalian species. However, calcium may influx via NCX if I_{CaL} is inhibited.[6] This may help explain the small contractions still present after administration of verapamil (see Figure 5.5).

L-type calcium channels are activated through phosphorylation by protein kinases such as protein kinase A (PKA). PKA activation increases I_{CaL} by increasing the fraction of channels that are available to open during depolarization.[29] PKA has other areas of activity in the contracting myocyte including phosphorylating RyR to induce CICR and phosphorylating PLB to increase SR calcium uptake. PKA can further phosphorylate myosin binding protein C and troponin I to affect myofilament contraction. These collectively account for the positive inotropy and lusitropy observed after G_s-mediated activation, for example after application of Iso.[6]

In studies on rodent cardiomyocytes, Iso has been shown to increase cell shortening and increase I_{CaL} over control (untreated) myocytes.[4,16,56] The EC_{50} for Iso-induced cAMP accumulation in the adult mouse ventricular myocyte is approximately

110 nM,[23] very similar to the concentration used in the majority of these studies. Our experimental findings agree with these reports, in that we observed an approximate two-fold increase in contraction in myocytes treated with 100 nM Iso (see Figures 5.10 and 5.13).

Iso is an agonist of β adrenergic receptors (βAR) in the heart. βAR are GPCR which couple to G_s to increase cAMP, which can then activate PKA. β1AR are the predominant cardiac subtype in mouse myocytes.[23] In addition to stimulating myocyte contraction, β1AR activation also induces myocyte relaxation by increasing Ca^{++} sequestration in the SR.[64] β2AR, on the other hand, have been proposed to couple to both G_s and G_i.[65] However, since β2AR are less abundant, stimulation of both β1AR and β2AR by Iso ultimately increases cell shortening in myocytes. A schematic of Iso-mediated increases in APD and contraction is presented in Figure 5.20.

G_i-coupled receptor agonists act in opposition to G_s-coupled receptor agonists to decrease AC and cAMP. CCh is a widely used agonist of acetylcholine receptors (mainly muscarinic) in the heart. CCh can decrease Iso-stimulated cell shortening in rat myocytes through a pertussis toxin (PTX)-sensitive mechanism, indicating involvement of G_i.[16] Although most of the reported literature agrees that CCh acts in a negative inotropic manner, there have been isolated reports in which CCh has been shown to increase contractions.[52] It should be noted, however, that those studies using guinea pig ventricular myocytes were performed in high $[Ca^{++}]_o$ (5.4 mM), at low frequency (0.2 Hz, or 12 bpm), and using extremely high concentrations of CCh (100 μM). Our results (see Figures 5.10 and 5.13) demonstrated negative inotropy when 100 nM CCh was

administered to mouse ventricular myocytes. There are three signaling pathways that can account for the CCh-induced negative inotropy: (i) activation of the inwardly rectifying current I_{KAch};[25,66] (ii) inactivation of AC and cAMP;[23] and (iii) activation of PI3K activity to reduce I_{CaL}.[15]

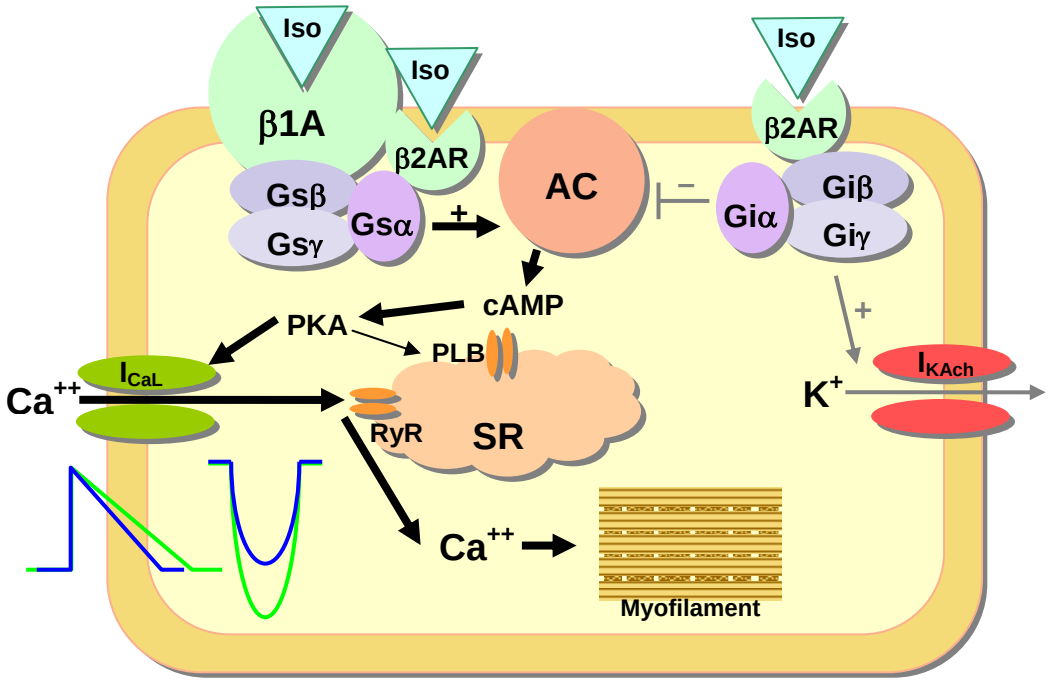

Figure 5.20 Signaling Pathways for Iso-induced Inotropy in Adult Mouse Ventricular Myocytes. G_s-coupled activation by β1AR predominates, increasing cAMP, PKA and $[Ca^{++}]_i$. Both APD and cell shortening increase (baseline, blue).

ACh is a muscarinic receptor agonist released by the vagus nerve following parasympathetic activation to the heart. Binding of ACh or CCh to M_2R activates a weakly inwardly rectifying K^+ ion current (I_{KAch}) mediated by $G_{i\beta\gamma}$ subunits.[34,35] Bradycardia results from I_{KAch}-mediated hyperpolarization, which can suppress spontaneous depolarization (I_f currents) in sino-atrial node cells.[21,66] K_{ACh} also exhibits an outward current at membrane potentials above the resting potential. Thus, this

outward K^+ current becomes activated during overshoot, plateau, and repolarization phases of the AP and results in a shortened APD.[13,49] A schematic of CCh-mediated decreases in APD and contraction is presented in Figure 5.21.

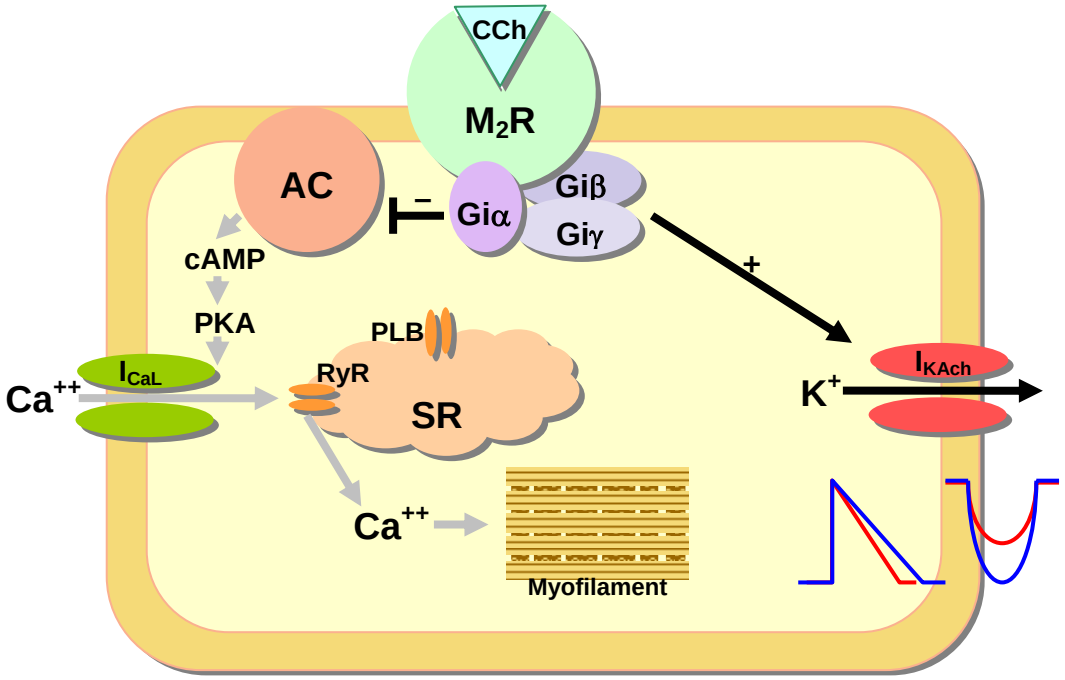

Figure 5.21 Signaling Pathways for CCh-induced Inotropy in Adult Mouse Ventricular Myocytes. $G_{i\alpha}$-coupled activation by M_2R decreases Ca^{++}. $G_{i\beta\gamma}$ activates I_{KAch}. Both APD and cell shortening decrease (baseline, blue).

5.5.3 Role of S1P in APD and negative inotropy

In 1993 Banach, et al.[5] reported that serum contains a PTX-sensitive lipid factor which could antagonize βAR-stimulated AC activity on L-type calcium channels. Later studies by this lab and others identified that S1P and other related molecules (e.g. sphingosylphosphorylcholine and LPA) could depress contractility through inhibiting I_{CaL} or by activating an I_{KAch}-like current in myocytes.[1,13,14,16,21,24,38] Further, these findings

on S1P-induced negative inotropy and/or bradycardia have been replicated in a number of animal species including rabbit,[21] cats,[51] rats,[45] and mice.[19]

S1P can activate I_{KAch} at nanomolar concentrations (see Figure 5.15).[13,49,61] Other S1P mimetics have similar responses. For example, FTY720-P also activates I_{KAch} in isolated mouse atrial myocytes.[33] Although FTY720-P activates a number of S1P receptor isoforms, including $S1P_1$ and $S1P_{3,}$[12] the absence of FTY720-P-induced bradycardia in $S1P_3$-null mice,[19] suggests strong involvement of $S1P_3$.

While S1P routinely caused decreased contractions in adult mouse ventricular myocytes, in some instances S1P has been noted to cause a slight initial increase in contraction. However, these small increases were nearly always followed by a sustained decrease in cell shortening. Nanomolar concentrations of S1P can cause rapid and transient increases in $[Ca^{++}]_i$ in $S1P_1$ expression systems.[50] These transient increases in $[Ca^{++}]_i$ were shown to be mediated via a PLC-IP_3 pathway involving $G_{i\beta\gamma}$. It has also been observed in rat and dog myocardium that S1P may not inhibit AC,[57,58] but in fact, may actually increase sinoatrial rate (in dogs).[58]

5.5.4 Role of S1P Receptor Isoforms in APD and Negative Inotropy

S1P receptor isoform expression in the mammalian heart is primarily limited to $S1P_{1-3}$. Our studies showed $S1P_1$ to be expressed most prominently in adult mouse ventricular myocytes (see Figure 5.7). In fact, $S1P_1$ expression levels were almost 2-fold greater than $S1P_3$. Other investigators have found high levels of $S1P_1$ in mouse heart[67] and isolated human[25,43] and rat myocytes.[38,45,54] $S1P_3$ has also been routinely identified in

myocardium of various species,[19,38] but $S1P_2$ is generally expressed in only small amounts or may be lacking entirely.[19,25] In agreement with this, we found that $S1P_2$ expression levels were negligible (see Figures 5.7 – 5.8). It is interesting to note that $S1P_2$-null mice have hemodynamic parameters comparable to wild-type mice, even during challenge with the βAR agonist dobutamine.[41] Thus, $S1P_2$ appears to be less relevant to studies on myocyte contractility, and our investigations focused appropriately on the roles of $S1P_1$ and $S1P_3$ in the regulation of S1P-mediated events.

To isolate $S1P_1$-activation and its response to cell shortening, we used two approaches. The first was to use the $S1P_1$-selective compound SEW2871. SEW2871 is a highly selective agonist for $S1P_1$ (with a reported EC_{50} of 20.7 nM in the mouse) which has low activity for other S1P receptor subtypes, even at concentrations up to 10 μM. Furthermore, SEW2871 exhibits receptor internalization and recycling similar to that induced by S1P.[28,55] However, SEW2871 is reportedly approximately 10 times less potent than S1P at $S1P_1$ activation.[55] Thus, we used SEW2871 at concentrations equal to, or 10 times greater, than those of S1P. We found that SEW2871 was approximately as effective as S1P in reducing cell shortening in normal mouse ventricular myocytes as S1P (see Figure 5.12). This represented our initial evidence that $S1P_1$ is strongly involved in negative inotropy. Our second approach was to use myocytes isolated from $S1P_3$-null mice. Under these conditions, the $S1P_1$ receptor was selectively activated. Again (see Figure 5.13), S1P resulted in similar changes in contractility.

In an attempt to identify and then investigate $S1P_3$-specific responses to cell shortening, we used the $S1P_1$-selective antagonist VPC23019. Although VPC23019 is a competitive antagonist for both $S1P_1$ and $S1P_3$, it is more potent at the $S1P_1$ receptor (7.9

pK_i for $S1P_1$ vs. 5.9 pK_i for $S1P_3$).[17] Our findings with myocytes isolated from $S1P_3$-null mice and treated with VPC23019 verified that this compound effectively antagonized $S1P_1$ receptors. Thus, pre-treating wild-type myocytes with VPC23019 and then challenging with S1P (in the continued presence of VPC23019) is an effective paradigm to study $S1P_3$ contributions. The results with VPC23019 (see Figure 5.14) were similar to those with SEW2871, and suggest that the $S1P_3$ isoform, in addition to $S1P_1$, is involved with negative inotropy in ventricular myocytes.

$S1P_3$ (shown through experiments with $S1P_3$-null mice) has been associated with decreases in heart rate.[19,55] This is of interest because $S1P_3$ can couple to G_q in addition to G_i. In myocytes, PLC activation by G_q can convert PIP_2 to DAG and IP_3. DAG can activate protein kinase C (PKC), which, in turn, can both positively and negatively modulate I_{CaL}.[29] IP_3 receptors found on the SR of ventricular myocytes can increase $[Ca^{++}]_i$ when activated. And, PIP_2 has been shown to control channel gating of K_{Ach}.[44] Therefore, G_q activation by $S1P_3$ could potentially have complicated and counteracting effects. However, because of the slower kinetics of downstream effectors (vs. CICR),[6] IP_3 receptors may be less effective in altering beat-to-beat contractions.

Signaling via G_q is less prominent in the mouse than in the rat.[23] The potential for $S1P_3$ signaling through G_q may therefore be less relevant in myocytes isolated from the mouse. This does not preclude, however, the signaling pathways of $S1P_3$ through G_i. In fact, G_i may be more likely to be involved with decreasing contractility and reducing APD since activation of I_{KAch} in atrial myocytes is PTX sensitive.[13,25] Furthermore, activation of I_{KAch} by the $G_{\beta\gamma}$ dimer requires PIP_2 (as do all inwardly rectifying K^+ channels).[59] Thus, enzymatic pathways that deplete PIP_2 (e.g. G_q-PLC) will reduce the

activity of the channel. This gives further evidence that G_i is most likely the more important modulator of myocyte beat rate and contractility.

We have examined the role of $S1P_1$ and I_{KACh} in contributing to decreased cell shortening by taking advantage of the application of a specific blocker. There are a limited number of blockers targeting inward rectifying K^+ channels. However, one such compound is tertiapin, a small peptide (21 amino acids) from the venom of honey bees.[20] Tertiapin selectively blocks I_{KACh} in cardiac myocytes by acting on the extracellular surface of the ion channel molecule(s).[18,30,66] It has little activity on other inward rectifying K^+ currents such as I_{K1} or I_{KATP} and does not affect either I_{Kv} or I_{CaL}.[18,30] Tertiapin (10-100 nM) reduces both the inward and outward components of ACh-stimulated K^+ currents,[30] and reduces the negative chronotropic responses induced by ACh in Langendorff-perfused hearts.[18] The k_d of tertiapin is ~8 nM and its IC_{50} is approximately 30 nM.[18,27,30] Accordingly, we pre-treated myocytes with 100 nM tertiapin prior to concurrent application of S1P (100 nM). Although a decrease in cell shortening was still observed (see Figure 5.16), it was smaller than what we had previously observed when I_{KACh} was not blocked (see Figure 5.9). This leads us to speculate that the negative inotropy observed in S1P-treated adult mouse ventricular myocytes is comprised of two individual components: (i) one pathway that acts via $G_{i\alpha}$ to reduce I_{CaL} and CICR, and (ii) another equally important pathway that acts via $G_{i\beta\gamma}$ to activate I_{KACh} and reduce APD, with additional consequences on $[Ca^{++}]_i$. This latter contribution was explored further using mathematical modeling.

5.5.5 Model Predictions of the Effect of APD Reduction on $[Ca^{++}]_i$

Contraction strength in myocytes has been shown to be affected by the frequency as well as the amplitude and duration of calcium transients (see Figures 5.6 and 5.17).[6] Furthermore, $[Ca^{++}]_i$ has been shown to be regulated by APD due to the markedly altered Ca^{++} influx due to I_{CaL} (see Figure 5.17). Using a mathematical model of the adult mouse ventricular myocyte, we demonstrate that alterations in ADP through positive and negative inotropic modulators (e.g. Iso and CCh) can alter I_{CaL} and $[Ca^{++}]_i$ (see Figure 5.18). Like CCh, S1P can attenuate $I_{KAch.}$[26] However, pre-treatment with CCh has no effect on S1P-activation of I_{KAch},[13] indicating that the two compounds share no common receptor agonism.

Results from these simulations using the mouse ventricular myocyte are in agreement with other experimental and modeling studies using S1P. In the guinea pig atrial myocyte, for example, application of S1P causes a concentration-dependent decrease in APD (see Figure 5.15).[49] Additionally, a model of the human atrial myocyte[48] has also been utilized by our laboratory to demonstrate that incorporation of a S1P-activated I_{KAch} current shortens APD (Giles, unpublished data).

We further explored the relationship between APD and $[Ca^{++}]_i$ using our model of the adult mouse ventricular myocyte. These simulations suggest that APD is positively correlated with total I_{CaL} flux. This provides a mechanism to help explain the experimental findings presented in this chapter. As proposed, activation of $S1P_1$ and $S1P_3$ receptor isoforms by S1P stimulates I_{KAch}. Outward flux of K^+ then increases the rate of repolarization and shortens APD. The shorter APD means less calcium flux through I_{CaL}. In addition, activation of $S1P_1$ and $S1P_3$ directly decreases I_{CaL} via G_i-

coupling to further alter repolarization and attenuate CICR. The loss of $[Ca^{++}]_i$ by these two mechanisms lessens calcium-mediated myofilament contraction strength and results in reduced cell shortening. A schematic of S1P-mediated changes in APD and contraction is presented in Figure 5.22.

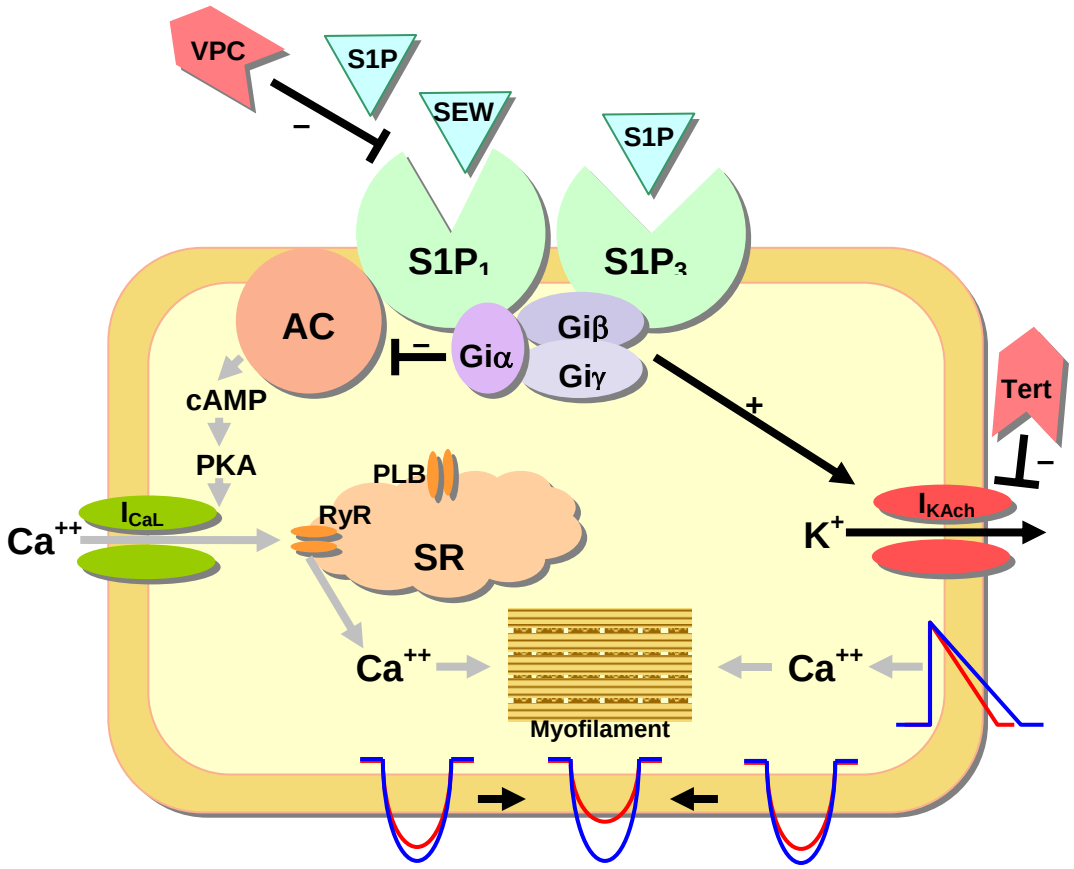

Figure 5.22. Proposed Signaling Pathways for S1P Receptor-activated Negative Inotropy in Adult Mouse Ventricular Myocytes. Activation of $S1P_1$ or $S1P_3$ by S1P or activation of $S1P_1$ by SEW2871 causes $G_{i\alpha}$-mediated inhibition of adenylyl cyclase (AC) and reduced production of cAMP. Reduction in cAMP levels, fails to activate protein kinase A (PKA), which, in turn, fails to activate L-type calcium channel currents (I_{CaL}). The net result is less calcium induced calcium release from the sarcoplasmic reticulum (SR) and less contractile force within the myofilaments, represented by the contraction curves on the left (baseline, blue). Simultaneously, $G_{i\beta\gamma}$ dimer activates acetylcholine-like potassium channel (I_{KAch}) which shortens action potential duration (baseline, blue) and decreases time for calcium influx. VPC23019 selectively antagonizes $S1P_1$ allowing S1P to react with $S1P_3$ only.

5.5.6 Limitations of Our Work

Our studies used data from mouse ventricular myocytes that were field-stimulated at either 1 or 2 Hz. It is generally accepted that increasing stimulus frequency increases contractile force. However, Antoons et al.,[2] demonstrated that, at least for the mouse, increases in $[Ca^{++}]_i$ transient amplitudes with increasing frequency (1 – 4 Hz) were modest and that overall changes in $[Ca^{++}]_i$ were minimal due to offset between simultaneous decreased I_{CaL} and increased SR release.

In these studies, orientation of the myocytes with regards to field stimulus direction was not monitored. In general, the stimulator was near, but not touching the myocyte. A study using pig myocytes has reported that alignment of the cells with the stimulating electrodes seemed to be important to contraction.[22] This paper reported that contractions stopped if the cell was aligned parallel with the electrodes, but resumed if greater or equal to a 25° offset. We, however, observed no qualitative differences with orientation of field stimulator. This may be due to the custom-design of our probe, whereas the other studies may have used more traditional parallel electrodes, or mistakenly used myocyte pairs as the experimental preparation.

An additional report has suggested that field stimulation, as compared to current-clamp stimulation, may increase time to peak contraction (by approximately 19 ms) and that shortening is sodium-independent and involves L-type Ca^{++} channels and/or NCX.[9] While the reported stimulation methods were similar to those used in our studies, the previous study was on rat myocytes, and the isolation and maintenance protocol for the

cells differed greatly. Furthermore, NCX in the mouse normally represents <10% of total calcium entry.[37]

There are limitations with any mathematical model. The model upon which these simulations was based has an acknowledged inability to reproduce accurately inactivation of L-type calcium channels. Regardless, the authors of this model have shown it to accurately reproduce experimental observations of Ca^{++} fluxes in mouse myoctes and to accurately reproduce findings from voltage-clamp experiments for a number of other major ionic currents, including fast sodium and nearly all of the potassium currents.[10] Thus, there is a reasonable level of confidence in the ability of this model to investigate situations of the adult mouse ventricular myocyte. As such, we utilized the model to explore the relationship between APD and $[Ca^{++}]_i$.

5.6 Acknowledgments

This Chapter is based on a manuscript in submission to the *American Journal of Physiology: Heart and Circulatory Physiology* (Landeen LK, Hu BS, Haga JH, Aroonsakool N, Giles WR. Mechanisms of the Negative Inotropic Effects of Sphinogine-1-Phosphate in Adult Mouse Ventricular Myocytes). The Doctoral candidate (LL) was the principal investigator/author of this work.

We would like to sincerely thank Dr. Richard L. Proia (National Institute of Diabetes and Digestive and Kidney Diseases) for making his S1P transgenic mice available to us. We also thank Dr. Masahiko Hoshijima and Ms. Kim Weldy (UCSD) for maintenance of the $S1P_3$-null breeding colonies. Training on myocyte field stimulation was provided by Dr. Ken Spitzer (University of Utah).

5.7 References

1. Alewijnse,A.E., Peters,S.L. & Michel,M.C. Cardiovascular effects of sphingosine-1-phosphate and other sphingomyelin metabolites. *Br. J. Pharmacol.* 143, 666-684 (2004).

2. Antoons,G., Mubagwa,K., Nevelsteen,I. & Sipido,K.R. Mechanisms underlying the frequency dependence of contraction and [Ca(2+)](i) transients in mouse ventricular myocytes. *J. Physiol.* 543, 889-898 (2002).

3. Arya,M. *et al.* Basic principles of real-time quantitative PCR. *Expert. Rev. Mol. Diagn.* 5, 209-219 (2005).

4. Balogh,J. *et al.* Phospholipase C and cAMP-dependent positive inotropic effects of ATP in mouse cardiomyocytes via P2Y11-like receptors. *J. Mol. Cell Cardiol.* 39, 223-230 (2005).

5. Banach,K., Bunemann,M., Huser,J. & Pott,L. Serum contains a potent factor that decreases beta-adrenergic receptor-stimulated L-type Ca^{2+} current in cardiac myocytes. *Pflugers Arch.* 423, 245-250 (1993).

6. Bers,D.M. Cardiac excitation-contraction coupling. *Nature.* 415, 198-205 (2002).

7. Bers,D.M. & Guo,T. Calcium signaling in cardiac ventricular myocytes. *Ann. N. Y. Acad. Sci.* 1047:86-98 (2005).

8. Bers,D.M. & Weber,C.R. Na/Ca exchange function in intact ventricular myocytes. *Ann. N. Y. Acad. Sci.* 976:500-12 (2002).

9. Bokenes,J., Sjaastad,I. & Sejersted,O.M. Artifactual contractions triggered by field stimulation of cardiomyocytes. *J. Appl. Physiol.* 98, 1712-1719 (2005).

10. Bondarenko,V.E., Szigeti,G.P., Bett,G.C., Kim,S.J. & Rasmusson,R.L. Computer model of action potential of mouse ventricular myocytes. *Am. J. Physiol Heart Circ. Physiol* 287, H1378-H1403 (2004).

11. Bouchard,R.A., Clark,R.B. & Giles,W.R. Effects of action potential duration on excitation-contraction coupling in rat ventricular myocytes. Action potential voltage-clamp measurements. *Circ. Res.* 76, 790-801 (1995).

12. Brinkmann,V. & Lynch,K.R. FTY720: targeting G-protein-coupled receptors for sphingosine 1-phosphate in transplantation and autoimmunity. *Curr. Opin. Immunol.* 14, 569-575 (2002).

13. Bunemann,M. *et al.* Activation of muscarinic K^+ current in guinea-pig atrial myocytes by sphingosine-1-phosphate. *Journal of Physiology* 489, 701-707 (1995).

14. Bunemann,M. *et al.* A novel membrane receptor with high affinity for lysosphingomyelin and sphingosine 1-phosphate in atrial myocytes. *EMBO J.* 15, 5527-5534 (1996).

15. Chesley,A. *et al.* The beta(2)-adrenergic receptor delivers an antiapoptotic signal to cardiac myocytes through G(i)-dependent coupling to phosphatidylinositol 3'-kinase. *Circ. Res.* 87, 1172-1179 (2000).

16. Cremers,B. *et al.* Modulation of myocardial contractility by lysophosphatidic acid (LPA). *J. Mol. Cell Cardiol.* 35, 71-80 (2003).

17. Davis,M.D., Clemens,J.J., macdonald,T.L. & Lynch,K.R. Sphingosine 1-phosphate analogs as receptor antagonists. *J. Biol. Chem.* 280, 9833-9841 (2005).

18. Drici,M.D., Diochot,S., Terrenoire,C., Romey,G. & Lazdunski,M. The bee venom peptide tertiapin underlines the role of I(KACh) in acetylcholine-induced atrioventricular blocks. *Br. J. Pharmacol.* 131, 569-577 (2000).

19. Forrest,M. *et al.* Immune cell regulation and cardiovascular effects of sphingosine 1-phosphate receptor agonists in rodents are mediated via distinct receptor subtypes. *J. Pharmacol. Exp. Ther.* 309, 758-768 (2004).

20. Gauldie,J., Hanson,J.M., Rumjanek,F.D., Shipolini,R.A. & Vernon,C.A. The peptide components of bee venom. *Eur. J. Biochem.* 61, 369-376 (1976).

21. Guo,J., MacDonell,K.L. & Giles,W.R. Effects of sphingosine 1-phosphate on pacemaker activity in rabbit sino-atrial node cells. *Pflugers Arch.* 438, 642-648 (1999).

22. Hedgepath,K.R., Mukherjee,R., Wang,Z. & Spinale,F.G. The relation between changes in myocyte orientation and contractile function with electrical field stimulation. *Basic Res. Cardiol.* 92, 385-390 (1997).

23. Hilal-Dandan,R., Kanter,J.R. & Brunton,L.L. Characterization of G-protein signaling in ventricular myocytes from the adult mouse heart: differences from the rat. *J. Mol. Cell Cardiol.* 32, 1211-1221 (2000).

24. Hilal-Dandan,R. *et al.* Lysophosphatidic acid induces hypertrophy of neonatal cardiac myocytes via activation of Gi and Rho. *J. Mol. Cell Cardiol.* 36, 481-493 (2004).

25. Himmel,H.M. *et al.* Evidence for Edg-3 receptor-mediated activation of *I*K.ACh by sphingosine-1phosphate in human atrial cardiomyocytes. *Molecular Pharmacology* 58, 449-454 (2000).

26. Himmel,H.M., Pietsch,M., Streller,U., Graf,E.M. & Ravens,U. Changes in morphology and inward rectifier currents in human atrial myocytes depend on culture conditions. *Basic Res. Cardiol.* 97, 434-444 (2002).

27. Jin,W. & Lu,Z. A novel high-affinity inhibitor for inward-rectifier K^+ channels. *Biochemistry.* 37, 13291-13299 (1998).

28. Jo,E. *et al.* $S1P_1$-selective in vivo-active agonists from high-throughput screening: off-the-shelf chemical probes of receptor interactions, signaling, and fate. *Chem. Biol.* 12, 703-715 (2005).

29. Kamp,T.J. & Hell,J.W. Regulation of cardiac L-type calcium channels by protein kinase A and protein kinase C. *Circ. Res.* 87, 1095-1102 (2000).

30. Kitamura,H. *et al.* Tertiapin potently and selectively blocks muscarinic K(+) channels in rabbit cardiac myocytes. *J. Pharmacol. Exp. Ther.* 293, 196-205 (2000).

31. Klabunde,R.E. Cardiovascular Physiology Concepts. Lippincott Williams & Wilkins, Philadelphia, PA (2005).

32. Kono,M. *et al.* The sphingosine-1-phosphate receptors $S1P_1$, $S1P_2$, and $S1P_3$ function coordinately during embryonic angiogenesis. *J. Biol. Chem.* 279, 29367-29373 (2004).

33. Koyrakh,L., Roman,M.I., Brinkmann,V. & Wickman,K. The heart rate decrease caused by acute FTY720 administration is mediated by the G protein-gated potassium channel I. *Am. J. Transplant.* 5, 529-536 (2005).

34. Krapivinsky,G. *et al.* The G-protein-gated atrial K^+ channel I_{KACh} is a heteromultimer of two inwardly rectifying K(+)-channel proteins. *Nature.* 374, 135-141 (1995).

35. Krapivinsky,G., Krapivinsky,L., Wickman,K. & Clapham,D.E. G beta gamma binds directly to the G protein-gated K^+ channel, IKACh. *J. Biol. Chem.* 270, 29059-29062 (1995).

36. Lee,M.J. *et al.* Sphingosine-1-phosphate as a ligand for the G protein-coupled receptor EDG-1. *Science.* 279, 1552-1555 (1998).

37. Li,L., Chu,G., Kranias,E.G. & Bers,D.M. Cardiac myocyte calcium transport in phospholamban knockout mouse: relaxation and endogenous CaMKII effects. *Am. J. Physiol.* 274, H1335-H1347 (1998).

38. Liliom,K. *et al.* Sphingosylphosphocholine is a naturally occurring lipid mediator in blood plasma: a possible role in regulating cardiac function via sphingolipid receptors. *Biochem. J.* 355, 189-197 (2001).

39. Liu,Y. *et al.* Edg-1, the G protein-coupled receptor for sphingosine-1-phosphate, is essential for vascular maturation. *J. Clin. Invest* 106, 951-961 (2000).

40. Livak,K.J. & Schmittgen,T.D. Analysis of relative gene expression data using real-time quantitative PCR and the 2(-Delta Delta C(T)) Method. *Methods* 25, 402-408 (2001).

41. Lorenz,J.N., Arend,L.J., Robitz,R., Paul,R.J. & MacLennan,A.J. Vascular dysfunction in $S1P_2$ sphingosine 1-phosphate receptor knockout mice. *Am. J. Physiol Regul. Integr. Comp Physiol.* 292, R440-R446 (2007).

42. MacDonell,K.L., Severson,D.L. & Giles,W.R. Depression of excitability by sphingosine-1-phosphate in rat ventricular myocytes. *American Journal of Physiology* 275, H2291-H2299 (1998).

43. Mazurais,D. *et al.* Cell type-specific localization of human cardiac S1P receptors. *J. Histochem. Cytochem.* 50, 661-670 (2002).

44. Mirshahi,T., Jin,T. & Logothetis,D.E. G beta gamma and KACh: old story, new insights. *Sci. STKE.* 2003, E32 (2003).

45. Nakajima,N. *et al.* Expression and characterization of Edg-1 receptors in rat cardiomyocytes: calcium deregulation in response to sphingosine 1-phosphate. *Eur. J. Biochem.* 267, 5679-5686 (2000).

46. Nakajima,T. *et al.* Troglitazone inhibits voltage-dependent calcium currents in guinea pig cardiac myocytes. *Circulation* 99, 2942-2950 (1999).

47. Nishizawa,T. *et al.* Overexpressed cardiac Gsalpha in rabbits. *J. Mol. Cell Cardiol.* 41, 44-50 (2006).

48. Nygren,A. *et al.* Mathematical model of an adult human atrial cell: the role of K^+ currents in repolarization. *Circ. Res.* 82, 63-81 (1998).

49. Ochi,R., Momose,Y., Oyama,K. & Giles,W.R. Sphingosine-1-phosphate effects on guinea pig atrial myocytes: Alterations in action potentials and K^+ currents. *Cardiovasc. Res.* 70, 88-96 (2006).

50. Okamoto,H. *et al.* EDG1 is a functional sphingosine-1-phosphate receptor that is linked via a Gi/o to multiple signaling pathways, including phospholipase C activation, Ca^{2+} mobilization, Ras-mitogen-activated protein kinase activation, and adenylate cyclase inhibition. *J. Biol. Chem.* 273, 27104-27110 (1998).

51. Oral,H., Dorn,G.W. & Mann,D.L. Sphingosine mediates the immediate negative inotropic effects of tumor necrosis factor-alpha in the adult mammalian cardiac myocyte. *J. Biol. Chem.* 272, 4836-4842 (1997).

52. Protas,L., Shen,J.B. & Pappano,A.J. Carbachol increases contractions and intracellular Ca^{++} transients in guinea pig ventricular myocytes. *J. Pharmacol. Exp. Ther.* 284, 66-74 (1998).

53. Reuter,H. *et al.* Na(+)--Ca^{2+} exchange in the regulation of cardiac excitation-contraction coupling. *Cardiovasc. Res.* 67, 198-207 (2005).

54. Robert,P. *et al.* EDG1 receptor stimulation leads to cardiac hypertrophy in rat neonatal myocytes. *J. Mol. Cell Cardiol.* 33, 1589-1606 (2001).

55. Sanna,M.G. *et al.* Sphingosine 1-phosphate (S1P) receptor subtypes $S1P_1$ and $S1P_3$, respectively, regulate lymphocyte recirculation and heart rate. *J. Biol. Chem.* 279, 13839-13848 (2004).

56. Sugishita,K. *et al.* Cellular basis for the acute inhibitory effects of IL-6 and TNF-alpha on excitation-contraction coupling. *J. Mol. Cell Cardiol.* 31, 1457-1467 (1999).

57. Sugiyama,A., Aye,N.N., Yatomi,Y., Ozaki,Y. & Hashimoto,K. Effects of sphingosine 1-phosphate, a naturally occurring biologically active lysophospholipid, on the rat cardiovascular system. *Jpn. J. Pharmacol.* 82, 338-342 (2000).

58. Sugiyama,A., Yatomi,Y., Ozaki,Y. & Hashimoto,K. Sphingosine 1-phosphate induces sinus tachycardia and coronary vasoconstriction in the canine heart. *Cardiovasc. Res.* 46, 119-125 (2000).

59. Sui,J.L., Petit-Jacques,J. & Logothetis,D.E. Activation of the atrial KACh channel by the betagamma subunits of G proteins or intracellular Na^+ ions depends on the presence of phosphatidylinositol phosphates. *Proc. Natl. Acad. Sci. U. S. A.* 95, 1307-1312 (1998).

60. Taha,T.A., Argraves,K.M. & Obeid,L.M. Sphingosine-1-phosphate receptors: receptor specificity versus functional redundancy. *Biochim. Biophys. Acta* 1682, 48-55 (2004).

61. van Koppen,C. *et al.* Activation of a high affinity Gi protein-coupled plasma membrane receptor by sphingosine-1-phosphate. *J. Biol. Chem.* 271, 2082-2087 (1996).

62. Vandecasteele,G. *et al.* Muscarinic and beta-adrenergic regulation of heart rate, force of contraction and calcium current is preserved in mice lacking endothelial nitric oxide synthase. *Nat. Med.* 5, 331-334 (1999).

63. Xia,M. *et al.* Functional expression of L- and T-type Ca^{2+} channels in murine HL-1 cells. *J. Mol. Cell Cardiol.* 36, 111-119 (2004).

64. Xiao,R.P. Cell logic for dual coupling of a single class of receptors to G(s) and G(i) proteins. *Circ. Res.* 87, 635-637 (2000).

65. Xiao,R.P. *et al.* Coupling of beta2-adrenoceptor to Gi proteins and its physiological relevance in murine cardiac myocytes. *Circ. Res.* 84, 43-52 (1999).

66. Yamada,M. The role of muscarinic K(+) channels in the negative chronotropic effect of a muscarinic agonist. *J. Pharmacol. Exp. Ther.* 300, 681-687 (2002).

67. Zhang,G., Contos,J.J., Weiner,J.A., Fukushima,N. & Chun,J. Comparative analysis of three murine G-protein coupled receptors activated by sphingosine-1-phosphate. *Gene* 227, 89-99 (1999).

CHAPTER 6

CONCLUSION

6.1 Summary of Major Findings

The actions of sphingosine-1-phosphate (S1P) through its G-protein coupled membrane receptor isoforms were investigated in fibroblasts and myocytes of the adult myocardium. Activation of and signaling pathways via these receptors are known to result in a number of distinct cellular responses.[5,6,14,16] Using cardiac fibroblasts (CFb) and myocytes of both the mouse and rat, functional responses in differentiation, migration, contraction, and ionic currents were studied.

While there is much known about the effects of S1P on myocyte action potential and activation of potassium (K^+) current, the majority has been published on non-murine species.[3,8,13] Further, the literature is lacking regarding actions of S1P on fibroblasts isolated from adult myocardium. These studies were initiated in part to contribute to the growing body of knowledge on the varied physiological responses that S1P can have within cells of the heart.

CFb are essential components of myocardium. They not only facilitate the structural and organizational architecture of the heart, but they are important contributors to paracrine signaling. Additionally, these cells are electrotonically coupled to myocytes and can directly participate in regulating the action potential of myocytes.[1,10,11] Therefore, study of their cell signaling and physiology is important in a number of emerging disciplines. However, in order to conduct meaningful studies on CFb, relatively pure populations of cells are required. A protocol was developed based on a differential

plating procedure and negative selection steps using magnetically activated antibodies (anti-CD11b). This protocol demonstrated significant reduction of resident macrophage (MΦ) levels in CFb isolates. Furthermore, it was demonstrated that the use of commonly used cytoskeletal markers (e.g. vimentin and smooth muscle α-actin) to identify CFb is less reliable than the use of more CFb-specific markers, such as discoidin domain receptor 2 (DDR2),[7] due to co-expression by non-CFb contaminating cell types (e.g. MΦ).

Using this protocol, primary isolated, purified mouse CFb were shown to express S1P receptor isoforms $S1P_{1-3}$. The relative levels of these receptor subtypes, however, could be modulated with time and by culture conditions. Whereas $S1P_3$ was expressed the highest upon initial isolation, levels of $S1P_2$ increased with extended time in culture. Direct co-culture with MΦ or exposure to known MΦ-secreted factors altered S1P receptor levels in CFb relative to controls. Factors that demonstrated modulating effects included transforming growth factor beta 1 (TFGβ1), tumor necrosis factor alpha (TNFα), and platelet-derived growth factor BB (PDGF-BB). TGFβ1 tended to down-regulate whereas TNFα tended to up-regulate. This was observed for all three S1P receptor isoforms. PDGF-BB caused increases in S1P3 expression levels the strongest. This was shown to be specific to PDGF-BB and not a common mechanism of tyrosine kinase receptors, since administration of insulin-like growth factor 1 (IGF-1) failed to illicit a similar response.

The ability of effector molecules which are components of the $S1P_2$ and $S1P_3$ signaling pathways to alter S1P receptor expression levels was demonstrated. Disruption

of $S1P_2$-$G_{12/13}$-Rho signaling[17] through the use of a Rho-associated kinase inhibitor, decreased $S1P_2$ expression using a culture protocol in reduced serum (which was shown previously to augment $S1P_2$). Similarly, disruption of $S1P_3$-$G_{12/13}$-Rac signaling[17] through a Rac 1 inhibitor decreased $S1P_3$ expression using a protocol in PDGF-BB (which was shown previously to augment $S1P_3$). Thus, S1P receptor expression in adult mouse CFb appears to be sensitive to downstream, intracellular events or membrane-associated regulators. These may serve in a feedback sensing manner. $S1P_3$ was further shown to be necessary for CFb migration in response to PDGF-BB. Cross activation of PDGF-BB and $S1P_1$ has been suggested in other cell systems. The data presented here suggests that PDGF-BB may also activate $S1P_3$ in cells that require this receptor for migration.

Until recently, no electrophysiological characterization of K^+ ion channel expression in CFb had been reported. Building on the data published by others in this laboratory,[4,15] various aspects of mouse and rat CFb electrophysiology were assessed, including the response of rat CFb to S1P. These assessments were performed using novel patch-clamping technology platforms by AVIVA Biosciences, Inc. and Nanion, Inc. Both K_v and K_{ir} currents were identified by patch-on-a-chip platforms. However, compared to conventional patch clamping methods, chip platforms were more likely to activate mechanosensitive ion channels. Therefore, S1P activation was studied by conventional techniques in rat CFb. S1P was found to strongly activate time-dependent inward and outward currents in adult rat CFb that resembled TRP ion channel currents.

Lastly, mouse ventricular myoycte contractility was investigated experimentally and these findings were integrated and explored through mathematical modeling[2] to

characterize signaling pathways involved in S1P-regulated negative inotropy. Similar to carbachol (CCh)-G_i activation of acetylcholine-like K^+ currents (I_{KACh}) which decrease action potential duration (APD) and reduce cell shortening,[19] S1P was also found to activate I_{KACh} and to decrease cell shortening (partially). This was demonstrated to occur through $S1P_1$ (which exclusively couples to G_i) using a selective inhibitor of I_{KACh}, tertiapin, and myocytes isolated from $S1P_3$-null mice. It was further demonstrated that activation of either $S1P_1$ or $S1P_3$ can reduce cell shortening via $G_{i\alpha}$-coupled inactivation of L-type calcium (Ca^{++}) channel currents (I_{CaL}). Again, these responses were similar to those observed with CCh.[18] The consequences of alterations in APD and I_{CaL} were more fully explored using a mathematical model of the adult mouse myocyte. This model confirmed experimental findings on the action of G_i and G_s towards myocyte cell shortening and how APD is integrally linked to Ca^{++} influx and intracellular Ca^{++} concentrations ($[Ca^{++}]_i$).

In conclusion, the investigations performed as part of this Dissertation provide significant insights regarding the effects of S1P on cells of the myocardium, namely ventricular fibroblasts, myocytes and macrophages. The resulting manuscripts (Landeen L.K., Aroonsakool N., Haga J.H., Hu B.S., Giles W.R., Sphingosine-1-Phosphate Receptor Expression in Cardiac Fibroblast Cells is Modulated by in vitro Culture Conditions, *American Journal of Physiology: Heart and Circulatory Physiology*, 2007, in press; Landeen L.K., Aroonsakool N., Haga J.H., Hu B.S., Giles W.R., Effects of Sphinogine-1-Phosphate On Myocyte Contractility, *American Journal of Physiology: Heart and Circulatory Physiology*, 2007, in preparation) will meaningfully contribute to the growing body of knowledge regarding S1P and cardiac physiology.

6.2 Future Considerations

One important future area of investigation regarding these studies would be the confirmation of message expression of the S1P receptor isoforms with protein data. Significant efforts were made using Western blotting methods, however, the availability of specific and quality antibodies is severely lacking. In fact, most published articles on S1P receptors tend to report message levels instead of protein levels. Further, when several prominent labs working in the field of S1P research were contacted, they all expressed their lack of success with protein determinations. It is not readily clear why more suitable antibodies are not commercially available, considering the high volume of published papers in the field. Having protein measurements would greatly improve the interpretation of these and other's findings.

Loss of $S1P_1$ is embryonically lethal.[12] $S1P_1$ was shown in the studies presented in Chapter 5 to be a critical contributor towards myocyte contractility after application of S1P. It would be important to confirm these findings, which utilized pharmacological approaches, by alternative means, such as through the use of RNA interference (RNAi) techniques. RNAi could also be used to determine whether other species have similar signaling pathways that contribute to the negative inotropic effects of S1P, especially in species that have more prominent G_q activity than that reported for the mouse.[9]

It has been recently shown by Chilton and Giles (2007, in submission) that rabbit myocytes and CFb can form gap junction communications during in vitro co-culture. This intercellular coupling does not alter APD, since APD are similar in both coupled and non-coupled (i.e. single cultures of) myocytes. However, application of S1P (at nanomolar concentrations) to coupled CFb-myocytes causes rapid loss of excitability. It

would therefore be worthy of note to reproduce selected studies from Chilton and Giles using cells isolated from the adult mouse ventricular myocardium. In particular, it would be of great consequence to perform such studies using CFb that have first had their S1P receptor expression profiles modulated (using the methods described in Chapter 3, using CFb isolated from S1P receptor-deficient mice, or using RNAi knock-down methods) to see the contributions of specific receptor subtypes on myocyte APD. Similar experiments could also be performed whereby myocytes with S1P receptor deficiencies are used.

Lastly, since many of these experiments were performed using isolated cells, it would be informative to see if these findings held consistent when using intact tissue. This could be accomplished perhaps using either isolated strips of ventricle or in Langendorff-perfused whole-heart studies. The contributions of S1P receptor isoforms to myocyte contractility could again be studied using pharmacological approaches or using S1P receptor knock-out mice. An understanding of such findings in more intact tissue would be a better bridge to understanding of the physiological situation in higher mammals.

6.3 References

1. Baudino,T., Carver,W., Giles,W.R. & Borg,T.K. Cardiac Fibroblasts: friend or foe? *Am. J. Physiol Heart Circ. Physiol.* ., (2006).

2. Bondarenko,V.E., Szigeti,G.P., Bett,G.C., Kim,S.J. & Rasmusson,R.L. Computer model of action potential of mouse ventricular myocytes. *Am. J. Physiol Heart Circ. Physiol* 287, H1378-H1403 (2004).

3. Bunemann,M. *et al.* Activation of muscarinic K^+ current in guinea-pig atrial myocytes by sphingosine-1-phosphate. *Journal of Physiology* 489, 701-707 (1995).

4. Chilton,L. *et al.* K^+ currents regulate the resting membrane potential, proliferation, and contractile responses in ventricular fibroblasts and myofibroblasts. *Am. J. Physiol Heart Circ. Physiol* 288, H2931-H2939 (2005).

5. Fukushima,N., Ishii,I., Contos,J.J., Weiner,J.A. & Chun,J. Lysophospholipid receptors. *Annu. Rev. Pharmacol. Toxicol.* 41:507-34., 507-534 (2001).

6. Futerman,A.H. & Hannun,Y.A. The complex life of simple sphingolipids. *Eur. Mol. Biol. Organization* 5, 777-782 (2004).

7. Goldsmith,E.C. *et al.* Organization of fibroblasts in the heart. *Dev. Dyn.* 230, 787-794 (2004).

8. Guo,J., MacDonell,K.L. & Giles,W.R. Effects of sphingosine 1-phosphate on pacemaker activity in rabbit sino-atrial node cells. *Pflugers Arch.* 438, 642-648 (1999).

9. Hilal-Dandan,R., Kanter,J.R. & Brunton,L.L. Characterization of G-protein signaling in ventricular myocytes from the adult mouse heart: differences from the rat. *J. Mol. Cell Cardiol.* 32, 1211-1221 (2000).

10. Kamkin,A., Kiseleva,I., Lozinsky,I. & Scholz,H. Electrical interaction of mechanosensitive fibroblasts and myocytes in the heart. *Basic Res. Cardiol.* 100, 337-345 (2005).

11. Kohl,P., Kamkin,A.G., Kiseleva,I.S. & Noble,D. Mechanosensitive fibroblasts in the sino-atrial node region of rat heart: interaction with cardiomyocytes and possible role. *Exp. Physiol* 79, 943-956 (1994).

12. Liu,Y. *et al.* Edg-1, the G protein-coupled receptor for sphingosine-1-phosphate, is essential for vascular maturation. *J. Clin. Invest* 106, 951-961 (2000).

13. Ochi,R., Momose,Y., Oyama,K. & Giles,W.R. Sphingosine-1-phosphate effects on guinea pig atrial myocytes: Alterations in action potentials and K^+ currents. *Cardiovasc. Res.* 70, 88-96 (2006).

14. Pyne,S. & Pyne,N.J. Sphingosine 1-phosphate signalling in mammalian cells. *Biochem. J.* 349, 385-402 (2000).

15. Shibukawa,Y., Chilton,E.L., Maccannell,K.A., Clark,R.B. & Giles,W.R. K+ currents activated by depolarization in cardiac fibroblasts. *Biophys. J.* 88, 3924-3935 (2005).

16. Spiegel,S. & Milstien,S. Sphingosine-1-phosphate: an enigmatic signalling lipid. *Nat. Rev. Mol. Cell Biol.* 4, 397-407 (2003).

17. Taha,T.A., Argraves,K.M. & Obeid,L.M. Sphingosine-1-phosphate receptors: receptor specificity versus functional redundancy. *Biochim. Biophys. Acta* 1682, 48-55 (2004).

18. Vandecasteele,G. *et al.* Muscarinic and beta-adrenergic regulation of heart rate, force of contraction and calcium current is preserved in mice lacking endothelial nitric oxide synthase. *Nat. Med.* 5, 331-334 (1999).

19. Yamada,M. The role of muscarinic K(+) channels in the negative chronotropic effect of a muscarinic agonist. *J. Pharmacol. Exp. Ther.* 300, 681-687 (2002).